UNIVERSITÀ DI PISA

ENGINEERING PHD SCHOOL "LEONARDO DA VINCI"

PhD Thesis

SUSTAINABLE BIOCOMPOSITES FROM RENEWABLE RESOURCES AND RECYCLED POLYMERS

VU THANH PHUONG

Supervisor:

Professor Andrea Lazzeri

PhD Course in

CHEMICAL ENGINEERING AND MATERIAL SCIENCE

(SSD ING-IND/22)

XXIII cycle

2010 - 2012

Contents

Abstract

Chapter 1. General introduction

Chapter One reports on a review of sustainable biocomposite materials. The concepts on sustainable materials, renewable resources, biopolymers, biocomposites, are summarized from the literatures as background theories for this thesis. The situation of plastic materials and its effects on the environment, health, disposal matter (landfills, incinerations, mechanical and biorecycling) are defined to explain why the applications of biopolymers and biocomposites are necessary for research and industry. Current applications and the market of biopolymers, biofibers, and biocomposite materials are reported and analyzed. The availability of current biofibers or natural fibers on the market are listed and compared with mechanical properties and their economic value as oppose to non-biodegradable materials such as glass, carbon fibers, etc. Moreover, biopolymer and bio-based materials are being developed not only on quantity, but also for the quality of materials. In addition to this, their prices are getting cheaper. Therefore, biocomposites will become potential materials for diversified applications in the future. The investigation into current research and applications of biopolymer and biocomposites are essential to find new research directions for this thesis and its application to develop new materials that have high mechanical and thermo resistance and biodegradability. Specially, some new tendencies and new challenges found in the development of biopolymer-like celluluse diacetate, polylactic acid, starch and biocomposites are discussed. Consequently, not only the research presented in this thesis has been focused on industrial application, but also on the solution of some critical environmental problem.

Chapter 2. "Green" biocomposites based on cellulose diacetate and regenerated cellulose microfibers: Effect of plasticizer content on morphology and mechanical properties

In Chapter Two, The mechanical properties of biocomposites based on CDA considered in the literature are still not satisfactory in view of their possible applications, and the use types of processing are not economically viable on an industrial scale. In particular, the thermal characteristics of the materials developed and their matrix-filler interactions were not much investigated. So far, there are no

publications about the effects of multi plasticizers on physical properties, thermal stability and morphology of cellulose diacetate/cellulose fibers composites under melt processing. Since both the cellulose diacetate and Lyocell fibers can be produced from renewable forest biomass, their manufacturing does not imply any competition for land and water required for food production. From that reasons, a new processing method was developed for cellulose diacetate (CDA) based biocomposites by melt processing. The new strategy developed in this work makes use of two different plasticizers: a primary "external-type" or "non-reactive-type" plasticizer, Triacetin (TA), added prior to extrusion to enhance the "processing window" of the polymer and a secondary "internal-type" or "reactive-type", Glycerin Polyglycidyl Ether (GPE), added during the extrusion step to reduce the amount of potential volatiles or leachable products in the final product and to help in the reduction of viscosity and thus further improving processability. The thermo-mechanical properties and the morphology of biocomposites with Lyocell microfibers, other wood based fillers, which are typically considered as a reference to produce "green" biocomposites from natural resources, have been analyzed.

Chapter 3. Compatibilization of Poly(lactic acid)/ Polycarbonate blends through reactive blending and in-situ copolymer formation.

To diversify the biopolymers from different resources and combine them with recyclable polymers from oil, we developed new biodegradable copolymers based on Polylactic acid and aromatic polycarbonates through a process of reactive blending in the molten state by the presence of a multi-catalyst. Maintaining the mechanical properties of materials at high temperatures are preferably suitable for the production of materials for different industrial sectors such as transportation, electronics and the electrical equipment industry. Polylactic acid is currently the most used biopolymer, but the materials produced with it are brittle and have low thermo resistance. To extend the functional ability of PLA to different applications such as electric components, food trays, car components, etc. The melting blends of Polylactic acid (PLA) and Polycarbonate bisphenol A (PC) prepared in different temperatures are investigated for the mechanical properties, thermo resistance and morphology. The blends show phase separation; the adhesion between two phases of polymers are poor due to high surface tension of each

components. The multi-catalyst (tetrabutylammonium tetraphenylborate-TBATBP and Tricaetin-TA) is added to increase the interaction between the two phases in order to enhance the mechanical properties and thermo resistance of materials. The dynamic mechanical thermal analysis test shows a new peak in tan δ that does not occur in the blends with a catalyst. This new peak appears at a temperature T_{gp} lower than the T_g of PC and higher than the T_g of PLA. This aspect is related to the presence of PC-blocks in the copolymer. The tensile, thermogravimetric Analysis (TGA), differential scanning calorimetry (DSC), scanning electron microscopy (SEM), transmission electron microscope (TEM) and aerobic biodegradability tests confirmed that the copolymer was formulated under the action of catalysts. However, the Size Exclusion Chromatography (SEC), Nuclear magnetic resonance (NMR) and Fourier Transform Infrared Spectroscopy (FITR) do not show direct evidence of a change in the materials' structure due to similar polar function groups of PLA and PC. The new copolymer has been investigated regarding its mechanical properties, morphology, thermal properties and biodegradation behavior to satisfy the understanding of all the properties of these potential materials, which will serve for broadening the application of bio- and biobase-polymers on the market. Moreover, it will be used as a matrix for biocomposites with required high mechanical properties and thermo resistance.

Chapter 4. Biocomposites based on Poly(lactic acid)-graft-Polycarbonate bisphenol A copolymers and regenerated cellulose microfibers.

After the development of a copolymer matrix with high mechanical properties and thermal resistance, in this chapter we move back to our main focus to develop bio-base composite materials. The blended Polylactic acid (PLA)/ polycarbonate bisphenol A (PC) copolymer and Lyocell fibers with different fiber contents and investigated the composites in terms of their mechanical properties, thermo resistance and relaxation structure, which are shown in Chapter Four. On the physical mixing, the adhesion between two phases of polymers and the interaction between the fibers and matrix are poor. Therefore, not only do the Lyocell fibers reduce the thermo resistance of composites, but they also decrease the elongation at break of materials. However, the presence of multi-catalysts not only formulates a new copolymer, but also increases the interaction between the fibers and polymer matrix,

therefore counterbalancing the negative properties of the PLA/PC/Ly composites. The in-situ-transesterification reaction of the polymer during melt-blending which enables to obtain the reaction between the ester group of the polylacti acid and the hydroxyl function of cellulose fibers. Exploiting catalysts for formulating copolymers to increase the interaction between fibers and the matrix can open new methods for producing biocomposites.

Chapter 5. Analysis on the influence of interface interactions on the mechanical properties of nanofiller- and short fiber- reinforced polymer composites

Chapter Five developed a new method to estimate the interface shear strength of the fiber and polymer matrix. The Pukánszky's model for tensile strength, originally developed for filled composites, has been recently used with success for short fiber-reinforced composites and various nanocomposites, although no theoretical justification has been provided so far for this new use. Despite its simplicity and widespread use to characterize nanoparticle- and short fiber-reinforced composites, the adimensional Pukánszky interaction parameter *B*-factor is not related to physical-mechanical parameters such as the interfacial shear strength, τ, and other experimental variables such as the filler aspect ratio (a_r) and orientation factor.

In this thesis Pukanszky's equation has been analyzed in terms of the Kelly-Tyson model for the prediction of composite strength. In this way it was possible to establish a direct link between Pukanszky's interaction parameter *B* and fundamental material parameters such as tensile strengths of the matrix and of the fibers, the aspect ratio of the fibers, and the orientation factor and the interfacial shear strength IFSS. It was also possible to determine the minimum value of *B* for which it is possible to predict the tensile strength of the composite from the modified rule of mixtures, as well the maximum value that B can achieve in the case of continuous aligned fibers with the same type of matrix, fibers and interface shear strength. Moreover, a critical volume fraction, φ_{crit}, was defined corresponding to the minimum amount of filler content necessary for the composite strength to be greater than the strength of the unreinforced matrix, i.e. corresponding to the case $\sigma_c=\sigma_m$. It was also shown that for this condition $B_{crit}\cong 3$.

From this analysis it was possible to express the interfacial shear strength in terms of *B* and other material parameters, Eq. (13). From such equation, it is possible to verify the monotonical relation between B and IFSS that has been suggested previously in the literature.

A few examples of calculations of the IFSS, τ , from Pukánszky's interaction factor B have been provided, using published literature values relating to nanocomposites with organically modified nanoclays and carbon nanotubes, as well as composites reinforced with short natural fibers. All results obtained fall within the value expected from similar literature values and below the maximum predicted according to the von Mises criterion, $\tau = \sigma_m/\sqrt{3}$.

The new equations presented in this work provide a theoretical basis for the use of Pukánszky's model in the case of nanocomposites and discontinuous fiber composites. Compared to the traditional Kelly-Tyson approach, the interaction factor B enables to give a rapid estimate of the interface shear strength even when fundamental material constants such as fiber tensile strength, aspect ratio and orientation factor as well as the stress in the matrix when the composites breaks, cannot be simply evaluated. This new approach can therefore be appreciated in research and in the development of new composites in industrial environments.

Chapter 6. General conclusions

In the final chapter the results of the thesis will be compared with original aims of this research and the new materials developed will be evaluated. The advantages and disadvantages of each biopolymer and biocomposite produced will be summarized, based on their mechanical properties, thermal resistance, and morphology. From this viewpoint, some of the materials will be developed on an industrial scale for the production of "green composites" with a pilot extrusion machine. The results of this thesis could not only be applied to Italian plastic companies but to the whole European bioplastic industry,and in general to all enterprises active in the most advanced countries of the world .

Chapter 1: General Introduction

I. PLASTICS AND SUSTAINABILITY: CURRENT ISSUES AND OPEN PROBLEMS

Today, plastic materials are widely used due to their diversity in terms of type, properties, and their applications in our daily lives. In fact, plastic materials are the first choice for the production of almost all components because they are durable, light, safe, chemical and water resistant, easy to process and are cost effective. Regarding industry, plastic materials can be applied in packaging (37%), construction (20.6%), automobile manufacturing (7.5%), electronic devices (5.6%), as well as in other applications (27.3%). This wide range of application has lead to a sudden increase in their development in recent years, not only in technology advancement, but also in the sheer quantity of production. According to the European plastic market organization report, the amount of plastics production has increased more than five hundred percent from 1976 to 2010 [1].

Despite these positive aspects, more than 90% of plastic or polymer materials available in the market are produced from oil. As the use of plastics increases, the number of oil fields necessary to meet this demand is insufficient. Moreover, the polymer is durable and has a high molecule weight, leading to a long lifetime on land and sea for hundreds of years. In addition, the production and degradation process of plastic can produce large quantities of carbon dioxide and toxic gas, adding to the greenhouse effect and therefore contributing to worldwide climate change [2-3].

To summarize the positive and negative effects that plastics have on the environment, the European Union has released some framework conditions for plastics expressed in Europe [1,4].

Policy Framework	**Legal framework**
* **General Polices** - *Sustainable Resource Strategy:* + Promotion of energy efficient production + Resource use: promote recovery + and recycling (landfill no future option), drive use of Recycling and Resource Management (RRM - "low carbon economy") - *EU Integrated Product Policy:* + Conception of products with the highest possible degree of sustainability – from the cradle to the grave - *Sustainable Industrial product policy (SIP)* *** Specific Initiatives on European Level** - *Green paper on market-based instruments for environmental technologies* + Discusses / proposes measures like labeling, eco-taxes, CO_2 -trading, VAT, standardization, PR campaigns - *Sustainable Industrial Policy on bio-based products* +Lead Markets Initiative for bio-based products +EU Policy Leaders Browne and Sarkozy proposal of VAT Reduction (5% in EU)	*** European Packaging** * **Packaging Waste Directive** - Allow composting of packaging * **Germany** - Germany Packaging Ordinance: Regulation of compostable plastic packaging - Certificate biopackaging will be exempted from recycling obligation until 2012. Value is € 0.5-0.8 for bioplastic. - Exemption planned of deposit for beverage bottles with > 75% RRM until 2012. Supported by Coca Cola. * **France:** Law on Agriculture includes mandatory use of disposable retail carry bags, cotton buds and waste bags by 2012 (challenged by European Commission - therefore pending) * **Italy:** Intended mandatory bio-degradable bags from 2009 pending (Challenged by EC) ***UK/ Austria/ Cities:** Looking for specific recycling solutions and look for biodegradable packaging. * **Netherlands:** Subsidies from Ministry of Environment for bringing down cost of compostable packaging; taxation of fossil-based polymers * **Belgium:** Compostable bags exempted from packaging tax pending. Value of € 0.3/kg

In the analysis of the policy and legal framework for plastic production and its applications, two main tendencies emerge that regard both the plastics industry and the plastics market.

- *Recycling plastic materials*

- *Using renewable resources or sustainable materials to produce bioplastics, which are biodegradable, bio-based, compostable, and fast arriving in new applications*

II. PLASTIC RECYCLING

Manufacturing plastics requires large quantities of energy, labor, natural resources, water and harmful chemicals, which can strongly effect the environment and human health. They are also are durable and persist for long periods of time, therefore greatly affecting the environment. The Association of Plastic Manufactures in Europe has concluded that 1.8 tons of oil are saved for every ton of recycled polyethylene produced [5]. Recycling plastic also reduces energy consumption, reduces the amount of solid waste going to the landfill and helps reduce the greenhouse effect, along with saving precious natural resources.

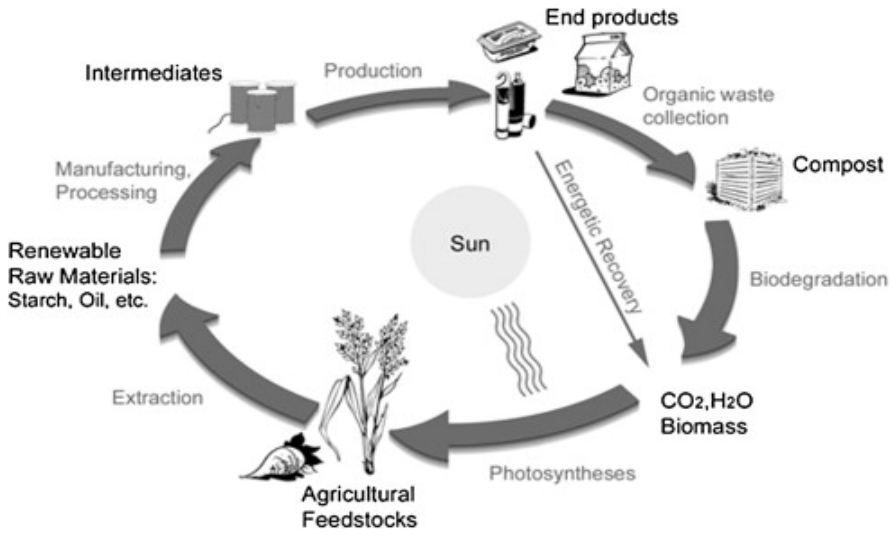

Figure 1. Life cycle of plastic materials [6]

Despite the positive effects of recycling plastics, many applications do not utilize pristine polymers such as trays, pots, toys, electric components, and house construction components, impacting the development of the plastic recycling industry and market. Several polymers can be recycled such as low density polyethylene (LDPE), high-density polyethylene (HDPE) , polypropylene (PP), PVC (Polyvinyl chloride), , polystyrene (PS) and polyethylene terephthalate (PET) , from bottles, trays, film, tubes, shopping bags, as well as polycarbonate of bisphenol A (PC), and acrylonitrile butadiene styrene copolymer (ABS) from electric components, cups, and toys [6-7].

III. CONCEPT OF SUSTAINABLE BIO-BASED MATERIALS

3.1 Renewable resources.

Until now, this concept has not been defined officially in scientific terms. The definition of "renewable resources" according to Wikipedia is a "*natural resource (such as wood or solar energy) that can be replenished naturally with the passage of time, either through biological reproduction or other naturally recurring processes*" [8].

In terms of plastic materials, only those polymers that are produced from renewable resources, natural renewable energy, agriculture resources such as cellulose, corn, starch, natural sugar, or those resources that can be re-produced from nature can be called a biopolymer or a bioplastic. Conversely, almost all plastics are produced from petroleum. Following the definition of the European Bioplastic Organization, bioplastics can be bio-based, biodegradable or both [9].

3.2 Bio-based materials

The American Society for Testing and Materials (ASTM) defined a bio-based material as "*an organic material in which carbon is derived from a renewable resource. A commodity or resource that is inexhaustible or replaceable by new growth) via biological process (ASTM D6866) [10]*". The product must be produced 100% from natural resources, but is not necessarily biodegradable or compostable.

As of now, bioplastics do not have many advantageous properties, as compared to the polymers from oil, because it is a new field in research and development. However, they present several benefits that are environmentally friendly, for example:

+ They need less time to break down after being discarded, so that means there will no longer be tons of plastic dominating our landfills;

+They are produced from renewable resources, so the bioplastics will be easy to renew or recycle because they were produced from biomass, or also animal fats, meats or other tissues;

+ They are good for the environment because there is no harm done to the earth when recovering fossil fuels. Also, in this process there are very few greenhouse gasses and harmful carbon emissions, thereby decreasing the greenhouse effect. Moreover, bioplastic production needs less energy and few harmful chemicals [11-16].

3.3 Biodegradable plastics

Similar to bio-based plastics, a biodegradable plastic was defined by the American Society for Testing and Materials as *"a degradable plastic in which the degradation results from the action of naturally occurring microorganisms such as bacteria, fungi, and algae. Biodegradable plastics must biodegrade in specific environments such as soil, compost, or marine environments (ASTM D6866)"* [10]. Biodegradable plastics can be made from oil or natural resources; it is not important where the materials come from, they need only to meet the requirements defined above.

3.4 Compostable plastics

" A plastic that degrades by biological processes during composting to yield CO_2, water, inorganic compounds and biomass at a rate consistent with other known compostable materials and leaves no visible, distinguishable or toxic residues. Toxic residues important for compost quality include heavy metal content and serotoxins (ASTM D6400) [17]"

3.5 Main types of Bioplastics and Applications [18-21]

Biodegradable/ compostable	**Name**	**Application**
Synthetic Polyesters (BASF, Mitsubishi, etc.)	polybutyleneadipate/ terephthalate (PBAT), polysuccinate (PSN), polybutylene succinate adipate (PBSA),	Films, toughening agents for brittle biopolymers, bottles, etc.
Biodegradable/ compostable and Bio-based	**Name**	**Application**
NatureWorks, Purac/ Synbra, Futerro, Sidaplax, etc	Polylactic acid (PLLA, PDLA)	Rigid containers, film, barrier coating, cosmetic covers, etc.
Novamont, Sphere-Biotec, Plastic, etc	Starch based materials	Loose fill, bags, films, trays, wrap films, etc
Innovia, Acetati, etc	Cellulose based materials, Cellulose diacetate (CDA), etc	Glass components, helmets, car components, food trays, etc
BASF, FKUR, etc	PLA compounds/blends	Films, tomato clips, tree-pots, etc.
Metabolix,, KaneKa, Biomer, etc,	Polyhydroxyalkanoate (PHA), polyhydroxybutyrate (PHB), polyhydroxyhexanoate (PHH)	Films, barrier coatings, medicines, trays, etc.
Bio-based	**Name**	**Application**
Dupont	Bio-PDO based polymers, 1,3 propanediol (PDO), DuPont Sorona, DuPont Cerenol	Textile Fibers, Automotive Refinishing, etc.
Braskem, DOW	PE, PP from Bioethanol	Cups, food trays, films, medicines, food packaging, beverage bottles, etc.
Solvin	PVC from Bioethanol	Pipes, etc.
Arkema, BASF, etc.	Polyamides PA 6.6.9/6.10	Car components, bumpers, electric components, etc.

Table1. Several types of bioplastics and their applications.

3.6 Sustainable materials

Similar to the concept of renewable resources, a consensus definition for sustainable materials does not yet exist. According to Mohanty *et al.* [22], a sustainable, bio-based product is defined as *"a bio-based product derived from renewable resources having recycling capability and triggered biodegrability with commercial viability and environmental acceptability"*.

Furthermore, in terms of polymers, the Institute for Local Self-Reliance and European Plastic Organization [5-23] established that *"a sustainable polymer is a plastic material that addresses the needs of consumers without damaging environment, health, and economy. Feedstock for the production of sustainable plastics must be renewable, such as plants, with preference to the use of by products or over production. Synthesis, production and processing of sustainable polymers should use less net water and non-renewable energy, emit less greenhouse gases and have a smaller carbon-footprint than their non-sustainable counterparts, while still being economically viable."*

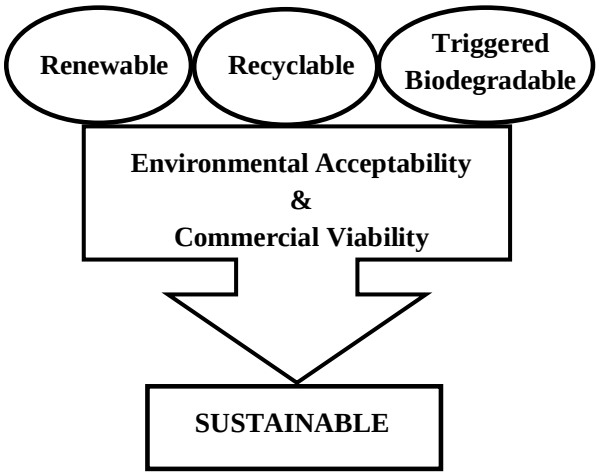

Figure 2. Concept of "sustainable" bio-based product by Mohanty *et al.* [22].

According to the definitions above, biopolymers or polymers produced from renewable resources can be considered sustainable materials. Biocomposites or composites made completely or partially from bio-resources (only the matrix or fiber) are also regarded as sustainable materials. In the expression of this concept, we can ascertain that sustainable materials could be biodegradable, whether they are recycled or

not; but they must be produced from renewable materials. Regarding to development of friendly environmental materials, biocomposites are considered the most important candidates for the development of sustainable materials because they have high mechanical properties, are thermo resistant, and are cost effective, especially those based on biopolymer matrices and renewable fibers and fillers.

Considering those problems regarding the environment and the tendency of material development, sustainable materials have emerged as the materials of the future. For this reason, in 2009 the Sustainable Biomaterials Collaborative Network elaborated new principles for the development of sustainable biomaterials such as: the elimination of single-use products that can neither be recycled nor composted; avoiding fossil fuel-based materials; developing materials and products derived from renewable feedstock; growing feedstock as a resource for manufacturing biomaterials; and investigating the effect of sustainable materials on the environment, health, and social and economic justice [24].

IV. BIOCOMPOSITES

Composite materials have been around for many years. Over the past 30 years, the composite technology markets have developed greatly, especially on glass, carbon, aramid fibers, laminate, and thermoset. However, the composites based on long glass fibers or laminates and thermoset are still limited in their application in smaller and cheaper applications such as such as pots, trays, boxes, fishing cases, tubes, other car parts, chairs, etc. because they have a low elongation at break, are flexible and their processing is too expensive. Therefore, a choice was made to base composite materials on a thermoplastic matrix and short fibers and fillers. At the same time, processing methods, such as single/twin screw extrusion and injection, were updated in order to adapt to economic requirements.

Based on the development of composite materials and the appearance of new bio-based materials as well as the problems of plastic materials with the environment, a new brand of composite materials was formulated and called biocomposites to include totally or partially bio-based materials. This means that they can have a matrix, fiber or both, which are produced from renewable resources. Materials can be

completely or partially biodegradable such as polypropylene/wood fibers, polylactic acid/glass fibers, polyamide/cellulose fibers, and polycarbonate/lignin.

4.1 Current applications of biocomposites and recent research tendencies

Nowadays, predictions about "peak oil" and the limits of oil production together with the consideration that the risk of environmental damage when drilling flor oil and gas and the extraction costs are increasing higher as these resources become less accessible, make biocomposites that present a wide range of advantageous properties especially important in engineering applications . Biocomposites are therefore receiving much consideration from many research groups, and industrial companies all over the world, more specifically in the automotive industry due to their low environmental impact and their cost effectiveness. Biocomposites can present the same performance for lower weights and, at the same weight as other composites, present 25-30% higher mechanical properties [22]. Depending on different components of the car, the fiber and matrix are selected to adapt with the using requirement of each components. Since petroleum plastics are still cheaper and easier to process than biopolymers, car components are being produced from polypropylene and biofibers such as flax, hemp, and kenaf. The goal is to decrease the lifetime of the material or it will be consumed naturally by bacteria, so the environmental impact of product will be reduced.

Biocomposites are not only promising materials for the automotive industry, but also for agriculture, the packaging field, construction and house components [25]. In agriculture, pots or tomato clips together with other articles are produced from biocomposites. Most of them are produced from polylactic acid, PHB or starch and wood fibers [22, 26, 27]. Their lifetime is short and can become fertilizer once used. This tendency will increase the life cycle of materials in nature as well as decrease the environmental impact. Moreover, biocomposites are the best candidates for choosing materials in packaging applications due to different requirements of the mechanical properties, size, and diversification in uses such as food packaging, containers for cosmetics, chemicals, fish transport, and biological eggs. All of them have a short lifetime and are 100% biodegradable.

From the potential applications above, the development of biocomposites are following four tendencies [22, 27-30]:

• Develop new processing techniques to obtain new types or treatment biofibers using physical or chemical methods to obtain inexpensive yet high mechanical properties, cellulose content, uniformity, and high surface energy;

• Modification of the polymer matrix through functionalization, blending to increase the mechanical properties, thermo, oxygen, and chemical resistance, etc;

• Using a coupling agent or catalyst to modify the polymer matrix and/or increase the interaction of polymer and biofibers;

• Develop or select the best conditions for processing materials.

Due to the many different types of polymers and biopolymers, researchers have focused their attention on modifying the polymer matrix and the interaction with fibers, since it is rather easy to combine or enhance positive properties through the combination of different polymers. However, natural fibers such as kenap, helm, flax, tencel, coir, and coconut are not abundant [28,29]. The main goal of industry and research is to develop a processing technology in order to obtain a fiber that presents high physical properties, surface tension, cellulose content, and geometry. Moreover, fiber manufacturers are pushing to decrease the cost of processing together with diversifying the types of fibers in order to adapt the prices to the composite materials. The applications dictate the technical processes used for the composites. For example, traditional processing methods such as RTM, sheet molding, and resin transfer molding are used for long biofibers and thermoset. For short fibers and thermo plastics, extrusion and injection are fashionable, but it is not easy to find the best processing conditions for each material. Indeed modeling and research regarding processing is still an open field [27]. Typically the choice of processing method is adjusted according to the fundamental theory on rheology of the polymer and the experience of operator. In this thesis, we selected extrusion and injection for our processing method because it is easy to develop for industry and inexpensive to produce.

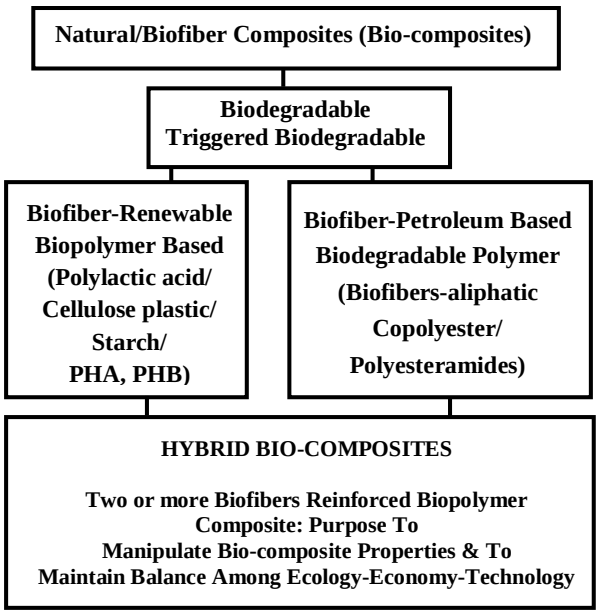

Figure 3. Classification of biocomposites according to Mohanty *et al.* [22].

4.2 Natural fibers/biofibers

Biofibers have become increasingly popular in recent years because it has high mechanical properties when compared to glass or carbon fibers, is inexpensive, has a low density, is renewable and environmentally friendly being completely biodegradable. Along with the development of biocomposites, biofibers will become fashionable materials for the future, and this development will bring about a new revolution in materials technology [22-30].

There are different biofibers on the market made from biomass or renewable resources. Faruk *et al.* [27] has classified them into six categories: "bast fibers (jute, flax, hemp, ramie and kenaf), leaf fibers (abaca, sisal and pineapple), seed fibers (coir, cotton and kapok), core fibers (kenaf, hemp and jute), grass and reed fibers (wheat, corn and rice)," and finally wood flour, and regenerated cellulose fibers. In particular, the bamboo and coir fibers are undergoing development in recent years not only in quantity, but also in quality [31,32]. However, they are still coarse materials and have not made much progress for production as other commercial fibers have.

Lignocellulosic Fiber	Density (g/cm^3)	Tensile Strength (MPa)	Young's Modulus (GPa)
Bagasse (Saccharum officinarum)	0.34 - 0.49	135 - 222	15 - 17
Bamboo (Bambusa vulgaris)	1.03 - 1.21	106 - 204	
Banana (Musa sapientum)	0.67- 1.50	700 - 800	27 - 32
Buriti (Mauritia flexuosa)	0.63 - 1.12	129 - 254	
Coir (Cocos nucifera)	1.15 - 1.52	95 - 220	4 - 6
Cotton (Gossypium M.)	1.51- 1.60	287 - 800	6 - 13
Curaua (Ananas erectifolium)	0.57 - 0.92	117 - 3000	27 - 80
Flax (Linum usitatissimum)	1.30 - 1.50	344 - 1035	26 - 28
Hemp (Cannabis sativa)	1.07	389 - 690	35
Jute (Corchorus capsularis)	1.30 - 1.45	393 - 800	13 - 27
Piassava (Attalea funifera)	1.10 - 1.45	109 - 1750	5 - 6
Pineapple (Ananas comoscus)	1.44 - 1.56	362 - 1627	35 - 83
Ramie (Boehmeria nivea)	1.5	400 - 1620	61 - 128
Sisal (Agave sisalana)	1.26 - 1.50	287 - 913	9 - 28
Soft wood (spruce)	0.46 - 1.50	112 - 1000	11 - 40
Hard wood (birch)	0.67 - 1.50	300 - 1500	30 - 80
E-glass	2.50 - 2.58	2000 - 3450	70 - 73
Carbon	1.78 - 1.81	2500 - 6350	230 - 400
Aramid	1.44	3000 - 4100	63 - 131

Table 2. Density and Mechanical Properties of Selected LCFs [28-35].

The main problem of biofibers is that they are not uniform and that they contain a lot of natural chemical compounds such as lignin, wax, fat, hemicellulose, and water. They can reduce the physical properties of fibers as well as the interaction between fibers and matrix. The weak interface between the fiber and polymer matrix will affect the stress transfer from the matrix to the fibers, so it will reduce the mechanical properties of the final materials. Moreover, the natural compounds are also affected by the processing condition, because the materials will be easily degraded at high processing temperatures by the absorption of moisture such as lignin [36]. To avoid that problem, modifying the natural fiber has received much consideration before processing with composites. Two main processing methods are formulated as physical and chemical methods [27].

The physical methods for treating fibers are stretching, thermal treatment, and adding plasma. The principles of the physical method is to activate the surface energy of the fiber or to increase the wetting of the fiber in order to enhance the interaction with the polymer matrix. The stretching and thermal treatments are inexpensive, but are not efficient when compared to the plasma method. Treating fibers with plasma has been quite popular over the last 10 years, activating the surface oxidation of fiber. Normally, this method is applied to the cellulose fibers and hydrophylic matrix. However, it is neither economic nor easy to degrade the cellulose fibers due to the high-energy requirement for the treatment process. In addition, this method is limited in efficiency due to an increase in the compatibilization between the fiber and matrix such as Hemp/PP, Flax/polyester, and Sisal/HDPE[38-42].

Unlike the principle of physical methods, chemical methods are based on changing the chemical structure of biofibers. It is a more economic, popular and presents diversified applications. Normally, the chemical method focuses on changing the chemical composition of the fiber or modifying the hydroxyl functions on the fiber surface. Not only does it enhance the adhesion of the fibers to the polymer matrix, it also increases the other properties of the composites such as water absorption and thermal resistance. The chemical treatment methods include silane, alkaline, acetylation, and enzyme treatments used as coupling agents. The alkaline treatment is a simple and wide application for biofibers because it removes some substances such as lignin, wax, oil from the surface of the fibers. This method interrupts the hydrogen bonding in the fiber structure, therefore improving the surface roughness. The effect of the alkaline method to mechanical properties and wetting ability of lignocellulose fibers were investigated [43-51]. The alkaline treatment is the first step of fiber treatment before processing. The silane coupling agent used the amino group in the compound to react with OH groups on the surface of fibers to not only increase the surface energy, but also to activate some chemical groups that easily react with the polar groups in the polymer matrix [52-55]. This method is used mostly for glass fibers and epoxy matrix composites, but is still useful for cellulose fibers. A bit different than the silane coupling agent, the

acetylation method uses the acetyl group to react with the OH group of fibers to increase the hydrophobic character on the surface of fiber, decreasing the water absorption of the composite [56-65].

Using a coupling agent for the treatment of fibers or increasing the chemical bond between fibers and matrix in biocomposite is an attractive focus not only in research, but also for industrial applications. The selection of the coupling agent must depend on the polar or active functions of the matrix. The coupling agent will form a chemical link between fibers and the matrix by reacting with polar groups in both. For example, MA-*g*-PP and MA-*g*-PE [66-68] are chosen for biocomposites based on polypropylene or polyethylene and biofibers. The MA coupling agents are produced as commercial products such as SEBS-*g*-MA [69] and MAH-*g*-PP[70]. The grafted polymers with MA are designed by the requirement properties of the final materials such as good wetting, thermal and oxidation resistance [71-76]. There are also some coupling agents with epoxy terminated short polymer chains such as epoxy functionalized soybean oil [77-78], where the epoxy functions can react with the OH groups of biofibers.

When using coupling agents for processing, the materials must be completely dried to avoid reactions with water in the biofibers. Although the coupling agent increases the interaction of the fiber and matrix, they may also give rise to crosslinking reactions between polymer chains in the matrix, making the matrix brittle. It is still a challenge for biocomposite technology to select a coupling agent which can increase the mechanical properties of the matrix, the interaction between fibers and the matrix, and the processability of materials. Moreover, as mentioned above, the lignocellulosic fibers are still not uniform, different chemical compounds such as lignin, wax, and fats will be affected by the biodegradation of fiber as well as the physical properties and efficiency of the treatment method. Confronted with these issues, Lenzing AG, Lenzing, Austria has invented a new type of cellulose fiber called Lyocell, also known as Tencel, an artificial microfiber made from regenerated wood pulp cellulose. It is produced by spinning bleached wood pulp dissolved in a nontoxic (“green”) organic solvent, N-Methylmorpholine-N-oxide or MMNO, which can recovered by washing the freshly spun cellulose microfibers in water, later purified, and recycled. Tencel fibers have 100% cellulose, a high surface

energy, are uniform, and have an especially high aspect ratio [79]. For this reason, these promising fibers have been selected to reinforce the biopolymer matrix in this thesis.

4.3 Biopolymer matrices for composites

In order to adapt to the environmental conditions and requirements of the market, bioplastic production has increased suddenly over the past few years, from 249,000 metric tons in 2009 to 1.16 million metric tons in 2011 [9]. Following the analysis of the European plastic organization, the amounts of polylactic acid (PLA), polyhydroxyalkanoate (PHA), cellulose acetate and starch will increase rapidly in the next few years [9,19]. More specifically, bioplastics will be combined with biofibers to produce "green composites" with 100% biodegradable materials. Thanks to these developments, bioplastics are being used for different applications such as food packaging, construction, automobile manufacturing, electronic devices, medical products, and for products that can be found around the house. However, they still have some limited properties such as brittleness, low toughness, and low thermo resistance, which must be improved if they are to replace traditional plastics in the future. More specifically, polylactic acid and cellulose derivatives, which are selected as a polymer matrix in this thesis, are remarkable polymer matrices for biocomposites having reasonable prices and diversified manufacturers. That is why they are not only considered in research, but also in industrial applications.

4.3.1 Cellulose Acetate

Cellulose plastics and their derivatives come from materials that are found in nature. They are produced through the reaction of polysaccharides and acetic anhydride from wood pulp. In the past, the production of cellulose acetate came from paper recycling. The most important thermoplastic cellulose esters are cellulose acetate (CA), cellulose diacetate (CDA), cellulose acetate butyrates (CAB), cellulose acetate propionates (CAP) and nitrocellulose [80]. The biodegradation properties of cellulose acetate depends on the degree of substitution acetate (DS), Cantor and Mechalas found that CA is biodegradable when the DS is less than 2.4 [81]. However, the glass temperature of cellulose plastics is quite near the decomposition temperature. Therefore, they are generally too difficult to be processed through

conventional melt processing methods without the addition of plasticizers. At present, only plasticized formulations of cellulose esters have commercial utility as extruded films or sheets. For this reason, the formulation of cellulose acetate with plasticizers is critical to its performance and has been the subject of considerable research and industrial application.

As it is known, the major plasticizers of cellulose acetate are phthalate compounds, such as diethyl phthalate (DEP) and dioctyl phthalate (DOP). This family of plasticizers has a relatively high rate of migration and volatilization because of a low molecular weight [81]. Moreover, CA was plasticized by the other commercial compound such as Poly(caprolactonetriol) [82], polyethylene glycol, propylene glycol, dibutyl phthalate [83], glycol and TA as multi-plasticizers [84]. Most papers on the use of plasticizers were only focused on improving the processibility of cellulose acetate. The plasticized cellulose derivatives have high mechanical properties and thermal resistance. They are applied to injection processing to produce helmets, glass frames, sport accessories, automotive components, finishing rods, construction and house components.

Cellulose derivatives are also modified by blending them with other non-biopolymers to improve different properties of materials such as elongation at break, thermo resistance, flexibility, and moisture absorption. For example, CAP was blended with polyethersulfone (PES) [85], Nylon 6,6 [86], polyethyleneimine [87], polyestercarbonate [88], and vinyl polymers [89-90]. Almost all blends were applied to production components, which were exposed to the environment. In addition, the presence of cellulose acetate in the materials decreased the environmental impact factor of the materials, especially for non-bioplastics.

Moreover, the combination of CA and the other biopolymers or biodegradable polymer received much consideration from researchers and industry to increase biodegradation ability, biodegradation time, as well as the conditions of biodegradation. This method is commonly used for film production based on cellulose acetate such as poly(3-hydroxybutyrate) (PHB) [91], polylactic acid (PLA) [92], and starch [93]. The blends with biopolymers from natural resources are mostly applied for medicine or films production.

Moreover, CA is also blended with some polymers produced using petroleum-based feedstock biodegradable such as poly(butylene succinate) [94], or not like polymethyl methacrylate (PMMA) [95], etc. With these blends it is possible to produce films for packaging because the materials show elongation at break and are sufficient biodegradability.

Nevertheless, the big problem of these materials is found in the processing method. Almost all studies on blends of cellulose derivatives with other polymers used the solvent mixing method. The structure of such blends was thus porous and not durable. Cellulose acetate is immiscible with most polymers. Therefore, some maleic anhydride (MA) or epoxy terminated coupling agent or some transesterifaction catalyst must be used in order to increase the interaction [96].

As mentioned above, cellulose acetate usually requires plasticizers for industrial processing, especially for extrusion. However, the plasticized cellulose acetate has a limit for application over long periods of time. In fact, the plasticizers can be released and can decrease the mechanical properties of materials such as elongation at break, toughness, etc. Moreover, the problems of immiscibility with other polymers forces the producer to change the process method, since the solvent mixing method can only be applied for lab scale and research, since it will not be economically viable for industrial processing. In addition, the development of cellulose derivative composites is still limited, although the materials are biodegradable and come from natural resources such as lignin [97-98]. Most publications on cellulose derivatives date were published in the period 1994 to 2002; after that they have not received attention from research, but it still remains a possible product for the market. For this reason, in this thesis, we aim to produce composites based on this old biodegradable polymer that can quickly be adapted to real life applications, easy to apply for industrial processing and the production of biocomposites.

4.3.2 Polylactic acid

Polylactic acid (PLA) is made from a natural resource - corn starch. PLA is formulated from the condensation polymerization of D or L lactic acid or ring opening polymerization of the lactide. So, there are PDLA and PLLA polymers on the current market. It is completely biodegradable, compostable, and

the materials can maintain their mechanical properties without rapid hydrolysis even in high humidity conditions. Moreover, the prices of PLA are about 2 to 4 USD/kg, very competitive with the other petroleum plastics in the current market [99]. For these reasons, PLA is the most used biopolymer now. The amount of PLA produced is about 140,000 tons per year and its production will increase by two or three times that over the next few years. There are several companies producing PLA such as Natureworks, Purac, Samsung, etc.

PLA is a semi-crystalline polymer having medium tensile strength and Young's modulus. However, the thermal resistance of these materials is not high, T_g = 60 ^oC, and they have a low fracture toughness and are also brittle materials (the elongation more or less 7%) [99]. To increase the mechanical properties of PLA, especially tensile strength and Young's modulus, many studies focuses on PLA reinforced with different types of biofibers to obtain biocomposites for diversified applications. The composites based on PLA and biofibers are expected not only to increase the mechanical properties, but also to decrease the cost, the energy consumption, the environmental impact as well as to accelerate the development of biofibers. New strategies open the possibility for replacing synthesized fibers in polymer composites with the presence of PLA. In recent years, there have been many publications on biocomposites and their products on the market based on PLA, such as Kenaf/PLA [100], Jute/PLA [101], wood flour/PLA [102], cellulose fibers/PLA [103], Flax/PLA [104], etc. However, the poor wetting ability between hydrophilic microfibers and hydrophobic polymeric matrices would lead their simple mechanical mixtures to composites with poor interfacial adhesion and limited mechanical strength and ductility. Moreover, one of the problems of this composite is its poor interaction between the fibers and matrix since PLA has a high surface tension. In order to enhance the adhesion between the PLA and fiber, several treatment fiber methods have been tried such as silane, acetylation, and alkaline [105-109]. Besides maleic anhydride [110] and (4,40-thiodiphenol) (TDP) [111], also MA-*g*-PP was added as a coupling agent for the composite [112]. Although this modification increases the interaction of matrix and fibers, the composite

remained still too brittle because of the original properties of the matrix. These properties also limit the amount of fibers in the composite during processing and application.

Currently, there are two options for reducing the brittleness of the materials. These are using plasticizers and adding the other polymer with high elongation at break. The principle of both cases decreases the T_g and interaction between polymer chains of PLA. That means the tensile strength and Young's modulus of PLA will be reduced. There are a number of plasticizers such as Polyethylene glycol (PEG) [113] and Triacetin [114]. Similar to cellulose acetate, the plasticizers will affect the mechanical properties of PLA if used over a long period of time. Moreover, the toughening agents for PLA are quite diversified and include poly(vinyl acetate) [115], poly(caprolactone) [116], and poly(butylenesuccinate) (PBS) [117], etc. More specifically, Poly(butylenadipate-co-terephthalate) (PBAT, Ecoflex®) produced by the BASF company is the most popular toughening agent for PLA. The elongation at break of polylactic acid increases more than 200% when adding 50 wt% of PBAT [118-120]. Ecoflex can be blended to starch, PHA, and PHB [120] to increase the flexibility of the materials. The plasticizers and toughening agent are used to produce films based on PLA for different applications. Similar to the plasticizers PBAT and PBS have a low T_g, slightly decrease tensile strength but because of the high surface tension of PLA are not soluble in this polymer and phase separate into a dispersion of small and soft rubber particles. In addition, the toughening agents also present a poor interaction with fibers in the composite. Hence, this will limit the application of PLA based composites in fields where materials with high thermal resistance, flexibility and fracture toughness are required such as food trays, electrical components, etc. As the aim of this thesis, we try to develop a new type of biopolymer composites based on PLA to adapt with the conditions mentioned above. In addition, the biocomposites with new formulations will also be investigated in order to improve the interaction between the fiber and matrix so it will enhance the mechanical properties and environmental impact of materials.

V. THE AIMS OF THE THESIS:

Despite their potential, considering the long-term environmental issues and the progressive resource depletion, the use of materials derived from renewable resources still often conflicts with problems in the regular provision of raw materials, property variability, high processing costs and low properties of the final products. In order to enhance the development of engineered biocomposite products that meet the diverse needs of users and to maximize the sustainability of natural resources, research needs to implement a biotechnological, materials science and an engineering approach in order to improve biocomposite performance. Biocomposites, or more specifically "green composites", consist of biofibers and bioplastic matrices from renewable resources. Thermoplastics have a lower impact on the environment than thermosets because of their recyclability. Moreover, biopolymers and natural fiber composites are commercially available from a number of companies. The automotive industry is the largest potential user of biocomposites. Due to small production runs, material costs are typically higher than for fossil fuel equivalents. Manufacturing energy costs may be higher too. In Europe, where legislation ensures the polluter pays, large car companies are making significant effort to adopt natural fiber composites in the non-structural parts of their cars because they can be composted. This is a much cheaper form of disposal than landfill or incineration.

This thesis treats the valorization of forest resources for the production of bio-based products with the additional contribution to solve the problems related to materials produced from petro-derived resource, to waste disposal, to the use of energy consumption and polluting chemical pathways and to the use of hazardous substances. Effort will be devoted to the promotion of the use of wood derived fibers to replace glass fibers and mineral fillers, in automotive interior and exterior parts; and as a component in composite materials with biodegradable polymeric matrices for application in the packaging (cardboard, containers, etc.) and agriculture sector (mulching, greenhouse, tomato clips, pots, etc.).

However, the biopolymer matrix still presents limited properties such as being brittle, having low thermal resistance, difficult for processing, etc. In order to succeed in the focus above and diversify the

application of materials, the polymer matrix must be modified in order to increase the mechanical properties, processability (Chapter 2 with cellulose diacetate matrix) and thermal resistance, and morphology and toughness (Chapter 3 with PLA/PC blends matrix). It is also common knowledge that in case of weak adhesion at the fiber-polymeric matrix interphase, the amount of fibers that can be loaded in the composites without problems of dispersion is limited since fiber agglomeration will lead to a material with poor mechanical properties and difficult to process. The modification of plant material (e.g., through physical, chemical, or biological means) has been generally considered necessary prior to its use in the manufacturing of natural fiber-reinforced thermoplastic composites. The amounts and properties of the coupling agent are crucial for the properties of the composites. The appropriate coupling agents need to be adjusted to the chemical composition of the polymer matrix. Each matrix/reinforcement pair requires a different coupling agent such as glycerin polyglycidyl ether (Chapter 1) or transesterification agents (Chapter 4).

It seems very useful to determine the strength of a biopolymer-natural fiber interface to evaluate the optimal level of physical, chemical or biological modification of such interface. In the current theory, the interaction between the fibers and polymer matrix, often described in term of 'adhesion', is generally related to the interfacial shear strength (τ or IFSS) and is almost only applied for continuous fiber composites. Several experimental methods have been developed for their determination. These can be divided into two general categories: single (direct testing) and multiple fiber tests (indirect testing). The experimental methods for single fibers are mainly the pull-out and the fragmentation tests that provide measures of IFSS [121-122]. Several methods have been recently developed for deriving values for τ(the IFSS) from the tensile stress-strain curve of the composite and the fiber length distribution based on the modifications of the Kelly-Tyson equation [123-124]. There are also some methods provided by Bader and Bowyer [125-127], Thomason and Fu and Lauke to estimate the IFSS of fibers and matrix. However, they can only be applied to continuous or long fibers. The interface shear strength between short fibers and fillers has not received much consideration and development from the theory of mechanical

properties. For that reason, in the last chapter (Chapter 5) of this thesis, a new model will be developed for predicting the IFSS of nanofillers, short natural fibers and the polymer matrix based on the developments of the Pukánszky and Kelly-Tyson theories.

VI. REFERENCES

1. Plastics Europe Market Research Group (PEMRG). www.plasticseurope.org (accessed on March 25, 2013).

2. VISY Recycling, www.visyrecycling.com.au (accessed on March 25, 2013).

3. http://ec.europa.eu/environment/integration/research/newsalert/pdf/IR1.pdf (accessed on March 25, 2013).

4. Science for Environment Policy, Plastic Waste: Ecological and Human Health Impacts, 2011, http://ec.europa.eu/environment/integration/research/newsalert/index_en.htm (accessed on March 25, 2013).

5. European Bioplastic website information, http://www.european-bioplastics.org (accessed on March 25, 2013).

6. APME (Association of Plastics Manufacturers in Europe). http://www.wasteonline.org.uk/resources/InformationSheets/Plastics.htm (accessed on March 25, 2013).

7. Plastics Recycling - New Zealand Institute of Chemistry, http://nzic.org.nz/ChemProcesses/environment/14E.pdf (accessed on March 25, 2013).

8. From Wikipedia, http://en.wikipedia.org/wiki/Renewable_resource (accessed on March 25, 2013).

9. European Bioplastic Organization. http://www.european-bioplastics.org (accessed on March 25, 2013).

10. ASTM D6866. http://www.astm.org/Standards/D6866.htm (accessed on March 25, 2013).

11. Advancing the chemical Science. http://www.rsc.org/Education/Teachers/Resources/Inspirational/resources/6.1.2.pdf (accessed on March 25, 2013).

12. News from BioStockPro website. http://www.biostockspro.com/7-advantages-of-biodegradable-plastics/ (accessed on March 25, 2013).

13. Harding KG, Dennis JS, Blottnitz H, Harrison STL. Environmental analysis of plastic production processes: Comparing petroleum-based polypropylene and polyethylene with biologically-based poly-β-hydroxybutyric acid using life cycle analysis. Journal of Biotechnology 2007;130:57-66.

14. Misra M, Nagarajan M, Reddy J, Mohanty AK. Bioplastics and green composites from renewable resources: where we are and future directions. 18th International Conference on Composite Materials, 21-26 August 2010, Jeju, South Korea.

15. Vink ETH, Rabago KG, Glassne DA, Gruber PA. Applications of life cycle assessment to NatureWorks polylactide (PLA) production. Polymer Degradation and Stability 2003;80:403-419.

16. Williams J, Renewable Polymers, Renewable Materials Factsheet.www.nnfcc.co.uk (accessed on March 25, 2013).

17. ASTM 6400. http://www.astm.org/Standards/D6400.htm (accessed on March 25, 2013).

18. Williams J, Renewable Polymers, Renewable Materials Factsheet, www.nnfcc.co.uk (accessed on March 25, 2013)..

19. Biomass Magazine, http://biomassmagazine.com/articles/8183/european-bioplastics-releases-2016-market-forecast (accessed on March 25, 2013).

20. European Bioplastic Association. http://en.european-bioplastics.org/market/global-prod-capacity_total/ (accessed on April 4, 2013).

21. Karlsson S, Albertsson AC. Biodegradable polymers and environmental interaction. Polymer Engineering and Science 1998;38:1251–1253.

22. Mohanty AK, Misra M Drzal LT. Sustainable Bio-composites from renewable resources: opportunities and challenges in the green materials world. Journal of Polymers and the Environment 2002;10:19-26.

23. Institute for Local Self-Reliance. http://www.sustainableplastics.org/ (accessed on March 25, 2013).

24. Sustainable Biomaterials Collaborative. http://www.sustainablebiomaterials.org (accessed on March 25, 2013).

25. Forbioplast FP7 Project. http://www.forbioplast.eu (accessed on March 25, 2013).

26. Ramesh BNG, Anitha N Rani RHK. Recent trends in biodegradable products from biopolymers. Advanced Biotech 2010;9:30-34.

27. Faruk O, Bledzki AK, Fink H-P, Sain M. Biocomposites reinforced with natural fibers: 2000–2010.Progress in Polymer Science 2012;37:1552–1596.

28. Monteiro SN , Lopes FPD, Barbosa AP, Bevitori AB, Da Silva ILA, Da Costa LL. Natural lignocellulosic fibers as engineering materials.An Overview. Metallurgical and Materials Transactions A 2011;42:2963-2974.

29. Bledzki AK, Gassan J. Composites reinforced with cellulose based fibres. Progress in Polymer Science 1999;24:221–274.

30. Alvarez-Chavez CR, Edwards S, Moure-Eraso R, Geiser K. Sustainability of bio-based plastics: general comparative analysis and recommendations for improvement. Journal of Cleaner Production 2012;23:47-56.

31. Okubo K, Fujii T, Yamamoto Y. Development of bamboo-based polymer composites and their mechanical properties. Composites Part A 2004;35:377–383.

32. Tran LQN, Fuentes CA, Dupont-Gillain C, Vuur AW, Verpoest I. Wetting analysis and surface characterisation of coir fibres used as reinforcement for composites. Colloids and Surfaces A 2011;377:251–260.

33. Satyanarayana KG, Guimara JL, Wypych F. Studies on lignocellulosic fibers of Brazil. Part I: Source, production, morphology, properties and applications. Composites Part A 2007;38:1694–1709.

34. Kalia S, Kaith BS, Kaur I. Pretreatments of natural fibers and their application as reinforcing material in polymer composites. A review. Polymer Engineering Science 2009;49:1253–1272.

35. Klason C, Kubat J, Stromvall HE. The efficiency of cellulosic fillers in common thermoplastics. Part 1. Filling without processing aids or coupling agents. International Journal of Polymeric Materials and Polymeric Biomaterials 1984;10:159–187.

36. Mohanty AK, Misra M, Hinrichsen G. Biofibres, biodegradable polymers and biocomposites: an overview. Macromololecular Materials Engineering 2004;276:1–24.

37. Eichhorn SJ, Baillie CA, Zafeiropoulos N. Current international research into cellulosic fibres and composites. Journal of Materials Science 2001;36:2107–2113.

38. Gassan J, Gutowski VS. Effects of corona discharge and UV treatment on the properties of jute-fibre epoxy composites. Composites Science and Technology 2000;60:2857–2863.

39. Ragoubi M, Bienaimé D, Molina S, George B, Merlin A. Impact of corona treated hemp fibres onto mechanical properties of polypropylene composites made thereof. Industrial Crops and Products 2010;31:344–9.

40. Pizzi A, Kueny R, Lecoanet F, Massetau B, Carpentier D, Krebs A, Loiseau F, Molina S, Ragoubi M. High resin content natural matrix–natural fibre biocomposites. Industrial Crops and Products 2009;30:235–240.

41.Marais S, Gouanvé F, Bonnesoeur A, Grenet J, Poncin-Epaillard F, Morvan C, Metayer M. Unsaturated polyester composites reinforced with flax fibers: effect of cold plasma and autoclave treatments on mechanical and permeation properties. Composites Part A 2005;36:975–86.

42. Martin AR, Manolache S, Mattoso LHC, Rowell RM, Dense F. Plasma modification of sisal and high-density polyethylene composites: effect on mechanical properties. In: Natural Polymers and Composites Proceedings 2000:431–436.

43. Huda MS, Drzal LT, Mohanty AK, Misra M. Effect of chemical modifications of the pineapple leaf fiber surfaces on the interfacial and mechanical properties of laminated biocomposites. Composite Interfaces 2008;15:169–91.

44. Goda K, Sreekala MS, Gomes A, Kaji T, Ohgi J. Improvement of plant based natural fibers for toughening green composites-effect of load application during mercerization of ramie fibers. Composites Part A 2006;37:2213–2220.

45. Ray D, Sarkar BK, Rana AK, Bose NR. The mechanical properties of vinylester resin matrix composites reinforced with alkali-treated jute fibres. Composites Part A 2001;32:119–27.

46. Qin C, Soykeabkaew N, Xiuyuan N, Peijs T. The effect of fibre volume fraction and mercerization on the properties of all-cellulose composites. Carbohydrate Polymers 2008;71:458–467.

47. Brígida AIS, Calado VMA, Gonçalves, LRB, Coelho MAZ. Effect of chemical treatments on properties of green coconut fiber. Carbohydrate Polymers 2010;79:832–838.

48. Iannace S, Ali R, Nicolais L. Effect of processing conditions on dimensions of sisal fibers in thermoplastic biodegradable composites. Journal of Applied Polymer Science 2001;79:1084–1091.

49. Mohanty AK, Khan MA, Misra M, Hinrichsen G. Natural fibre reinforced biodegradable matrix composite: effect of surface modification of jute on the performance of jute–biopol composites. Polymeric Materials: Science and Engineering , Proceedings of the American Chemical Society 2000;82:29–30.

50. Rout J, Tripathy SS, Nayak SK, Misra M, Mohanty AK. Scanning electron microscopy study of chemically modified coir fibers. Journal of Applied Polymer Science 2001;79:1169–1177.

51. Bledzki AK, Fink HP, Specht K. Unidirectional hemp and flax EP and PP-composites: influence of defined fiber treatments. Journal of Applied Polymer Science 2004;93:2150–2156.

52. Pothan LA, Thomas S. Polarity parameters and dynamic mechanical behavior of chemically modified banana fiber reinforced polyester composites. Composites Science and Technology 2003;63:1231–40.

53. Cantero G, Arbelaiz A, Llano-Ponte R, Mondragon I. Effects of fibre treatment on wettability and mechanical behavior of flax/polypropylene composites. Composites Science and Technology 2003;63:1247–1254.

54. Ismail H, Khalil HPSA. The effects of partial replacement of oil palm wood flour by silica and silane coupling agent on properties of natural rubber compounds. Polymer Testing 2000;20:33–41.

55. Khalil HPSA, Ismail H. Effect of acetylation and coupling agent treatments upon biological degradation of plant fibre reinforced polyester composites. Polymer Testing 2000;20:65–75.

56. Bledzki AK, Mamun AA, Lucka-Gabor M, Gutowski VS. The effects of acetylation on properties of flax fibre and its polypropylene composites. eXPRESS Polymer Letters 2008;2:413–22.

57. Seavey KC, Glasser WG. Continuous cellulose fiber-reinforced cellulose ester composites. II. Fiber surface modification and consolidation conditions. Cellulose 2001;8:161-169.

58. Seena J, Koshy P, Thomas S. The role of interfacial interactions on the mechanical properties of banana fibre reinforced phenol formaldehyde composites. Composite Interfaces 2005;12:581–600.

59. Tserki V, Zafeiropoulos NE, Simon F, Panayiotou C. A study of the effect of acetylation and propionylation surface treatments on natural fibres. Composites Part A 2005;36:1110–1118.

60. Hill CAS, Khalil HPSA. Effect of fiber treatments on mechanical properties of coir or oil palm fiber reinforced polyester composites. Journal of Applied Polymer Science 2000;78:1685–1697.

61. Khalil HPSA, Ismail H, Rozman HD, Ahmad MN. Effect of acetylation on interfacial shear strength between plant fibres and various matrices. European Polymer Journal 2001;37:1037–1045.

62. Zafeiropoulos NE, Baillie CA, Hodgkinson JM. Engineering and characterisation of the interface in flax fibre/polypropylene composite materials. Part II. The effect of surface treatments on the interface. Composites Part A 2002;33:1185–90.

63. Zafeiropoulos NE, Williams DR, Baillie CA, Matthews FL. Engineering and characterisation of the interface in flax fibre/polypropylene composite materials. Part I. Development and investigation of surface treatments. Composites Part A 2002;33:1083–1093.

64. Zafeiropoulos NE, Baillie CA. A study of the effect of surface treatments on the tensile strength of flax fibres: Part II. Application of Weibull statistics. Composites Part A 2007;38:629–638.

65. Zafeiropoulos NE, Dijon GG, Baillie CA. A study of the effect of surface treatments on the tensile strength of flax fibres: Part I. Application of Gaussian statistics. Composites Part A 2007;38:621–628.

66. Mohanty S, Nayak SK, Verma SK, Tripathy SS. Effect of MAPP as a coupling agent on the performance of jute–PP composites. Journal of Reinforced Plastics and Composites 2004;23:625–637.

67. Mishra S, Naik JB, Patil YP. The compatibilising effect of maleic anhydride on swelling and mechanical properties of plant fiber-reinforced novolac composites. Composites Science and Technology 2000;60:1729–1735.

68. Yang HS, Kim HJ, Park HJ, Lee BJ, Hwang TS. Effect of compatibilizing agents on rice-husk flour reinforced polypropylene composites. Composite Structures 2007;77:45–55.

69. Liu H, Wu Q, Zhang Q. Preparation and properties of banana fiber-reinforced composites based on high density polyethylene (HDPE)/nylon-6 blends. Bioresource Technology 2009;100:6088–6097.

70. Gassan J, Bledzki AK. Possibilities to improve the properties of natural fiber reinforced plastics by fiber modification–jute polypropylene composites. Applied Composite Materials 2000;7:373–385.

71. Okuboa K, Fujiia T, Thostenson ET. Multi-scale hybrid biocomposite: Processing and mechanical characterization of bamboo fiber reinforced PLA with microfibrillated cellulose. Composites Part A 2009;40:469–475.

72. Joseph PV, Joseph K, Thomas S, Pillai CKS, Prasad VS, Groeninckx G, Sarkissova M. The thermal and crystallisation studies of short sisal fibre reinforced polypropylene composites. Composites Part A 2003;34:253–66.

73. Li X, Zhang J, He J, Reddy DJP, Rajulu AV. Tensile properties of Hildegardia fibers reinforced polypropylene biocomposites. Journal of Composite Materials 2010;44:1681–1688.

74. Aranberri-Askargorta I, Lampke T, Bismarck A. Wetting behavior of flax fibers as reinforcement for polypropylene. Journal of Colloid and Interface Science 2003;263:580–589.

75. Bledzki AK, Gassan J, Mildner I. Transcrystallization of polypropylene on different modified jute fibers. Composite Interfaces 2001;8:443–452.

76. Bismarck A, Aranberri-Askargorta I, Springer J, Lampke T, Wielage B, Stamboulis A, Shenderovich I, Limbach HH. Surface characterization of flax, hemp and cellulose fibers; surface properties and the water up take behavior. Polymer Composites 2002;23:872–94.

77. Tran P, Graiver D, Narayan R. Biocomposites synthesized from chemically modified soy oil and biofibers. Journal of Applied Polymer Science 2006;5:69-75.

78. Miyagawa H, Misra M, Drzal LT, Mohanty AK. Novel biobased nanocomposites from functionalized vegetable oil and organically-modified layered silicate clay. Polymer 2005;46:445-453

79. Lenzing company, http://www.lenzing.com/ (accessed on March 25, 2013).

80. Drzal LT, Mohanty AK, Misra M. Environmentally Benign Powder Impregnation Processing and Role of Novel Water Based Coupling Agents in Natural Fiber-Reinforced Thermoplastic Composites. Polymer Preprint. Polymer Division of Polymer Chemistry. American Chemical Society 2001; 42:31–32

81. Cantor P A, Mechalas, BJ, Biological degradation of cellulose acetate reverse-osmosis membranes. Journal of Polymer Science Part C 1969;28:225–241.

82. Ceccorulli G, Pizzoli M, Scandola M. Effect of a low molecular weight plasticizer on the thermal and viscoelastic properties of miscible blends of bacterial poly(3-hydroxybutyrate) with cellulose acetate butyrate. Macromolecules 1993;26:6722–6726.

83. Rao PR, Diwan PV. Permeability studies of cellulose acetate free films for transdermal use: influence of plasticizers. Pharmaceutical Acta Helvetica 1997;72:47–51.

84. Lee SH, Shiraishi N. Plasticization of cellulose diacetate by reaction with maleic anhydride, glycerol, and citrate esters during melt processing. Journal of Applied Polymer Science 2001;8:243–250.

85. Rahimpour A, Madaeni SS. Polyethersulfone (PES)/cellulose acetate phthalate (CAP) blend ultrafiltration membranes: preparation, morphology, performance and antifouling properties. Journal of Membrane Science 2007;305:299–312.

86. Shashidhara GM, Guruprasad KH, Varadarajulu A. Miscibility studies on blends of cellulose acetate and nylon 6. European Polymer Journal 2002;38:611–614.

87. Chen Z, Deng M, Chen Y, He G, Wu M, Wang J. Preparation and performance of cellulose acetate/polyethyleneimine blend microfiltration membranes and their applications. Journal of Membrane Science 2004;235:73–86.

88. Yoshioka SLM, Shiraishi N, Polymer blend of cellulose acetate butyrate and aliphatic polyestercarbonate. Journal of Applied Polymer Science 2000;77:2908–2914.

89. Jinghua Y, Xue C, Alfonso GC, Turturro A, Pedemonte E. Study of the miscibility and thermodynamics of cellulose diacetate-poly(vinyl pyrrolidone) blends. Polymer 1997;38:2127–2133.

90. Miyashita Y, Suzuki T, Nishio Y. Miscibility of cellulose acetate with vinyl polymers. Cellulose 2002;9:215–223.

91. Zhang LL, Deng XM. Biodegradable polymer blends of poly(3-hydroxybutyrate) and hydroxyethyl cellulose acetate. Polymer 1997;38:6001–6007.

92. Teramoto Y, Nishio Y. Cellulose diacetate-graft-poly(lactic acid)s: synthesis of wide-ranging compositions and their thermal and mechanical properties. Polymer 2003;38:2701–2709.

93. Mayer JM, Elion GR, Buchanan CM, Sullivan BK, Pratt SD, Kaplan DL. Biodegradable blends of cellulose acetate and starch: production and properties. Journal of Macromolecular Science: Part A 1995;32:775-785.

94. Uesaka T, Nakane K, Maeda S, Ogihara T, Ogata N. Structure and physical properties of poly(butylene succinate)/cellulose acetate blends. Polymer 2000;41:8449–8454.

95. Bhat DK, Kumar MS. Biodegradability of PMMA blends with some cellulose derivatives. Journal Polymer Environment 2006;14:385–392.

96. Rao V, Ashokan PV, Shridhar MH. Studies on the compatibility and specific interaction in cellulose acetate hydrogen phthalate (CAP) and poly methyl methacrylate (PMMA) blend. Polymer 1999;40:7167–7171.

97. Wu RL, Wang XL, Li F, Li HZ, Wang YZ. Green composite films prepared from cellulose, starch and lignin in room-temperature ionic liquid. Bioresource Technology 2009;100:2569–2574.

98. Park HM, Misra, M, Drzal LT, Mohanty AK. “Green” nanocomposites from cellulose acetate bioplastic and clay: effect of eco-friendly triethyl citrate plasticizer. Biomacromolecules 2004;5:2281–2288.

99. Information from NatureWorks LLC, http://www.natureworksllc.com/ (accessed on March 25, 2013).

100. Hidayata A, Tachibana S. Characterization of polylactic acid (PLA)/kenaf composite degradation by immobilized mycelia of Pleurotus Ostreatus. International Biodeterioration & Biodegradation 2012;71:50-54.

101. Hu R, Lim JK. Fabrication and mechanical properties of completely biodegradable hemp fiber reinforced polylactic acid composites. Journal of Composite Materials 2007;41:1655-1669.

102. Petinakis E, Yu L, Edward Y, Dean K, Liu H, Scully AD. Effect of matrix–particle interfacial adhesion on the mechanical properties of poly(lactic acid)/wood-flour micro-composites. Journal of Polymers and the Environment 2009;17:83-94.

103. Mathew AP, Oksman K, Sain M. Mechanical properties of biodegradable composites from poly lactic acid (PLA) and microcrystalline cellulose (MCC). Journal of Applied Polymer Science 2005;97:2014–2025.

104. Oksman K, Skrifvars M, Selin JF. Natural fibres as reinforcement in polylactic acid (PLA) composites. Composites Science and Technology 2003;9:1317-1324.

105. Huda MS, Drzal LT, Mohanty AK, Misra M. Effect of fiber surface treatments on the properties of laminated biocomposites from poly(lactic acid) (PLA) and kenaf fibers. Composites Science and Technology 2008;68:424–432.

106. Lee BH, Kim HS, Lee S, Kim HJ, Dorgan JR. Bio-composites of Kenaf fibers in polylactide: role of improved interfacial adhesion in the carding process. Composites Science and Technology 2009;69:2573–2579.

107. Ochi S. Mechanical properties of Kenaf fibers and Kenaf/PLA composites. Mechanics of Materials 2008;40:446–452.

108. Nishino T, Hirao K, Kotera M, Nakamae K, Inagaki H. Kenaf reinforced biodegradable composite. Composites Science and Technology 2003;63:1281–1286.

109. Le Duigou A, Davies P, Baley C. Interfacial bonding of flax fibre/poly(l-lactide) bio-composites. Composites Science and Technology 2010;70:231–239.

110. Oksman K, Mathew AP, Bondeson D, Kvien I, Manufacturing process of cellulose whiskers/polylactic acid nanocomposites, Composite Science and Technology 2006;55:2774-1784.

111. Wong S, Shanks RA, Hodzic A. Effect of additives on the interfacial strength of poly(l-lactic acid) and poly(3-hydroxy butyric acid)-flax fibre composites. Composites Science and Technology 2007;67:2478–84.

112. Meng QK, Hetzer M, Kee DD. PLA/clay/wood nanocomposites: nanoclay effects on mechanical and thermal properties. Journal of Composite Materials 2011;10:1145-1158.

113. Martin O, Avérous L. Poly(lactic acid): plasticization and properties of biodegradable multiphase systems. Polymer 2001;42:6209–6219.

114. Zhongjie R, Dong LS, Yang Y. Dynamic mechanical and thermal properties of plasticized poly(lactic acid). Journal of Applied Polymer Science 2006;101:1583–1590.

115. Gajria AM, Dave V, Gross RA, McCarthy SP. Miscibility and biodegradability of blends of poly(lactic acid) and poly(vinyl acetate). Polymer 1996;37:437–444.

116. Wang L, Ma W, Gross RA, McCarthy SP. Reactive compatibilization of biodegradable blends of poly(lactic acid) and poly(ε-caprolactone). Polymer Degradation and Stability 1998;59:161-168.

117. Bhatia A, Gupta R, Bhattacharya S, Choi H. Compatibility of biodegradable poly (lactic acid) (PLA) and poly (butylene succinate) (PBS) blends for packaging application. Korea-Australia Rheology Journal 2007;19:125-131.

118. Xiao H, Lu W, Yeh JT. Crystallization behavior of fully biodegradable poly (lactic acid)/poly (butylene adipate-co-terephthalate) blends. Journal of Applied Polymer Science 2009;112:3754–3763.

119. Ren J, Fu H, Ren T, Yuan W. Preparation, characterization and properties of binary and ternary blends with thermoplastic starch, poly(lactic acid) and poly(butylene adipate-co-terephthalate). Carbohydrate Polymers 2009;77:576–582.

120. Coltelli MB, Maggiore ID, Bertoldo M, Signori F, Bronco S, Ciardelli F. Poly(lactic acid) properties as a consequence of poly(butylene adipate-co-terephthalate) blending and acetyl tributyl citrate plasticization. Journal of Applied Polymer Science 2008;110:1250–1262.

121. Hull D, Clyne TW. An introduction to composite materials, 2nd ed 1996, Cambridge University Press, Cambridge.

122. Matthews FL, Rawlings RD. Composite materials: engineering and science, 1999, CRC Press, Boca Raton.

123. Kelly A, Tyson WR. Tensile properties of fibre-reinforced metals: Copper/tungsten and copper/molybdenum. Journal of the Mechanics and Physics of Solids 1965;13:329-350.

124. Piggott MR. Short fibre polymer composites: A fracture-based theory of fibre reinforcement. Journal of Composite Materials 1994;28:588-606.

125. Fu SY, Lauke B. Effects of fibre length and fibre orientation distributions on the tensile strength of short-fibre-reinforced polymers. Compos Science and Technology 1996;56:1179-1190.

126. Bowyer WH, Bader MG. On the reinforcement of thermoplastics by perfectly aligned discontinuous fibres. Journal of Materials Science 1972;7:1315-1321.

127. Bader MG, Bowyer WH. An improved method of production for high strength fibre-reinforced thermoplastics. Composites 1973;4:150-156.

Chapter 2

"Green" Biocomposites Based on Cellulose Diacetate and Regenerated Cellulose Microfibers: Effect of Plasticizer Content on Morphology and Mechanical Properties

I. INTRODUCTION

Plastic materials are widely spread in everyday life with diversified applications. Most of the plastics of common use are currently produced from fossil fuels, consumed and discarded into the environment, ending up with very long time for degradation and relevant problems of collection and disposal which often end up in landfills or incineration. The increasing pressure on manufacturers by new environmental and waste management policies, consumers demand and also the escalation of oil prices is steering the trends of polymer technology away from traditional materials. For these reasons, the new field of biodegradable and bio-based polymers, which have some environmental friendly properties (materials in which the production is based on renewable resources, characterized by low energy consumption, low CO2 emissions, with possibility for composting, biomethanation or recycling), has received growing consideration which has been so far focused specifically on starch based products, PLA (Polylactic acid), PHA (Poly hydroxyl alkanoates) in particular PHB (Poly hydroxyl butyrate), cellulose derived plastics [1], etc. The production of these materials is based on annually renewable agricultural and biomass feedstocks. Moreover biopolymers derived from natural sources can capture markets currently dominated by products based exclusively on petroleum feedstock [2-3].

However, biodegradable polyesters like PLA and PHA generally present some disadvantages over oil based plastics such as low fracture toughness, low glass transition temperature (T_g), high moisture absorption, difficult processing as well as limited applications. Cellulose diacetate (CDA), the most important cellulose derived biopolymer, from an industrial point of view, is a thermoplastic material produced through the esterification of cellulose. Cellulose acetate has been reported to be potentially biodegradable [4], so that new applications of CDA may be envisaged not only for packaging and automotive but also for medical and pharmaceutical applications, in the production of biocomposite materials and other bio-related fields. A variety of raw materials such as cotton, recycled paper, wood cellulose, and sugarcane are used in making cellulose esters in powder form [5-6]. CDA possesses high glass transition temperature (T_g), which results in limited processability compared with typical commodity plastics. In addition, it has low solubility in common solvents and cannot be melt processed as raw material because it starts to decompose before melting. Therefore, CDA requires the use of plasticizers to reduce its T_g and processing temperature. The role of plasticizers is to decrease the intermolecular forces among the polymer chains, resulting in a softened and more flexible polymeric matrix. Traditionally plasticization of CDA has been accomplished using citrate, phthalates, glycerol derivatives, phosphates, triacetin, etc. Phthalate esters, historically the most common industrially used plasticizers for CDA, have been subjected to environmental scrutiny as a health threat and thus there is now a serious concern about their long-time use. In order to improve the processing of CDA, some studies explored new plasticizers such as poly(caprolacton triol) [7], polyethylene glycol, propylene glycol and dibutyl phthalate [8]. Others combined maleic anhydride, glycol and TA as multi-plasticizers [9]. Their research improved the processing of CDA based materials but at the expenses of their mechanical properties. On the basis of the examined literature, TA was chosen to improve CDA processing in this study, as an environmentally sustainable (“eco-friendly”) plasticizer because of its low toxicity and fast biodegradability [10-11]. Moreover, the solubility of triacetin in CDA is high and triacetin is a very effective plasticizer of CDA. A thermodynamic study has shown that the enthalpy for

mixing is exothermal over the whole range of compositions and the Gibbs energy of the mixing of the CDA/TA blend has a minimum corresponding to about 40 wt% Triacetin [12]. It was also found a fall in the entropy of the system following the formation of solvates between the functional groups of CDA and triacetin for TA concentrations up to about 40 wt%, followed by an increase in the entropy of the system as a result of disturbance of the interchain interaction in CDA on its solvation for larger concentrations.

In order to improve mechanical properties, cellulose diacetate was blended with Poly (vinyl pyrrolidone), Poly (vinyl acetate), Poly (N-vinyl pyrolidone – co - vinyl acetate) [13-14], Poly(caprolactone monoacrylate) [15]. A number of trials were made to extend the cellulose diacetate chain through reaction with octadecenyl succinic anhydrides [16] and also with other biopolymer such as Polylactic acid and starch [17-18]. Most of the research related with cellulose diacetate used solvents to dissolve the materials and then proceed with processing. This induced a porous structure and reduced the toughness of the materials. A few researchers used a melt processing approach to improve the performance of cellulosic plastics [19]. Moreover, several studies have tried to develop biocomposite based on cellulose diacetate with natural fibers and fillers [20], while others used organically modified clay to produce “green” nanocomposites [21]. The suitability of cellulose fibers for thermoplastics in general and biopolymers in particular were investigated because of ecological advantages, high mechanical properties in terms of Young’s modulus and tensile strength, low density and dimensional stability [20,22]. Glasser et al. reported the preparation of composites based on continuous rayon and lyocell fibers reinforced cellulose acetate butyrate (CAB) and other commercially-available thermoplastic cellulose esters by using solution impregnation. The fibers were also surface modified by acetylation to change the interfacial adhesion between the cellulose fiber and cellulose ester matrix, but no significant increase in strength of the composites was observed, leading the Authors to the conclusion that interfacial stress transfer is not a limitation in this system [23-25], although this result could be easily anticipated by anybody knowledgeable enough in the mechanics of continuous fiber reinforced composites. Until very recently, the properties of composites prepared with cellulose esters reinforced with short lyocell fibers

(Ly) have not been considered [26]. From this study, it was shown that the Young's modulus of lyocell/cellulose acetate butyrate (CAB) composites increased from 2 GPa for neat CAB to 4 GPa for a composite with a lyocell fiber content of 34.8% (v/v). Similar trend was obtained for flax/CAB biocomposites which showed higher modulus than lyocell/CAB composites, with values of 5 GPa for a flax/CAB composite with the same composition. Moreover, tensile strength of lyocell/CAB composites with fiber content higher than 16.7% (v/v) resulted in lower values than neat CAB, indicating a high probability of failure cracks on lyocell/CAB composite samples when increasing fiber composition. In addition, compared to neat CAB, elongation at break decreased for all the composites studied.

In summary, the mechanical properties of biocomposites based on CDA considered in the literature are still not satisfying, in view of their possible application, and use types of processing with are not economically viable on an industrial scale. In particular, the thermal characteristics of the materials developed and their matrix-filler interactions were not much investigated. So far, there are no publications about the effect of multi plasticizers on physical properties, thermal stability and morphology of cellulose diacetate/cellulose fibers composites under melt processing.

Since both the cellulose diacetate and Lyocell fibers can be produced from renewable forest biomass, their manufacture does not imply any competition for land and water required for food production. The interest in the research on biocomposites based on CDA/Lyocell fibers is the development of high-performance, environmentally-friendly, sustainable, potentially biodegradable biomaterials.

II. EXPERIMENTAL DETAILS

2.1 Materials

Cellulose diacetate (CDA, CAS # 9004-35-7) type LS/SS was kindly supplied by the Acetati Company – Italy, with a degree of substitution of 2.4. Triacetin (TA, also known as glycerin triacetate or 1,2,3-triacetoxypropane, CAS # 102-76-1) was purchased from Aldrich Chemicals as primary plasticizer,

while a water soluble epoxy resin, polyglycidyl ether of glycerin (GPE), with an Epoxy Equivalent Weight, EEW = 135 ~ 155 g/eq, type EJ300, purchased by Joong-ang Special Industry Co – South Korea, was used as secondary plasticizer (scheme 1). Tencel® FCP-10/400 microfibers, shown in Figure 1, with a diameter of about 10.5 µm and an average fiber length of 390 µm, corresponding to an aspect ratio, ar = 37, were kindly provided by Lenzing AG, Lenzing, Austria. According to this manufacturer, these fibers have a density: 1.5 g/cm³, a Young's modulus of 10 –15 GPa, a tensile strength of 570 MPa and an elongation at break of 11 %. Microcrystalline cellulose with a diameter of 20 µm and ar = 2-4 was obtained by Aldrich Chemicals [27-28], lignocellulosic fibers type Filtracel EFC 1000, with a diameter of 63.9 µm, a density of 1.5 g/cm3, and ar = 6.8 purchased from Rettenmaier & Söhne Gmbh – Germany, were used as reference reinforcements since they have been very well characterized in the literature [29-30]. All materials were dried overnight under vacuum at 100 °C before processing.

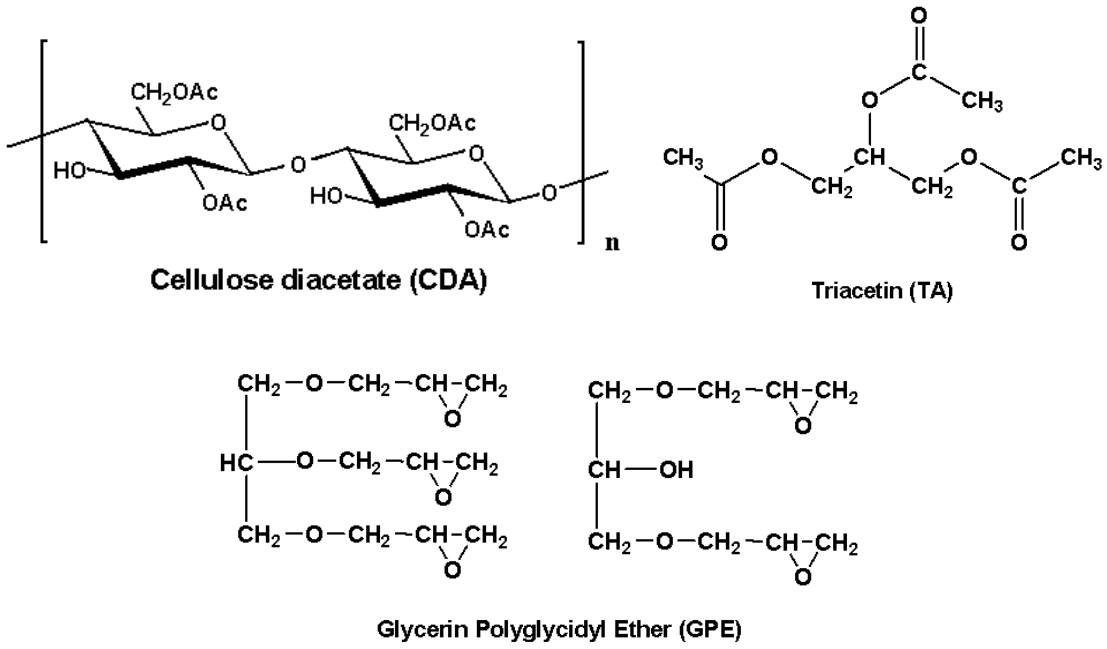

Scheme 1. Chemical structure of CDA, GPE, TA

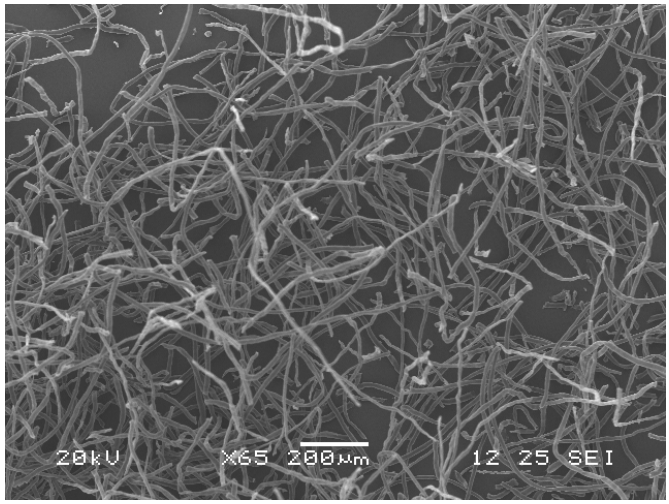

Figure 1. SEM micrographs for Lyocell fiber

2.2 Processing

A cellulose diacetate (CDA) powder was mechanically mixed about 10 minutes with different ratios of primary plasticizer (TA) by means of a high speed mixer. After this mixing stage, the fillers and the secondary plasticizer (GPE) were added and mixed for extra 10 minutes, in the same equipment. The resulting mixtures were processed with a MiniLab II Haake Rheomex CTW 5 conical twin-screw extruder (Thermo Scientific Haake GmbH, Karlsruhe, Germany), at a screw rate of 80 rpm/min and a cycle time of 30 seconds, in the temperature range from 170 °C to 210 °C, depending on the material formulation. The processing temperature was chosen for each system at level below the onset of degradation phenomena, evidenced by the appearance of a dark coloring of the material, accompanied by a very brittle behavior. The content of Triacetin in this study was varied from 20 to 40 wt%. In fact, based on our preliminary testing, it is not possible to process CDA with less than 20 wt% TA, because for lower TA contents the melt processing temperature of the plasticized CDA exceeds its decomposition temperature. Prior experiments in our lab also showed that exceeding 40 wt% TA the main mechanical properties (elastic modulus, tensile strength, and elongation at break) of materials become unacceptably low. As mentioned in the introduction, this can be explained by the fact that the functional groups of CDA are completely

solvated by triacetin when the TA content reaches 40 wt%. Beyond this value, further increases in TA concentration just separate the individual CDA molecules decreasing their interchain interactions.

The role of GPE is to increase the interactions of the fibers with the matrix thus acting as coupling agent. In our preliminary testing, we tried different GPE contents: 5, 10 and 20 wt% GPE, but we observed a decrease in the mechanical properties of the composites for concentrations beyond 5 wt%. This can be explained by the fact that the chemical structure of GPE is similar to TA, so adding more GPE would have negative effects – in term of excessive plasticization – like using higher amounts of TA.

The content of Lyocell fibers was limited to a maximum 10 wt% (corresponding to 12 vol%) for physical limitation of the feeding system of the MiniLab extruder (maximum 7 cm3) with a low apparent volume filler. After extrusion, the molten materials were transferred through a preheated cylinder to the Haake MiniJet II mini injection molder (Thermo Scientific Haake GmbH, Karlsruhe, Germany), to obtain ASTM D638 V dog-bone tensile bars used for measurements and analysis. The specimens were placed in plastic bags for vacuum sealing to prevent moisture absorption.

2.3 Characterization methods

Tensile tests were performed at room temperature, at a crosshead speed of 10 mm/min, by means of an Instron 4302 universal testing machine (Canton MA, USA) equipped with a 10 kN load cell and interfaced with a computer running the Testworks 4.0 software (MTS Systems Corporation, Eden Prairie MN, USA).

Thermogravimetric Analysis (TGA) was run under the flow of nitrogen gas, at a scanning speed of 10 °C/min, from room temperature to 1000 °C, using a TGA 1000 instrument (Rheometric Scientific Inc., USA).

Dynamic mechanical thermal analysis (DMTA) was carried out on a Gabo Eplexor® 100N (Gabo Qualimeter GmbH, Ahlden, Germany). Test bars were cut from the tensile bar specimens (size: 20 x 5 x 1.5 mm) and mounted in tensile geometry. The temperature used in the experiment ranged from -100 °C to 170 °C, at a heating rate of 2 °C/min and frequency of 1 Hz.

The morphology of the composites was studied by scanning electron microscopy (SEM) using a JEOL JSM-5600LV (Tokyo, Japan), by analyzing the fracture surfaces of samples, broken in liquid nitrogen. Prior to SEM analysis all the surfaces were sputtered with gold.

The chemical bonding between Lyocell fibers and polymer matrix through GPE were analyzed by using a Nicolet 380 spectrometer with diffuse reflectance accessory (DRIFT). The composite was dissolved in acetone to remove the polymer matrix (CDA) and then the fibers were drying under vacuum at 100°C in 24 hours. Lyocell fibers were mixed with potassium bromide (KBr) in order to obtain the DRIFT spectra. During the DRIFT measurement, pure potassium bromide was chosen as background.

III. THEORETICAL ANALYSIS

3.1 Constitutive equations

The stress-strain curve of polymers and composites can be approximated to a number of idealized constitutive equations. Brittle polymers often show a linear elastic stress-strain relationship $\sigma = E\varepsilon$ up to fracture, while a few exhibit a perfectly elastic-plastic behavior:

$$\sigma = E\,\varepsilon \qquad \text{for } \sigma \leq \sigma_y$$

$$\sigma = \sigma_y \qquad \text{for } \sigma > \sigma_y \qquad (1)$$

where E is the elastic modulus and σ_y the yield stress.

A number of polymers and composites, instead show an increase in stress upon stretching beyond their yield point (strain hardening). If the stress increases linearly with elongation both before and after yielding, the material follows the perfectly linear elastic – linear strain hardening model (bilinear hardening for short). The stress-strain relation may be represented by:

$$\sigma = E\,\varepsilon \qquad \text{for } \sigma \leq \sigma_y$$

$$\sigma = \sigma_y + E_p(\varepsilon - \varepsilon_y) \qquad \text{for } \sigma > \sigma_y \qquad (2)$$

where ε_y is the yield strain, satisfying the relation $\varepsilon_y = \sigma_y / E$ and E_p the strain hardening modulus (sometimes called tangent modulus), corresponding to the constant work hardening slope. The ratio $b = E_p/E$ is defined as the strain hardening ratio.

The physical ground for the bilinear model can be given by the Neo-Hookean approach for true stress σ_{true} [31]:

$$\sigma_{true} = \sigma_y + G_R(\lambda^2 - \frac{1}{\lambda}) \quad (3)$$

where G_R is the rubbery strain-hardening modulus and λ is the draw ratio. This gives for the engineering stress σ_{eng}:

$$\sigma_{eng} = \frac{\sigma_y}{\lambda} + G_R(\lambda - \frac{1}{\lambda^2}) \quad (4)$$

Considering the relation $\lambda = 1 + \varepsilon$:

$$\sigma_{eng} = \frac{\sigma_y}{(1+\varepsilon)} + G_R\left[(1+\varepsilon) - \frac{1}{(1+\varepsilon)^2}\right] \quad (5)$$

Expanding the second term in square brackets, we get, neglecting terms with superior order:

$$\sigma_{eng} = \sigma_y + 3G_R\varepsilon \quad (6)$$

Comparing the two expressions, it is apparent that $E_p = 3\ G_R$.

From the Neo-Hookean theory, the strain hardening modulus may be expressed as:

$$E_p = 3nkT \quad (7)$$

where *n*, *k*, and *T* represent the network density (number of chains per unit volume in the network), Boltzmann's constant, and the absolute temperature, respectively.

In this way, the strain hardening modulus can be directly put in relation to entanglement network density, at a given temperature.

3.2 Young's modulus

Several theoretical expressions have been developed for the prediction of the elastic modulus of short fiber composites. One of the most successful approaches considers long straight discontinuous fibers, completely embedded in a continuous matrix, making use of the so-called shear-lag concept [32]. This model introduces some simplifying assumptions, such as: (1) uniform alignment of the fibers within the matrix; (2) stress transfer by shear along the length of the fiber-matrix interface; (3) perfect elastic, isotropic behavior of both matrix and fiber; (4) perfect bonding between the two materials at the interface.

However, it is now well established that the prediction of composite modulus calculated by the Cox's model does not provide sufficiently accurate estimations when the fiber aspect ratio is small [33], as in the present work. The predicted modulus obtained by the Cox's model is significantly smaller than the experimentally observed values for short fiber composites. In fact, the Cox's model neglects the stress transfer across the fiber ends, $\sigma_f(\pm L/2) = 0$.

Since the early work of Cox, several improvements have been proposed to the original shear lag analysis and some of these developments have been recently reviewed [34-37]. In particular Kim has proposed the following modified equation for the elastic modulus of short fiber composites, E_C^{Kim}, taking into account both fiber end traction forces and stress concentration effects [30-32]:

$$E_C^{Kim} = E_f \varphi_f \left\{ 1 + \left(\sqrt{\frac{E_m}{E_f}} - 1 \right) \frac{\tanh(\beta a_r)}{\beta a_r} \right\} + E_m (1 - \varphi_f) \qquad (8)$$

where E_f, E_m are the fiber and matrix Young's modulus, respectively, φ_f is the fiber volume fraction and β is given by:

$$\beta = \sqrt{\frac{2E_m}{E_f (1 + \upsilon_m) \log(\frac{P_f}{\varphi_f})}} \qquad (9)$$

where ν_m is the matrix Poisson's modulus and P_f is the fiber packing factor.

Of all the micromechanics equations, Halpin-Tsai's semi-empirical equations are accurate and straightforward. Halpin and Tsai showed that the Hermans solution to Hill's self consistent model can be

reduced to a simpler approximate analytical form and extended its use to a wide variety of reinforcement geometries [38]. For the longitudinal modulus, the Halpin-Tsai's equation gives the following expression:

$$E_{Cl}^{HT} = \frac{1+2a_r\lambda_l\varphi_f}{1-\lambda_l\varphi_f}E_m \tag{10}$$

with

$$\lambda_l = \frac{\left(\frac{E_f}{E_m}\right)-1}{\left(\frac{E_f}{E_m}\right)+2a_r} \tag{11}$$

while the transverse modulus takes the form:

$$E_{Ct}^{HT} = \frac{1+2a_r\lambda_l\varphi_f}{1-\lambda_l\varphi_f}E_m \tag{12}$$

where

$$\lambda_l = \frac{\left(\frac{E_f}{E_m}\right)-1}{\left(\frac{E_f}{E_m}\right)+2} \tag{13}$$

For composites with fibres oriented randomly in a plane, the Halpin-Tsai's equations give:

$$E_C^{HT} = \frac{3}{8}E_{Cl}^{HT} + \frac{5}{8}E_{Ct}^{HT} \tag{14}$$

A more rigorous model for short fibers or particulate reinforced composites inclusions has been proposed by Tandon and Weng [39], on the basis of the solutions found by Eshelby on an ellipsoidal inclusion surrounded by an infinite matrix [40] and the concept of average stress introduced by [41] Mori and Tanaka[1].

3.3 Yield stress

[1] For the complexity of the Tandon-Weng model, the relevant equations are not reported here for brevity and we refer to the original paper for more details [34].

Many models have been proposed in the specific literature to predict yield stress of composites. The Pukánszky's model [42] describes the effects of the volume filler fraction (φ_f) and the interfacial interaction on tensile yield stress of particulate filled polymers:

$$\sigma_c = \sigma_m \frac{1-\varphi_f}{1+2.5\varphi_f} \exp(B\varphi_f) \quad (15)$$

The parameter B is an interaction parameter that considers the capacity of stress transmission between various components. The terms σ_c and σ_m are yield stress of composite and matrix, respectively. The term $\exp(B\varphi_f)$ considers the interaction, while the $(1-\varphi_f)/(1+2.5\varphi_f)$ term indicates the effective decrease of useful cross section due to filler introduction. Interfacial interaction depends on the thickness of the interphase, and the strength of the interaction as shown in the following equation:

$$B = \left(1 + A_f \rho_f \tau\right) \ln \frac{\sigma_i}{\sigma_m} \quad (16)$$

where A_f, ρ_f, τ, σ_i are the specific surface area, the density of the filler, the thickness of the and the strength of interphase, respectively. The parameter B can be easily calculated by knowing the yield stress of composites filled with different volume percentages of particle fillers.

IV. RESULTS AND DISCUSSION

4.1 Mechanical properties of CDA-based blends and composites

Figure 2 shows typical stress-strain curves for cellulose diacetate (CDA) blends with different amounts of plasticizers and their composites with Lyocell cellulose fibers and the mechanical properties of materials are summarized in Table 1. All curves appear to follow an almost ideal elastic-plastic behavior, closely following Equation 1.

In this series of materials, the content of TA was varied from 20% to 40% to prevent the degradation of CDA during melt processing. As expected, the tensile strength of materials decreased with increasing TA amount while the elongation at break increased (Figure 3). Considering the strain

hardening modulus, *Ep*, we observe a strong decrease between 20-30 wt%, followed by a less rapid decrease beyond this value (Figure 4). As discussed above, a decrease of this parameter can be directly explained with a loss of entanglement density caused by the presence of the plasticizer (Equation 7).

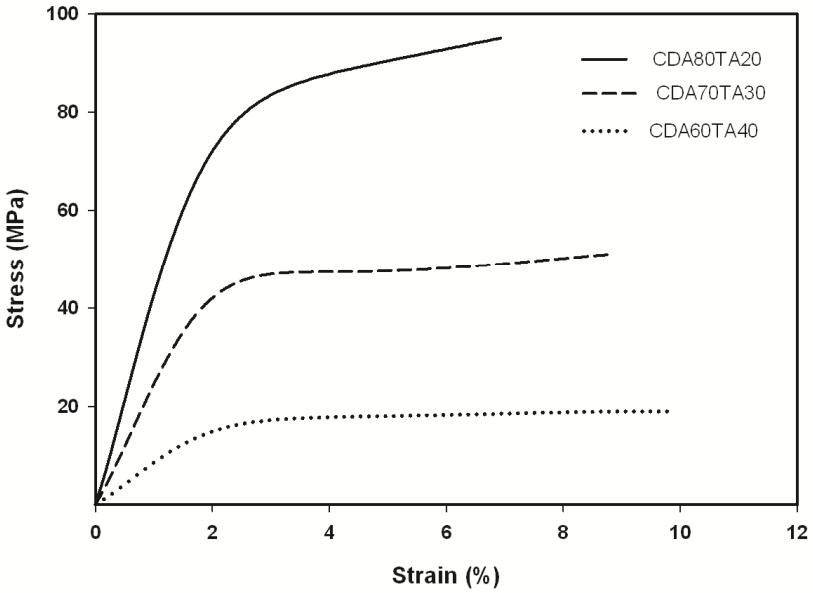

Figure 2a. Stress-strain curves for CDA/TA blends with different amount of TA

Samples name	CDA (%)	TA (%)	GPE (%)	Lyocell (%)	Elastic Modulus (GPa)	Tensile Strength (MPa)	Strain at break (%)
CDA80TA20	80	20	0	0	4.54 ± 0.2	93.3 ± 2	6.85 ± 0.6
CDA70TA30	70	30	0	0	2.67 ± 0.1	49.3 ± 1.5	8.68 ± 0.5
CDA60TA40	60	40	0	0	0.96 ± 0.1	19.7± 1.3	9.35 ± 0.7
(CDA80TA20)Ly10	80	20	0	10	5.57 ± 0.3	98.4 ± 3	6.8 ± 0.1
(CDA70TA30)Ly10	70	30	0	10	3.57 ± 0.1	54.6 ± 0.3	8.19 ± 0.8
(CDA60TA40)Ly10	54	36	0	10	1.81 ± 0.1	27.2 ± 0.1	9.5% ± 0.4

CDA80TA20GPE5	76	19	5	0	3.67 ± 0.08	80.5 ± 1	9.04 ± 0.4
CDA70TA30GPE5	66.5	28.5	5	0	1.75 ± 0.03	33 ± 0.5	9.38 ± 0.2
CDA60TA40GPE5	57	38	5	0	0.34 ± 0.01	10.4 ± 0.4	8.55 ± 0.1
(CDA80TA20GPE5)Ly10	68	17	5	10	4.78 ± 0.15	95.3 ± 4	7.21 ± 0.5
(CDA70TA30GPE5)Ly10	59.5	25.5	5	10	2.48 ± 0.08	44.2 ± 0.3	10 ± 0.6
(CDA60TA40GPE5)Ly10	51	34	5	10	1.4 ± 0.14	21.4 ± 0.6	9.8 ± 0.2
(CDA80TA20GPE5)Ly10	76	19	5	Ly -10%	4.78 ± 0.15	95.3 ± 4	7.21 ± 0.5
(CDA80TA20GPE5)Re10	76	19	5	Re - 10%	5.1 ± 0.2	92 ± 3	4.73 ± 0.3
(CDA80TA20GPE5)MCC10	76	19	5	MCC - 10%	4.58 ± 0.1	79.3 ± 3.7	6.91 ± 0.4

Table 1. Mechanical properties of materials with different amounts of plasticizers and several types of natural fibers

This behavior indicates that the optimum content for TA as primary plasticizer is about 20-30 wt%, where tensile strength and modulus values are still high. Exceeding a TA content of 30 wt% does not seem advantageous, because the plasticizer reduced the interaction of polymer chains to such an extent that mechanical properties are substantially hampered.

On the other hand, the data of Table 1 show also that the addition of 5% Glycerin Polyglycidyl Ether (GPE) – the secondary plasticizer – to these blends not only facilitates melt processing but also enhances the values of elongation at break with a concomitant small decrease in tensile strength, more limited in comparison with the effect of the addition of an analogous amount of TA (Figure 3).

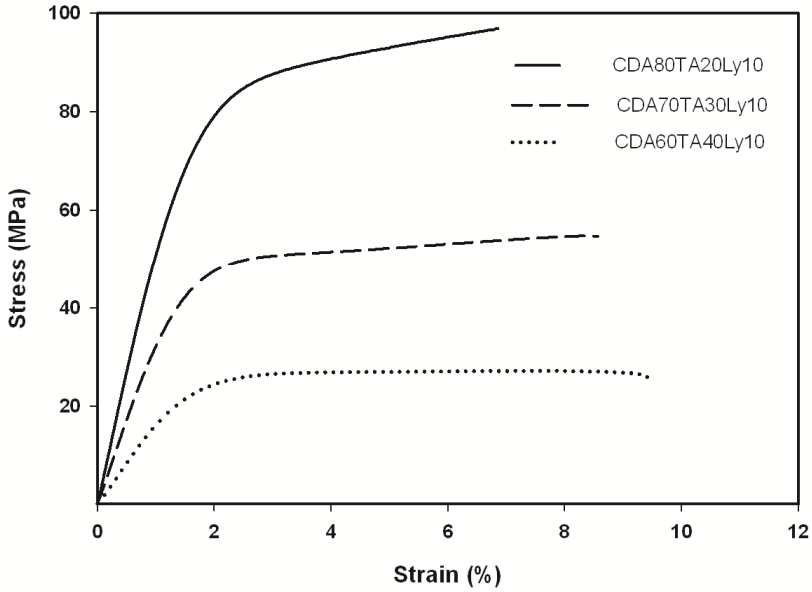

Figure 2b. Stress-strain curves for CDA/TA/Ly based blends with different amount of TA

Mechanical properties of plasticized CDA blends were substantially improved by the addition of Lyocell fibers. The elongation at break of the composite materials was unchanged compared to the corresponding matrix (Figure 3), while the tensile strength and Young's modulus increased significantly (Figure 3 and Table 1). The preservation of the values of elongation at break, even in presence of fibers acting as reinforcement, suggests good adhesion between the fibers and the polymer matrix. This hypothesis is also supported by comparing the experimental modulus data with some theoretical models which assume good adhesion between the fibers and the matrix (Figures 5a and 5b). Using the modulus values for the CDA plasticized at different TA contents, the Kim's equation (8) and Tandon-Weng's model provides estimates of the composite modulus which are very close to experimental data, while the Halpin-Tsai's equations (8) to (14) seems to provide a lower bound value for the Young's modulus of the materials.

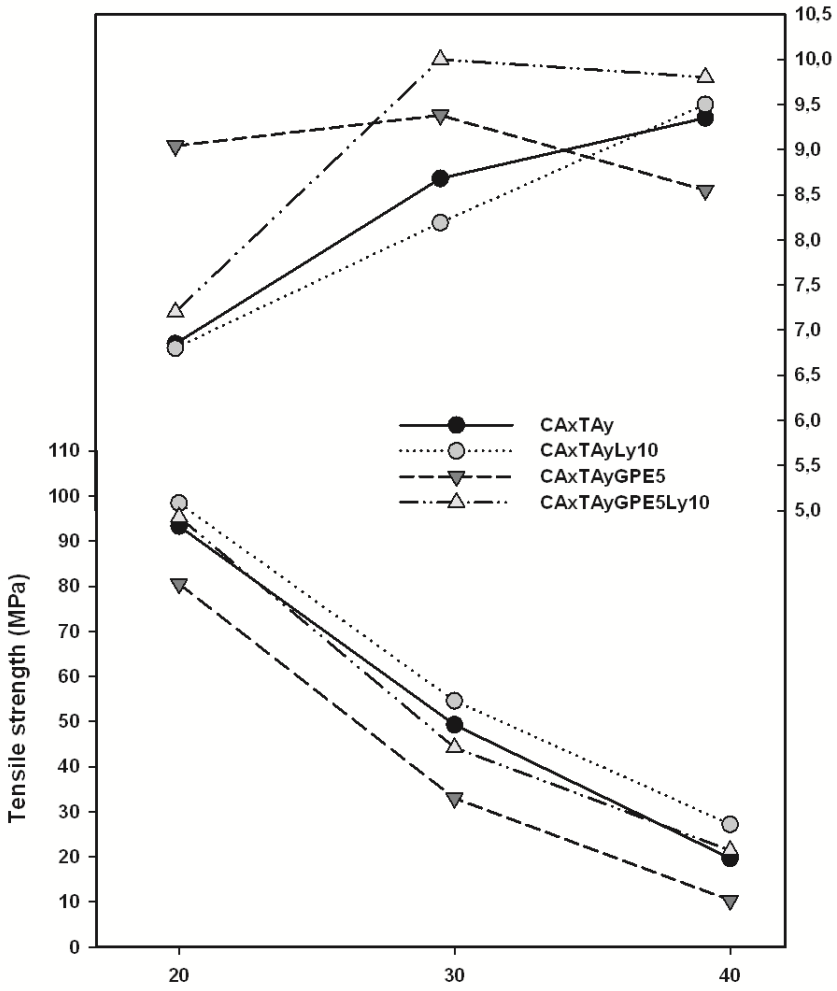

Figure 3. Mechanical properties for CDA/TA/GPE blends with different amount of TA and GPE

The Cox's model enables an estimation of the critical aspect ratio, i.e. the ratio between the length where shear stress transfer occurs and the diameter of the fiber [43]:

$$a_c = 2.303\sqrt{\frac{E_f(1+\nu_m)}{E_m}}\log\sqrt{\frac{\pi}{4\varphi_f}} \qquad (17)$$

Using a value of 12.5 GPa for the fibre modulus and the values of Table 1 for Em, the critical aspect ratio can be estimated to vary from a minimum of 2.9 for (CDA80TA20)Ly10 to a maximum of

10.6 for (CDA60TA40E5)Ly10. Since the Lyocell fibers own an aspect ratio of 37, this ensures a proper stress transfer from the matrix to the fibers and the buildup of the tensile stress in the fibers up to the maximum value achievable in a corresponding composite reinforced with continuous fibers of the same type, even for the softest matrix tested in this work.

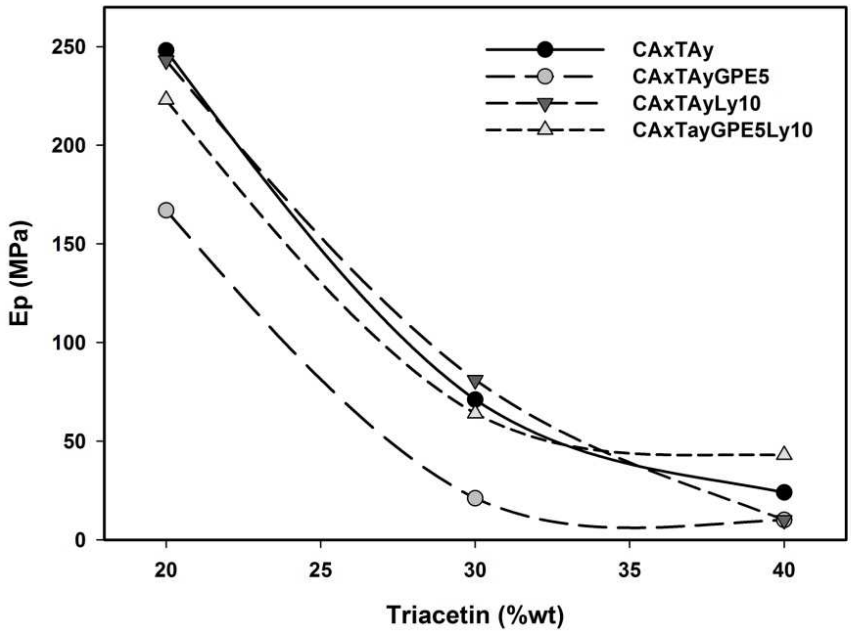

Figure 4. Hardening modulus of materials with different plasticizers content

The addition of GPE improves the adhesion between the fibers and the polymer matrix. This effect can be measured quantitatively by using the B-factor according to Pukánszky's equation (15). For example, for the composite based on TA-plasticized CDA reinforced with Lyocell fibres – (CA80TA20)Ly10 – a B-value of 3.77 could be estimated, while for the composite with same fiber volume fraction but with the matrix modified by the further addition of GPE –(CA80TA20GPE5)Ly10 – a B-value of 4.86 was obtained. On increasing the triacetin content the B-factor for the matrix modified with GPE is always larger than for the reference material (Figure 6), but the difference between B-factors referring to the same TA content progressively increases, and this divergence is particularly relevant at 40 wt% TA. Thus it seems that GPE is more effective on the yield stress on increasing TA content.

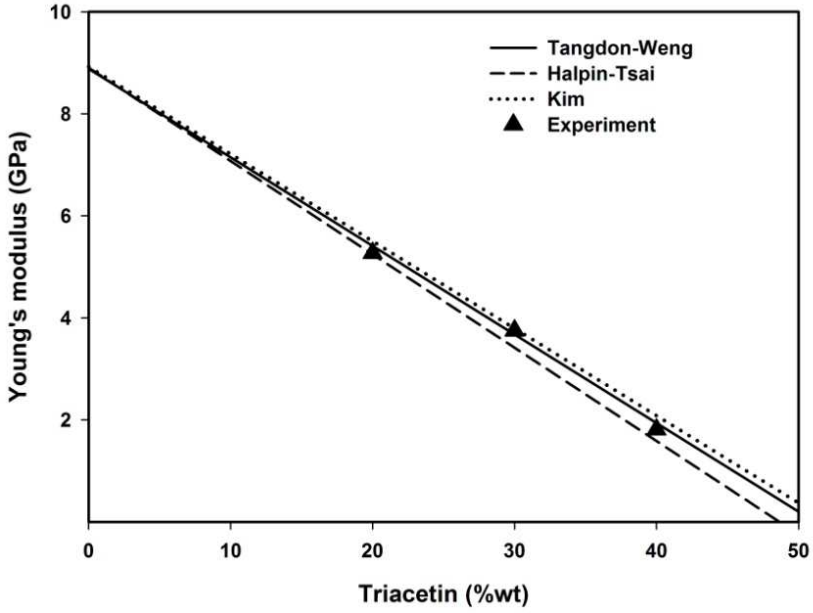

Figure 5a. Young's modulus for (CDAxTAy)Ly10 at different TA content. Comparison between experimental data and theory prediction

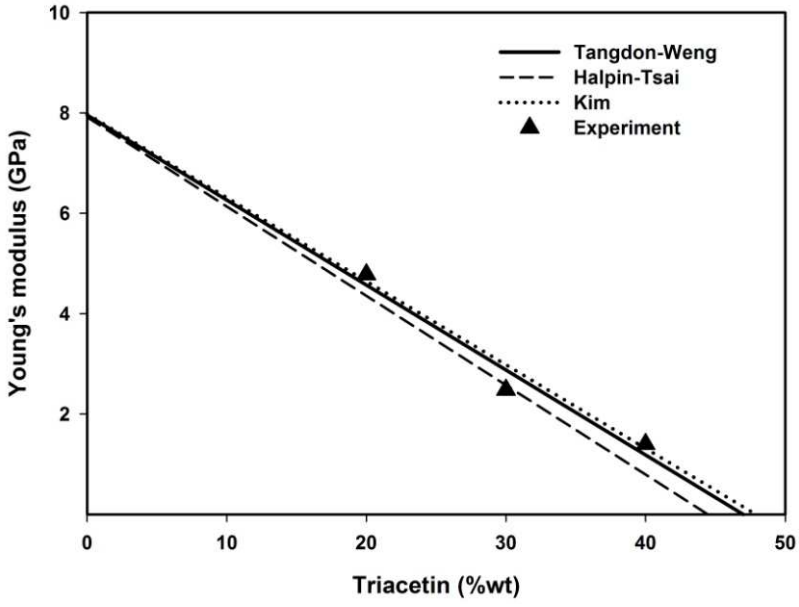

Figure 5b. Young's modulus for (CDAxTAyGPE5)Ly10 at different TA content. Comparison between experimental data and theory prediction

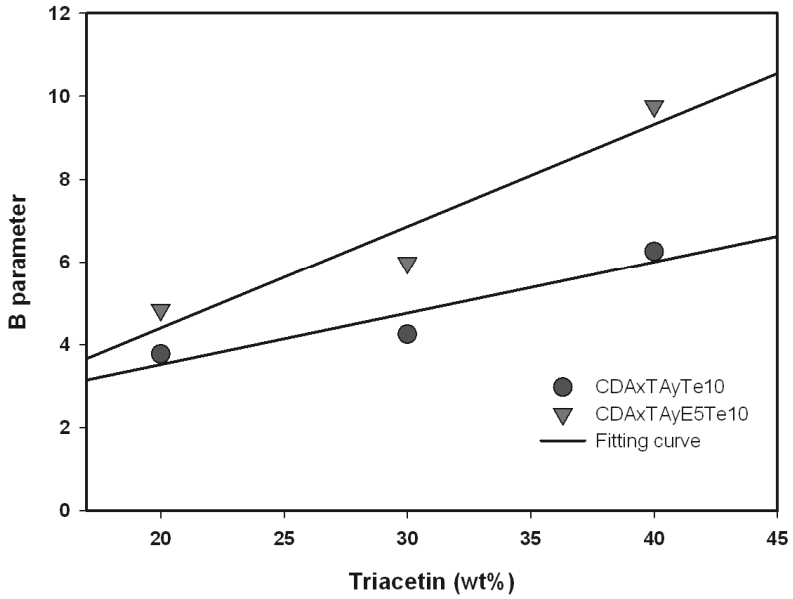

Figure 6. Pukánszky's B parameter of materials with different content of plasticizer

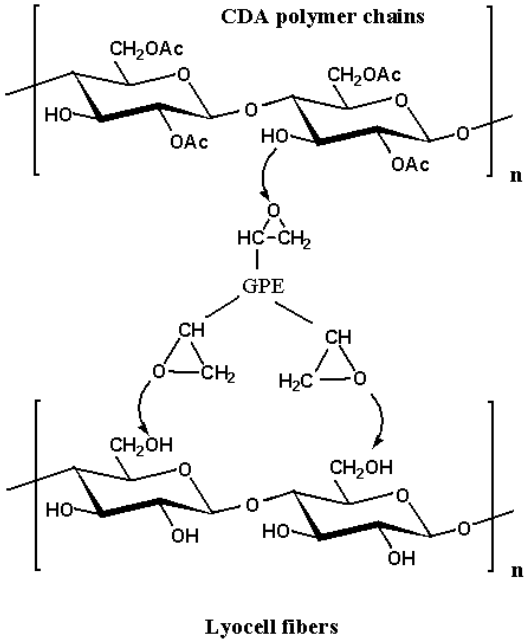

Scheme 2. Mechanism reaction of GPE with Cellulose diacetate and Lyocell fibers

This suggests the hypothesis that epoxy groups of GPE could react with the hydroxyl groups present on both the Lyocell fibers and along the cellulose diacetate chains, during melt processing, improving the fiber-matrix interactions. Thus the fibers could be covalently bonded to the CDA matrix by means of a glycerin polyglycidyl ether bridging molecule (scheme 2).

To test this hypothesis, samples of (CDA80TA20)Ly10 and (CDA80TA20GPE5)Ly10 were dissolved in acetone to remove CDA from the Lyocell fibers and check for the evidence of ester groups. As shown in Figure 7, the fibers obtained from the composite without GPE show an FTIR spectra totally overlapping with that of the original Lyocell fibers, while those removed from the composite with GPE modified matrix show an additional peak at 1730 cm^{-1}, corresponding to the stretching of C=O bonds, which clearly indicates that the molecule now contains a carbonyl group, not present in the cellulose fibers solvent removed from the composite without GPE. This can be interpreted as an indirect proof of the presence of CDA molecules attached to the surface of the Lyocell fibers. The GPE seems thus to behave both like a plasticizer for the CDA matrix and like a coupling agent. To better assess the potential of Lyocell fibers in CDA, it is interesting to compare the behavior of other natural fibers in the same matrix.

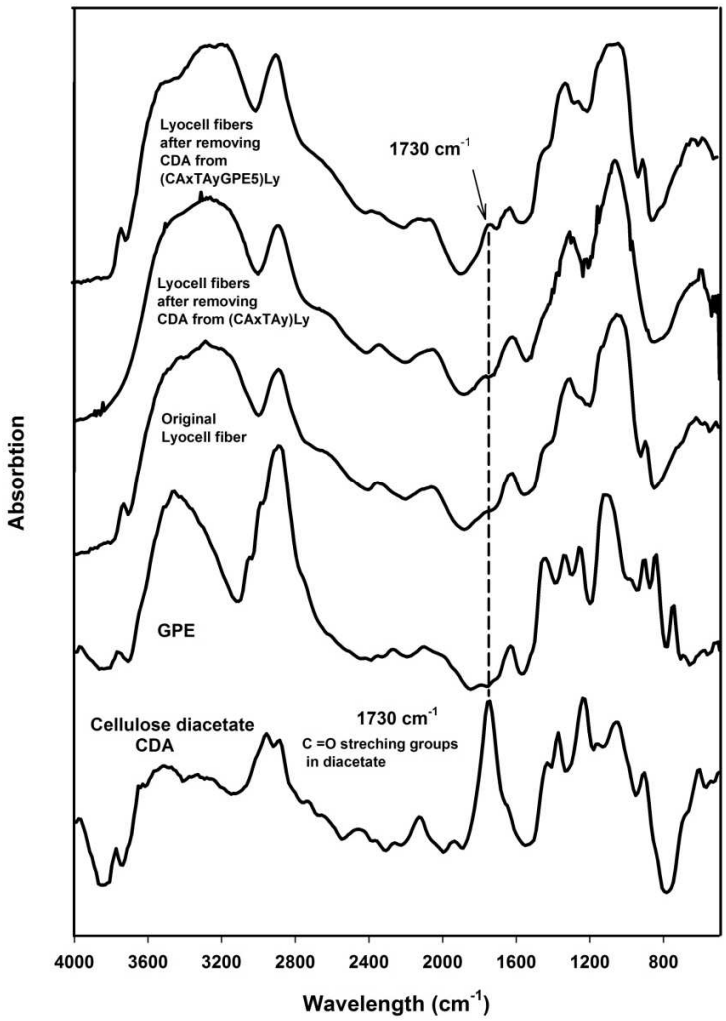

Figure 7. FTIR spectra (see text for details)

Table 1 compares the tensile strength of composites based on cellulose diacetate and wood flour (Rettenmaier) and microcrystalline cellulose at fixed content of multi-plasticizers (20% TA and 5% GPE). The tensile strength and elongation at break of Lyocell fibers/plasticized CDA (CA80TA20GPE5) composites are higher than for the corresponding composites reinforced with the lignocellulosic fibers (Rettenmaier EFC 1000, Re for short), particularly as far as the elongation at break is concerned, while the composite with microcrystalline cellulose show an intermediate behavior. For these composites, however, the Young's modulus pursues a different pattern, with the composites with lignocellulosic fibers

showing the highest value, followed by the composites reinforced with Lyocell fibers, while the composites filled with microcrystalline cellulose presents the smallest values. In fact, Lyocell fibers have the highest aspect ratio, so one would expect that the composites with these fibers should have the highest modulus, and the slightly higher stiffness of the composites with lignocellosic fibers can be explained by their higher inherent Young's modulus due to the presence of lignin in these fibers. On the other hand, the elastic modulus of composites with microcrystalline cellulose (MCC) shows the lowest value because of their small aspect ratio. In fact, using Equation (17) and a Young's modulus of 25 GPa [44] a critical aspect ratio (arc) of 4.6 can be estimated for MCC, that is a value above the actual aspect ratio (ar = 2-4) of this type of fibers. The same calculation provides a value of arc = 3.3 for the lignocellulosic fibers, by assuming a Young's modulus of 13.5 GPa [45]. Since for these fibers ar = 6.7, this ensures a superior stress transfer between the matrix and the reinforcement respect to the MCC fibres.

While the tensile strength of composites with Lyocell and lignocellulosic fibers are quite similar, the elongation at break of the samples with Lyocell fibers is sensibly higher. This can also be explained with presence of lignin in Rettenmaier fibers which makes these fibers stiffer than the Lyocell but more brittle.

4.2 Thermal behavior

The thermogravimetric and derivative thermogravimetric curves of CDA blends with different amounts of plasticizers are reported in Figures 8a and 8b, respectively, the corresponding data are accounted for in Table 2. The pure CDA degrades in a single step starting from an initial temperature, Ti = 320 °C to the final temperature Tf = 480 °C, with a DTG peak temperature at 410 °C, which can be attributed to the thermal degradation of acetate functional groups and glucose rings in the polymer chains.

In CDA samples with plasticizers, two degradation steps were observed, instead. The first degradation interval observed at lower temperatures, can be related to the TA content, since the temperature of complete degradation decreases and the DTG peak is broadened with increasing plasticizer content.

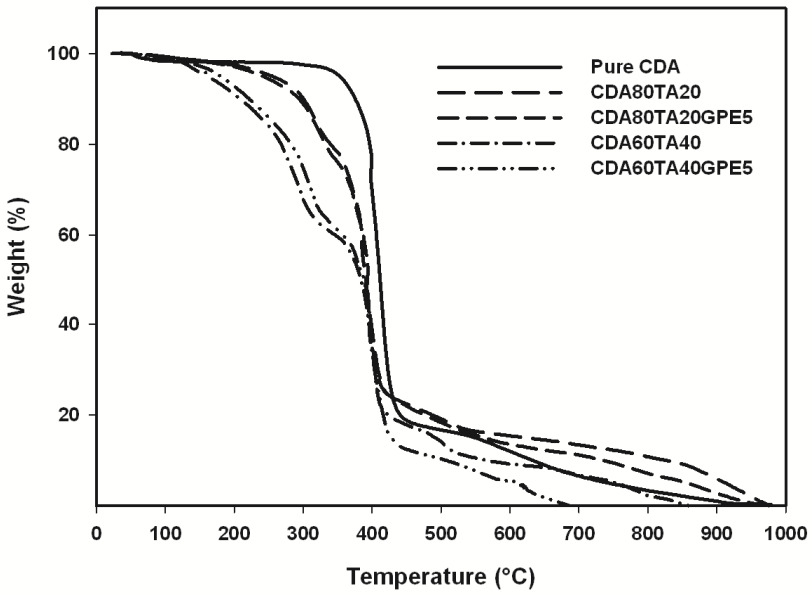

Figure 8a. TGA curves for CDA/TA/GPE blends with different amounts of TA and GPE

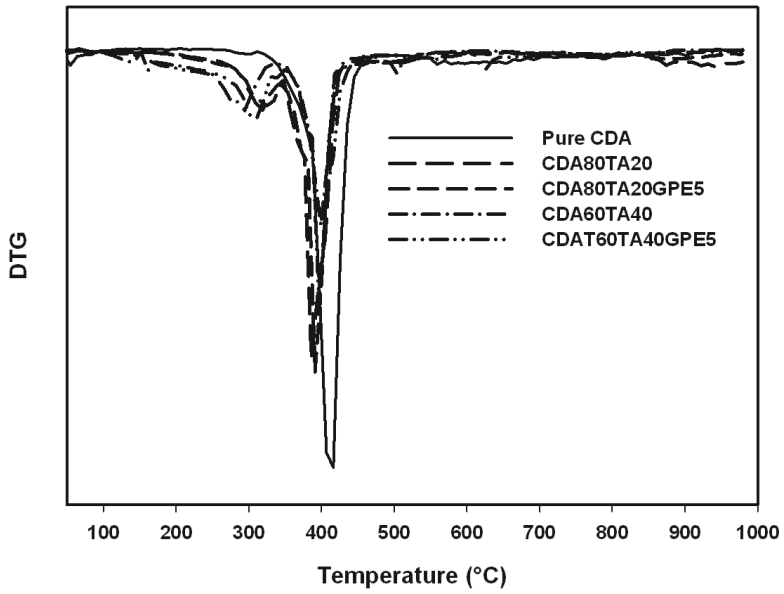

Figure 8b. DTG curves for CDA/TA/GPE blends with different amount of TA and GPE

The temperature of this peak is around 310 °C, higher than the boiling temperature and near to the decomposition temperature of TA. The weight loss related to this peak is consistent with the amount of

TA added, so it was assessed that there was practically no loss of plasticizers during processing, via volatilization. The second degradation peak starts at about 340 °C, which is near to the initial degradation temperature of pure CDA. Since the first DTG degradation peak is attributed to TA and the second to CDA, this suggests the presence of just physical interactions (van der Waals and hydrogen bonding) between CDA and TA. Besides, the thermal stability of materials was slightly changed in the samples where GPE was present. Although there are no specific DTG peaks that can be associated to the degradation of GPE, probably masked by other peaks since only a small amount of GPE (5%) is present in these materials, the DTG peak for CDA60TA40GPE5 is about 10 °C higher of the corresponding peak for CDA60TA40. This suggests interactions between TA and GPE which increase the thermal stability of the blend

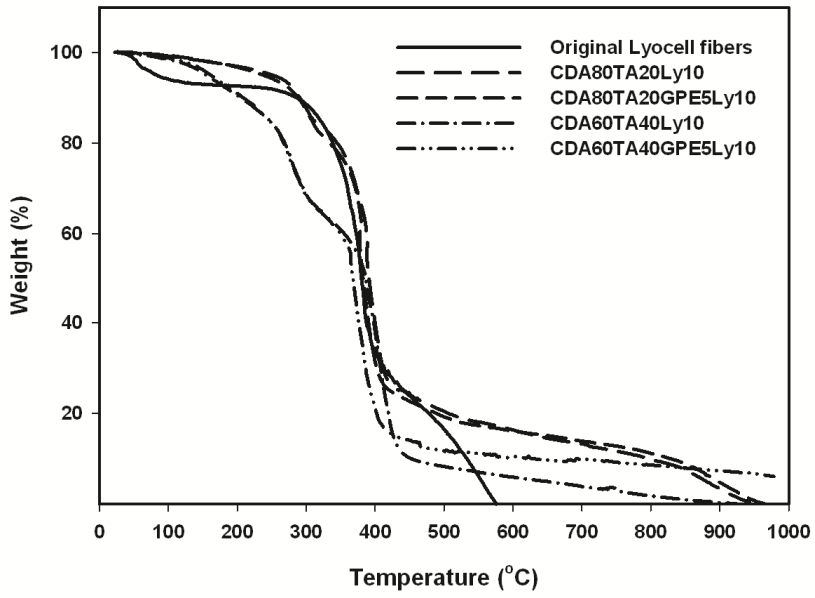

Figure 9a. TGA curves for CDA/TA/GPE/Lyocell fibers (10phr) composites with different amounts of TA and GPE.

Figures 9a and 9b shows the thermogravimetric and derivative thermogravimetric curves of CDA and 10 wt% of Lyocell fibers with different plasticizer content. The thermal behavior of Lyocell

reinforced CDA composites is similar to that shown by the corresponding matrix. In the thermogravimetric curve of Figure 9a, the first stage is related to the decomposition of TA, but the starting temperature and DTG peak temperature are about 10 degrees lower than in samples without fibers. This phenomenon might suggest a reduced interaction between TA and CDA molecules.

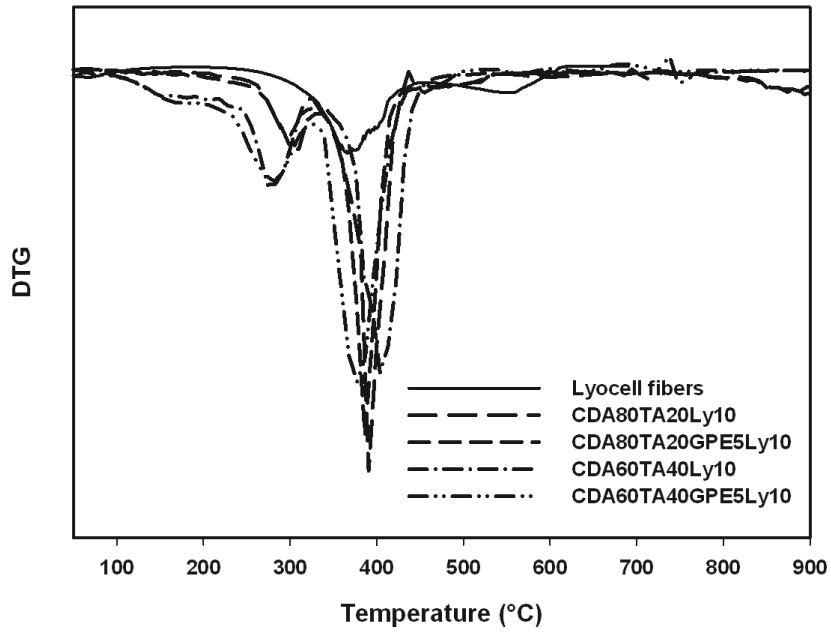

Figure 9b. DTG curves for CDA/TA/GPE/Lyocell fibers (10phr) composites with different amounts of TA and GPE

No specific weight loss interval seems to be associated to the degradation of Lyocell fibers. Similar to GPE, the effect of Lyocell fibers is not clear due to their small amount. Moreover, the degradation interval of Lyocell fibres is partially overlapping to that of CDA. In fact, pure Lyocell fibers show an initial degradation temperature Ti = 220 °C, compared to a corresponding value of 310 °C for CDA, and a final decomposition temperature Tf = 420 °C (450 °C for CDA) with a DTG peak at 380 °C (410 °C for CDA). Thus, in the second stage, the initial temperature for the composite is lower than the corresponding matrix without fibers because, the Ti of Lyocell fibers is shifted 90 °C lower respect to CDA. On the contrary, the DTG temperature peak in second stage of CDA80TA20Ly10 is 386 °C which

is close to the degradation peak of Lyocell fibers. Meanwhile, the DTG temperature peak of CDA60TA40Ly10 is 406 °C, quite similar to pure CDA (410 °C). This might be a consequence of a higher level of interaction between fibers and CDA in the composites with lower TA content.

Blends	**First stage**			**Second stage**		
	Temperature range, ^{0}C	Temperature peak, ^{0}C	Wt loss, %	Temperature range, ^{0}C	Temperature peak, ^{0}C	Wt loss, %
Pure CDA	310-980	410	100	-	-	-
CDA80TA20	200-340	310	20	340-960	390	100
CDA80TA20GPE5	200-347	320	20	347-960	392	100
CDA60TA40	130-345	305	40	345-855	402	100
CDA60TA40GPE5	140-346	316	42	346-675	392	100
Lyocell fibers	220-572	380	100	-	-	-
(CDA80TA20)Ly10	190-315	290	18	315-940	386	100
(CDA80TA20GPE5)Ly10	190-336	304	20	336-954	377	100
(CDA60TA40)Ly10	120-332	277	37	312-905	406	100
(CDA60TA40GPE5)Ly10	130-352	280	40	352-1000	383	94

Table 2. Thermogravimetric data of CDA/TA/GPE5/Ly10 with different amounts of plasticizers

It was also shown in the analysis of the tensile tests, that exceeding a TA content of 30 wt% does not seem advantageous, so this results further supports the view that there is a maximum level of this

plasticizer which should not be overcome to avoid substantial degradation of the physical-mechanical properties.

The presence of GPE introduces some differences in the thermogravimetric curve of Lycell fiber reinforced cellulose diacetate. Comparing the second stage decomposition of (CDA80TA20)Ly10 and (CDA80TA20GPE5)Ly10, (CDA60TA40)Ly10 and (CDA60TA40GPE5)Ly10, we observe that the initial temperature is clearly higher for the samples including GPE. This further suggests that a chemical bonding is formed between Lyocell fibers and cellulose diacetate through epoxy function of GPE.

4.3 Relaxation transitions, structure

Figure 10a presents the DMTA spectrum for cellulose diacetate and its composites with different plasticizer content. The temperature dependence of storage modulus and loss tangent is shown in this figure. Considering the curves with TA only, we observe two major transitions for the blends at 20 and 30% TA, while for the sample with 40% TA three tan δ peaks are visible. The high temperature peak corresponds to the glass transition of CDA [46-47]. The addition of plasticizer leads to a linear decrease in the α-transition temperature of CDA (Figure 10) which can be fitted with Gordon and Taylor [48] equation (18):

$$T_g = \frac{x_1 T_{g1} + k_{GT}(1-x_1)T_{g2}}{x_1 + k_{GT}(1-x_1)} \qquad (18)$$

using the values of $T_{g\,1}$ = -68 °C for triacetin and $T_{g\,2}$ = 195 °C for pure CDA [47,49], and an interaction parameter k_{GT} = 0.96. These data are in agreement with previously published research work [12] and they can be explained by the large miscibility of CDA and TA [50].

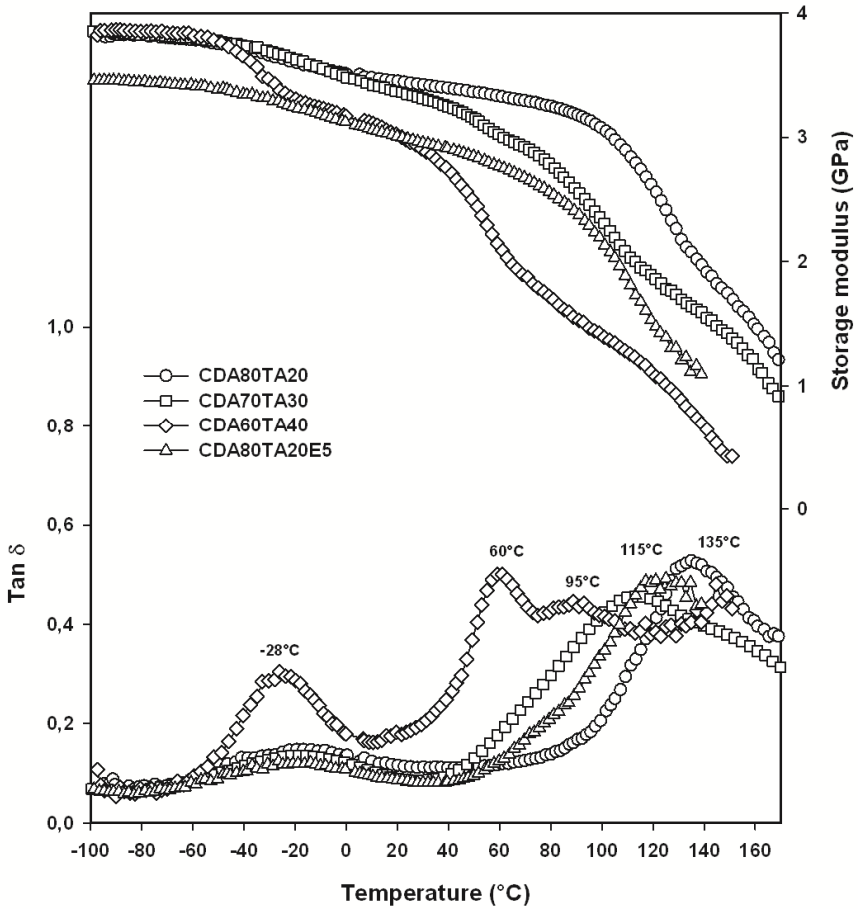

Figure 10a. DMTA curves for CDA/TA/GPE blends with different amounts of TA and GPE

The low temperature peak at -28 °C, normally defined as the β-peak, is sometimes associated with the movement of the glucose ring units or to water associated with hydroxymethyl groups [46]. The sample at 40% TA shows an additional peak in loss tangent at about 60 °C while the β-peak at -28 °C is much more pronounced than the other two samples. The additional peak at 60 °C can be probably identified with the β^*-peak discussed by Scandola [47] as a water-related relaxation. This explanation does not seem to hold in the present case since no weight loss associated with water can be identified in the thermogravimetric curve for CDAxTAy blends. In fact the materials were dried before extrusion and kept in a close environment prior to testing, so water pick-up was minimum. Pukánszky and co-workers

[46] also reported about a β'-peak associated to a relaxation of structural units larger than a single glucose ring and dependent upon sample preparation conditions.

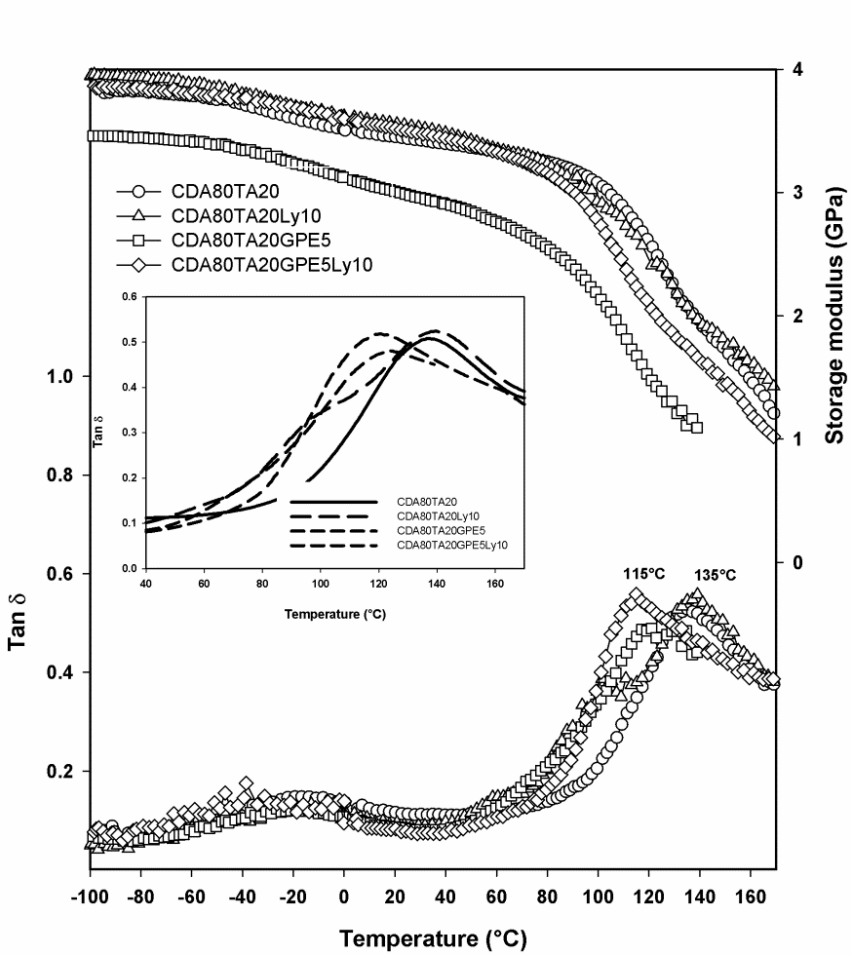

Figure 10b. DMTA curves for CDA/TA/GPE/Lyocell fibers composites with different amounts of TA and GPE

The fact that this transition is present only in the sample with larger TA content can lead us to a tentative explanation. At low TA content, the molecules of this plasticizer intercalate between the chains of polymers, spacing them apart and increasing the "free volume". This increased space between polymer molecules enables to reduce the activation energy for the cooperative motions of the main chain and has the effect of significantly lowering the glass transition temperature of CDA. At higher TA content, a critical value of free volume is reached where several glucose ring along the chain have enough space to

cooperative move even below the T_g of the polymer. This could explain both the increase in intensity of the β-peak increases in intensity and the appearance of the β'-peak.

Comparing the loss tangent vs. temperature curve for CDA80TA20 and CDA80TA20GPE5, we notice that there are no new peaks that can be associated to GPE, although, the α-transition temperature of CDA is further reduced by about 20 °C. This means that the second plasticizer is also miscible with cellulose diacetate, and only one homogeneous phase is present in the system. We have shown that a reaction between epoxy groups of GPE and hydroxyl functions of Lyocell fibers is likely to have occurred, so a similar reaction might occur between GPE molecules and CDA polymer chains. Although the specific study of the detailed mechanism of interaction between GPE and CDA is beyond the purposes of this work, it is likely that GPE behaves like an internal plasticizer while TA is an external plasticizer.

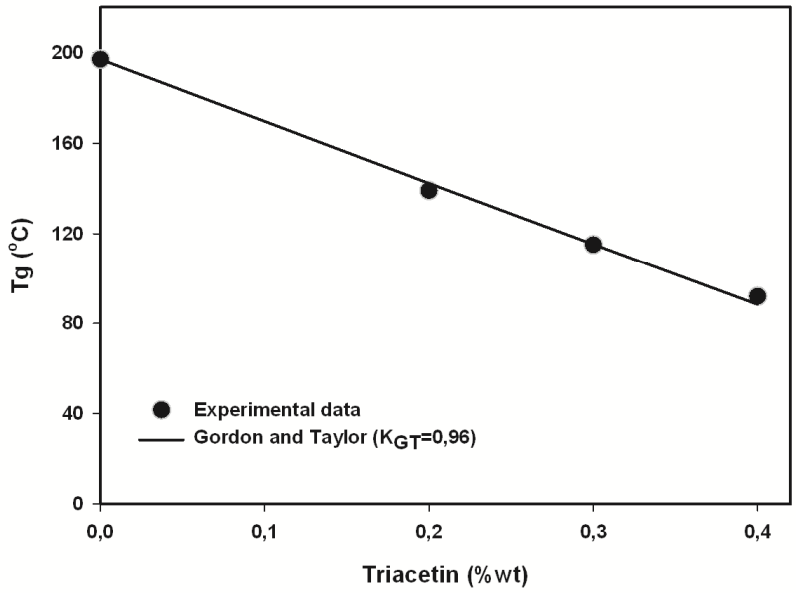

Figure 11. Glass transition temperature versus triacetin content for CDA/TA blends

Moreover, the curves of storage modulus versus temperature shown in Figures 10a and 10b, indicate that, while modulus is obviously decreased by an increase in the plasticizer content, the addition

of Lyocell fibers compensates this loss in stiffness. Considering the loss tangent versus temperature curves, it is possible to observe that the α-transition temperature of CDA is unchanged in presence of the fibers – compare curves for CDA80TA20 and (CDA80TA20)Ly10. On the other hand, the addition of Lyocell fibers is also accompanied by the appearance of a shoulder in the α-peak of the tan δ curve, which may indicate a new hidden peak related to the presence of the fibers, around 95 °C, partially overlapping with the glass transition of CDA. A possible explanation is that the Lyocell fibers have just physical interactions with the polymeric matrix. This shoulder disappears when GPE is added to the composite. Moreover, the glass-transition peak is shifted further down in temperature, at about 115 °C, in presence of GPE. This further supports the hypothesis of an increased interaction between fibers and the reactive plasticizer.

4.4 Morphology

The fracture surfaces of cellulose diacetate with different amounts of plasticizer are reported in Figure 12a, b, c. The morphology of these blends appears homogeneous also at high plasticizer content as well as in the presence of GPE. That means that both plasticizers are compatible with CDA. Moreover, the good interaction between Lyocell fibers and polymer matrix is confirmed by examining Figures 13a, b and c. With 20% TA, it is clear that most of the fibers were stressed until break, just a small amount of them being pulled-out. The amount of pulled-out fibers seems to increase upon increasing TA content, as shown in Figures 13a and 13c images. This is a consequence of the reduction of yield stress of the matrix which lowers the interface shear strength and leads to an increase in the critical fiber length, as discussed previously. However, figures 13a, and b show that the adhesion of fibers to the polymeric matrix was improved by the addition of GPE. By combination of tensile testing, DMTA, FTIR and TGA studies, it could be concluded that chemical interactions are established between Lyocell fibers and polymer matrix through the epoxy functions of GPE.

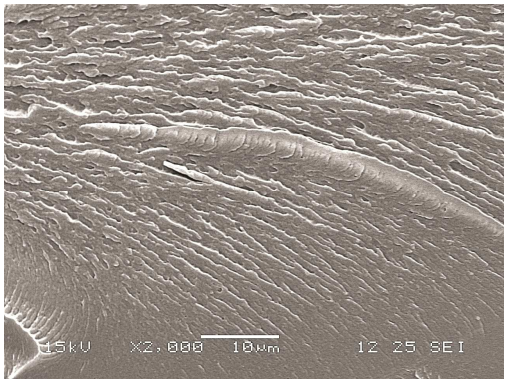

CDA (80phr)/ TA (20phr)

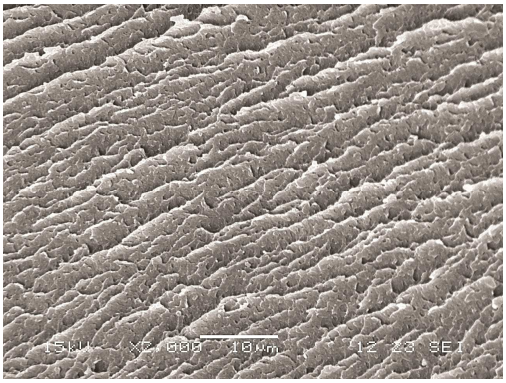

CDA (80phr)/ TA (20phr)/ GPE (5phr)

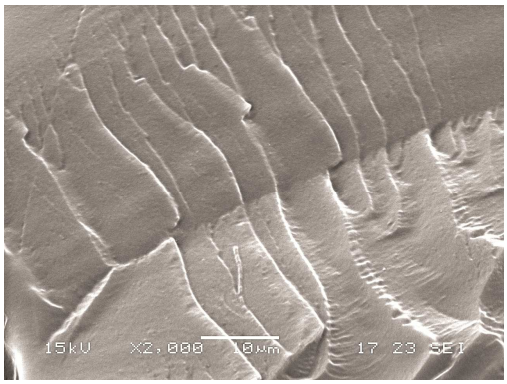

CDA (60phr)/ TA (40phr)

Figure 12. SEM micrographs for CDAx/TAy matrix

Moreover, the morphology of different natural fibers can be observed in Figures 13d and 13e. In case of microcrystalline cellulose and lignocellulosic fibers, a certain number of fiber agglomerates with sizes of the order of about 100 µm can be noted. Meanwhile, microcrystalline cellulose and wood flour presented better interaction with polymer matrix than Lyocell fibers because of their surface roughness. In particular, wood flour has also about 15 % content of lignin, which could have reacted with GPE, during extrusion.

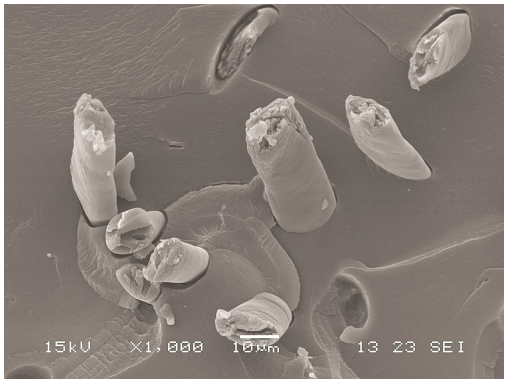

CDA (80phr)/TA (20phr)/Ly (10phr)

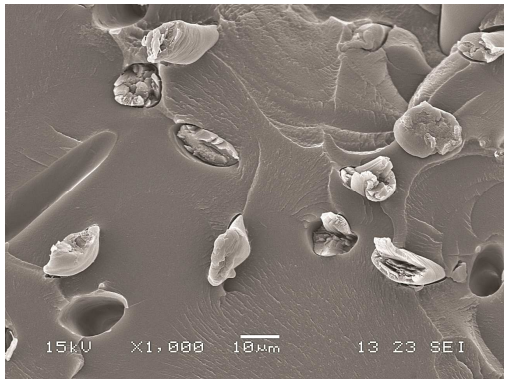

CDA (80phr)/ TA (20phr)/
GPE (5phr)/Ly (10phr)

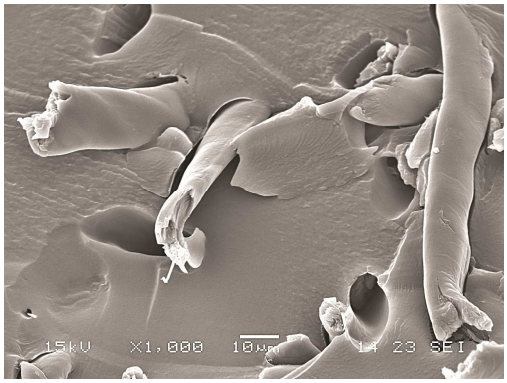

CDA (60phr)/TA (40phr)/Ly(10phr)

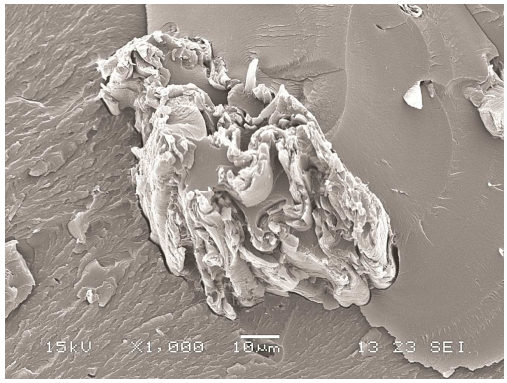

CDA (80phr)/ TA (20phr)/
GPE (5phr)/Re (10phr)

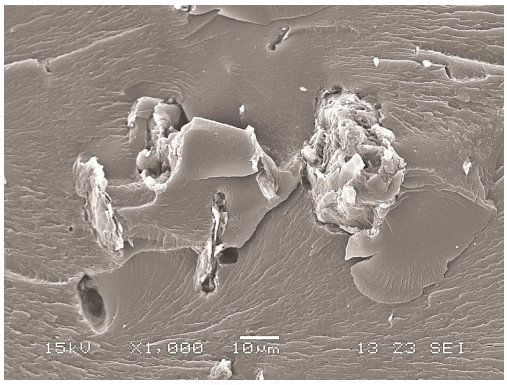

CDA (80phr)/ TA (20phr)/ GPE (5phr)/MMC(10phr)

Figure 13. SEM micrographs for CDAx/TAy/ fibers composites

On the other hand, the mechanical properties of composites with CDA and wood flour and microcrystalline cellulose (MCC) cellulose do not present better mechanical properties respect to those

prepared with Lyocell fibers, possibly because of the low aspect ratio and not uniform geometry for wood flour and MCC.

V. GENERAL DISCUSSION

Although CDA is a long time known and used polymer, biocomposites based on CDA have not received recently as much attention in R&D as those based on other biopolymers such as polylactic acid, as attested by the limited recent literature on CDA based composites, despite the fact that cellulose is the most abundant biopolymer on our planet. One of the reasons is related to the difficult processability since the processing temperature for CDA is very close to the degradation temperature. Thus, there is the need for the addition of plasticizers such as phthalates which make the material not suitable for composting or biodegradation.

Thus, as mentioned above, some studies considered different plasticizers, more compatible with the envinronment like triethyl citrate or triacetin, blending with other biopolymers and producing biocomposites.

Triacetin is a relatively low viscosity liquid (at 20 °C = 23 mPa•s) that can easily diffuse into CDA molecules, leading to a rapid depression of its T_g, thus enabling a larger processing window for plasticized CDA. On the other hand, the GPE used in this study shows a much higher viscosity (at 25 °C about 250 mPa•s), thus higher temperatures and much longer times are required for its diffusion into CDA. Also GPE has shown to be capable of reacting with the matrix, thus acting more as an internal plasticizer. Thus, the new strategy developed in this work, which makes use of a system of two different plasticizers:

- a primary “external-type” or “non-reactive-type” plasticizer added prior to extrusion to enhance the “processing window” of the polymer.
- a secondary “internal-type” or “reactive-type”, added during the extrusion step to reduce the amount of potential volatiles or leachable products in the final product and to help in the reduction of

viscosity and thus further improving processability, may prove as an extremely useful approach in establishing a new process route for CDA based biocomposites.

On the other hand, many natural fibers used in composites possess a limited aspect ratios, and their non-homogeneity in both fiber diameter and fiber length and their size distribution, results in limited property enhancement, and little materials reproducibility.

Lyocell, also known as Tencel, is an artificial microfiber made from regenerated wood pulp cellulose. It is produced by spinning bleached wood pulp dissolved in a nontoxic (“green”) organic solvent, N-Methylmorpholine-N-oxide or MMNO, which can recovered by washing the freshly spun cellulose microfibers in water, and later purified, and recycled. Both fiber diameter and fiber length can be accurately controlled during the production process.

In this study, we investigated Lyocell fibers reinforced CDA biocomposites and the effect of the content of two plasticizers (TA and GPE). In first instance it was considered the performance of the system, with and without regenerated cellulose microfibers, varying the TA amount from 20% to 40% by weight. Then GPE was evaluated as not only as a second plasticizer but also to improve the interactions between the fibers and the polymer matrix and consequently to target an increase in stiffness. The resulting materials showed excellent mechanical properties, much better than those reported in the literature for CDA composites prepared with traditional plasticizers and fillers. A comparison with other eco-friendly fillers like wood flour and microcrystalline cellulose, tested in this paper, showed that cellulose diacetate composites with Lyocell fibers showed superior dispersion in the polymer matrix, and higher mechanical properties, related to the higher aspect ratio of these fibers and to the good bonding with the polymeric matrix.

Without overlooking the difficulty of scaling-up a process from lab-scale to industrial-scale, this new approach enables to envisage potential innovative biocomposites, based on a readily available natural resource.

VI. CONCLUSIONS

The mechanical properties, thermal stability and morphology of biocomposites based on cellulose diacetate, plasticized with a combination of reactive and non-reactive plasticizers and reinforced with fibers from natural resources, were investigated.

Values of tensile strength and Young's modulus decreased with increasing the plasticizer content. A good compromise between processing and mechanical properties for the composites with Lyocell cellulose fibres was obtained for the systems where CDA is plasticized with 20 wt% TA. The presence of GPE not only improved processability but also increased values of elongation at break in the materials produced.

Thermo-gravimetric analysis confirmed that only physical interactions (hydrogen and van der Waals forces) are established between CDA and TA while stronger interactions (covalent bonds) are observed by the introduction of GPE.

The glass transition temperature T_g decreased due to effect of the primary plasticizer, as investigated by DMTA testing.

SEM micrographs evidenced that, in samples with 20 wt% TA, the fibers were stressed until break, with just a small amount being pulled-out. Fiber pull-out was more evident with increasing the plasticizer contents. The adhesion of the polymeric matrix with the fibers improved by the addition of GPE, possibly because of the formation of strong chemical bonds with polymer matrix through the epoxy groups of GPE.

Besides, the mechanical properties of cellulose diacetate composite with different natural filler were determined as a reference. They showed high tensile strength as well as a good dispersion of fibers within the polymer matrix. However, the lower aspect ratio of the filler and the less uniform dispersion in the polymer matrix prevented the achievement of the same level of mechanical properties obtained by the composites with Lyocell fibers.

Considering both processing conditions, economic aspects and availability of raw materials on the market, bio-composites based on plasticized CDA reinforced with regenerated cellulose (Lyocell) microfibers could become an interesting option for the production of “green” biocomposites.

Acknowledgment

The authors gratefully acknowledge the financial support of the FORBIOPLAST (Forest Resource Sustainability through Bio-Based-Composite Development) project – Contract No. 212239-FP7-KBBE, funded by the European Commission under the 7th Framework Programme (FP7) (http://www.forbioplast.eu). Thanks to Dr Barbara Gospietro of Acetati Spa – Verbania (Italy) for providing us with cellulose diacetate, Dr Markus Gobl of Lenzing Aktiengesellschaft – Lenzing (Austria) for providing us the Tencel fibres and to the Joong-Ang Special Industry Co., Ltd, Seoul (South Korea) for providing Glycerin Polyglycidyl Ether. The authors wish also to acknowledge Ms Irene Anguillesi for performing DMTA and TGA tests.

** This chapter was published on Composites: Part A 43 (2012) 2256–2268*

VII. REFERENCES

1. Yu L, Dean K, Li L. Polymer blends and composites from renewable resources. Progress in Polymer Science 2006;31:576-602.

2 .Mohanty AK, Misra M, Hinrichsen G. Biofibers, biodegradable polymers and biocomposites: An overview. Macromolecular Materials and Engineering 2000;276-277:1-24.

3. Scholz C, Gross RA (eds). Polymers from renewable resources - Biopolyesters and biocatalysis. In: ACS Symposium Series 764 2001, American Chemical Society, Washington DC.

4. Buchanan CM, Gardner RM, Komarek RJ. Aerobic biodegradation of cellulose acetate. Journal of Applied Polymer Science 1993;47:1709-1719.

5. Edgar KJ, Buchanan CM, Debenham JS, Rundquist PA, Seiler BD, Shelton MC, Tindall D. Advances in cellulose ester performance and application. Progress in Polymer Science 2001;26:1605-1688.

6. Filho GR, Monteiro DS, Meireles CdS, de Assunção RMN, Cerqueira DA, Barud HS, Ribeiro SJL, Messadeq Y. Synthesis and characterization of cellulose acetate produced from recycled newspaper. Carbohydrate Polymers 2008;73:74-82.

7. Meier MM, Kanis LA, de Lima JC, Pires ATN, Soldi V. Poly(caprolactone triol) as plasticizer agent for cellulose acetate films: influence of the preparation procedure and plasticizer content on the physico-chemical properties. Polymers for Advanced Technologies 2004;15:593-600.

8. Rao PR, Diwan PV. Permeability studies of cellulose acetate free films for transdermal use: Influence of plasticizers. Pharmaceutica Acta Helvetiae 1997;72:47-51.

9. Lee SH, Shiraishi N. Plasticization of cellulose diacetate by reaction with maleic anhydride, glycerol, and citrate esters during melt processing. Journal of Applied Polymer Science 2001;81:243-250.

10. Lee SH, Lee SY, Nam JD, Lee Y. Preparation of cellulose diacetate/ramie fiber biocomposites by melt processing. Polymer -Korea 2006; 30:70-74.

11. Lee SY, Cho MS, Nam JD, Lee Y. Melting processing of biodegradable cellulose diacetate/starch composites. Macromolecular Symposia 2006;242:126-130.

12. Rabinovich IB, Pet'kov VI, Zarudayeva SS. Physicochemical analysis of mixtures of cellulose diacetate with triacetin and thermodynamic characteristics of the process of mixing them. Polymer Science USSR 1985;27:2040-2047.

13. Jinghua Y, Xue C, Alfonso GC, Turturro A, Pedemonte E. Study of the miscibility and thermodynamics of cellulose diacetate-poly(vinyl pyrrolidone) blends. Polymer 1997;38:2127-2133.

14. Miyashita Y, Suzuki T, Nishio Y. Miscibility of cellulose acetate with vinyl polymers. Cellulose 2002;9:215-223.

15. Wang D, Xuan Y, Huang Y, Shen J. Synthesis and properties of graft copolymer of cellulose diacetate with poly(caprolactone monoacrylate). Journal of Applied Polymer Science 2003;89:85-90.

16. Takihara T, Yoshida Y, Isogai A. Reactions between cellulose diacetate and alkenylsuccinic anhydrides and characterization of the reaction products. Cellulose 2007;14:357-366.

17. Teramoto Y, Nishio Y. Cellulose diacetate-graft-poly(lactic acid)s: synthesis of wide-ranging compositions and their thermal and mechanical properties. Polymer 2003;44:2701-2709.

18. Lee SH, Teramoto Y, Wang S, Pharr GM, Rials TG. Nanoindentation of biodegradable cellulose diacetate-graft-poly(L-lactide) copolymers: Effect of molecular composition and thermal aging on mechanical properties. Journal of Polymer Science Part B 2007;45:1114-1121.

19. Mohanty AK, Wibowo A, Misra M, Drzal LT. Development of renewable resource–based cellulose acetate bioplastic: Effect of process engineering on the performance of cellulosic plastics. Polymer Engineering & Science 2003;43:1151-1160.

20. Wollerdorfer M, Bader H. Influence of natural fibres on the mechanical properties of biodegradable polymers. Industrial Crops and Products 1998;8:105-112.

21. Park HM, Misra M, Drzal LT, Mohanty AK. “Green” Nanocomposites from cellulose acetate bioplastic and clay: effect of eco-friendly triethyl citrate plasticizer. Biomacromolecules 2004;5:2281-2288.

22. Grunert M, Winter WT. Nanocomposites of cellulose acetate butyrate reinforced with cellulose nanocrystals. Journal of Polymers and the Environment 2002;10:27-30.

23. Seavey KC, Ghosh I, Davis RM, Glasser WG. Continuous cellulose fiber-reinforced cellulose ester composites. I. Manufacturing options. Cellulose 2001;8:149-159.

24. Seavey KC, Glasser WG. Continuous cellulose fiber-reinforced cellulose ester composites. II. Fiber surface modification and consolidation conditions. Cellulose 2001;8:161-169.

25. Franko A, Seavey KC, Gumaer J, Glasser WG. Continuous cellulose fiber-reinforced cellulose ester composites III. Commercial matrix and fiber options. Cellulose 2001; 8:171-179.

26. Carrillo F, Martin G, Lopez-Mesas M, Colom X, Canavate J. High modulus regenerated cellulose fiber-reinforced cellulose acetate butyrate biocomposites. Journal of Composite Materials 2011;45:1733-1740.

27. Panaitescu DM, Frone AN, Ghiurea M, Spataru CI, Radovici C and Iorga MD. Chapter 5: Properties of polymer composites with cellulose microfibrils in "Advances in composite materials - Ecodesign and analysis" book 2011:103-122.

28. Frone AN, Panaitescu DM, Donescu D. Some aspects concerning the isolation of cellulose micro and nanofibers. UPB Scientific Bulletin Series B 2011:1454-2331.

29. Renner K, Móczó J, Pukánszky B. Deformation and failure of PP composites reinforced with lignocellulosic fibers: Effect of inherent strength of the particles. Composite Science and Technology 2009;1653–1659.

30. Renner K, Kenyó C, Móczó J, Pukánszky B. Micromechanical deformation processes in PP/wood composites: Particle characteristics, adhesion, mechanisms. Composite Part A 2012; 1653–1661

31. Haward RN. The application of a simplified model for the stress-strain curves of polymers. Polymer 1987; 28:1485-88.

32. Cox HL. The elasticity and strength of paper and other fibrous materials. British Journal of Applied Physics 1952; 3:72-79.

33. Nardone VC, Prewo KM. On the strength of discontinuous silicon carbide reinforced aluminum composites. Scripta Metallurgica 1986;20:43-48.

34. Kim HG, Kwac LK. Evaluation of elastic modulus for unidirectionally aligned short fiber composites. Journal of Mechanical Science and Technology 2009;23:54-63.

35. Kim HG. A study on the prediction of elastic modulus in short fiber composite materials. Transactions of the Korean Society of Mechanical Engineers A 2005;29:318-324.

36. Kim HG. Effects of fiber aspect ratio evaluated by elastic analysis in discontinuous composites. Journal of Mechanical Science and Technology 2008;22:411-419.

37. Taya M, Arsenault RJ. A comparison between a shear lag type model and an eshelby type model in predicting the mechanical properties of short fiber composite. Scripta Metallurgica 1987;21:349-354.

38. Halpin JC, Kardos JL. The Halpin-Tsai equations: a review. Polymer Engineering and Science 1976;16: 344-352.

39. Tandon GP, Weng GJ. The effect of aspect ratio of inclusions on the elastic properties of unidirectionally aligned composites. Polymer Composite 1984;5:327-333.

40. Eshelby, JD. The determination of the elastic field of an ellipsoidal inclusion, and related problems. Proceedings of the Royal Society of London 1957;A241:376-396.

41. Mori T, Tanaka K. Average stress in the matrix and average elastic energy of materials with misfitting inclusions. Acta Metallurgica 1973;21:571–574.

42. Pukánszky B. Influence of interface interaction on the ultimate tensile properties of polymer composites. Composites 1990;21:255–262.

43. Robinson IM, Robinson JM, The influence of fibre aspect ratio on the deformation of discontinuous fibre-reinforced composites, Journal of Materials Science 1994;29:4663-4677.

44. Eichhorn SJ, Young RJ. The Young's modulus of a microcrystalline cellulose. Cellulose 2001;8:197–207.

45. Mirbagheri J, Tajvidi M, Ghasemi I, Hermanson JC. Prediction of the elastic modulus of wood flour/kenaf fibre/Polypropylene hybrid composites. Iran Polymer Journal 2007;16:271-278.

46. Számel G, Klébert S, Sajó I, Pukánszky B. Thermal analysis of cellulose acetate modified with caprolactone. Journal of Thermal Analysis and Calorimetry 2008;91:715-722.

47. Scandola M, Ceccorulli G. Viscoelastic properties of cellulose derivatives: 1. Cellulose acetate. Polymer 1985;26:1953-1957.

48. Gordon M, Taylor JS. Ideal copolymers and the second-order transitions of synthetic rubbers. i. non-crystalline copolymers. Journal of Applied Chemistry 1952;2:493-500.

49. Yuksel N, Baykara M, Shirinzade H, Suzen S. Investigation of triacetin effect on indomethacin release from poly(Methyl Methacrylate) Microspheres: Evaluation of Interactions Using FT-IR and NMR spectroscopies. International Journal of Pharmaceutics 2011;404:102-109.

50. Suvorova AI, Safronov AP, Mukhina EY, Peshekhonova AL. Thermodynamics of the interaction of Cellulose diacetate with plasticizer mixtures. Polymer Science USSR 1992;34:81-86

Chapter 3

Compatibilization of Poly(lactic acid)/Polycarbonate blends through reactive blending and *in-situ* copolymer formation

I. INTRODUCTION

The development of new materials derived from renewable sources is a goal of high technological and environmental importance. In this context, polymers derived from agricultural sources, such as polylactic acid (PLA) and its copolymers, are of great importance today [1]. Currently, one of the processes used in the production of PLA is that starting from corn starch [2]. Even though this product is of great interest, as compostable material derived by renewable resources, and has certain advantages when compared to traditional plastics, like high elastic modulus and transparency, the nature of polyester of PLA presents very important limitations such as high hydrolytic susceptibility, low thermal stability, brittleness and low crystallization rate. Improvement in PLA-based products are continuing either by the use of additives or through new formulation or copolymers. However, despite commercial advancements there is still considerable request for cost-effective methods to enhance PLA properties [2]. Its relatively low glass transition temperature (T_g), around 60°C, does not allow the polymer to maintain its mechanical properties in the temperature range during glass transition. Moreover, the possibility that further crystallization may occur at temperature values above the T_g may result in the dimensional instability of the manufactured items under the operating conditions. These features preclude the use of PLA-based materials in areas such as automotive parts, electrical and electronic equipment, as well as durable consumer goods such as mobile phones.

In principle, PLA-based materials that are able to maintain their mechanical properties in temperatures above T_g and below the melting temperature can be obtained:

a) by a crystallization process, either by reheating after moulding or through the use of nucleating and accelerating agents,

b) by physical mixing with a second polymer component, immiscible with the PLA, which is characterized by a glass phase having a high T_g [3].

In the instance of using crystallization, a well-known method is used where the PLA is reheated (annealed) after molding to improve the degree of crystallization; there is also the method of molding the PLA while a nucleating agent is added. The method of annealing after molding does not only present the problems of having a complicated molding process and a long molding period, but the annealing process requires the use of a die or something similar in order to avoid deformation involved with crystallization, therefore creating problems in terms of cost and productivity.

Regarding the method of adding a nucleating agent, the development of a crystallization nucleating agent to improve the degree and rate of crystallization is at an advanced state; however, even if a state-of-the-art crystallization nucleating agent is added, a crystallization period of about 2 minutes is required, and therefore it is not possible to use a molding cycle similar to that of a petroleum-derived and general-purpose resin. Furthermore, it is necessary to conduct crystallization at a temperature around 100 to 110°C, whereby it is not possible to conduct injection molding with a normal water cooled mold, presenting the problem of increasing the environmental impact due to a required high molding temperature. Moreover, when only polylactic acid is crystallized, a maximum heat deflection temperature (HDT) of around 55°C (at a load of 1.80 MPa) can be obtained even if sufficient crystallization is obtained through annealing or the like, whereby there is a problem of an insufficient heat resistance.

In order to avoid these problems, an investigation was carried out to prepare a copolymer by melt blending PLA with Polycarbonate (PC). In the patent literature blends of PLA with PC [4-6], as well as with some other commercially-available products [7-8] have been already described although with other

types of process. PC has been widely used as an engineering plastic with high thermal stability and mechanical properties (high tensile strength and elongation at break) [9]. However, most of the blends between different polymers are immiscible, and adhesion between the two polymers is weak due to high interfacial tension and weak entanglements. This happens when the polymers involved are incompatible. It is clear that the polymer system must exhibit a good adhesion between the phases in order to achieve good mechanical properties of polymer blends, and, above all, tensile strength.

There has been an extensive amount of literature investigating PLA blending and property modification, and its effects on characteristics such as biocompatibility or miscibility. In order to improve the compatibility between two immiscible components, a third component is added as a compatibilizer or catalyst in most cases. The compatibilizer can be either premade or formed *in situ* during melt blending. One successful application of reactive blending is the addition of peroxides to several PLA blends [10-13] by simultaneous melt blending. It was shown that the addition of peroxides to those polymers blends forms cross-linked and/or branched structures by heteroradical coupling reactions, which improve the compatibility of the polymer blends, the melt tensions, and the extrusion stability. The other reactive application is principally based on the reactions between end functional groups (i.e., A-OH or A-COOH) of PLA and other complementary functional groups (mainly epoxide groups) of the compatibilizers, for example, glycidyl methacrylate (GMA) [14-15], POE-g-GMA modifier [16], and the chain extension of PLA with multifunctional epoxide [17]. Similarly for polylactic acid, the blending of Polycarbonate with the other polymer ester improved phase interaction by using some coupling agent for reaction with both functional groups of two components [18 -19] or some catalyst for transesterification such as Dioctadecyl phosphate [20,21], Alkyl titanium [22], Tin(II) octoate [23], Tetrabutyltitanate [24], tetrabutylammonium tetraphenylboratetc [25], etc. Specifically, Polycarbonate was used as a good component for blending with polyethylene terephthalate (PET), which was known as a common polymer and widely applied over the last 20 years. Moreover, some studies applied transesterification to obtain the copolymer of PC and

semicrystalline PET to develop some advantageous properties such as transparency, stable processing, high thermal resistance and crystallinity of materials, etc. [20-23, 26-28].

However, PET is a polymer which can be recycled but that is not biodegradable. Nowadays, with the tendency of developing materials based on natural resources or more environmentally friendly, biobased-polymers and biocomposites have been the object of a growing interests both among researchers as well as industrialists. Of all the new biopolymers, PLA has become, over the past 10 years, the biopolymer with the fastest commercial growth, despite the previously mentioned disadvantages. Due to these reasons, only several studies were carried out on blended polylactic acid and polycarbonate (T_g ~160^{o}C)as to maintain the thermal resistance and to increase the biodegradation and recyclability of materials [23-24, 29-33].In particular, the literature makes reference to several patents and articles that described alloys based on PLA and aromatic polycarbonate (PC). However, the PLA/PC blends normally show a phase separation behavior and the interface between two phases is quite weak because of the high interfacial tension between polycarbonate and PLA. In these polymeric compounds, compatibilization agents of polymeric nature have also been used in order to improve the interface adhesion between the various phases. In these systems, however, the problem of limited compatibility between the phases due to the substantial difference in the chemical structure of the two components (PLA and PC) remains. Most studies used the extrusion method for processing, but the processing lasted over long periods of time (10 to 60 minutes). That condition is not realizable for industrial processing, because of the degradation of materials and of the energy cost. Although Kanzawa and Tokumitsu [33] added a toughening agent (PBAT) to PLA/PC blends, two steps of extrusion processing were needed and the thermal resistance was decreased by the presence of PBAT. In the other studies on PLA/PC blends [29-32], the thermal resistance and interface adhesion between the two components were slightly enhanced. Although the author used catalysts and compatibilizers for blending PLA and PC, little chemical evidence of their interaction could be demonstrated because of the presence of similar chemical functions in the polymer

chains of both polymers. Moreover, the biodegradation and thermal behavior of the blends were not much investigated.

From the above results, it is evident that there is a great need of new biodegradable copolymers based on polylactic acid and aromatic polycarbonates that maintain optimum mechanical properties, more specifically, tensile strength at temperatures that are higher than the glass transition of the PLA phase and preferably suitable for the production of materials for different industrial sectors such as transportation, electronics and the electrical equipment industry. In this work, new copolymers have been prepared by a process of reactive blending in the molten state, starting from mixtures of polylactic acid (PLA) and an aromatic polycarbonate (PC). The mixing conditions such as temperature and duration of mixing are selected to obtain interchange reactions between the base polymers. The procedure has been shown to lead to the obtainment of new materials with the structure of block copolymers, whose structure and molecular masses are advantageously adjustable by controlling the parameters of the mixing process. After that, the copolymer will be investigated regarding its mechanical properties, morphology, thermal and biodegradation behavior to satisfy the requirements of all the properties of these potential materials, which will serve for broadening the applications of bio-based polymers and composites to the market.

II. EXPERIMENTAL

2.1 Materials

Poly (L-lactic) acid was purchased from NatureWorks LLC having a nominal average molecular weight M_w = 199590 Da (IngeoTM 2002D Extrusion Grade), density 1.24g/cm^3. Polycarbonate of bisphenol A (Iupilon S3000) with a density of 1.20 g/cm^3 and average molecular weight M_w = 20 kDa was purchased from Mitsubishi Engineering Plastics. Triacetin (TA, also known as glycerin triacetate or 1,2,3-triacetoxypropane, CAS # 102-76-1) and Tetrabutylammonium tetraphenylborate (TBATPB, CAS # 15522-59-5) were purchased from Aldrich Chemicals. The chemical structure of these raw materials is showed in Scheme 1.

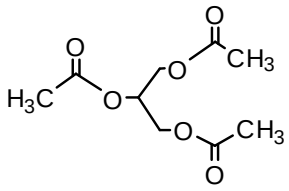

Triacetin (TA)

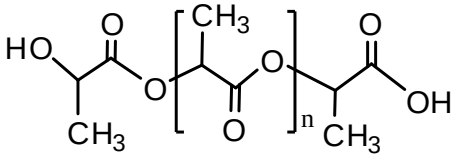

Polylactic acid (PLA)

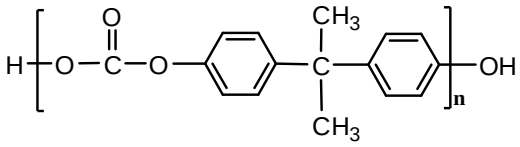

Polycarbonate Bisphenol A (PC)

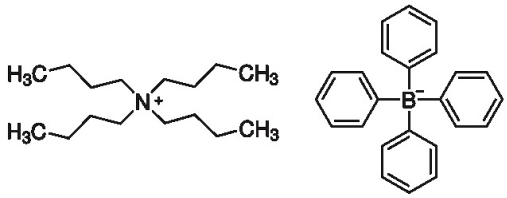

TetrabutylammoniumTetraphenylborate (TBATPB)

Scheme 1. Chemical structure of used raw materials.

2.2 Processing

The starting polymers were first dried at a temperature 60°C at a pressure of 1 mm Hg for four days. Then the polymers (PLA and PC) were mechanically mixed for about 10 minutes with different ratios of PLA/PC by means of a high speed mixer. After this mixing stage, the Triacetin and TBATPB were added and mixed for an extra 10 minutes using the same equipment. The resulting mixtures were processed with a MiniLab II Haake Rheomex CTW 5 conical twin-screw extruder (Thermo Scientific Haake GmbH, Karlsruhe, Germany).The mixing was conducted at a temperature of 210°C and 230°C with a screw speed of 100 rpm for a recycling time of one minute. After extrusion, the molten materials were transferred through a preheated cylinder to the Haake MiniJet II mini injection molder (Thermo Scientific Haake GmbH, Karlsruhe, Germany), to obtain ASTM D638 V dog-bone tensile bars used for measurements and analysis. The specimens were placed in plastic bags for vacuum sealing to prevent moisture absorption.

2.3 Characterization methods

Tensile tests were performed at room temperature, at a crosshead speed of 10 mm/min, by means of an Instron 4302 universal testing machine (Canton MA, USA) equipped with a 10 kN load cell and interfaced with a computer running the Testworks 4.0 software (MTS Systems Corporation, Eden Prairie MN, USA).

Differential scanning calorimetry (DSC) measurements were carried out for investigating the thermal behavior of materials with a TA Q200 instrument (TA Instruments, Newcastle, DE, USA) with nitrogen as the carrier gas and indium used for calibration. The samples were first heated from -100^{o}C to 250^{o}Cat 10^{o}C/min, and then cooled to -100^{o}C at 20^{o}C/min. Then, the second heating was investigated in the same conditions as the first heating.

Size exclusion chromatography (SEC) analysis was performed with a Jasco PLUS system consisting of a PU-2029 pump, CO-2063column oven set at 80^{o}C, RI-2031 differential refractometer, and UV-2077 UV detector, fitted with two PL-Gel Mixed D columns. Column calibration was performed with narrow distribution poly(styrene) standards. A 4 mg/mL solution of the polymer in THF (0.1% w/V) was filtered through a 0.2 mm membrane syringe filter and 20 mL was injected using the same solution as the eluent at 1 mL/min flow rate.

NMR ^{13}C spectra have been acquired on a BRUKER DRX400 Spectrometer in a deuterated chloroform. Excitation pulse for ^{13}C was calibrated to 30°C, and the repetition time was 1.5s. Proton irradiation was applied before each scan for Nuclear Overauser Enhancement and during FID acquisition of 1s for heteronuclear decoupling.

The chemical bonding of PLA and PC polymers was analyzed by using a Nicolet 380 spectrometer with Diffuse Reflectance Accessory (DRIFT). The composite was dissolved in choloroform, and the fibers were dried under a vacuum at 140^{0}C for 24 hours. The materials were mixed with potassium bromide (KBr) in order to obtain the DRIFT spectra. During the DRIFT measurement, pure potassium bromide was chosen as a background.

Thermogravimetric Analysis (TGA) was run under the flow of nitrogen gas at a scanning speed of 10 °C/min, from room temperature to 1000 °C, using a TGA 1000 instrument (Rheometric Scientific Inc., USA).

Dynamic mechanical thermal analysis (DMTA) was carried out on a Gabo Eplexor® 100N (Gabo Qualimeter GmbH, Ahlden, Germany). Test bars were cut from the tensile bar specimens (size: 20 x 5 x 1.5 mm) and mounted on a tensile geometry. The temperature used in the experiment ranged from -100 °C to 170 °C, at a heating rate of 2 °C/min and frequency of 1 Hz.

The morphology of the composites was studied by scanning electron microscopy (SEM) using a JEOL JSM-5600LV (Tokyo, Japan), by analyzing the fracture surfaces of the samples broken in liquid nitrogen. Prior to SEM analysis all the surfaces were sputtered with gold.

The transmission electron microscope (TEM) study, operated at 120 kV, was performed by using a JEOL 1210. The samples were trimmed with a Leica ULTRACUT E ultramicrotome room using a diamond-trimming knife and ultra-thin sectioned with a Leica ULTRACUT E ultramicrotome using a diamond knife. The section thickness was nominally 70 nm (setting).TEM-micrographs were made of representative areas of the samples at 3000X magnifications.

An aerobic biodegradability test of three materials was carried out under controlled composting conditions according to ISO 14855. The test materials were tested in the form of granulates. The composting inoculum was derived from an organic fraction of municipal solid waste that was aerated and stabilized under pilot-scale composting conditions over a period of more than 20 weeks. The compost was sieved to remove particles over 5 mm in size, and the fine fraction was then used as the inoculum. Control reactors contained only this inoculum without test material. The reactors were then placed in an incubator without light at 58°C ± 2°C and continuously aerated. During biodegradation, microorganisms present in the inoculum converted carbon in the reference or test material into CO_2. The gas leaving each individual reactor was analyzed at regular intervals for CO_2 and O2 content, and the gas flow rate was measured. Biodegradation was determined as the percentage of the carbon in the starting reference or test material

that was converted into CO_2. Continuation of the biodegradation test was possible since sufficient O_2 supply was present in the reactor headspace. The reactor also held a beaker containing an aqueous solution of KOH to absorb CO_2 released during the composting process. The tests were fully completed after 150 days.

II. THEORETICAL ANALYSIS

The Young's modulus of binary blends will change as the amount of polymers varies due to the different effects on the mechanical properties of constituent polymers and the phase behavior of blends. In the literature, there are several studies that attempt to predict the mechanical properties of binary polymer blends [34-35]. In particular Davies proposed for the modulus of blends with dispersed morphologies the following expression [34]:

$$E^{1/5}=\varphi_1 E_1^{1/5}+\varphi_2 E_2^{1/5} \qquad (1)$$

where $E_1$and E_2 are the elastic moduli of the two components.

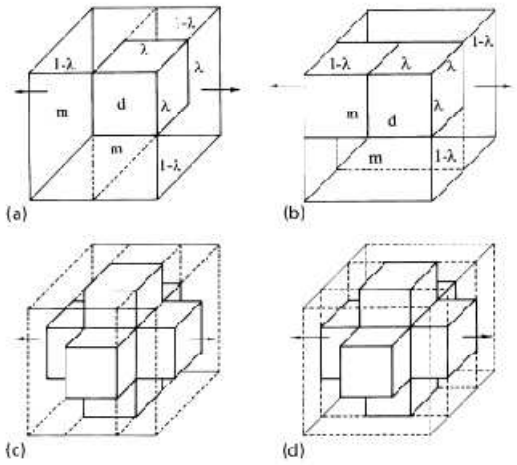

Figure 1. Three-dimensional models for the calculation of the modulus of dispersed polymer blends (a and b) and co-continuous polymer blends (c and d).

Another model to describe droplet/matrix blends, was proposed by Barentsen [35] who extended the combination of parallel and series elements as proposed by Takayanagi for two-dimensional geometries to a three-dimensional arrangement.

Barentsen's model can either be described as a series model of parallel parts (Fig. 1(a) and Eq. (1)) or a parallel model of serial linked parts (Fig. 1(b) and Eq. (2)). The unit cubes, as shown in Fig. 1(a) and (b), can be used for modeling polymer blends with a droplet/matrix morphology when the dispersed particles are evenly distributed in the matrix.

$$E_a = E_m \frac{\lambda^2 E_d + (1-\lambda^2)E_m}{(1-\lambda)\lambda^2 E_d + (1-\lambda+\lambda^3)E_m} \qquad (2)$$

$$E_b = (1-\lambda^2)E_m + \frac{\lambda^2 E_m E_d}{\lambda E_m + (1-\lambda)E_d} \qquad (3)$$

The modulus of the blend (E_a or E_b) is expressed as a function of a volume fraction ($\phi_d = 1-\phi_m = \lambda^3$), the modulus of the dispersed phase (E_d), and the modulus of the matrix (E_m).

However, in polymer blends, the morphology of the materials will be different as the proportions of each component vary. The morphology of the blends, which can show a changing phase behavior from phase-separation, to the formation of co-continuous phases and even phase inversion, will have a significant effect on the final properties and makes the prediction of such models, which do not consider the type of phase morphology, not fully reliable. In fact, both the Davies's and Barentsen's models, based only on the properties of the individual separated phases, do not fit well with the experimental data for co-continuous blends.

In a co-continuous morphology, the dispersed phase does not consist of separate particles in the matrix phase, but is interconnected and forms elongated domains, which extend throughout the matrix. To visualize co-continuity, Veenstra and co-workers proposed that the dispersed phases consist of three orthogonal bars of polymer 1 embedded in a unit cube where the remaining volume is occupied by

component 2. Repeating this unit cube in 3D shows that component 2 has the same framework as component 1, i.e. both the components are interconnected. In a similar manner to Barentsen, relations for a series model of parallel parts (Fig. 1(c) and Eq. (3)) and for a parallel model of serial-linked parts (Fig. 1(d) and Eq. (4)) can be derived [36] as:

$$E_c = \frac{(a^4 + 2a^3b)E_1^2 + 2(a^3b + 3a^2b^2 + ab^3)E_1E_2 + (2ab^3 + b^4)E_2^2}{(a^3 + a^2b + 2ab^2)E_1 + (2a^2b + ab^2 + b^3)E_2} \qquad (4)$$

$$E_d = \frac{a^2bE_1 + (a^3 + 2ab + b^3)E_1E_2 + ab^2E_2^2}{bE_1 + aE_2} \qquad (5)$$

Where *a* is related to the volume fraction of component 1 by $3a^2 - 2a^3 = \phi_1$ and *b* is related to the volume fraction of component 2 by $b = 1 - a$.

The model as depicted in Fig. 1(a) and equation (2) will be applied when the stiff component dominates and Fig. 2(a) and equation (3) as the stiff component is the minor phase. The same arguments can be used for the parallel model of serial-linked parts (Fig. 1(d) and Eq. (5)) and the series model of parallel-linked parts (Fig. 1(c) and Eq. (4)) that were derived for co-continuous blends.

IV. RESULTS AND DISCUSSIONS

4.1 The effect of processing conditions

To find the best conditions for processing Polylactic acid (PLA) and Polycarbonate of bisphenol A (PC) in extrusion, we chose the blend with PLA/PC having 40% and 60% in weight, respectively. The blends were processed with the temperatures and catalysts following the table below

Blends	PLA (wt%)	PC (wt%)	TBA-TBP (wt%)	Triacetin (wt%)	Extrusion temperature (^{o}C)
Blend 1	40	60			210
Blend 2	40	60		5	210
Blend 3	40	60	0.2		210
Blend 4	40	60	0.2	5	210
Blend 5	40	60			230
Blend 6	40	60		5	230
Blend 7	40	60	0.2		230
Blend 8	40	60	0.2	5	230

Table 2. Compositions of the blends PLA40/PC60 with different types of catalyst, and their processing temperatures.

Mixing was conducted at temperatures of 210°C and 230°C with a screw speed of 100 rpm, for a recycling time of 1 minute. The material was then injection moulded into ASTM D638V tensile bars. The chamber temperature was 210°C, the mould temperature 50°C, injection time 20s, and the injection pressure 790 mm Hg. Afterwards, the moulded samples were annealed at 80°C for 48 hours at a pressure of 1 mm Hg. The specimens for dynamic-mechanical analysis were obtained from the tensile bars. The samples were tested by using dynamical-mechanical thermal analysis (DMTA) and tensile testing.

4.1.1 Mechanical properties

Blend 1 is just a mechanical blend since no catalyst or co-catalyst was added. The mechanical behavior of this blend was very poor, as indicated by a tensile strength of 54.6 MPa and an elongation at break of 5.1%, as shown in Table 2, because of the reduced compatibility of the two starting polymers.

Blends	Tensile strength (MPa)	Young's modulus (GPa)	Elongation at break (%)
Blend 1	54.6	2.97	5.1
Blend 2	63.1	3.21	98.7
Blend 3	50.7	3.07	2.3
Blend 4	65.5	3.14	46.5
Blend 5	62	3.03	96.4
Blend 6	65.1	3.25	100.7
Blend 7	63.9	3.14	46.9
Blend 8	68.6	3.2	35.3

Table 2. Mechanical properties of the PLA40/PC60 blends.

The corresponding mechanical blend extruded at 230°C. Blend 5, showed a better mechanical behavior, associated with an elongation at break of 95.5%. This means that a higher extrusion temperature induced some transformations leading to improved compatibility. Blend 2 where triacetin was used as a catalyst displayed very ductile behavior, with an elongation at break of98.7%, an indication of excellent compatibility between the two polymer phases: PC-rich and PLA-rich. Blend 3was even more brittle than Blend 1, with an elongation at break of 2.3%, meaning that TBATPB is not active as a catalyst at this temperature (210 °C) because of the limited mixing time achievable in a twin-screw extruder. Blend 4, where both TBATPB and triacetin was added, showed even better mechanical properties than Blend 3, with a tensile strength of 65.5 MPa (corresponding to a 20.0% increase with respect to the mechanical blend), while maintaining an excellent value of elongation at break reaching 46.5%, thus showing the synergistic action of the TBATPB-triacetin co-catalyst system.

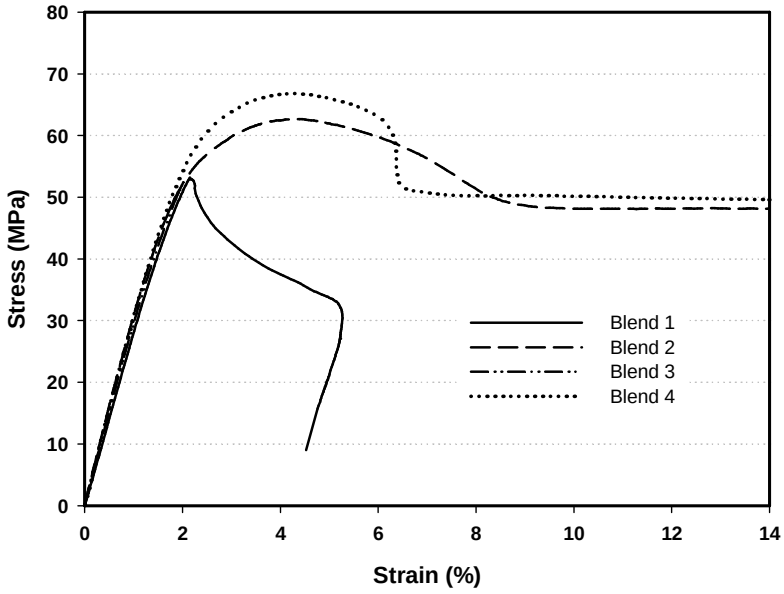

Figure 2. Tensile curve of the blends PLA40/PC60 with different types of catalysts at 210°C.

This is confirmed by comparing the stress-strain curves of the blends prepared at 230°C. As mentioned above, Blend 5, the simple mechanical mixture, shows a rather ductile behavior, with a tensile strength of 62 MPa and an elongation at break of 96.4%; but both Blends 6 and 7 show an increased yield strength of 65.1 and 63.9 MPa as well as an elongation at break of 100.7% and 46.9%, respectively. This indicates that both TBATPB and triacetin are active as catalysts at this temperature. The best mechanical performance is shown by Blend 8 where both catalysts are added during the extrusion, with a tensile strength of 68.6 MPa (with an increase of 12.1% respect to the mechanical mixture), while maintaining a very good elongation at break of 35.3%, thus confirming the synergistic action of the TBATPB-triacetin co-catalyst system in promoting the compatibility of the PLA-PC system by means of the formation of a copolymer.

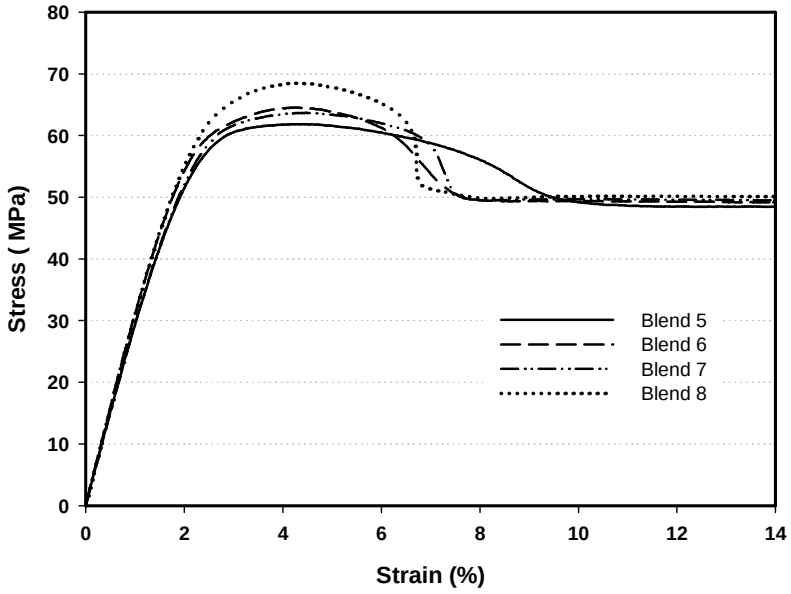

Figure 3. Mechanical properties of the blends PLA40/PC60

with different types of catalysts at 230°C.

4.1.2 DMTA (Dynamic mechanical thermal analysis)

The dynamic-mechanical analysis data, performed on rectangular samples having 10 dimensions of 20x5x1.5 mm, were analyzed in the range of temperature −100°C to 250°C with a heating rate of 2°C/min, and a frequency of 10 Hz. From the point of view of dynamical mechanical properties, the traces obtained by plotting tan δ versus temperature show a new peak that does not occur in the case of a simple physical mixture of two homopolymers. This new peak appears at a temperature T_{gp} lower than the T_g of PC. This aspect can be related to the presence of PC-blocks in the copolymer.

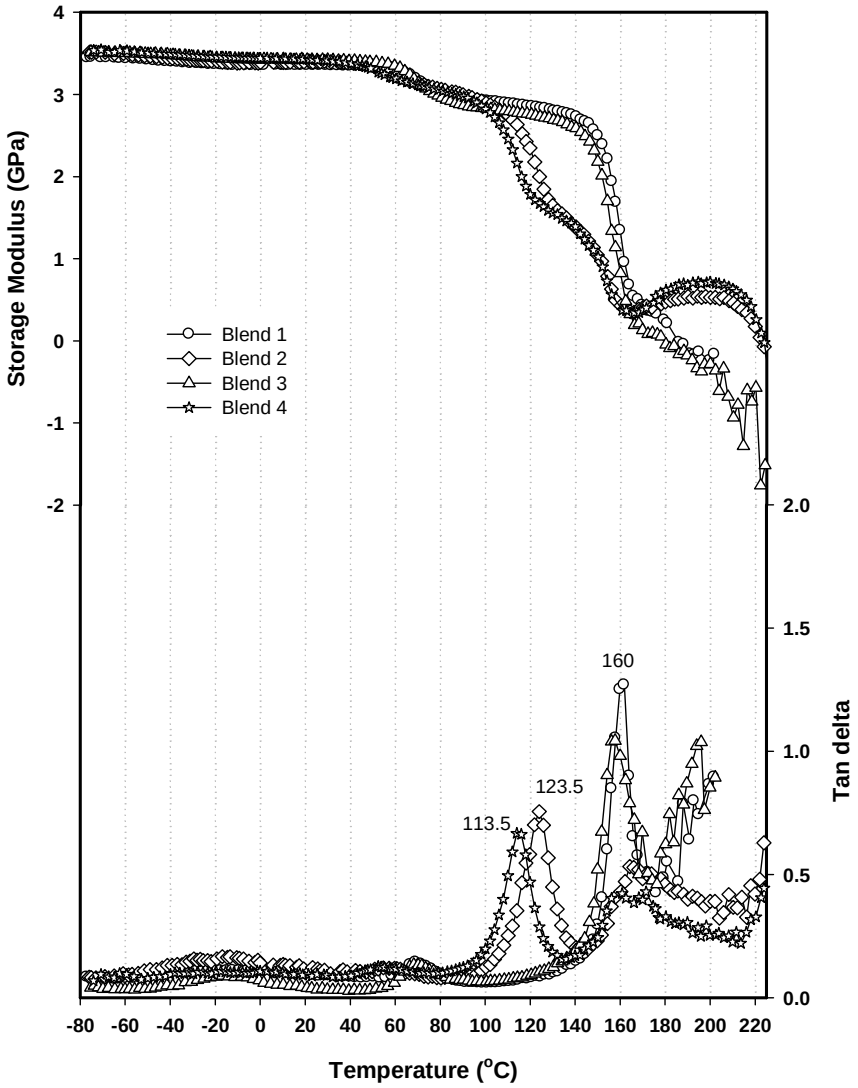

Figure 4. DMTA of the blends PLA40/PC60 with

different types of catalysts at 210°C.

For example, in Figure 3 for the blends extruded at210°C, these new peaks appear for Blend 2 (catalyst: triacetin only) and Blend 4 (TBATPB-triacetin co-catalyst system) at 123.5°C and 113.5°C, respectively, while they are not present for Blend 1 (mechanical mixture) and Blend 27 (catalyst: TBATPB only).

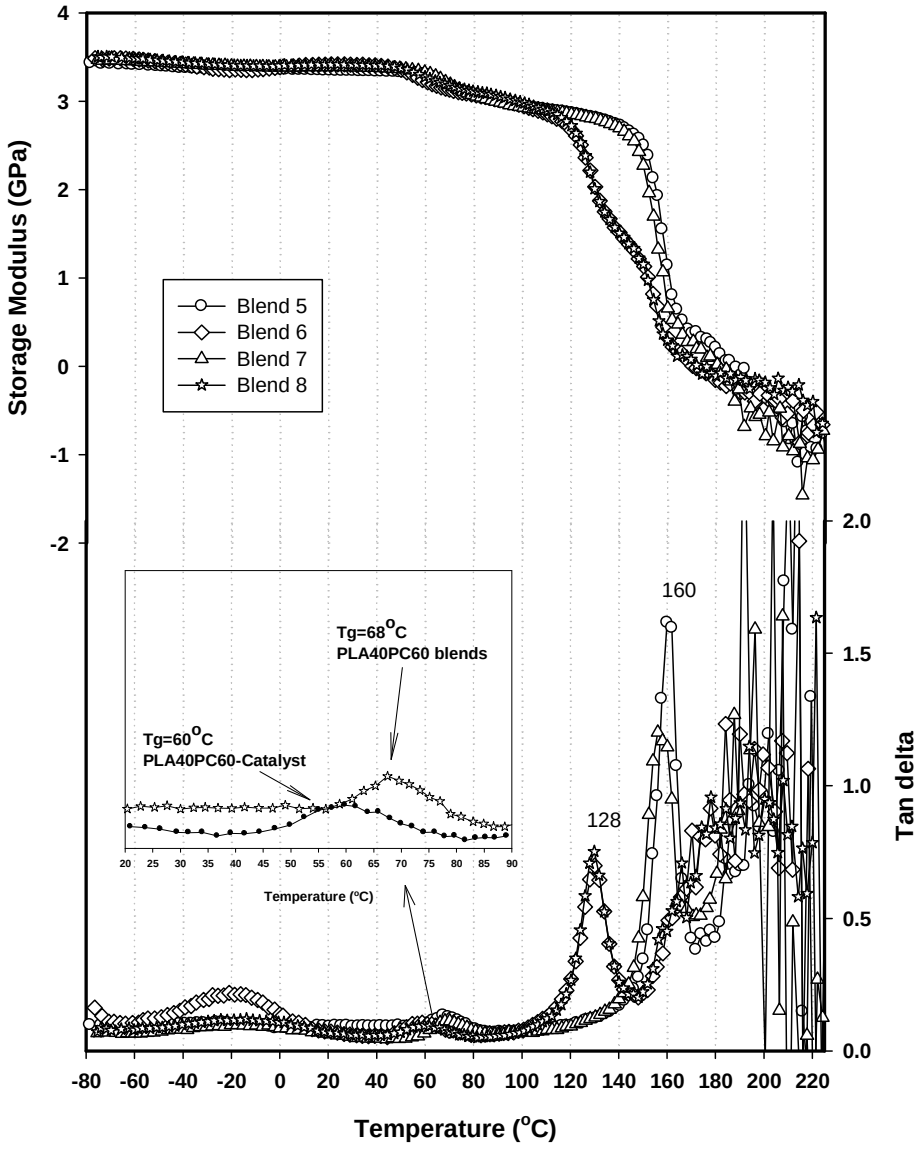

Figure 5. DMTA of the blends PLA40/PC60 with different types of catalysts at 230°C.

A similar analysis for the DMTA data shown in Figure 4 for the blends prepared at230°C can be carried out. Blend 6 (catalyst: triacetin only) and Blend 7 (TBATPB-triacetin co-catalyst system) show a new peak at 128°C, while the mechanical blend (Blend 5) shows a peak associated with the T_g of the PC phase at 160°C. Blend 31, where TBATPB is used as a catalyst, shows a peak at a slightly lower temperature, 155°C, and this can be explained with the occurrence of the transterification reaction leading

to PC blocks with lengths shorter than in the mechanical blend. The analysis of the DMTA data is consistent with the fact that these materials show a polyphase structure consisting of PLA domains dispersed in a matrix of PC, or vice versa, depending on the volume ratio of the components. In addition, for the PLA rich phase, there is an amorphous phase and a crystalline phase. The T_g transition temperatures of both PLA (50-70°C) and PC (155-160°C) are not, in general, much different from typical values of the two polymers PLA and PC, but a new peak appears at intermediate temperatures (110-130°C) for the copolymer.

A comparison is also made in Figure 5 between non-annealed samples of pure PLA, Blend 1 and Blend 4, showing how both blends have a much higher Young's modulus across and beyond the Tg of PLA. Also the modulus of PLA tends to increase starting from about 80°C to 120°C where it reaches a new maximum. This is associated to the partial crystallization of the PLA phase. A similar phenomenon is present in Blend 1, although with a much more limited entity, while it is not visible for Blend 4. This can be explained by the block-copolymer nature of this material. The PLA-blocks are shorter than in pure PLA or in the mechanical mixture with PC. Moreover, they are surrounded by rigid PC blocks that strongly limit molecular mobility and hinder the crystallization process. As proof of this statement, we can observe an increase in the modulus of Blend 4 above 160°C, which corresponds to the T_g of the PC blocks, up to 200°C, where the Young's modulus of the blend reaches a new maximum. This can be explained by the fact that when the PC-blocks are beyond their T_g, the PLA blocks recover their mobility and are able to crystallize.

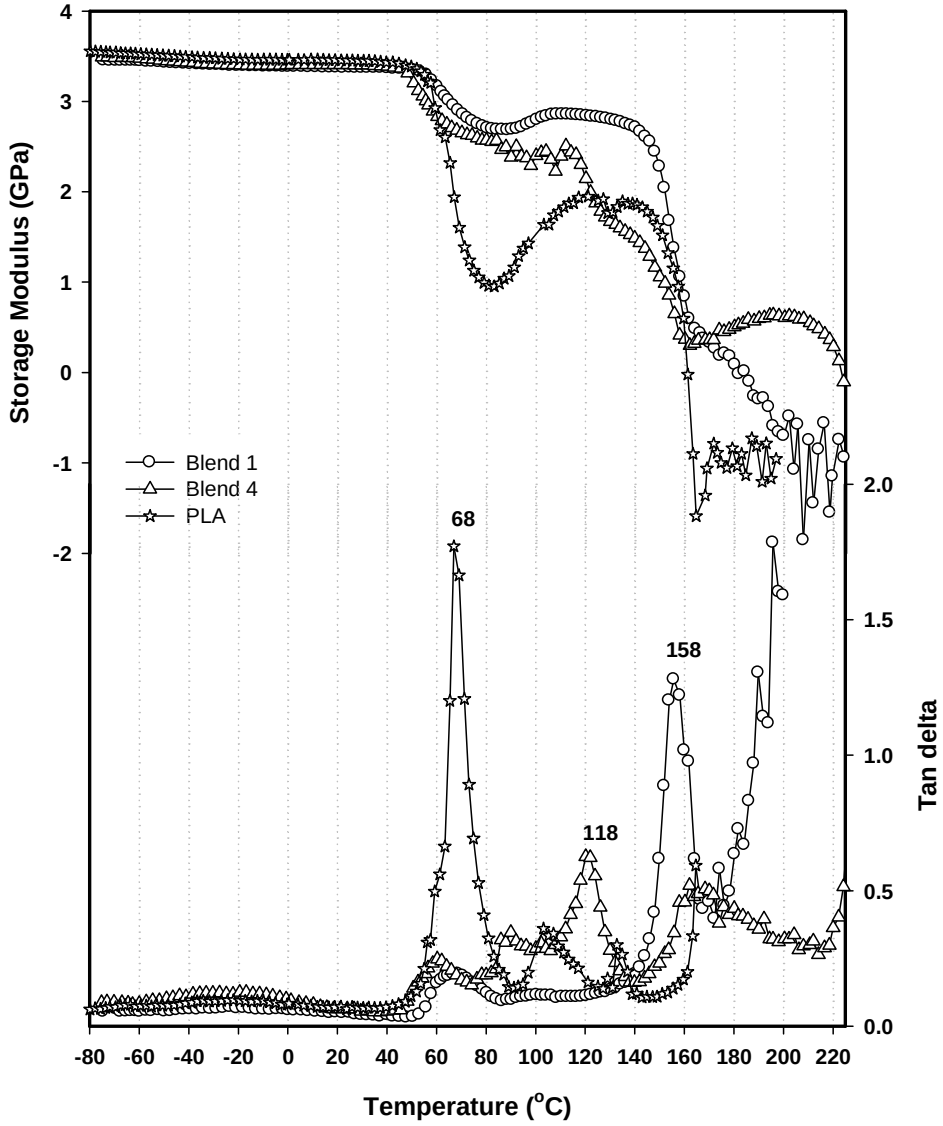

Figure 6. Comparison the storage modulus of materials by DMTA.

4.1.3 Thermogravimetric Analysis (TGA)

The thermogravimetric and derivative thermogravimetric curves of PLA40PC60 (Blend 1 to Blend 4) with and without catalyst at 210^{o}C are reported in Figures 8a and 8b, respectively, the corresponding data are accounted for in Table 3.

Formula	$T_{-10\%}$ (^oC)	$T_{-50\%}$ (^oC)	$T_{-70\%}$ (^oC)	T_{max}	Solid residue (%) at 800^oC
PLA	320.62	347.78	355.51	356.1	1.8
BLEND 1	346.32	389.49	430.43	358.75	8.9
BLEND 2	325.36	373.64	411.82	341.3	7.9
BLEND 3	341.14	385.32	423.01	353.48	8.0
BLEND 4	332.16	377.41	413.93	351.51	7.7
BLEND 5	335.71	379.05	412.06	349.72	7.4
BLEND 6	329.52	376.53	428.72	353.2	8.2
BLEND 7	330.7	372.6	397.02	356.2	7.3
BLEND 8	329.25	371.42	419.69	345.5	8.6
PC	439.4	506.1	528.54	508.95	21.34

Table 3. TGA and DTG of PLA40PC60 with and without catalysts in different processing temperatures.

The pure PLA degrades in a single step starting from 280^{o}C to the final temperature 427^{o}C, with a DTG peak temperature (T_{max}) at 356^{o}C. The T_{max} is the temperature at the maximum rate of weight lost, that is, the decomposition temperature. Moreover, the polycarbonate bisphenol A showed the degradation behavior in air with two stages. The main stage starts from 435^{o}C and ends at about 700^{o}C with 21.3% solid residue, the T_{max} of the main stage is 509^{o}C. A shoulder peak appears at 419^{o}C before the main peak. From the literatures, some complex chemical reactions take place at the first stage of thermal oxidative degradation including the free radical chain scission of the isopropylidene linkage and the branching and crosslinking reaction of molecular chains included by oxygen besides the reaction in inert atmosphere

[37]. Lee and Jang [38, 39] suggested that the initial step of thermal oxidative degradation of PC is an oxidative hydrogen cleavage from the isopopylidene linkage and then carbon-carbon scission, followed by hydrolysis and alcoholysis of carbonate. Oxygen may facilitate free radical branching reaction via the formation of peroxides and a high cross-linked structure with diaryl ester; ether and unsaturated carbonaceous bridges are formed above 440^{o}C.

The blends of PLA40PC60 with and without different catalysts at the processing temperature 210^{o}C created two main stages of degradation. The first stage is Polylactic acid and the second stage is polycarbonate bisphenol A. The degradation of the blend starts at the starting temperature of PLA and finishes at 547^{o}C before the end temperature of polycarbonate of bisphenol A. This thermal behavior is quite similar to the blends that were processed at 230^{o}C, which was shown in Figures 9A and 9B. Following the table and figures, the T_{max} of PLA in both cases did not also change with the presence of a catalyst. However, the T_{max} of PC was changed from 509^{o}C in pure polymer to 455^{o}C in blends. This phenomenon could possibly be explained by the fact that the degradation product of PLA could have facilitated the thermal degradation of PC. In both processing temperatures, the DTG peak of PLA degradation of blends is broader than in pure PLA, meaning that the thermal resistance of materials increases with the effect of polycarbonate. Moreover, the residual solid of the blends ranged between 7.2 and 8.5%, almost leaving behind the product of degradation PC. More specifically, Blends 2, 4, 6, and 8 having Triacetin as a catalyst, appeared to have a slight peak from 120^{o}C to 220^{o}C, and T_{max} of this peak was 180^{o}C. This peak was far from the boiling and degradation temperatures of Triacetin, 260^{o}C and 312^{o}C, respectively [40]. Thus, this peak started near the boiling temperature of acetic acid; we suggest that the Triacetin molecule could be broken down or could react in the presence of PLA and PC in order to formulate acid acetic or other hydrocarbon functions or molecules. However, this evidence needs to be carefully studied in the future with the support of FTIR and NMR in different decomposition temperatures of PC and PLA.

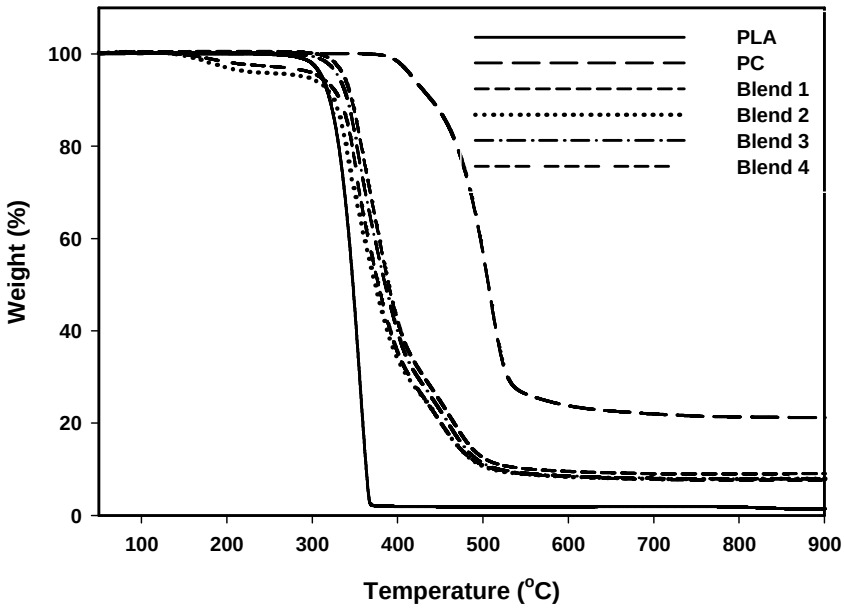

Figure 7A. TGA of the blends PLA40/PC60 with different types of catalysts at 210°C.

Following the data from Table 3, the temperature for obtaining 10% and 50% degradation percentages ($T_{10\%}$, $T_{50\%}$) of all blends at 230°C is quite similar until 400°C. After that, the decomposition temperatures ($T_{70\%}$) of blends at 70% degradation is different with and without a catalyst, which can be seen clearly in the small square in Figure 9A.

The increasing thermal resistance in the stage of Polycarbonate indicated that there are some specific interactions or chemical reactions between polylacticacid and polycarbonate of bisphenol A, which is quite similar to the thermal behavior of poly (vinyl chloride)/ethylene-vinyl acetate copolymer blends [41]. This fact is compatible with the analysis of DMTA and the tensile test above.

After investigating the effect of catalysts and temperatures on the formulation of copolymers in the blends, the middle peak (T_g ~128°C) between the T_g of PLA and PC in blends in DMTA testing serves as constructive evidence to confirm that the copolymer was formulated with the presence of Triacetin. It is possible that the reaction between PLA and PC could reach a maximum as processing at 230°C and with multiple catalysts (TA and TBATPB) thanks to the result above.

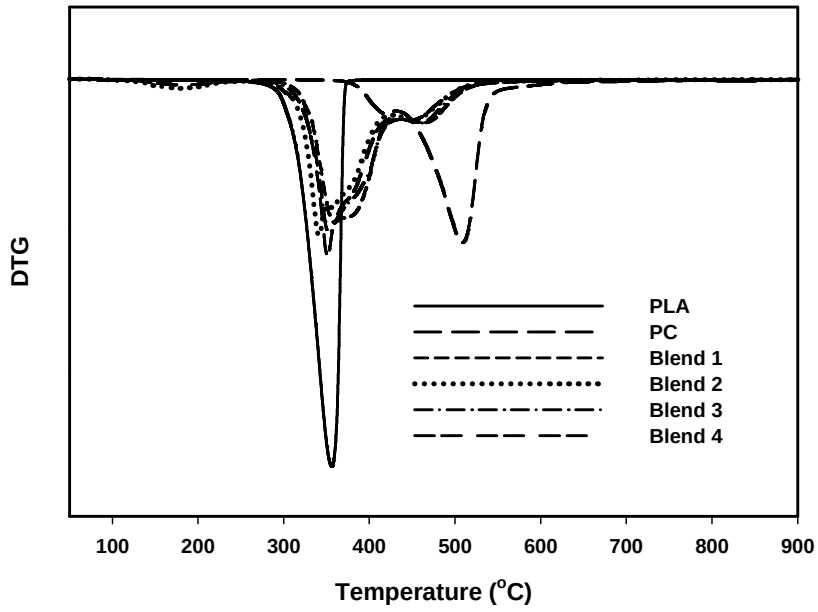

Figure 7B. DTG of the blends PLA40/PC60 with different types of catalysts at 210°C.

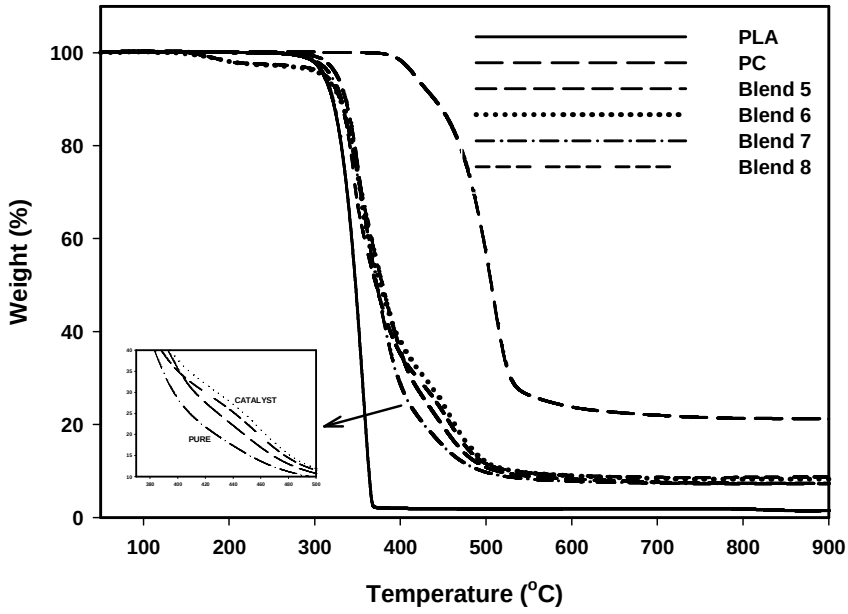

Figure 8A. TGA of the blends PLA40/PC60 with different types of catalysts at 230°C.

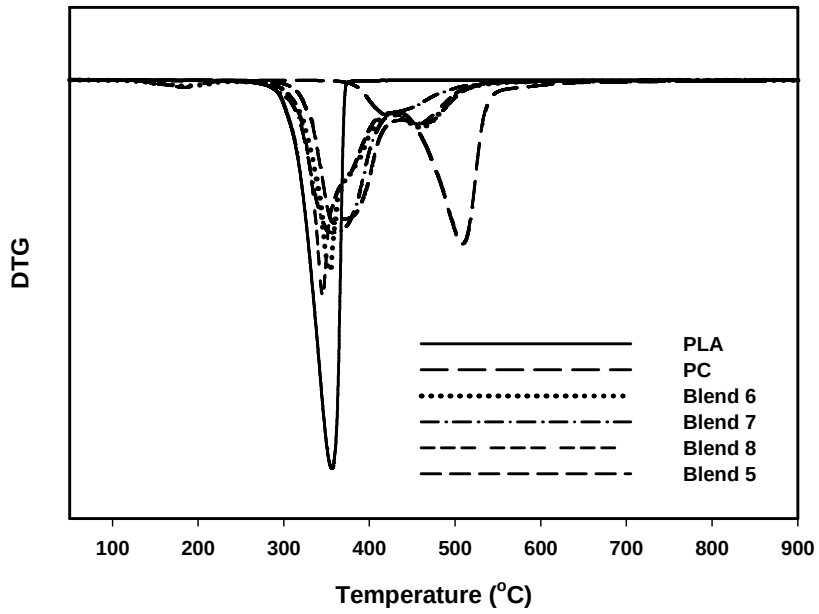

Figure 8B. DTG of the blends PLA40/PC60 with different types of catalysts at 230°C.

Following this part of research, it was decided to process the materials at 230°C with multiple catalysts for the investigation of different compositions of PLA and PC blends as changing in weight percent of each component and their characterization in terms of tensile tests, chemical analysis, and thermal, morphological and biodegradation analysis. This investigation will establish if most advantageous properties of PLA/PC blends occur at certain composition as well as the optimimum processing conditions in view of industrial applications.

4.2 Investigation of the full range of compositions

4.2.1 Mechanical properties

The mechanical properties of the blends of PLA and PC, at varying amount of their composition, are shown in Table 4. The tensile strength, Young's modulus and elongation at break of pristine Polycarbonate are 57.2 MPa, 2.25 GPa and 84.4%, respectively.

Blends	Tensile strength (MPa)	Young's modulus (GPa)	Elongation at break (%)
PC	57.2 ± 0.8	2.25 ± 0.06	84.4 ± 4.3
PC70PLA30	55.3 ± 0.3	2.86 ± 0.07	125 ± 3.3
PC60PLA40	55.2 ± 0.7	2.99 ± 0.17	126 ± 3.4
PC40PLA60	56.1 ± 0.7	2.98 ± 0.03	3.3 ± 0.5
PC30PLA70	51.1 ± 1.7	3.18 ± 0.08	2.3 ± 0.4
PC20PLA80	52.5 ± 2.3	3.38 ± 0.19	2.0 ± 0.1
PLA	60.4 ± 0.26	3.54 ± 0.12	4.1 ± 0.5

Table 4. Mechanical properties of physical blends with different amounts of PLA and PC.

As the amount of PLA increases, the Young's modulus of blends increases up to 3.54 GPa, i.e. the Young's modulus of pure Polylactic acid. The tensile strength of the blends do not change because of the tensile strength of pure PLA and PC is quite similar. However, the elongation at break of blends decreases from 126% for the blend with 60wt% PC down to 3.3 for the blend with 40 wt% of PC and neat the value of 4.1% for pure PLA. This point can be explained by a phase inversion, occurring around 50%, from a situation where PC is the matrix and PLA the dispersed phase to another condition where PLA is the continuous phase and PC is the discontinuous phase. It was worth noting that the elongation at break for the blend with 60wt% PC reaches the value of 126%, which is significantly higher than that of pure PC (84%), evidencing a strong toughening effect of the PLA domains in these blends.

Figure 9. Young's modulus of the blends with different amounts of PLA/PC, processed both in presence of catalysts and without (physical blends). The experimental data appear to fit well with Barentsen's model [35] at the two extremes of the composition range. In the middle range, the Young's modulus of the blends is substantially higher than what predicted by the Barentsen's model. A better fit can be obtained with the model proposed by Veenstra and his co-workers [36]; the higher values of

Young's modulus can be explained by a co-continuous phase behavior [43]. Moreover, the Young's modulus approached the parallel model and appears to be isotropic, which means that in these blends both phases fully contribute to the blend modulus in all directions. These results follow the general phase behavior of polymer blends [42] and have been confirmed by the morphological analysis (Figures 17 and 18 below). However, the big difference of elongation at break between PLA40PC60 and PLA60PC40 indicates that the phase inversion can occur at about 50 wt% of PLA. Above this concentration, the elastic modulus followed the trend predicted for a rigid PLA-rich matrix phase, with the PC domain dispersion; that is why the experimental data are fitted again with Barentsen's model, and the elongation at break rapidly decreased to the values characteristics of pristine PLA.

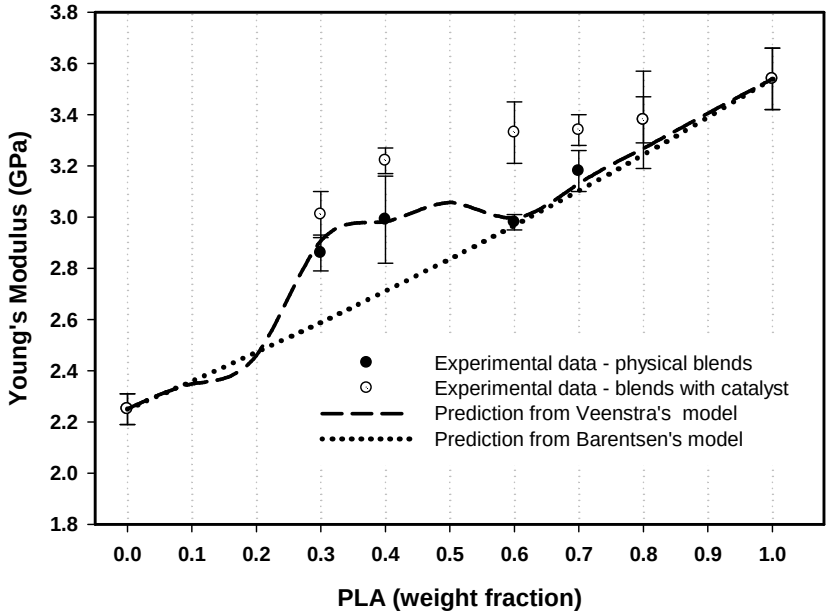

Figure 9. Young's modulus of the blends with different amounts of PLA/PC. Comparison between experimental data and theory prediction.

In figure 9, for the droplet/matrix morphologies, equation (2) has been used up to 20 wt% when PLA, the stiff component, is the matrix, while from 80 wt% to 100 wt%, where the stiff PLA component is the minor phase, equation (4) has been applied. In the case of co-continuous morphologies, when the

stiff PLA component dominates, from 50wt% to 60 wt% PLA, equations (3) has been used. In the range 20 wt% to 50 wt% PLA, equation (5) has been used. With these calculation, the experimental data and the theoretical models fit in a quite satisfactory way.

	Tensile strength (MPa)	Young's modulus (GPa)	Elongation at break (%)
PC	57.2 ± 0.8	2.25 ± 0.06	84.4 ± 4.3
PC70PLA30	58 ± 0.6	3.01 ± 0.09	110 ± 5.3
PC60PLA40	60.9 ± 0.7	3.22 ± 0.05	126 ± 3.6
PC40PLA60	51.9 ± 2.4	3.33 ± 0.12	2.0 ± 0.12
PC30PLA70	49.1 ±1.6	3.34 ± 0.06	1.8 ± 0.1
PC20PLA80	48.9 ± 1.1	3.38 ± 0.09	1.65 ± 0.1
PLA	60.4 ± 0.26	3.54 ± 0.12	4.1 ± 0.5

Table 5. Mechanical properties of blends with different amounts of PLA/PC with catalysts.

The Young's modulus of PLA/PC binary blends fit well the model of Veenstra [36] as can be seen in Figure 9. However, at all compositions, the Young's modulus of the blends prepared in the presence of a catalyst is always higher than the elastic modulus for the corresponding physical blends, as can be noted comparing the data in Tables 4 and 5. The Young's modulus of blends decreases for PC contents from 0 wt% to 30 wt% and then does not change much from 30 wt% to 40 wt%, which indicates that the materials start to reach a co-continuous phase morphology, which is similar to the behavior observed for physical blends.

It is interesting to observe that the experimental data of Young's modulus for the blends prepared in the presence of a catalyst is even greater than the theoretical predictions. Also the composition range for full co-continuity seems to be widened from 30-60 wt% PLA, for the physical blends to 20- 60 wt% PLA for the blends obtained in presence of the catalyst system. This can be explained by a reduced

interfacial tension for these blends, and is consistent with the hypothesis of the formation of a copolymer between polylactic acid and polycarbonate of bisphenol A, as a consequence of transesterification reaction between PC and PLA

4.2.2 Thermal behavior

The thermal behavior of materials was investigated by differential scanning calorimetry (DSC). Figure 10 shows the thermogram of the second scan with a heat rate of 10°C/minute.

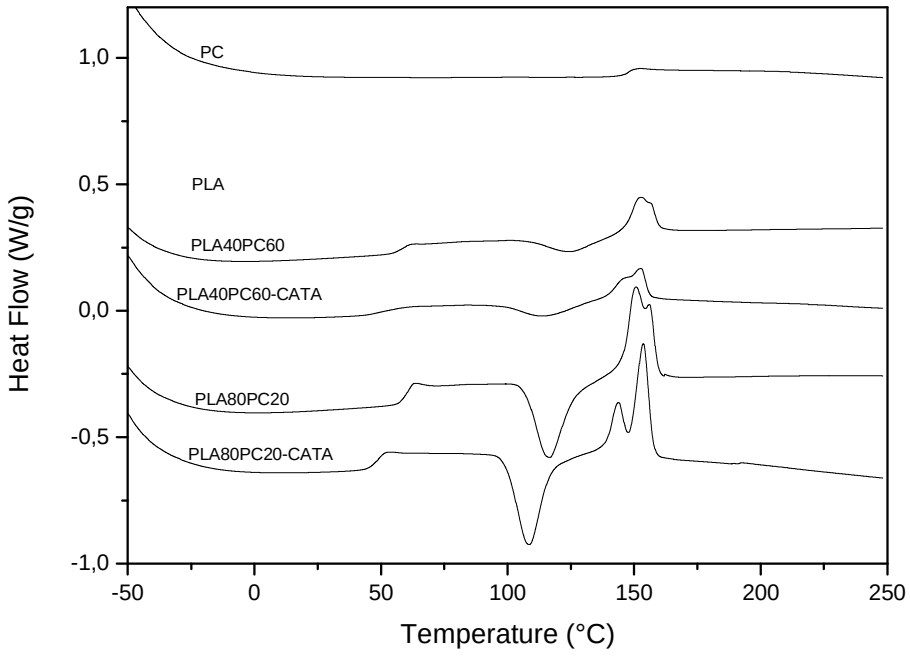

Figure 10. DSC thermogram(2nd scan) for PLA/PC blends prepared with and without catalysts.

The crystallinity of materials was calculated by using the formula $X_c = \frac{\Delta H_m / \phi_{PLA}}{\Delta H^0_m} * 100\%$, where ΔH^o_m is the theoretical heat of fusion of 100% crystalline PLA with a value of 93 J/g [40]. Upon the second scanning, the melting of pure PLA showed two peaks, which means that there are two types of crystalline phases in PLA. According to several studies, the crystalline phase of PLA depends on the crystallization temperature processing [45, 46]. Therefore, the disorder α' and order α phase of poly (L-

lactide) crystalline phases are formed at low (T_c< 100^{o}C) and high (T_c≥ 120^{o}C) temperatures, respectively. In our case, with the heat rate at 10^{o}C, 100^{o}C < T_c ≤120^{o}C, PLA crystalline formulated at the disorder-to-order phase transition, which was investigated by Zhang and his co-workers [47].

The glass transition temperature of pure PLA and PLA in blends did not differ and remained at about 59.1^{o}C, also in different formulations. However, this decreases to 48.8^{o}C with the existence of a catalyst in blends at 20% and 60% weight of PC. This fact indicates that Triacetin not only works as a catalyst, but also plays the role of a plasticizer on the Polylactic acid [48] because of the remaining triacetin amount. This is in agreement with the TGA data in Figures 7 and 6. Triacetin can reduce the interaction between polymer chains. The materials will be softer and can move easier to the glass state as the temperatures increase. Moreover, the crystalline temperature peak of PLA in blends is higher than pure in PLA because of the steric hindrance of polycarbonate chains on the crystallization of PLA. In addition, polycarbonate phases is an amorphous states, which affects to the percentage of crystallization process of PLA or (X_c) in the blends. Similar to the explanation above on the T_g, the action of the catalysts make the crystalline temperature peak of PLA in blends decrease, thereby increasing the percentage of crystallinity in all formulas as well as formulating the new disorder α' crystalline phase.

More specifically, the X_c of PLA in PLA80PC20-CATALYST is higher than the crystallinity percentage of pure PLA due to the effect of the catalysts. At low amounts of PC, the catalyst easily broke down the PC chains, and the broken chains will lower molecule weight than those of the original PC chains in blends without a catalyst. Hence, the polymer chain of PC is long and harmless for dispersion of the PLA phase matrix. Therefore, the dispersion of PLA will increase, and the PC molecules will avoid neighboring PC molecules. In this way, they can formulate a uniform complex in order to develop the crystalline of PLA, which acts as a nucleation in PLA. This phenomenon is similar to the role of PDLA in the crystalline processing of PLA in the study of Yamane and Sasai [49]. To the contrary, at high amounts of PC, the molecule will be large and voluminous; therefore it will very difficult to create the uniform complex with PLA or to prevent the crystalline formulation of PLA, which is clearly shown on the

thermogram of PLA40PC60 and PLA80PC20 by adding a catalyst. In this case, the crystalline percent of PLA is very low also when adding catalysts. The melting peak is not very clear, similar to the data of DMTA, so the materials can maintain the mechanical properties at high temperatures.

	T_g (°C)	T_{onset} (°C)	T_{cp} (°C)	ΔH_c (J/g)	ΔH_m (J/g)	ΔH (J/g)	X_c (%)
PLA	59,1	97,3	110	26,6	31,7	5,5	5,5
PLA80PC20	60,2	105,5	116,8	16,7	19,3	2,6	2,8
PLA80PC20-CATALYST	48,8	94,6	108,5	18,9	24,5	5,6	6,0
PLA40PC 60	58,8	109,2	125	2,1	3,4	1,3	1,4
PLA40PC60 - CATALYST	48,7	95,4	114,5	1,7	3,4	1,7	1,8
PC	147,4						

Table 6. Thermal analysis of blends by DSC testing.

The dynamic mechanical thermal analysis of blends without a catalyst was shown in Figure 11 after a crystalline at 80^{o}C in 24 hours. The first peak on the tan delta curve is the relaxation of pure PLA at 69^{o}C. The tan delta curve usually indicates the relaxation processes of the polymer. The major relaxation process is associated with the glass transition temperature (T_g) of PLA [50].

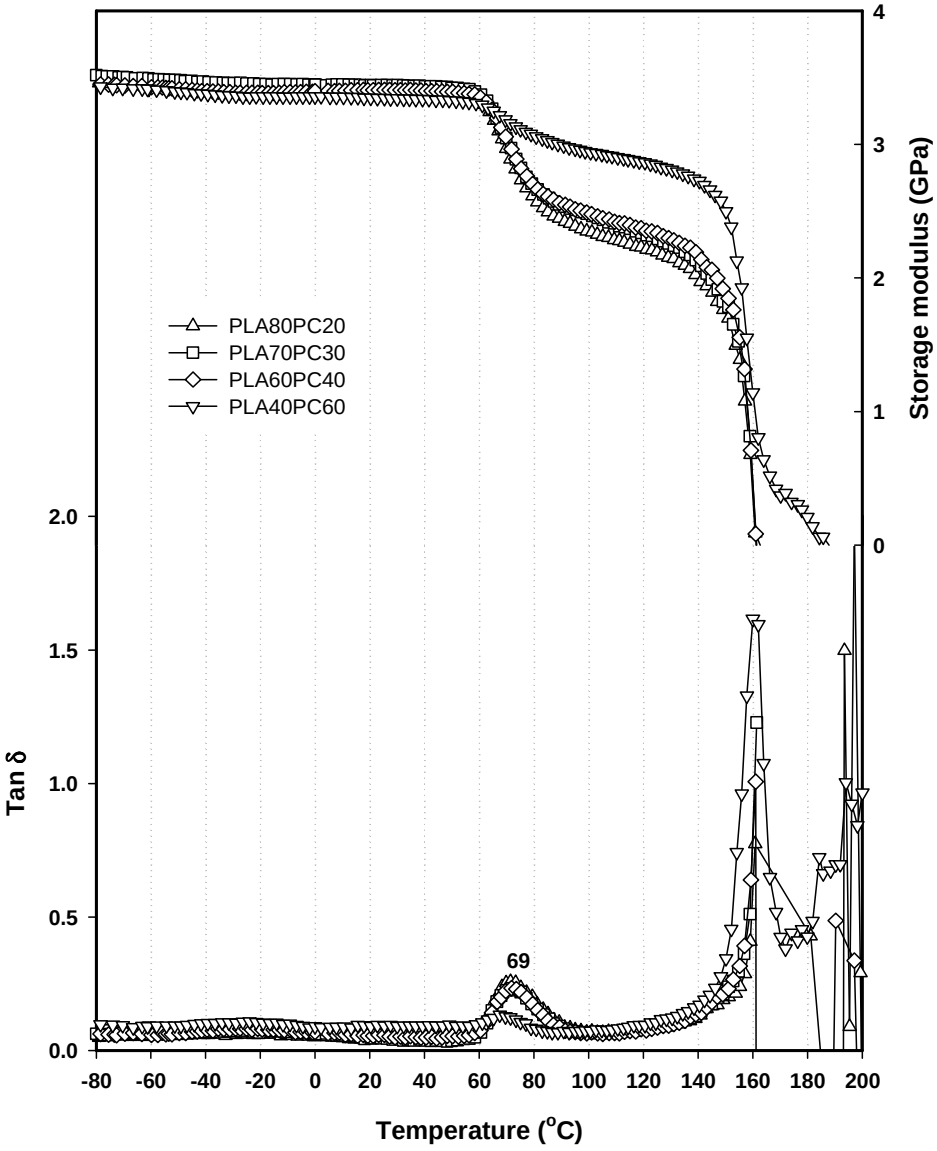

Figure 11. DMTA of the blends PLAx/PCy without catalysts at 230°C

after crystalline 24h at 80°C.

After the T_g of PLA, the storage modulus of blends enhanced as the content of PC increased because the thermal resistance of polycarbonate is high; in losing the storage modulus at 160°C, it will maintain the losing storage modulus of PLA by the interaction between the polymer chains. As mentioned in part A, the blends without a catalyst show two peaks at 69°C and 160°C, that is the T_g of PLA and PC,

respectively. This indicates that the blend is a separated phase, fitting well with SEM, TEM and mechanical property results. Furthermore, the height of the tan delta peak is associated with the mobility of the amorphous region in the polymer [51].As the amount of PC increases, the peak of PLA broadens, and the height of the tan delta peak decreases. Moreover, the peak of PC is sharpened and heightened because of the hindrance of the PC chains, decreasing the mobility of the PLA molecule in an amorphous phase.

In the presence of a catalyst, the blends showed the T_g of PLA at 60^{o}C in Figure 12, a reduction similar to the DSC analysis. Additionally, a new peak occurs between the temperature of PLA and PC. Similarly to the explanations above, this point is the most important evidence for the formulation of a new copolymer that is based on PLA and PC. In the crystalline condition, the middle peak on the tan delta curve did not change much as the amount of PC varied. The difference lies in the performance as exhibited in Figure 13, where the blends are not crystalline before testing. This dissimilarity can be explained by the consequence of the crystalline phase of PLA in the blends; they reduce the moving ability of the polymer chain, so the relaxation of the new copolymer is affected.

In Figure 13, with pure PLA, once the T_g the storage modulus decreases to 80^{o}C and then increases to 120^{o}C, implying that the crystallization of the PLA phase proceeds during a DMTA run (low scan rate). The decreasing storage modulus of PLA in blends starts and ends sooner than in the original PLA, although the quantity of losing storage modulus lessens at high amounts of PLA.

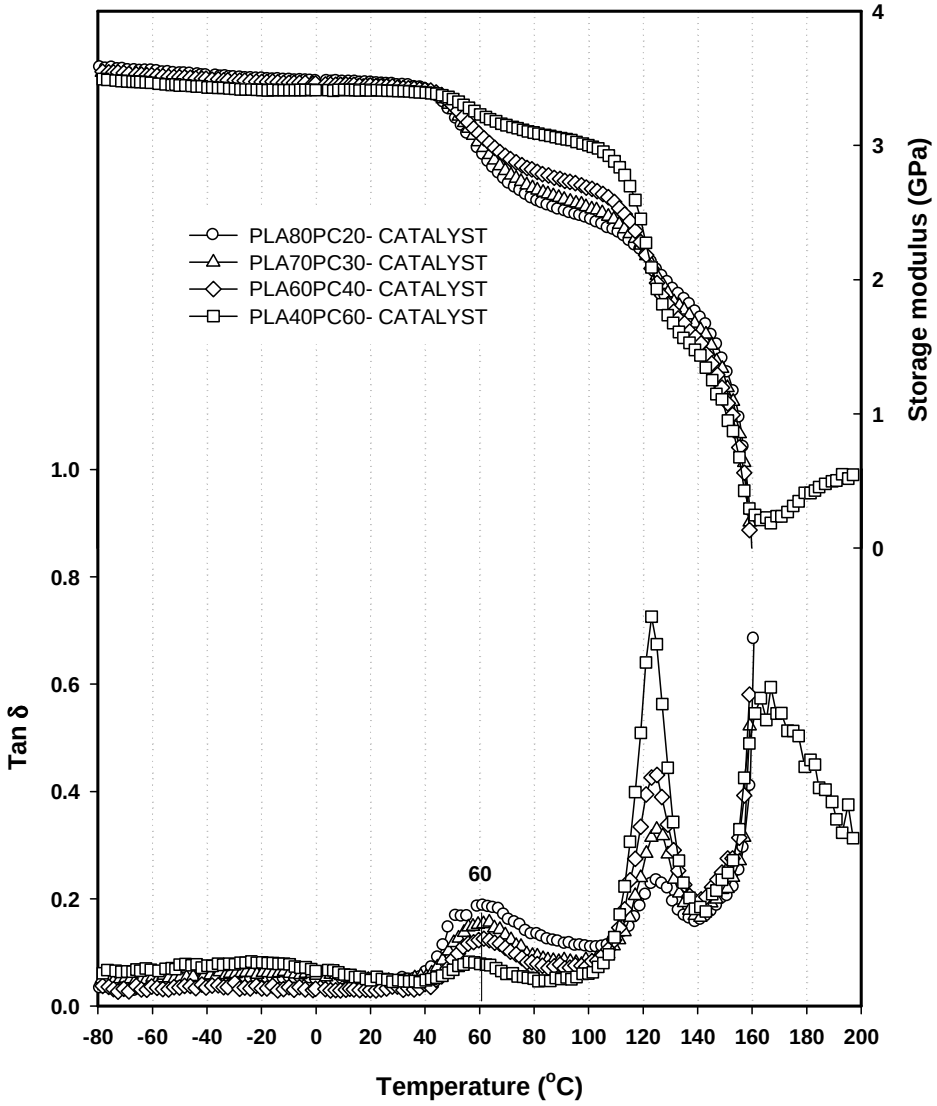

Figure 12. DMTA of the blends PLAx/PCy with catalyst at 230°C

after crystalline 24h at 80°C.

This fact again correlates well to the results of DSC in Figure 10 and indicates that the crystalline of PLA are prevented by high amounts PC. Figure 14 shows that the blends PLA40PC60-CATALYST and PLA30PC70-CATALYST do not decrease the storage modulus at the crystallization temperature zone of PLA, which is completely different from PLA40PC60 physical blends. This is the strong evidence to confirm that the catalyst makes a special interaction or chemical link between PLA and PC,

so the mobility chain of PLA was obstructed and the crystalline process did not happen. This is a significant point for the application of PLA, because the material can maintain the mechanical properties up to 100°C.

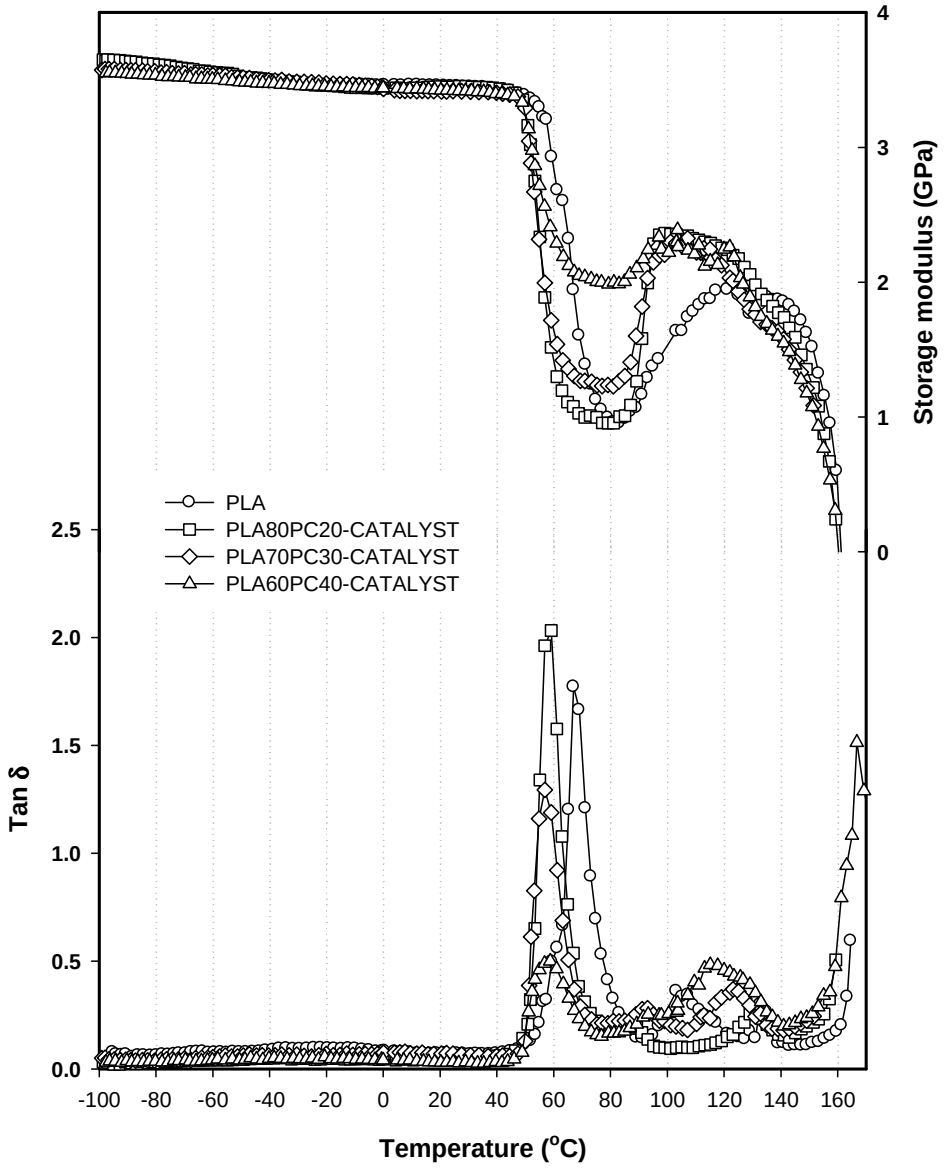

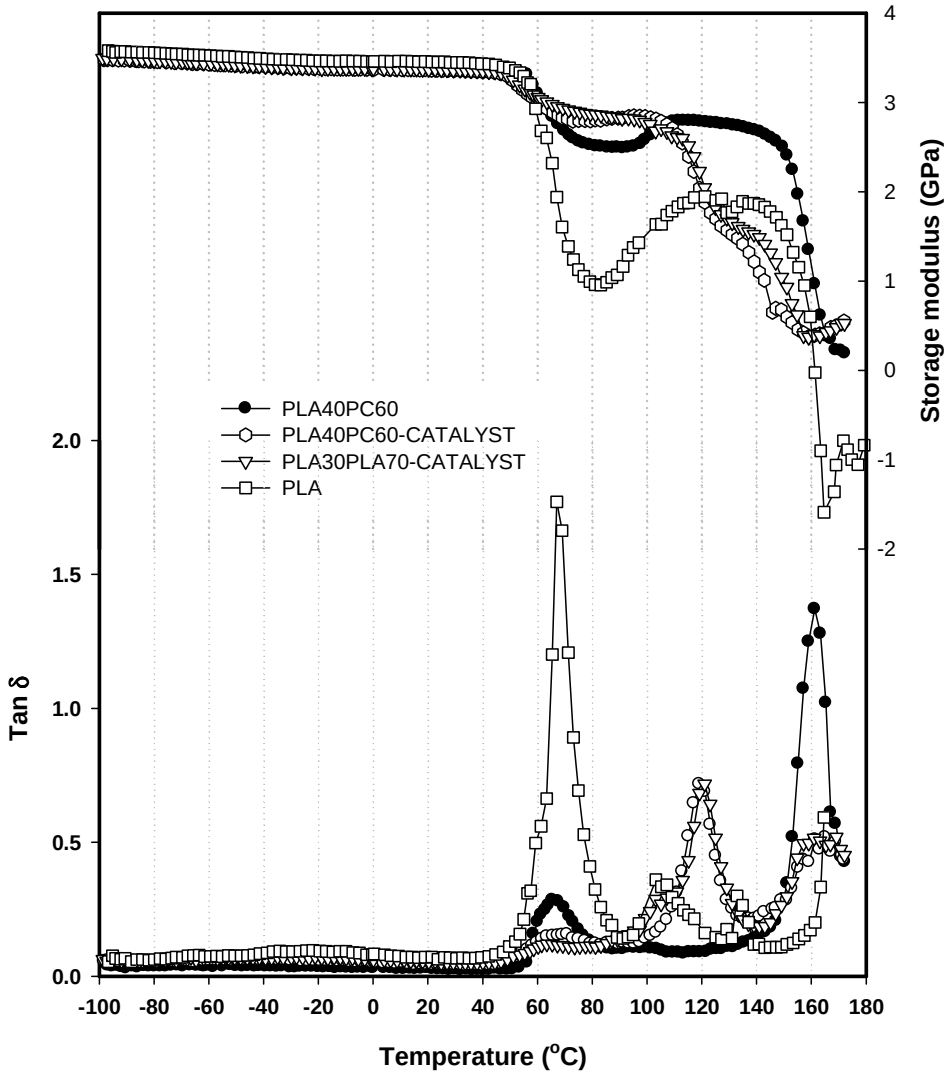

Figure 13A&B. DMTA of the blends PLAx/PCy with catalysts at 230°C.

Moreover, the temperature of the middle peaks or T_g of the new copolymer change with different amounts of PC, which also compares with the prediction models of glass transition temperatures on polymer blends suggested by Gordon Taylor [52] and complex polymer blends or copolymer system suggested by Kewei and Kalogeras [53,54]as seen in Figure 14. The different models for the glass transition temperature are reported as follows:

- Gordon-Taylor

$$T_g = \frac{\varphi_1 T_{g,1} + k_{GT}(1-\varphi_1)T_{g,2}}{\varphi_1 + k_{GT}(1-\varphi_1)} \quad (5)$$

- Kwei

$$T_g = \frac{\varphi_1 T_{g,1} + k_{Kw}(1-\varphi_1)T_{g,2}}{\varphi_1 + k_{Kw}(1-\varphi_1)} + q\varphi_1(1-\varphi_1) \quad (6)$$

- Kalogeras and Brostow

$$T_g = \varphi_1 T_{g,1} + (1-\varphi_1)T_{g,2} + \varphi_1(1-\varphi_1)\left[a_0 + a_1(2\varphi_1 - 1) + a_2(2\varphi_1 - 1)\right] \quad (7)$$

where "k_{GT}""k_{Kw}, *q*", " a_o, a_1, a_2" are adjustment parameters of equations (5), (6), (7), respectively.

By increasing the amount of PC, T_g slightly decreases and does not change from 40 wt.% to 60 wt.% of PC; at this point, it will increase. Therefore, this complex behavior of T_g does not fit the model of Gordon-Taylor when applied to a binary polymer with a simple interaction in an amorphous state of two polymer chains. In that equation, T_g versus the weight fraction follows a linear or hyperbolic function. However, the crystalline processing temperature of PLA is the same as the glass transition temperature of the new copolymer. Thus, the crystalline process will alter the transition temperature of the new copolymer complex as opposed to variations in each component's composition. Concerning this peculiar phenomenon, Kalogeras explains that in terms of microstructure, such intriguing variations may be partly attributed to the different types of segregation of the amorphous new copolymer and their relative contributions to the overall structure. To increase the degree of segregation, one finds: (a) inter-lamellar segregation (the amorphous new copolymer resides in the inter-lamellar region within the lamellar stack), (b) inter-fibrillar segregation (the amorphous chains are placed outside the lamellar stacks of the PLA crystalline component(s), but are still located within the spherulite), and/or (c) inter-spherulitic segregation (the amorphous phase is expelled from the lamellar stacks and resides at the inter-spherulitic

region of the PLA component) [54]. For this reason, Kwei and Kalogeras extended their original equation of the Gordon-Taylor model. Their results were applied and fit perfectly with the experimental data of the new copolymer of PLA and PC blends in the presence of a catalyst. Therefore, variations in T_g of the new copolymer are affected by the content of the PC present, but also by the crystalline processing from PLA.

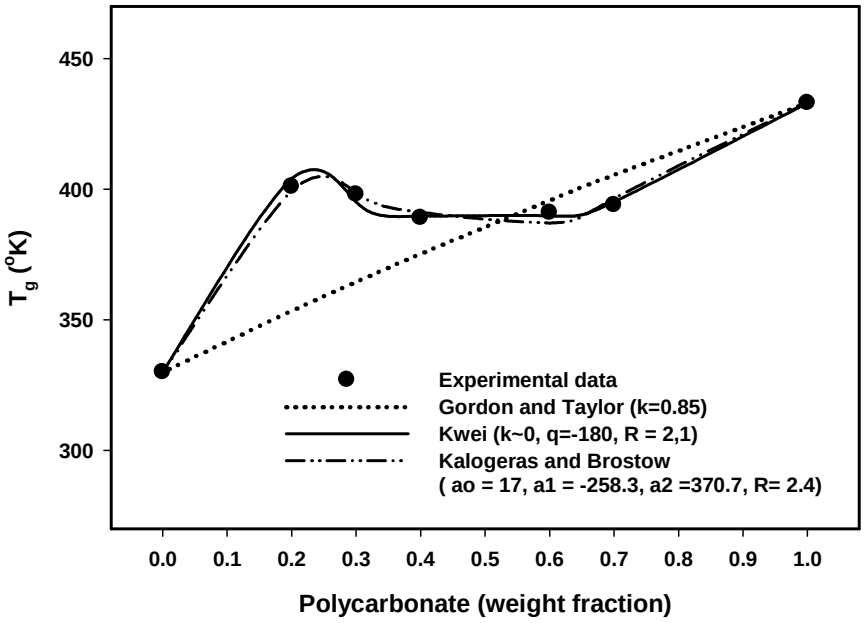

Figure 14. The new T_g of blends following the models in different weight percents of PC.

4.2.3 Structure analysis

An investigation of the distribution of molecular masses, the traces obtained by molecular exclusion chromatography (SEC), was performed by using the IR and UV detectors shown in Figure 15. The molecular weights relative to polystyrene standards of the two pure samples are reported in Table 7.

	Mn	Mw	Id
PLA	108000	175000	1,62
PC	24000	46000	1,92

Table 7. Molecular weight of PLA and PC.

From these curves there does not seem to emerge any evidence of actual grafting or transesterification as the curves of blends with catalysts when comparing the pure materials. The curve results to be chromatographic and consists of a peak at high elution times (lower molecular weights) due to polycarbonate, with a shoulder at shorter time due to the PLA. The data from SEC can be explained by the fact that the molcules in blends with a catalyst are not much affected by the transesterification. Following the mechanism of reaction, the PC chains were broken down using a catalyst, and then were re-reacted with PLA and PC; therefore the blending molecules did not vary much.

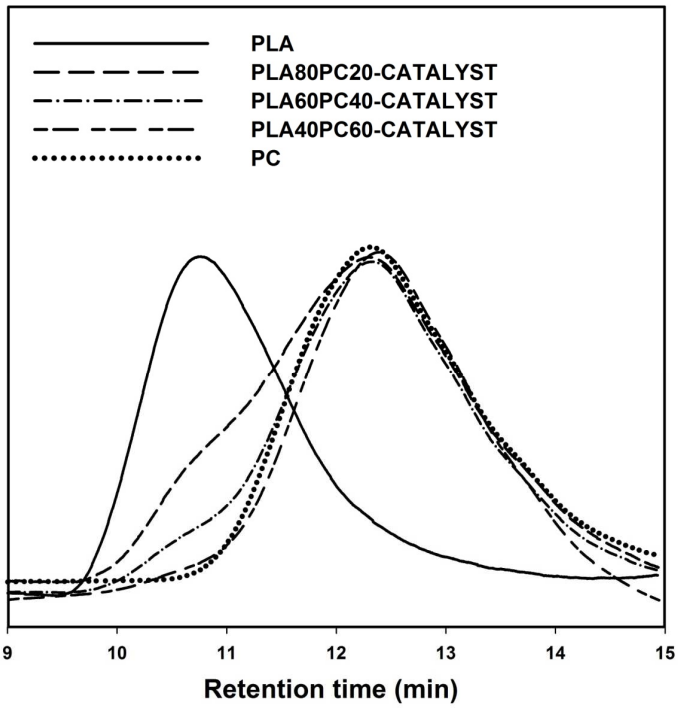

Figure 15. SEC analysis of PLAx/PCy with the presence of catalysts.

NMR spectra of the two pure polymers are rather simple as shown in Figure 16A. Small impurities are also present, but the assignment of the NMR signal is quite straightforward and accounts for the monomeric structure.

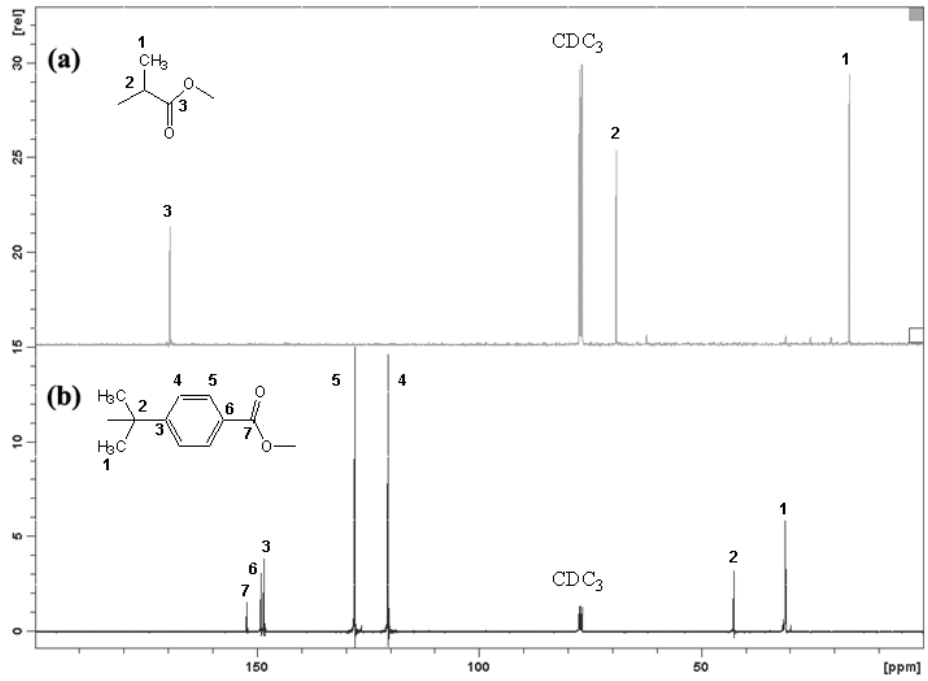

Figure 16A: NMR 13C of PLA80PC20 with catalysts.

In Figure 16B examples of physical blend (c) are reported as well as a mixture of the two polymers in the presence of the catalysts (d), where the weight ratio of PLA and PC were 80 and 20, respectively. Looking at the ^{13}C-NMR spectra, one cannot see any peculiar difference between the two samples. The signal marked with * in spectrum (d) is due to residual acetone present in the sample. In particular, at this stage, no evidence of copolymerization appears from the spectrum (d). The main signals coming from the starting polymers are all present and their intensity is in fair agreement with the weight ratio in both (c) and (d) spectra. Other smaller signals are visible, but they are also present in spectra (a) and (b) of the starting polymers. Since there are a lot of similar functions and hydrocarbon groups, the dectection by ^{13}C-NMR could be overlapped by the original function of the polymer. The problem will be similar also with FTIR testing.

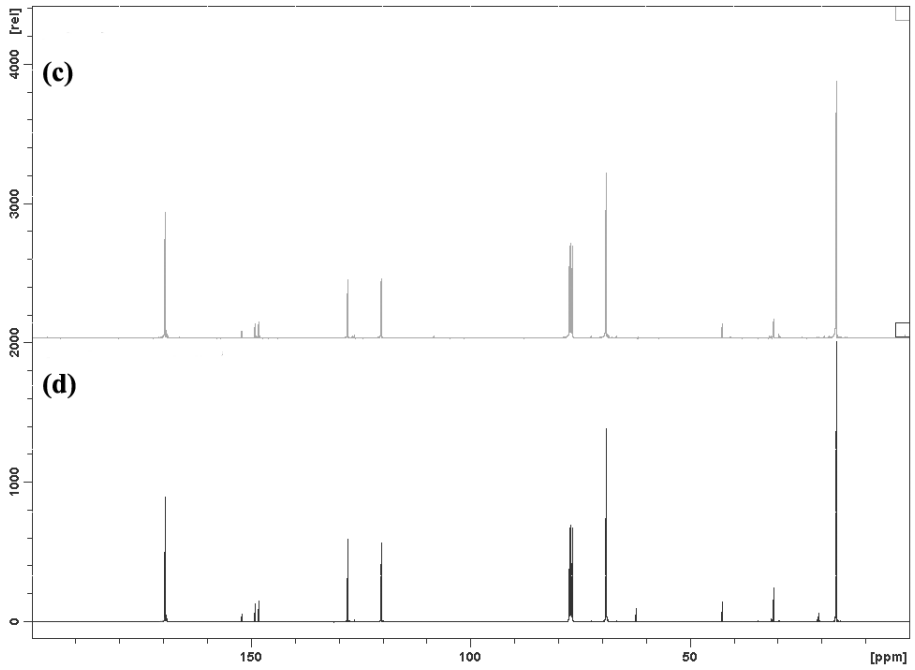

Figure 16B: NMR 13C of PLA80PC20 without catalysts.

Studies cannot show direct chemical evidence for the reaction between Polylactic acid and Polycarbonate bisphenol A, due to similar chemical functions in both polyesters. From the literature review of López and Ziebaa [55-56], the authors proposed the mechanism of reaction between PLA and PC in the presence of triacetin and of a transesterification catalyst (TBATPB), which is shown in Scheme 2. Triacetin will react with OH groups from polylactic acid and Polycarbonate under the melting conditions of extrusion and the effect of TBATBP to become glycerol. The Polycarbonate chain or PLA will be broken down by acting of glycerol and TBATBP through esterification reactions. Therefore the new PC and PLA chains will be formulated. New chains will be linked again with glycerol in the same mechanism to formulate new random copolymers. This fact can explain why there is not much change of the M_w of polymer blends.

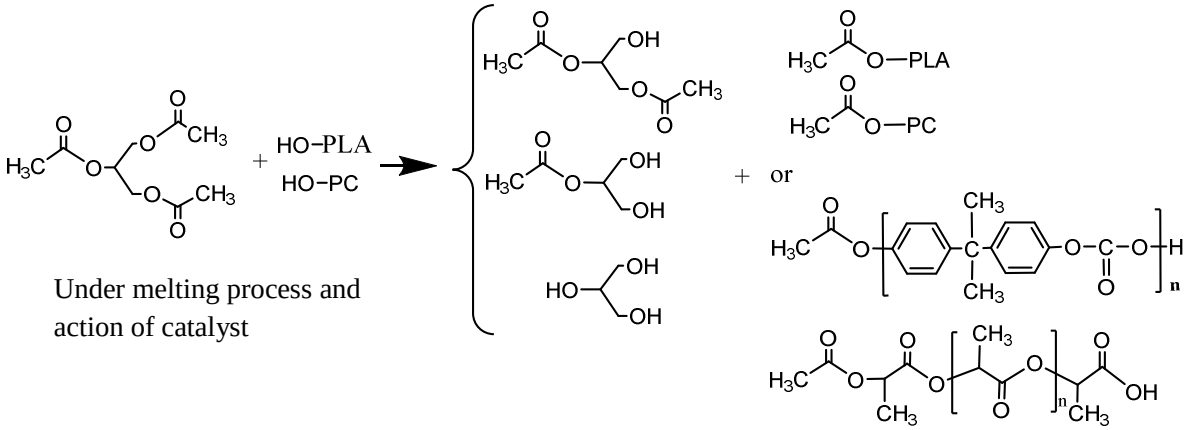

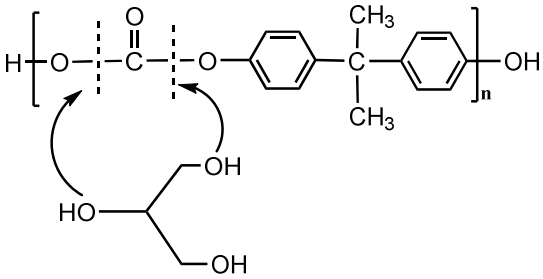

the Glycerin can attach to the PC, ➔ the polymer chains of PC broke down

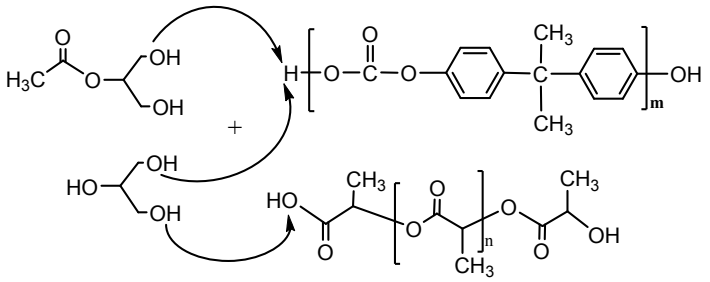

The broken PC polymer chains can react with PLA or itself to formulate random copolymer

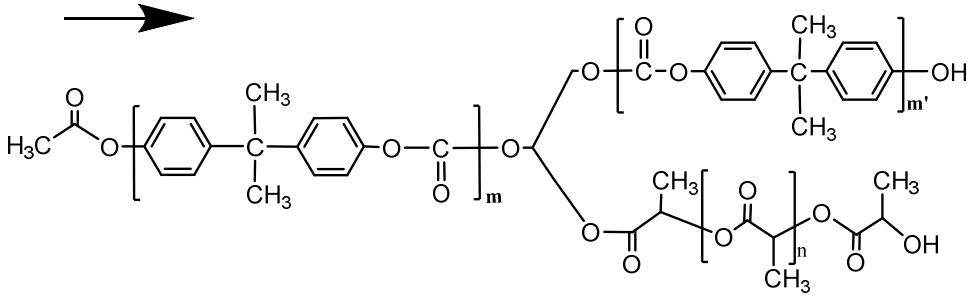

Scheme 2. Proposed mechanism of reaction between PLA and PC

in the presence of triacetin and of a transesterification catalyst.

4.2.3 Morphology

To investigate the effect of a catalyst on the morphology of blends, the scanning electron microscopy (SEM) was applied to the formulation of PLA80PC20. Regarding the physical blends, phase separation occurred with the PC domain and PLA matrix, which is shown clearly in Figures 17A and 17B with higher magnification. The surface tension of PC is high, so it will not be miscible with the PLA matrix. There is a large space between the PC spherical domain and the PLA matrix, therefore the materials will be brittle and will have a low elongation. The domain is not the same size; rather it is about 1µm to 3µm.

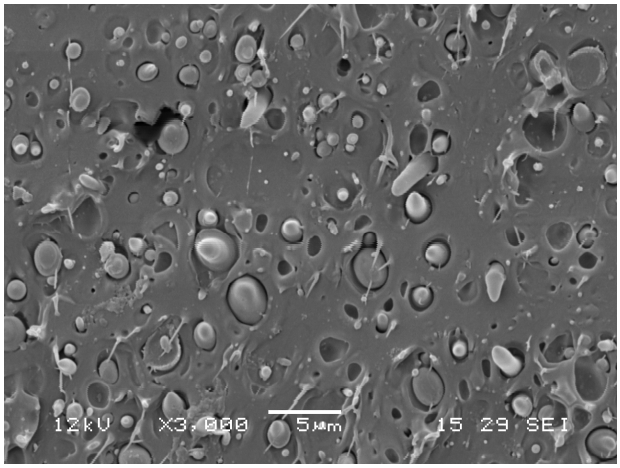

Figure 17A. SEM micrographs for PLA80/PC20 without catalysts.

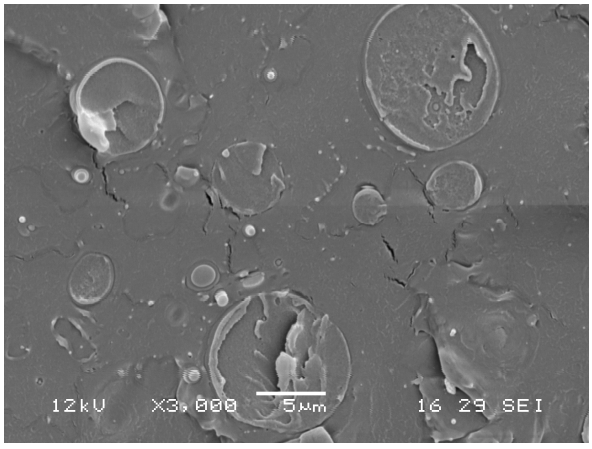

Figure 17B. SEM micrographs for PLA80/PC20 with catalysts.

However, in the same formula, by the action of catalyst, there is no space between PLA domains and PC matrix, only a light boundary between the two phases. It showed a new inter layer between the domain and the matrix, indicating that a new copolymer was formulated. The domain seemed flatter and bigger than in the physical blends of about 5µm -7µm. This is in agreement with the observation by the transmission electron microscope represented in Figures 18A and 18B.

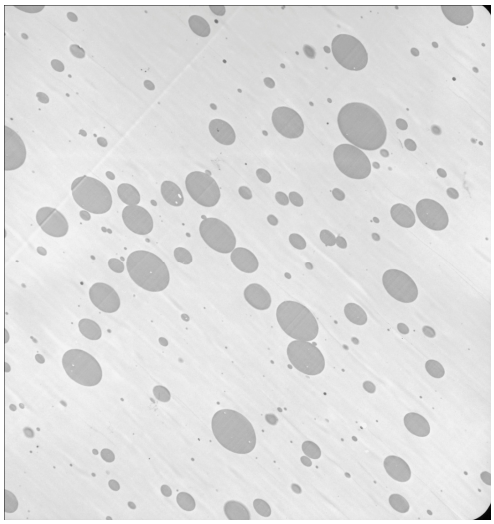

Figure 18A. TEM micrographs for PLA80/PC20 without catalysts.

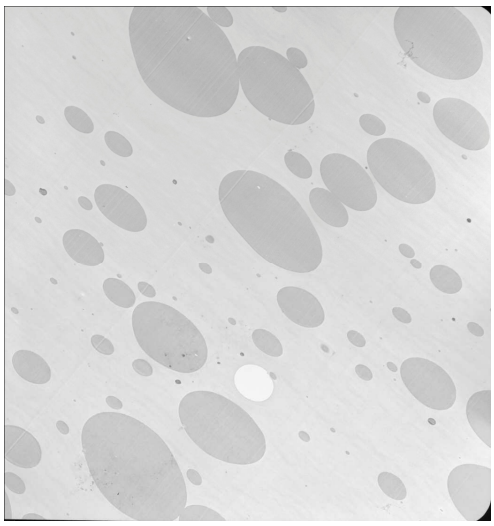

Figure 18B. TEM micrographs for PLA80/PC20 with catalysts.

This phenomenon can be explained by the decreasing the surface tension of the polycarbonate. To obtain a reaction between PLA and PC, the PC chain can be broken down through the effect of a catalyst in order to obtain the new copolymer; so the PC chain will be shorter than the original. That is why the domain size is larger, but thinner than in physical blends.

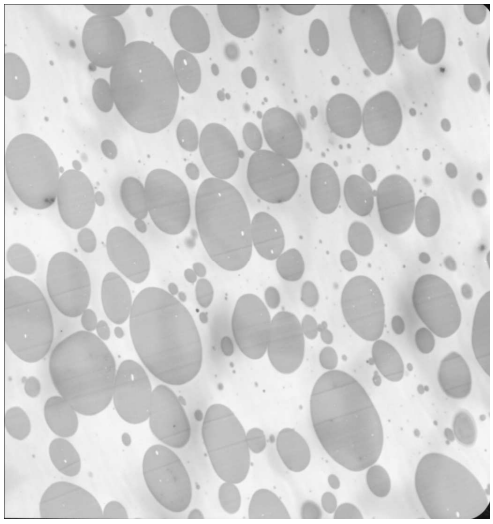

Figure 18C. SEM micrographs for PLA60/PC40 without catalysts.

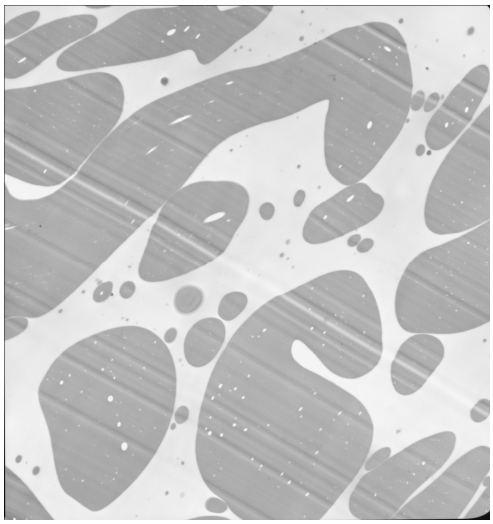

Figure 18D. SEM micrographs for PLA60/PC40 with catalysts.

Moreover, as the amount of PC in physical blends increases, the size of the domain will increase as exhibited in Figure 18C for PLA60PC40. This fact was applied to model the mechanical properties of the

blend. Furthermore, there seems to be some small sphere inside the PC domain, similar to a "salame" structure. Nevertheless, similar to the behavior of PLA80PC 20, with the presence of a catalyst, the domain in a separated phase is larger and moving towards a co-continuous phase, which is confirmed in Figure 18D.This fact deals with Young's modulus data in Figure 9. It implies that the blends mixed with a catalyst can obtain co-countinuous and invert phasesat low amounts of PC as compared to the physical blends. Therefore, the materials can obtain high Young's modulus and elongation at break at low contents of polycarbonate.

4.2.5 Biodegradation

The average percent biodegradation of PLA, PC and physical blends granulates are shown in Figure 19A. The pure polycarbonate is not completely degradated. Polylactic acid starts to degrade after 18 days. The degradation obtained 50wt% after about 55 days and 100wt% after about 80 days. After 150 days, the degradation is 138%. Biodegradation percentages above 100% are explained by a synergistic effect known as priming. A priming effect occurs if the compost inoculum in the test reactor is producing more CO_2 than the compost inoculum in the control reactors. This results in a net CO_2 production that does not come exclusively from the test item and, in the case of readily degradable products, in a measured biodegradation percentage exceeding 100%. As adding the polycarbonate, the speed of degradation decreases suddenly from 70 to 80 days. Then, they degrade fast and quite stably after 90days for PLA80PC20 and 100days for PLA70PC30, PLA60PC40. More specifically, PLA40PC60 blends degraded very slowly up to 120 days, because in this formula the materials performed co-continuous phase, and the high amount of PC can prevent the degradation factor on PLA. In summary, the percentage of degradation of blends is similar to the percentage of PLA, which came from the defect of the compost. That implies that the polymers in physical blends have only a physical interaction.

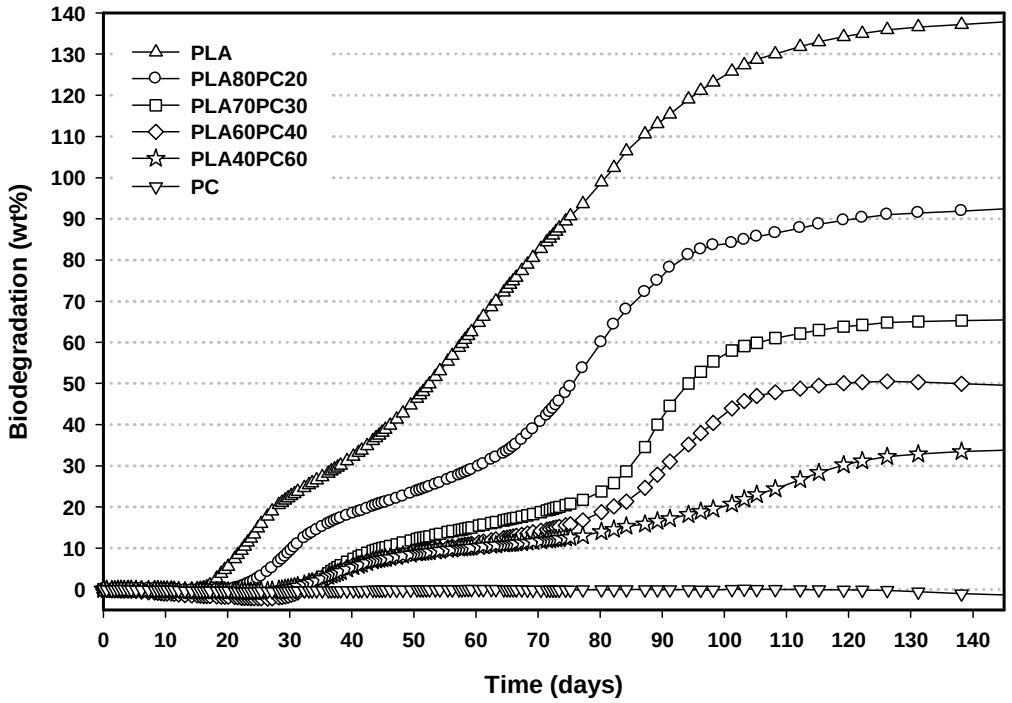

Figure 19A. Biodegradation test of the blends PLAx/PCy without catalysts.

On the other hand, PLA80PC20-CATALYST degradation in Figure 19B is different than physical blends. It starts to degrade after 10days and continuously increases over the next 90 days. However, the degradation amount of blends with a catalyst is higher than physical blends after 70 days, concluding that there are some differences as to the chemical structure of blends. It seems that the reaction of PC and PLA can break down the PC chain. Thus, the steric hindrance of the PC chains on PLA will decrease, so the degradation factor will be easy to digest the PLA polymer chains. Moreover, after 150 days, the final degradation amount of physical PLA80PC20 is higher than PLA80PC20-CATALYST. It can be explained that the amount of PLA reaction with PC prevented the degradation factor from the end chain. Finally, the degradation test showed that the presence of a catalyst could increase the speed of degradation, but could decrease the final degradation amount of materials. Yet, this fact is not much an effect to the application of the materials, because polycarbonate can be recycled after the degradation of the polylactic acid.

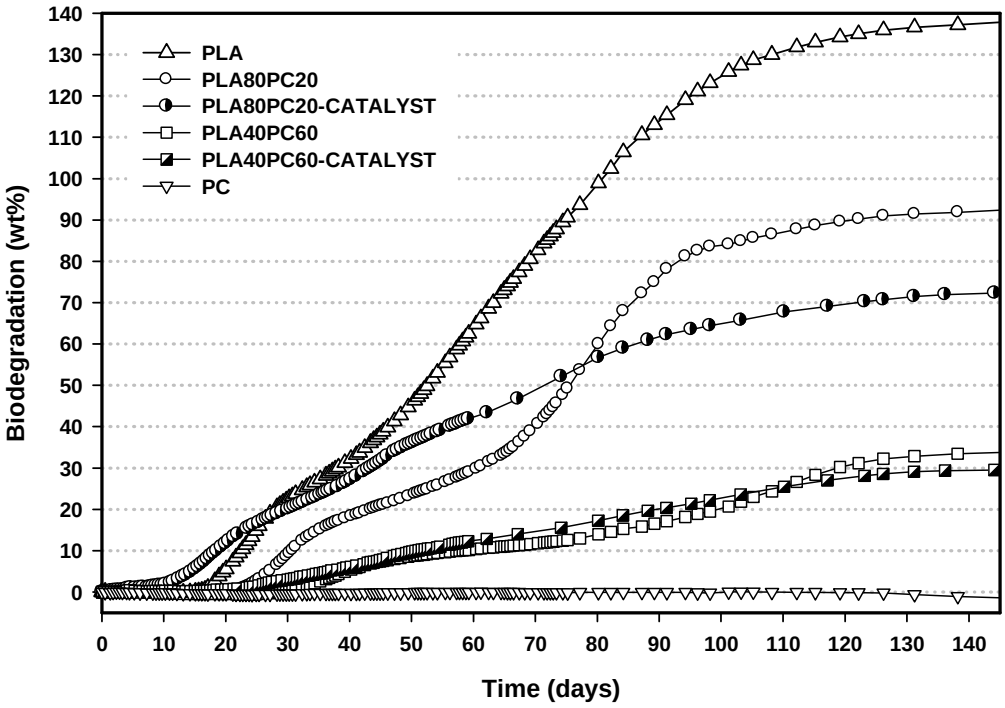

Figure 20A. Biodegradation test of the blends PLAx/PCy without and with catalysts.

V. CONCLUSIONS

The blends of polylactic acid and polycarbonate with and without a catalyst were investigated carefully. The effect of a catalyst and temperature on the mechanical properties of blends showed that the materials can obtain high miscibility processing at 230^{o}C. Additionally, the blends with multi-catalysts obtained a new peak on tan delta, which is between the relaxation temperature of PLA and PC. Moreover, the data of TGA shows an increasing thermal resistance in blends containing a catalyst. It indicates that the new copolymer is formulated on that processing condition.

The mechanical properties of blends with varying amounts of polylactic acid demonstrated that Young's modulus of blends would improve as the PLA amount is increased. The blends obtained the maximum elongation at break as the phases of blends were inverted. More specifically, they fit well with

some current models of mechanical properties. As the catalyst was added, Young's modulus of materials was enhanced thanks to the increasing interface of polymers by the formulation of new copolymers.

DSC and DMTA confirmed that as the content of PC increased, the crystallinity of materials was reduced. More specifically, the formula PLA40PC60 –CATALYST showed that the materials would not lose storage modulus after the temperature at T_g of PLA, namely no crystalline processing in that zone. Due to the catalyst, the links between PLA and PC were increased. Consequently, the PLA lessened the mobility and the crystalline process could not be obtained. These advantageous properties broadened the application ability of materials as compared to current polymers based on PLA.

In addition, the SEM and TEM confirmed once again the effect of a catalyst on the morphology of blends. The interaction between domain and matrix improved, and the size of the domains increased by reducing the surface tension of PC and new copolymer. The biodegradable test demonstrated that the materials combining a catalyst slightly decreased the weight percent of degradation after 70 days, but the speed of degradation was higher than with physical blends.

Chemical analysis could not give clear evidence of a chemical reaction between PLA and PCsince they have similar polar functions. However, with the results gained from DMTA, DSC, SEM, TEM and mechanical properties, the new copolymer is confirmed and its properties were investigated in order to approach the new matrix, which has a high thermo resistance. This could be developed into manufacturing "green" composite materials for different applications such as in phones, cars, and food trays.

* *This chapter was published on International Application Published Under the Patent Cooperation Treaty (PTC) - WO201205907A1-01/03/2012*

Acknowledgment

The authors gratefully acknowledge the financial support of the FORBIOPLAST (Forest Resource Sustainability through Bio-Based-Composite Development) project – Contract No. 212239-FP7-KBBE,

funded by the European Commission under the 7th Framework Programme (FP7) (http://www.forbioplast.eu). Thanks to Dr Markus Gobl of Lenzing Aktiengesellschaft – Lenzing (Austria) for providing us the Tencel fibres . The authors wish also to acknowledge Ms Irene Anguillesi for performing DMTA and TGA tests.

VI. REFERENCES

1. Johansson C, Bras J, Mondragon I, Nechita P, Plackett D, Simon P, Svetec DG, Virtanen S, Giacinti BM, Breen C,Clegg F, Aucejo S. Renewable fibers and bio-based materials for packaging applications - A review of recent developments. BioResources 2012;7:2506-2552.

2. Metha R, Kumar V, Bhunia H, UpadhyaySN. Synthesis of poly(lactic acid): a review. Journal of Macromolecular Science Part C 2005;45:325–349.

3. Liu H, Zhang J. Research progress in toughening modification of poly(lactic acid). Journal of Polymer Science Part B 2011;49:1051–1083.

4. Kido T, Yoshimura M, Yoka K. Japan published patent application 1995;109413.

5. Takehara A.Onoki T.Kageyama F. Japan published patent application 2007;131795.

6. Ishihara J, Kuyama H, Ozeki E, Ishitoku T, Tanaka M, Sakamoto N. Crosslinked polycarbonate and polylactic acid composition containing the same. European Patent Application 1999;EP0896013.

7. RTP Co. Website Engineering Bioplastic Compounds. Available at: http://www.rtpcompany.com/info/flyers/bioplastic.pdf. Accessed on March 2013.

8. PolyOne Co. Website. reSoundTM Biopolymer Compounds (RS1200-0001 &RS1200-0002). Available at: http://www.polyone.com/en-us/products/engresincompund/pages/reSound.aspx. Accessed on March 2013.

9. Robeson LM. Perspectives in polymer blend technology, Chapter 17, 1167-1200, in Polymer Blend Handbook, 2003, Ed. Utracky LA. Kluwer Academic Publisher, Netherlands.

10. Takeshi K, Katsuhisa T. Mechanical properties and morphological changes of poly(lactic acid)/polycarbonate/poly(butylene adipate-co-terephthalate) blend through reactive processing. Journal of Applied Polymer Science 2011;121:2908-2918.

11. Semba T, Kitagawa K, Ishiaku US, Hamada H. The effect of crosslinking on the mechanical properties of polylactic acid/polycaprolactone blends. Journal of Applied Polymer Science 2006;101:1816-1825.

12. Semba T, Kitagawa K, Ishiaku US,Kotaki M, Hamada H. Effect of compounding procedure on mechanical properties and dispersed phase morphology of poly(lactic acid)/polycaprolactone blends containing peroxide. Journal of Applied Polymer Science2007;103:1066-1075.

13. Wang R, Wang S, Zhang Y, Wan C, Ma P. Toughening modification of PLLA/PBS blends via in situ compatibilization. Polymer Engineering & Science2009;49:26-33.

14. Zhang N, Wang QF, RenJ,Wang L. Preparation and properties of biodegradable poly(lactic acid)/poly(butylene adipate-co-terephthalate) blend with glycidyl methacrylate as reactive processing agent. Journal of Material Science 2009;44:250-256.

15. Kumar M, MohantyS,Nayak SK, Parvaiz MR. Effect of glycidyl methacrylate (GMA) on the thermal, mechanical and morphological property of biodegradable PLA/PBAT blend and its nanocomposites. Bioresource Technology 2010;101:8406-8415.

16. Su ZZ, Li QY, Liu YJ, Hub GH, Wua CF. Compatibility and phase structure of binary blends of poly(lactic acid) and glycidyl methacrylate grafted poly(ethylene octane). European Polymer Journal 2009;45:2428-2433.

17. Corre YM, Duchet J, Reignier J, Maazouz A. Melt strengthening of poly (lactic acid) through reactive extrusion with epoxy-functionalized chains. RheologicaActa 2011;50:613-629.

18. Tjong SC, Meng YZ. Structural-mechanical relationship of epoxy compatibilized polyamide 6/polycarbonate blends. Materials Research Bulletin 2004;39:1791-1801.

19. Liang GG, Cook WD, Tcharkhtchi A, Sautereau H. Epoxy as a reactive plasticizer for improving polycarbonate processibility. European Polymer Journal 2011;47:1578-1588.

20. Marchese P, Celli A, Fiorini M. Influence of the activity oftransesterificationcatalysts on the phase behavior of PC-PET blends. Macromolecular Chemistry and Physics 2002;203:695-704.

21. MarcheseP,Celli A, Fiorini M, Gabalgi M. Effects of annealing on crystallinity and phase behaviour of PET/PC block copolymers. European Polymer Journal 2003;39:1081-1089.

22. Wilkinson AN, Cole D, Tattum SB. The effects of transesterification on structure development in PC-PBT blends. Polymer Bulletin 1995;23:751-757.

23. Yu T, Ren J, Gu S, Yang M. Synthesis and characterization of poly(lactic acid) and aliphatic polycarbonate copolymers. Polymer International 2009;58:1058-1064.

24. Warth H, Chen S, Wang, Y, Li H. US Patent 2010;US2010/0081739A1.

25. Penco M, Lazzeri A, Phuong TV, Cinelli P. International Patent Application 2012;WO2012025907A1.

26. Zhang GY, Ma JM, Cui BX, Luo XL, Ma DZ. Compatibilizingeffect of transesterificationcopolymers on bisphenol-A Polycarbonate/Poly(ethylene terephthalate) blends. Macromolecular Chemistry and Physics 2001;202:604-613.

27. Denchev Z, Sarkissiva M, Radusch HJ, Luepke T, Fakirow S. Sequential reordering in condensation copolymers, 4. Crystallization-induced sequential reordering in poly(ethylene terephthalate)/polycarbonate copolymers as revealed by the behavior of the amorphous phases. Macromolecular Chemistry and Physics 1998;199:215-221.

28. Aravind I, Pionteck J, Thomas S. Transreactions in poly trimethylene terephthalate/bisphenol-A polycarbonate (PC) blends analysed by pressure-volume-temperature measurements. Polymer Testing 2012;31:16-24.

29. Cho JK, Lee HT, Ha DH, Jung CD. US Patent 2012;US8133943B2.

30. Lee JB, Lee YK, Choi GD, Na SW, Park TS, Kim WN. Compatibilizing effects for improving mechanical properties of biodegradable poly (lactic acid) and polycarbonate blends. Polymer Degradation and Stability 2011;96:553-560.

31. Wang Y, Chiao SM, Hung TF, Yang SY.Improvement in toughness and heat resistance of poly(lactic acid)/polycarbonate blend through twin-screw blending: Influence of compatibilizer type. Journal of Applied Polymer Science 2012;125:E402-E412.

32. Yao M, Deng H, Mai F, Wang K, Zhang Q, Chen F, Fu Q. Modification of poly(lactic acid)/poly(propylene carbonate) blends through melt compounding with maleic anhydride. eXPRESS Polymer Letter 2011;5:937-949.

33. Kanzawa T, Tokumitsu K. Mechanical properties and morphological changes of poly(lactic acid)/polycarbonate/poly(butylene adipate-co-terephthalate) blend through reactive processing. Journal of Applied Polymer Science 201;121:2908-2918.

34. Davies WEA. The elastic constants of a two-phase composite material. Journal Physic D 1972;4:1325-1339.

35. Barentsen WM. PhD thesis, Eindhoven University of Technology, The Netherlands, 1972.

36. Veenstra H, Verooijen CJP, Lent JJB, Dam VJ, Boer PA, Nijhof HJA. The hydration of TENCEL® cellulose fibres studied using contrast variation in small angle neutron scattering. Polymer 2000;41:1871-1826.

37. Song L, He Q, Hu Y, Chen H, Liu L. Study on thermal degradation and combustion behaviors of PC/POSS hybrids. Polymer Degradation and Stability 2008;93:627-639.

38. Lee LH. Mechanisms of thermal degradation of phenolic condensation polymers. I. Studies on the thermal stability of polycarbonate. Journal Polymer Science A 1964;2:2859-2873.

39. Jang BN, Wilkie CA. A TGA/FTIR and mass spectral study on the thermal degradation of bisphenol A polycarbonate. Polymer Degradation and Stability 2004;86:419-430.

40. Phuong TV, Lazzeri A. “Green” biocomposites based on cellulose diacetate and regenerated cellulose microfibers: Effect of plasticizer content on morphology and mechanical properties. Composite Part A 2012;43:2256-2268.

41. Monteiro EEC, Thaumaturgo C. Surface phenomena and polymer miscibility of PVC/EVA blends. Composite Science and Technology 1997;57:1159-1165.

42. Potschke P, Paul DR. Formation of co-continuous structures in melt-mixed immiscible polymer blends. Journal of Macromolecular Science, Part C 2003;C43:87-141.

43. Williemse RC, Speijer A, Langeraar AE, Boer PD. Tensile moduli of co-continuous polymer blends. Polymer 1999;40:6645-6650.

44. Fischer EW, Sterzel HJ, Wegner G. Investigation of the structure of solution grown crystals of lactide copolymers by means of chemical reactions. Kolloid-Zu Z-Polymer 1973;251:980–990.

45. Zhang JM, Duan YX, Sato H, Tsuji H, Noda I, Yan S, Ozaki Y. Crystal modifications and thermal behavior of poly(l-lactic acid) revealed by infrared spectroscopy. Macromolecules 2005;38:8012-8021.

46. Cho TY, Strobl G. Temperature dependent variations in the lamellar structure of poly(l-lactide). Polymer 2006;47:1036-1043.

47. Zhang JM, Tashiro K, Tsuji H, Domb JA. Disorder-to-order phase transition and multiple melting behavior of Poly(l-lactide) investigated by simultaneous measurements of WAXD and DSC. Macromolecules 2008;41:1352-1357.

48. Ljungberg N, Wesslen B. The effects of plasticizers on the dynamic mechanical and thermal properties of poly(lactic acid). Journal ofApplied Polymer Science 2001;86:1277-1234.

49. Yamane H, Sasai K. Effect of the addition of poly(D-lactic acid) on the thermal property of poly(L-lactic acid). Polymer 2003;44:2569-2575.

50. Liu X, Dever M, Fair N, Benson RS. Thermal and mechanical properties of poly(lactic acid) and poly(ethylene/butylene succinate) blends. Journal Environment Polymer Degradation 1997;5:225-235.

51.Silverajah VS, Ibrahim AN, Yunus WZW, Hassan HA, Woei CB. A comparative study on the mechanical, thermal and morphological characterization of poly(lactic acid)/epoxidizedpalm oil blend. International Journal of Molecular Science 2012;13:5878-5898.

52. Gordon M, Taylor JS. Ideal copolymers and the second-order transitions of synthetic rubbers. i. non-crystalline copolymers. Journal Applied Chemistry 1952;2:493-500.

53. Kwei TK. The effect of hydrogen bonding on the glass transition temperatures of polymer mixtures. Journal Polymer Science letter 1984;22:307-313.

54. Kalogeras JM, Brostow W. Glass transition temperatures in binary polymer blends. Journal of Polymer Science Part B2009;47:80-95.

55. López DE, Goodwin AG, Bruce DA, Lotero E. Transesterification of triacetin with methanol on solid acid and base catalysts. Applied Catalysis A 2005;295:97–105.

56. Zięba A, Drelinkiewicz A, Chmielarz B, Matachowskia L, Stejskalc J. Transesterification of triacetin with methanol on various solid acid catalysts: A role of catalyst properties. Applied Catalysis A 2010;387:13-25.

Chapter 4

Biocomposites Based on Poly(lactic acid)-*graft*-Polycarbonate bisphenol A Copolymers and Regenerated Cellulose Microfibers

I. INTRODUCTION

In recent times, biodegradable polymer and bio-composites have received increasing consideration from researchers as well as in technology due to their potential in addressing environmental concerns, biomedical and industrial applications, packaging, and in electronic components. Biodegradable polymers are broken down in physiological environments through macromolecular chain scission into smaller fragments, and ultimately into simple and stable end products. The degradation may be due to aerobic or anaerobic microorganisms, biologically active processes (e.g., enzyme reactions) or passive hydrolytic cleavage. Recently, the critical discussion about the preservation of natural resources and recycling has led to renewed interest concerning biomaterials with a focus on renewable raw materials. The growing focus thus far has been paid to starch-based products, such as PLA (Polylactic acid), PHA (Poly hydroxyl alkanoates) in particular PHB (Poly hydroxyl butyrate), and cellulose derived plastics [1]. In the family of biodegradable polyesters, polylactides (i.e. PLA) have been singled out because they are renewable, biodegradable and compostable; moreover, they have very low or no toxicity and present a high mechanical performance, comparable to those of commercial polymers. However, the thermal stability of PLAs is generally not sufficiently high enough for them to be used as an alternative in many commercial polymer applications [2]. In order to increase the thermo resistance of polylactic acid, blending PLA with aromatic polyester such as Polycarbonate (PC) has been investigated [3-5], but there are also some commercial products available [6-7]. PC has been widely used as an engineering plastic having high

thermal stability and mechanical properties (high tensile strength and elongation at break), while its fracture toughness is still too low. In order to counterbalance these disadvantages, Suarez and his colleges used Acrylonitrile butadiene styrene (ABS) blended with PC through melting extrusion [8]. Subsequently, they found that in blends with PC, Polylactic acid can replace ABS, not only improving facture toughness, but also decreasing the environmental impact of materials [9]. However, the blends of PLA/PC are immiscible; adhesion between the two polymers is weak due to high interfacial tension and weak entanglements. Moreover, the materials showed a decrease in the modulus from 80-120^{o}C, which implied a crystallization process of the Polylactic acid. For these reasons, in the previous chapter we succeeded in increasing the interface between PLA and PC in melting extrusion through using a transesterification catalyst and formulating a new type of copolymer, which presents high mechanical properties, thermo resistance and morphology.

To continue the focus on increasing mechanical properties and producing the eco-materials, which are environmentally friendly, we applied cellulose fibers to new copolymers based on PLA and PC to produce bio-based or hybrid biodegradable composites. In the literature, PLA was blended as a matrix material for natural vegetable fibers or lignocellulosic fibers such as kenaf, flax, jute, hemp, bamboo, -based composites [10-17]. However, the incompatibility of natural or lignocellulosic fibers with the PLA matrix led to poor interfacial adhesion, leading to a decrease in the mechanical properties. Contrary to PLA, there is very little literature examining the reinforcement of PC and natural fibers [18] in the melting process. Since processing temperature of PC is high, it will be easy to degrade the natural fibers. Nevertheless, both PLA and PC matrices interact very poorly with natural fibers, because they have high surface tension; therefore the contact angle with the fibers will be low. Moreover, they are limited reactive functions, which can react or obtain physical interaction with polar functions on cellulose fibers. Enhanced interfacial adhesion for natural fiber-based composites can be achieved either by modifying the fibers and matrix chemical or physical treatments, or by using interfacial additives such as maleic anhydride, epoxide additive, or TBATBP for transesterification [19-30].

Moreover, many natural fibers possess a limited aspect ratio and are non-homogeneous in fiber diameter, length and size distribution. Therefore the proper stress could not transfer from the matrix to the fibers, and the buildup of the tensile stress in the fibers would result in limited property enhancement and reduced material reproducibility. Besides, the major constituents of natural fibers (lignocelluloses) are cellulose, hemicellulose and lignin. The amount of cellulose in lignocellulosic systems can vary depending on the species and age of the plant or species. Lignin is a phenolic compound that is generally resistant to microbial degradation [1]. Although the exact structural formula of lignin in natural fibers has not yet been established, most of the functional groups and units that make up the molecule have been identified. Lyocell, also known as Tencel, is an artificial microfiber made from regenerated wood pulp cellulose. It is produced by spinning bleached wood pulp dissolved in a nontoxic ("green") organic solvent, N-methylmorpholine-N-oxide or MMNO, which can then be recovered by washing the freshly spun cellulose microfibers in water, purified and then recycled. Both fiber diameter and length can be accurately controlled during the production process and without the lignin content. Based on these advantageous properties, Lyocell is the potential fiber that can increase the mechanical properties and thermo resistance of biocomposites, even though the interaction between the fibers and matrix is still poor. However, Lyocell is still a new type of fiber on the market, therefore studies on the effects of Lyocell fibers on the polymer matrix are limited and have not received much consideration as yet [31, 32].

As stated above, the aim of this study is to investigate the effects of the mechanical properties and thermo resistance of cellulose fibers (Lyocell) on composites based on blends of PLA and PC. We obtain the best results from the mechanism on transesterification process of the polymer in blends to increase the interaction between the fibers and matrix due to the reaction between the ester group and the hydroxyl function of cellulose fibers, as well as the effects of cellulose fibers on the formulated process copolymer. The results of this research can present new methods for the production of biocomposites as well as hybrid biodegradable composites.

II. EXPERIMENTAL DETAILS

2.1. Materials

Poly (L-lactic) acid was purchased from NatureWorks LLC having a nominal average molecular weight Mw = 199590 Da (NatureWorks® IngeoTM 2002D Extrusion Grade), density 1.24g/cm3. Polycarbonate bisphenol A (Mitsubishi Chemical Co-operation - Japan, branch S3000) had a density of 1.20 g/cm3 and an average molecular weight of Mw = 20 KDa. Triacetin (TA, also known as glycerin triacetate or 1,2,3-triacetoxypropane, CAS # 102-76-1) and tetrabutylammonium tetraphenylborate (TBATPB, CAS # 15522-59-5) were purchased from Aldrich Chemicals used as a transesterification factor or an interchange catalyst. The chemical structure of materials was performed as seen in Scheme 1.

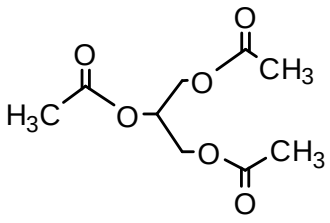

Triacetin (TA)

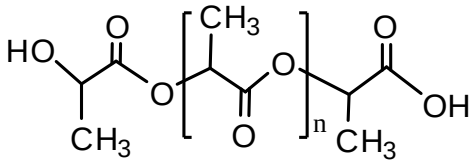

Polylactic acid (PLA

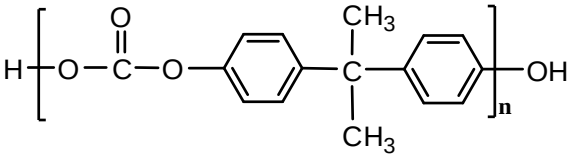

Polycarbonate Bisphenol A (PC)

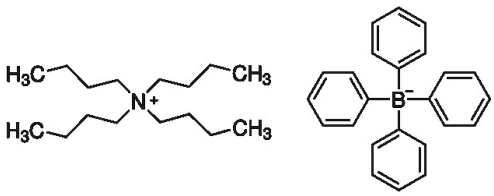

TetrabutylammoniumTetraphenylborate (TBATPB)

Scheme 1. Chemical structure of materials.

Tencel® FCP-10/400 microfibers with a diameter of about 10.5 µm and an average fiber length of 390 µm, corresponding to an aspect ratio ar = 37, were kindly provided by Lenzing AG, Lenzing, Austria. According to this manufacturer, these fibers have a density: 1.5 g/cm³, a Young's modulus of 10 –15 GPa, a tensile strength of 570 MPa, and an elongation at break of 11%. The morphology of Lyocell fibers

before processing is shown in Figure 1. All materials were dried overnight under a vacuum at 80°C before processing.

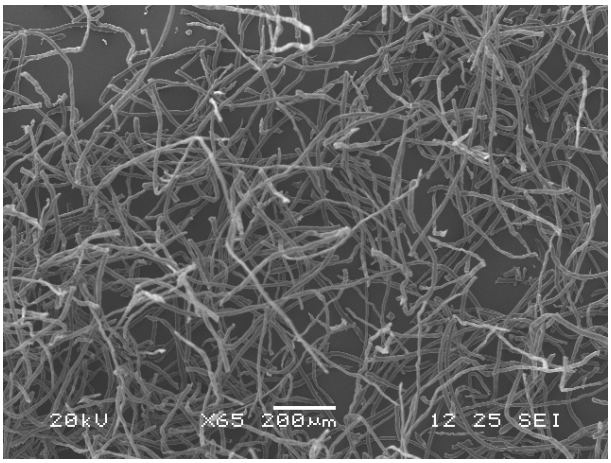

Figure 1. SEM of Lyocell fibers

2.2. Processing

Following the work in the previous chapter, we chose the ratio between PLA and PC to be 40% and 60% by weight, respectively. Then the matrix was blended with different contents of Lyocell fibers (5, 10, 15 wt%) with and without the presence of catalysts. The polymers (PLA and PC) were mechanically mixed for about 10 minutes with different ratios of Lyocell by means of a high-speed mixer. After this mixing stage, the Triacetin and TBATPB were added and mixed for an extra 10 minutes using the same equipment. The resulting mixtures were processed with a MiniLab II HaakeRheomex CTW 5 conical twin-screw extruder (Thermo Scientific Haake GmbH, Karlsruhe, Germany). The mixing was conducted at a temperature of 230 °C with a screw speed of 100 rpm, for a recycling time of 1 minute. After extrusion, the molten materials were transferred through a preheated cylinder to the Haake MiniJet II mini injection molder (Thermo Scientific Haake GmbH, Karlsruhe, Germany) to obtain ASTM D638 V dog-bone tensile bars used for measurements and analysis. The specimens were placed in plastic bags for vacuum sealing to prevent moisture absorption.

2.3. Characterization methods

Tensile tests were performed at room temperature at a crosshead speed of 10 mm/min by means of an Instron 4302 universal testing machine (Canton MA, USA), equipped with a 10 kN load cell and interfaced with a computer running the Testworks 4.0 software (MTS Systems Corporation, Eden Prairie MN, USA).

The chemical bonding of PLA-PC copolymers and Lyocell fibers was analyzed by using a Nicolet 380 spectrometer with the Diffuse Reflectance Accessory (DRIFT). The composites were dissolved in Tetrahydrofuran (THF) and the fibers were dried under a vacuum at 140^{o}C for 24 hours. The materials were mixed with potassium bromide (KBr) in order to obtain the DRIFT spectra. During the DRIFT measurement, pure potassium bromide was chosen as a background.

Thermogravimetric Analysis (TGA) was run under the flow of nitrogen gas at a scanning speed of 10 °C/min, from room temperature to 1000 °C, using a TGA 1000 instrument (Rheometric Scientific Inc., USA).

Dynamic mechanical thermal analysis (DMTA) was carried out on a Gabo Eplexor® 100N (Gabo Qualimeter GmbH, Ahlden, Germany). Test bars were cut from the tensile bar specimens (size: 20 x 5 x 1.5 mm) and mounted on a tensile geometry. The temperature used in the experiment ranged from -100 °C to 170 °C at a heating rate of 2 °C/min and frequency of 1 Hz.

The morphology of the composites was studied by scanning electron microscopy (SEM) using a JEOL JSM-5600LV (Tokyo, Japan) and by analyzing the fracture surfaces of the samples broken in liquid nitrogen. Prior to SEM analysis all the surfaces were sputtered with gold.

III. THEORETICAL ANALYSIS

Several theoretical expressions have been developed for predicting the elastic modulus of short fiber composites. One of the most successful approaches considers long straight discontinuous fibers that are completely embedded in a continuous matrix, making use of the so-called shear-lag concept [33]. This model introduces some simplifying assumptions, such as: (1) uniform alignment of the fibers within the

matrix; (2) stress transfer by shear along the length of the fibers-matrix interface; (3) perfect elastic, isotropic behavior of both matrix and fibers; (4) perfect bonding between the two materials at the interface.

3.1 Young's modulus

However, it is now well established that the prediction of the composite's modulus calculated by Cox's model does not provide sufficiently accurate estimations when the fiber's aspect ratio is small [34], as in the present work. The predicted modulus obtained by Cox's model is significantly smaller than the experimentally observed values for short fiber composites. In fact, Cox's model neglects the stress transfer across the fiber ends, $\sigma_f(\pm L/2) = 0$.

Since the early work of Cox, several improvements have been proposed to the original shear lag analysis, and some of these developments have been recently reviewed [35]. In particular, Kim has proposed the following modified equation for the elastic modulus of short fiber composites, E_C^{Kim}, taking into account both fibers end traction forces and stress concentration effects [36-38]:

$$E_C^{Kim} = E_f \varphi_f \left\{ 1 + \left(\sqrt{\frac{E_m}{E_f}} - 1 \right) \frac{\tanh(\beta a_r)}{\beta a_r} \right\} + E_m (1 - \varphi_f) \tag{1}$$

where β is given by:

$$\beta = \sqrt{\frac{2E_m}{E_f (1+\upsilon_m) \log(\frac{P_f}{\varphi_f})}} \tag{2}$$

Of all the micromechanics equations, Halpin-Tsai's semi-empirical equations are accurate and straightforward. Halpin and Tsai showed that the Herman's solution to Hill's self-consistent model can be reduced to a simpler approximate analytical form and extended its use to a wide variety of reinforcement geometries [39]. For the longitudinal modulus, the Halpin-Tsai's equation gives the following expression:

$$E_{Cl}^{HT} = \frac{1 + 2a_r \lambda_l \varphi_f}{1 - \lambda_l \varphi_f} E_m \tag{3}$$

with

$$\lambda_l = \frac{\left(\frac{E_f}{E_m}\right) - 1}{\left(\frac{E_f}{E_m}\right) + 2a_r} \tag{4}$$

while the transverse modulus takes the form:

$$E_{Ct}^{HT} = \frac{1 + 2a_r \lambda_l \varphi_f}{1 - \lambda_l \varphi_f} E_m \tag{5}$$

where

$$\lambda_l = \frac{\left(\frac{E_f}{E_m}\right) - 1}{\left(\frac{E_f}{E_m}\right) + 2} \tag{6}$$

For composites with fibers oriented randomly in a plane, the Halpin-Tsai's equations give:

$$E_C^{HT} = \frac{3}{8} E_{Cl}^{HT} + \frac{5}{8} E_{Ct}^{HT} \tag{7}$$

A more rigorous model for short fibers or particulate reinforced composites inclusions has been proposed by Tandon and Weng [40] on the basis of the solutions found by Eshelby on an ellipsoidal inclusion surrounded by an infinite matrix [41] and the concept of average stress introduced by [42] Mori and Tanaka.

3. 2 Yield stress

Many models have been proposed in the specific literature to predict yield stress of composites. Pukánszky's model [43] describes the effects of the volume filler fraction (φ_f) and the interfacial interaction on tensile yield stress of particulate filled polymers:

$$\sigma_c = \sigma_m \frac{1 - \varphi_f}{1 + 2.5\varphi_f} \exp(B\varphi_f) \tag{8}$$

Parameter *B* is an interaction parameter that considers the capacity of stress transmission among the various components. The terms σ_c and σ_m are yield stresses of the composites and matrix, respectively. The term $\exp(B\varphi_f)$ indicates the interaction, while the $(1-\varphi_f)/(1+2.5\varphi_f)$ term indicates the effective decrease of useful cross section due to filler introduction. Interfacial interaction depends on the thickness of the interphase, and the strength of the interaction is shown in the following equation:

$$B = \left(1 + A_f \rho_f \tau\right) \ln \frac{\sigma_i}{\sigma_m} \tag{9}$$

where A_f, ρ_f, τ, σ_i are the specific surface area, density of the filler, thickness of the interphase and strength of interaction, respectively. Parameter B can be easily calculated by knowing the yield stress of the composites filled with different volume percentages of particle fillers.

IV. RESULTS AND DISCUSSIONS

As mentioned above, we investigated the effects of catalysts in the formulation co-polymers through the transesterification process on the mechanical and thermo properties as well as the interaction between the fibers and polymer matrix. The matrix was selected as a fixed amount of PLA and PC, which are 40wt% and 60%wt, respectively. Subsequently, the matrix was blended with varying amounts of fibers (5, 10, 15% wt) with and without the presence of catalysts.

4.1 Mechanical properties

The mechanical properties of materials are shown in Table 1. In both cases, Young's modulus improves with increasing amounts of Lyocell fibers, while the elongation at break of the composites decreased when compared to the corresponding matrix.

According to Cox's model, an estimation of the critical aspect ratio is possible, i.e. the ratio between the length where shear stress transfer occurs and the diameter of the fibers [43]:

$$a_c = 2.303 \sqrt{\frac{E_f(1+\nu_m)}{E_m}} \log \sqrt{\frac{\pi}{4\varphi_f}} \tag{10}$$

Formulas	Tenisle strength (MPa)	Young's modulus (GPa)	Elogation at break (%)
PLA40PC60	55.2	2.99	126
(PLA40PC60)Te5	61.8	3.14	6.26
(PLA40PC60)Te10	63.1	3.49	3.6
(PLA40PC60)Te15	63	4.02	2.36
(PLA40PC60CATA)	60.9	3.22	126
(PLA40PC60CATA)Te5	66.7	3.5	4.52
(PLA40PC60CATA)Te10	67.2	3.84	3.75
(PLA40PC60CATA)Te15	68.4	4.2	3.16

Table 1. Tensile test of materials without and with catalysts

Using a value of 12.5 GPa for the fibers modulus and the values of Table 1 for E_m, the critical aspect ratio can be estimated to vary from 7 for (PLA40PC60)Ly5 to 5.6 for (PLA40PC60)Ly15 and from 6.8 to 5.4 in the same formulas in the presence of catalysts. Since the Lyocell fibers have an aspect ratio of 37, this ensures a proper stress transfer from the matrix to the fibers and the buildup of the tensile stress in the fibers up to the maximum value achievable in a corresponding composites reinforced with continuous fibers. However, in the blends without catalyst, the tensile strength of materials reduces from 10%wt of fibers, which showed in Figure 2.

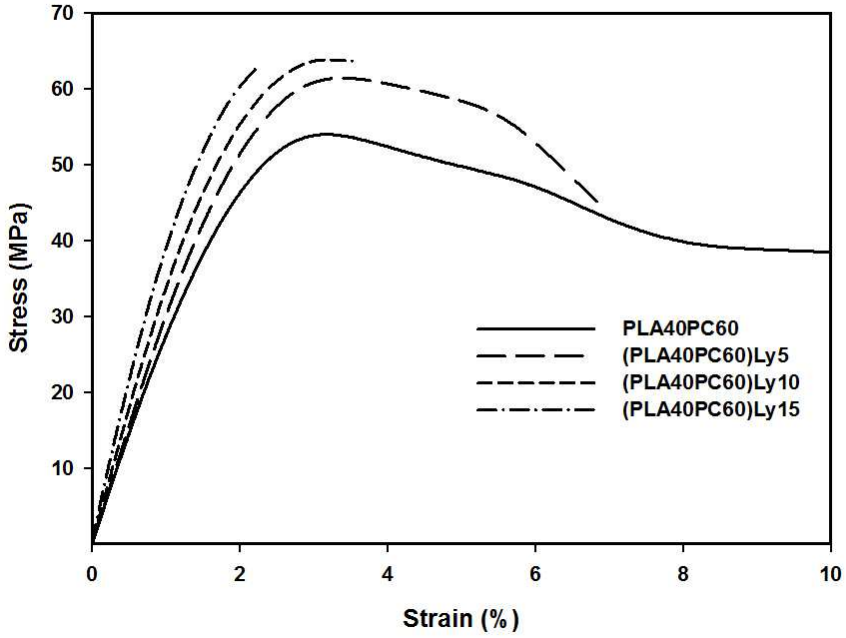

Figure 2. Tensile curve of the blends (PLA40/PC60)Ly with content of fibers

The composites cannot yield and become brittle at high fiber amounts. From the literature, the interaction between fibers and matrix is poor, therefore the structure of materials is weaker, although the aspect ratio condition showed that the stress can transfer from the fibers to the matrix. Meanwhile, the tensile strength of composites with an catalyst increases, while amount of Lyocell fibers increases, which is shown in Figure 3. Moreover, the elongation at break of composites is higher than the blends without a catalyst in the same amount of fibers. That enhancement indicates that the interaction between fibers and matrix is sufficient to maintain the structure of materials for transferring the stress from polymer to matrix.

The presence of catalysts improves the adhesion between the fibers and polymer matrix. This effect can be estimated quantitatively by using the B-factor according to equation (8). The B values of composites with and without catalysts are 4.2 and 5.1, respectively. The difference in B values point out the higher interaction between fibers and polymer matrix by acting of catalyst [43].

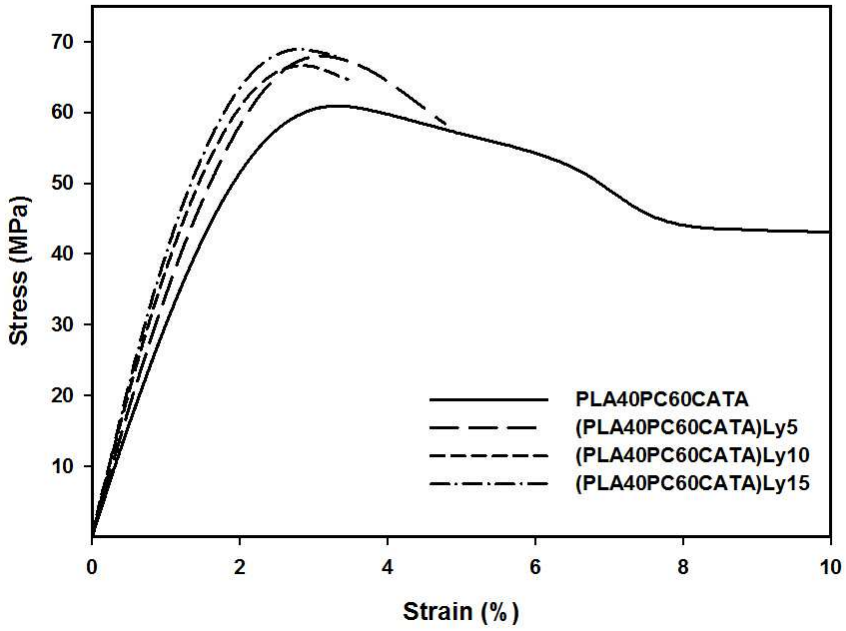

Figure 3. Tensile curve of the blends (PLA40/PC60/CATA)Ly with content of fibers

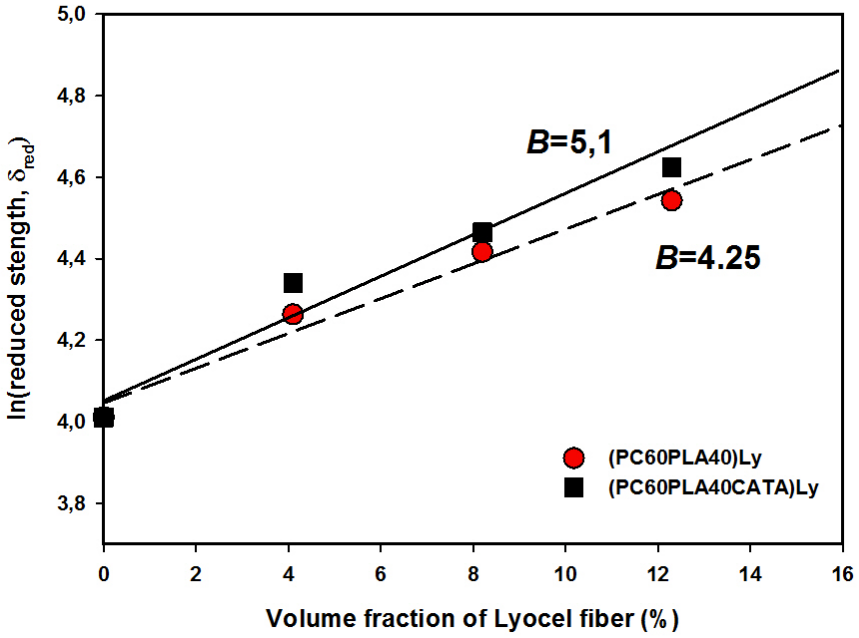

Figure 4. B factors of PLA40/PC60 composites without and with catalysts

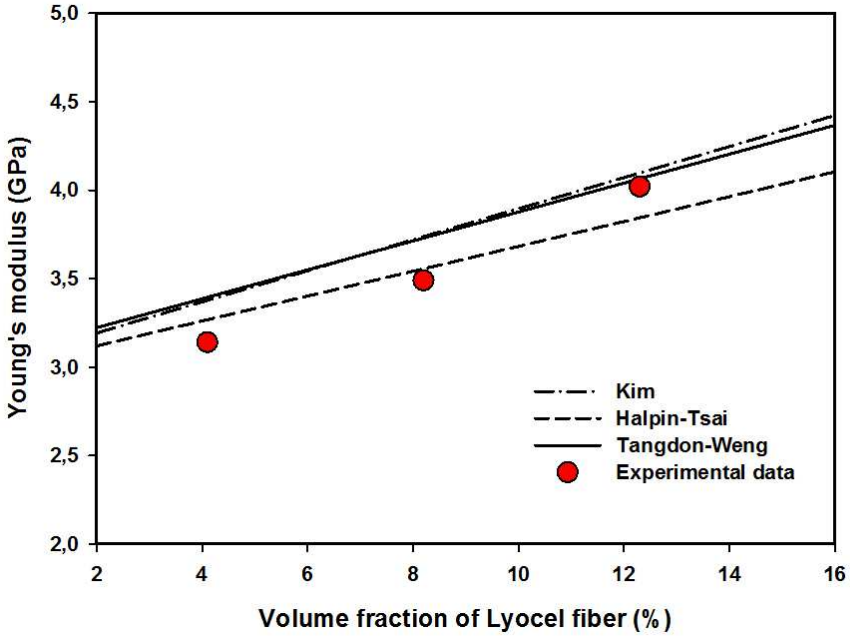

Figure 5. Comparison experimental data of (PLA40/PC60)Ly with theoretical models

Moreover, Kim's equation (1), Halpin-Tsai's equations (3) to (7) and Tandon-Weng's model provides estimates of the composites modulus. They were built up from the theory of long fibers, in which the perfect interaction between fibers and polymer matrix. The experimental data of composites are used to compare the models to authenticate the mechanical properties of materials. In Figure 5, the experimental data of composites without a catalyst show data far from the model values, while Young's modulus of blends with added catalysts fit well with Kim and Tangdon-Weng, which were developed in recent times and seem to be a better prediction than that of Halpin-Tsai. This implies that the interaction between the Lyocell fibers and polymer matrix is not only a perfect interaction, but also greater than in blends without a catalyst.

To investigate the effect of catalysts on the mechanical properties of composites, we suggested that there is reaction between hydroxyl groups (OH) of cellulose fibers and carboxyl functions (COOH) of polymers, which can be obtained through formulation process of copolymers under the transesterification mechanism of catalysts. The mechanism of this phenomenon was showed in Scheme 2.

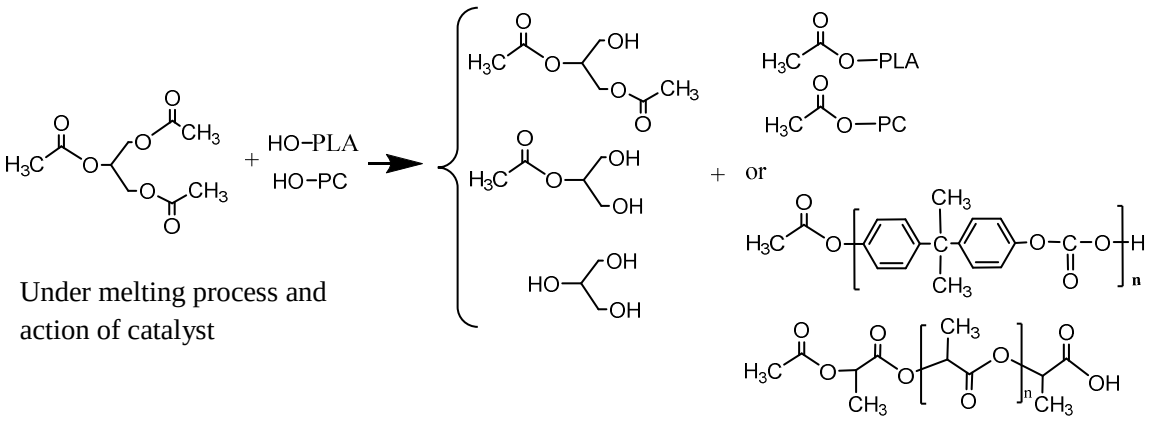

Under melting process and action of catalyst

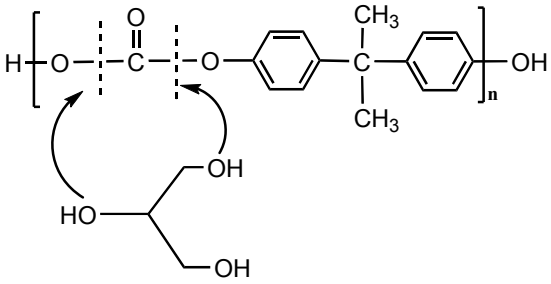

the Glycerin can attach to the PC, ➔ the polymer chains of PC broke down

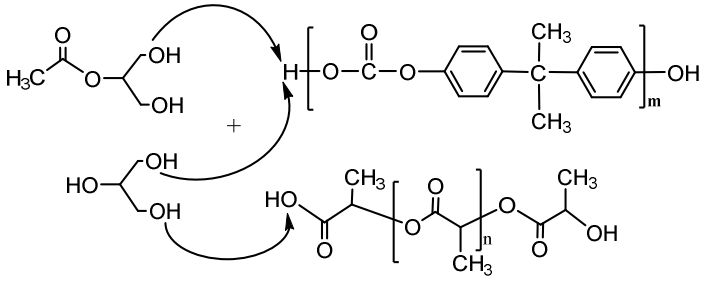

The broken PC polymer chains can react with PLA or itself to formulate random copolymer

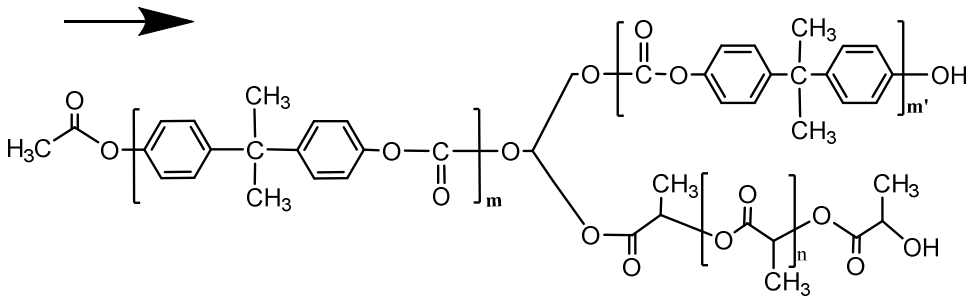

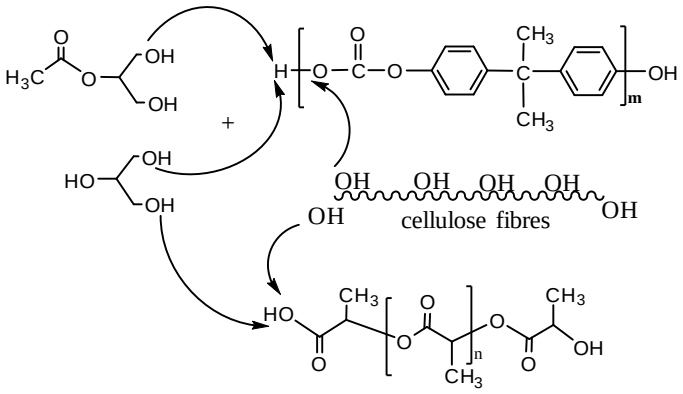

Scheme 2. Proposed mechanism of reaction between PLA/PC/Lyocell

in presence of triacetin and TBATPB

Triacetin can be modified by a transesterification agent (TBATBP) and OH functions in the end chain of PLA and PC in order to formulate glycerol. Glycerol can break down the original chains of PC and formulate new shorter PC chains, so that the amounts of COOH functions will increase. The TBATBP will accelerate the reactions between the polymers and the OH groups of cellulose fibers [45,46].

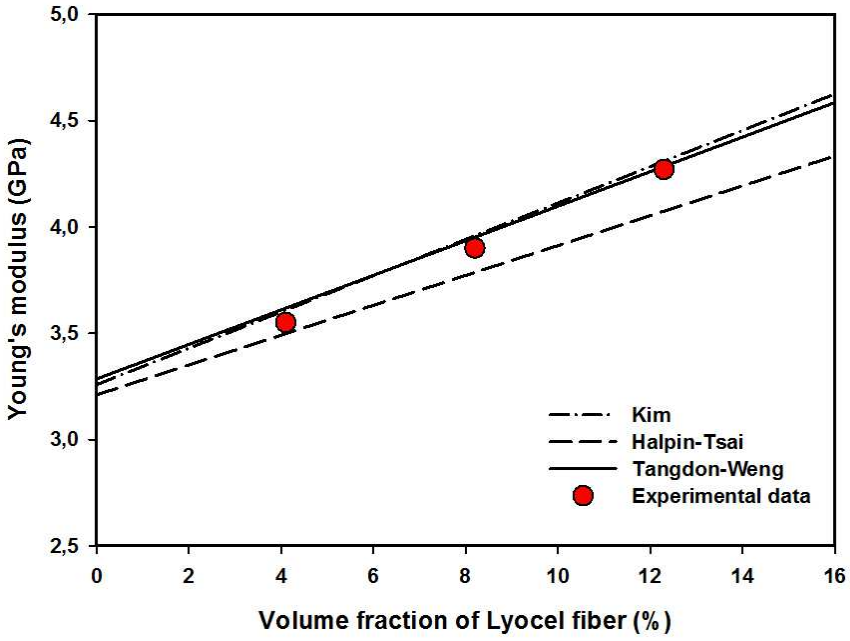

Figure 6. Comparison experimental data of (PLA40/PC60/CATA)Ly

with theoretical models

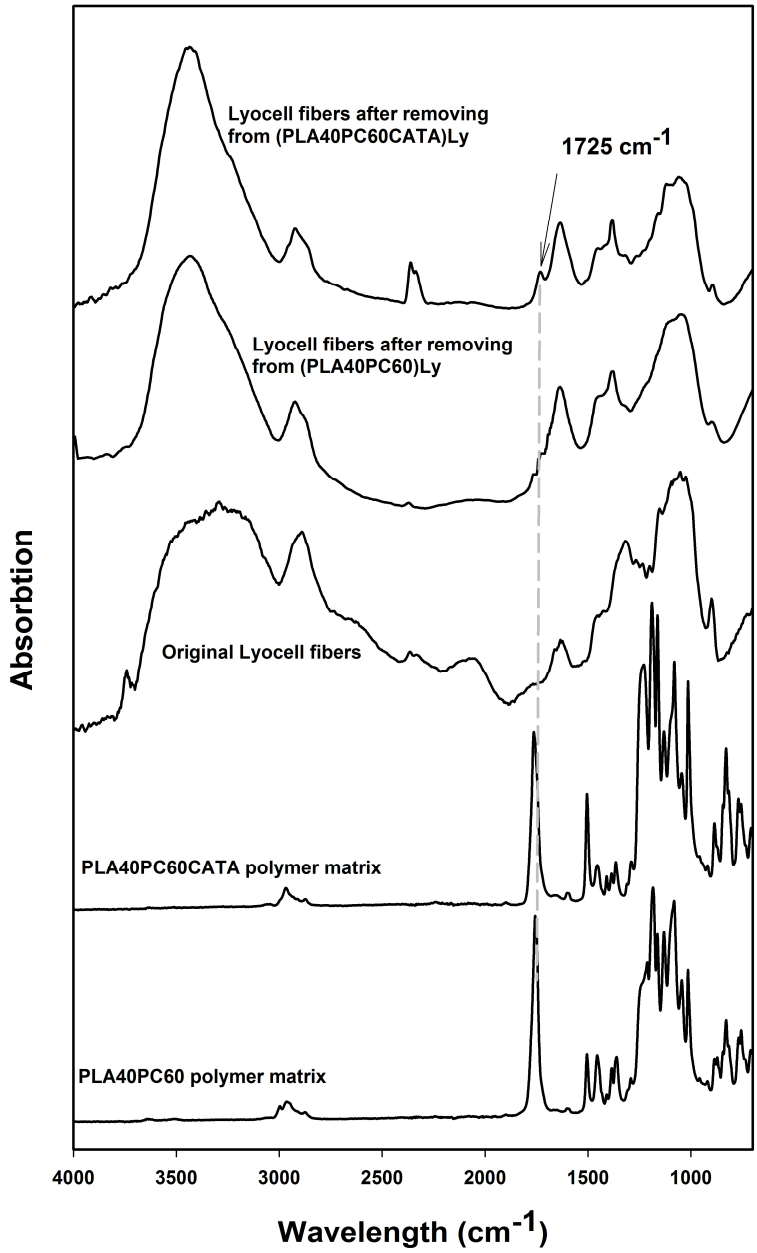

Figure 9. FTIR of fibers after processing with PLA40/PC60 with and without catalyst

To test this hypothesis, samples of (PLA40PC60)Ly15 and (PLA40PC60CATA)Ly15 were dissolved in THF to remove the polymer matrix from Lyocell fibers and examined for the ester group as evidence of a reaction between the fibers and matrix. The fibers were washed about five times using THF and Acetone and then dried under a vacuum in order to evaporate the solutions before testing FTiR. As

shown in Figure 9, the fibers obtained from the composites without catalysts show an FTIR spectra that completely overlap with that of the original Lyocell fibers, while those removed from the composites with a catalysts-modified matrix show an additional peak at 1725 cm^{-1}, corresponding to the stretching of C=O bonds in both PLA and PC, clearly indicating that the molecule now contains a carbonyl group, not present in the cellulose fiber solvent removed from the composites without TBATBP and Triacetin.

This can be interpreted as indirect proof of the presence of polymer molecules attached to the surface of the Lyocell fibers. Again, this fact not only confirmed the reaction between the fibers and polymer matrix, but also asserted our hypothesis on the mechanism of reaction.

4.2 Thermal behavior

The thermogravimetric and derivative thermogravimetric curves of PLA40PC60 blends with different amounts of Lyocell fibers are reported in Figure 7a and Figure 7b, respectively. The corresponding data are accounted for in Table 2.

Blends	**First stage**			**Second stage**		
	Temperature range, ^{0}C	Temperature peak, ^{0}C	Wt loss, %	Temperature range, ^{0}C	Temperature peak, ^{0}C	Wt loss, %
PLA40PC60	287-421	345	73	421-900	455	82
(PLA40PC60)Ly5	246-454	382	87	464-572	543	100
(PLA40PC60)Ly10	240-451	365	87	347-568	542	100
(PLA40PC60)Ly15	232-436	363	88	436-562	540	100
Lyocell fibers	220-572	380	100	-	551	-
PLA40PC60CATA	275-438	357	73	435-569	465	100

(PLA40PC60CATA)Ly5	267-452	388	76	452-594	579	100
(PLA40PC60CATA)Ly10	241-452	388	83	452-573	550	100
(PLA40PC60CATA)Ly15	238-452	388	86	452-558	545	100

Table 2. TGA analysis of materials

The TGA of PLA40PC60 blends shows that there are two main states of degradation. Degradation starts at an initial temperature, T_i=280°C, and the first stage temperature ends at 421°C with the DTG peak at 356°C, which can be attributed to the thermal degradation of Polylactic acid chains in the blends.

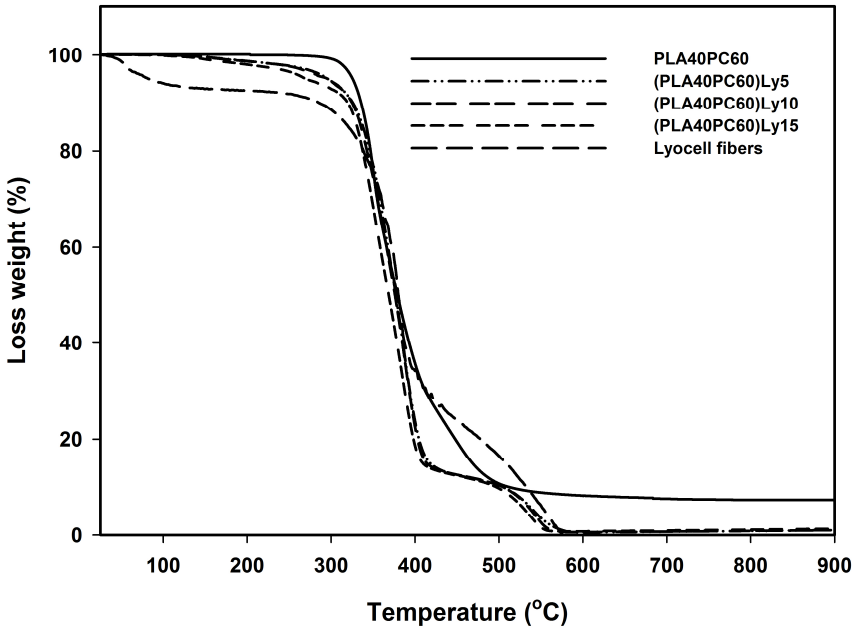

Figure 7A. TGA of the blends (PLA40/PC60)Ly with different content of fibers

The second stage of degradation ranges from 421°C to 900°C with a 7% solid residua. The DTG peak of this stage is 455°C and lower than the temperature of pure PC - 509°C. From literature PLA can facilitate the degradation temperature of PC, confirmed in our previous work or last chapter. When adding the Lyocell fibers, the starting degradation temperature of the composites is lowered than that of the

polymer blends-T_i=246°C. This change can be explained by the starting degradation temperature of Lyocell fibers - T_i =220°C.

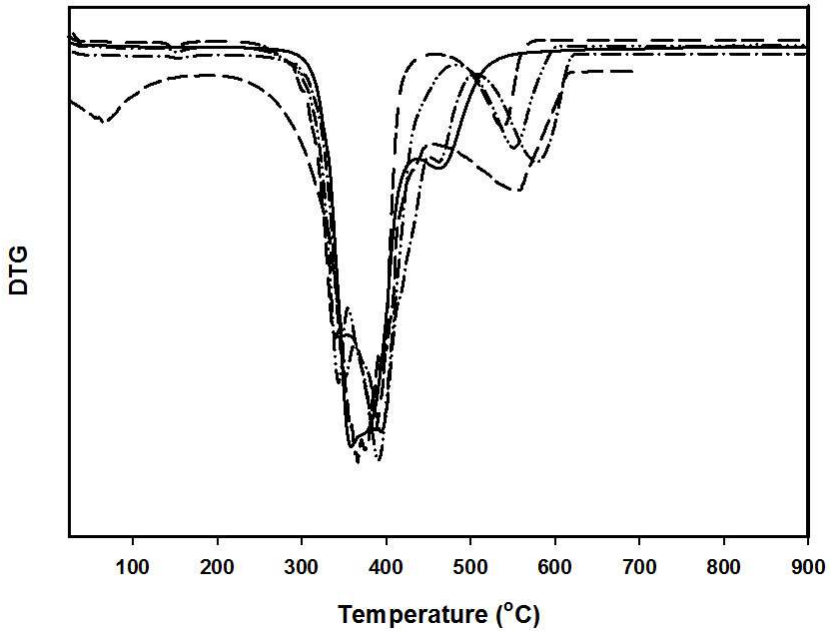

Figure 7B. DTG of the blends (PLA40/PC60)Ly with different content of fibers

In adding 5%wt Lyocell fibers, the DTG temperature peak of composites is 382°C, which is near the first stage peak of Lyocell fibers, but the DTG temperature decreases while increasing the fiber content. Moreover, the composites can be degraded completely after 572°C, having a different solid residua than the PLA40PC60 blends. In addition, the second stage peak of DTG for composites is 542°C, quite near the second stage of Cellulose fibers. Consequently, the Lyocell fibers acting as an agent can accelerate the degradation process of composites.

Meanwhile, the TGA and DTG of composites with the presence of catalysts performed can be seen in Figures 8A and 8B as well as in Table 2. Although the starting degradation temperature of PLA40PC60CATA-T_i = 275°C- is higher the corresponding one for PLA40PC60, the second stage temperature of blends with a catalyst related to degradation PC, is lower than blends without a catalyst.

This implies that the polymer chains of PC were broken down, similar to our reaction mechanism proposal and also confirmed by the last chapter. However, the starting degradation temperature of composites with a catalyst is higher than T_i of Lyocell fibers. The DGT curve shows that the temperature peak of composites is 388^{o}C even if the amount of fibers varies. This fact is completely different in blends without a catalyst. Furthermore, the DTG peak temperature in the second stage of composites is also higher than in the second stage of Lyocell fibers. This implies that there are some chemical interactions between the fibers and matrix, and that a new type of chemical link between the fibers and matrix are created. This is why cellulose fibers do not only facilitate the degradation of polymer matrix, but also preserve the DTG temperature even though the amount of fibers in the composites increases.

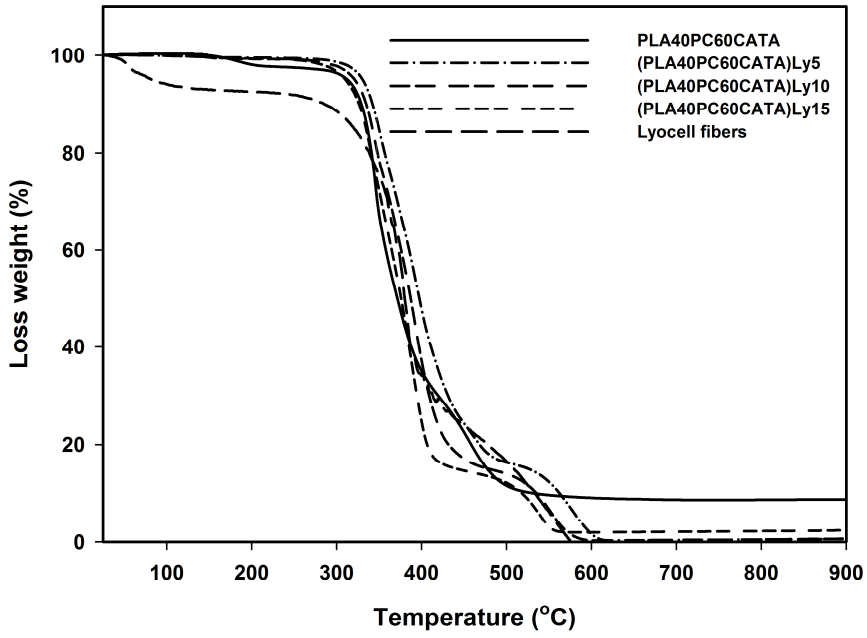

Figure 8A. TGA of the blends (PLA40/PC60/CATA)Ly with different content of fibers

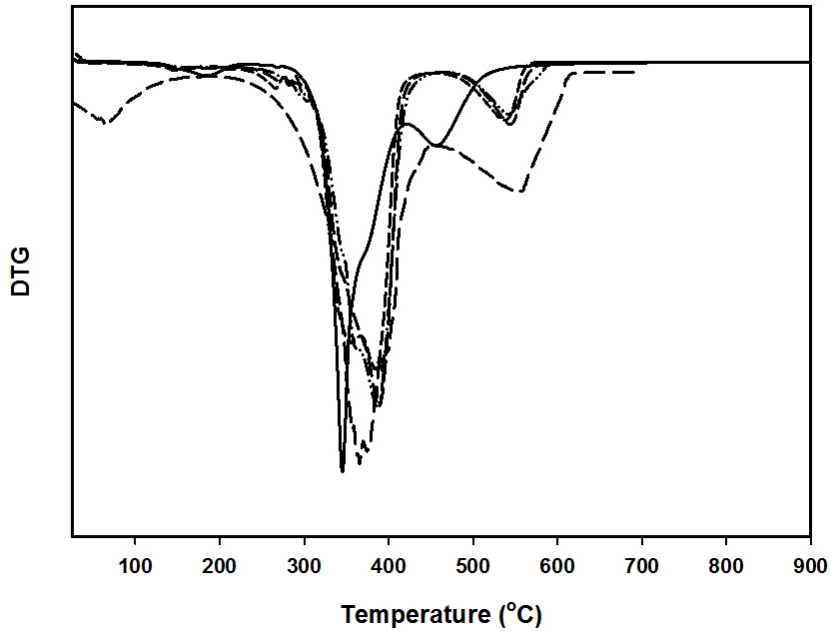

Figure 8B. DTG of the blends (PLA40/PC60/CATA)Ly with different content of fibers

4.3. Relaxation and structure

Figure 11a presents the DMTA spectrum for PLA40PC60 and its composites with different contents of Lyocell fibers. The temperature dependence of storage modulus and loss tangent is also shown in this figure. The temperature of loss tangent at 60^{o}C is representative for the glass transition temperature (T_g) of Polylactic acid [47], and the loss tangent at 160^{o}C is T_g of Polylactic acid. The DMTA of blends show that there is phase separation between Polylactic acid and polycarbonate in blends. The storage modulus decreases to 80^{o}C and then increases to 120^{o}C, implying that the crystallization of PLA phase proceeds during a DMTA run (low scan rate). The presence of fibers in the blend is not affected much by the glass transition temperature of both polymers, but it is slightly affected by the re-crystallization processing of Polylactic acid in blends. This fact was confirmed by the amount of losing storage modulus of composites as compared to PLA40PC60. This can be explained by the steric hindrance of fibers in the polymer matrix. Moreover, the Lyocell fibers show a higher storage modulus than the polymer matrix, which is well matched with tensile test above.

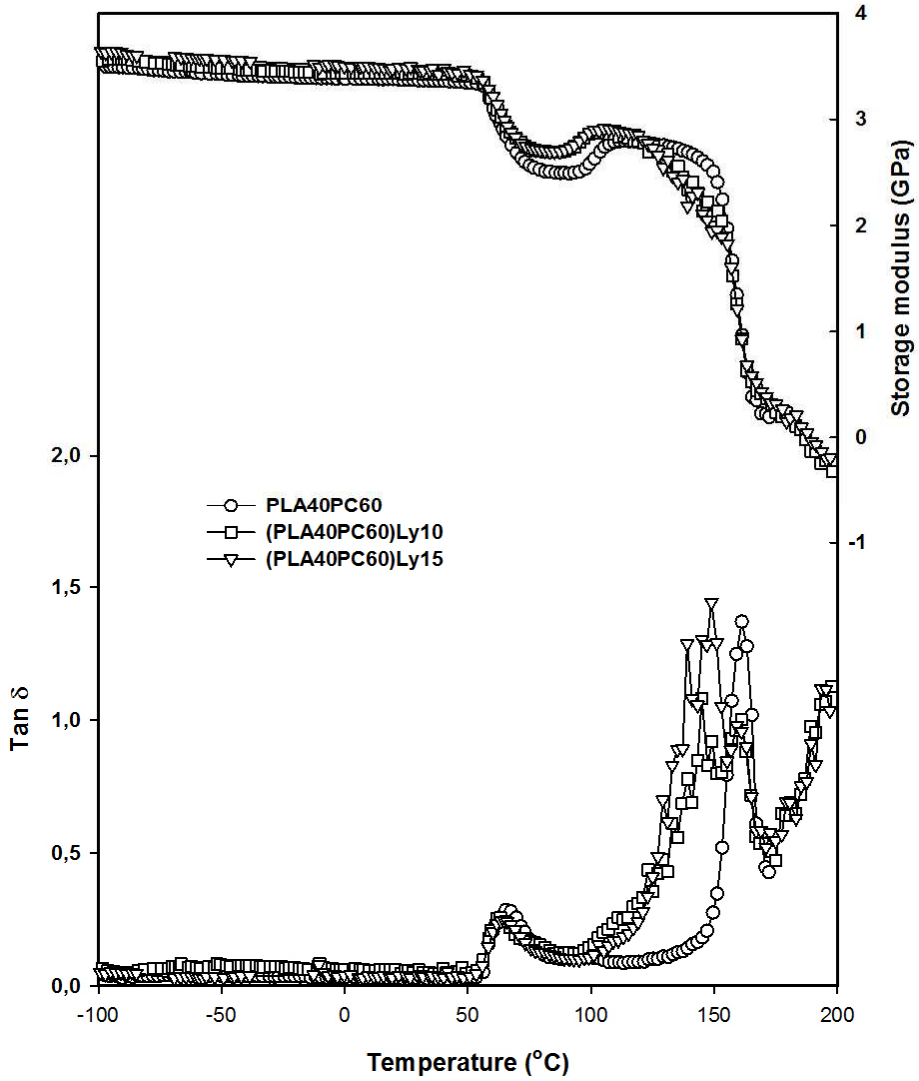

Figure 10. DMTA of the blends (PLA40/PC60)Ly with different content of fibers

However, the DMTA data of PLA40PC60 and composite blends with a catalyst shown in Figure 11B. In PLA40PC60CATA, there is a relaxation peak between the T_g of PLA and PC. It specify a T_g of new co-copolymer, which based on the reaction of PLA and PC. This co-copolymer is authenticated and the proposed mechanism of reaction in the last chapter as well as Scheme 2. Likewise, the low temperature peak at -28^{o}C, normally defined as the *β*-peak, is associated with the glucose ring units or to water associated with hydroxylmethyl groups [48]. Specifically, the *β*-peak is pronounced at high content

of fibers. In addition, the composites with 15%wt of fibers shows a new peak at 95°C, which is shoulder to the glass transition temperature of new copolymers. This behavior does not perform at low fiber contents as well as without catalysts. Consequently, we can conclude that the OH groups of fibers can react with a polymer matrix to formulate a new chemical interaction through the transesterification process. Besides, that chemical interaction enhances while the amount of fibers increases. That is why the new β-peak and shoulder of the T_g copolymer only performs at high fiber contents.

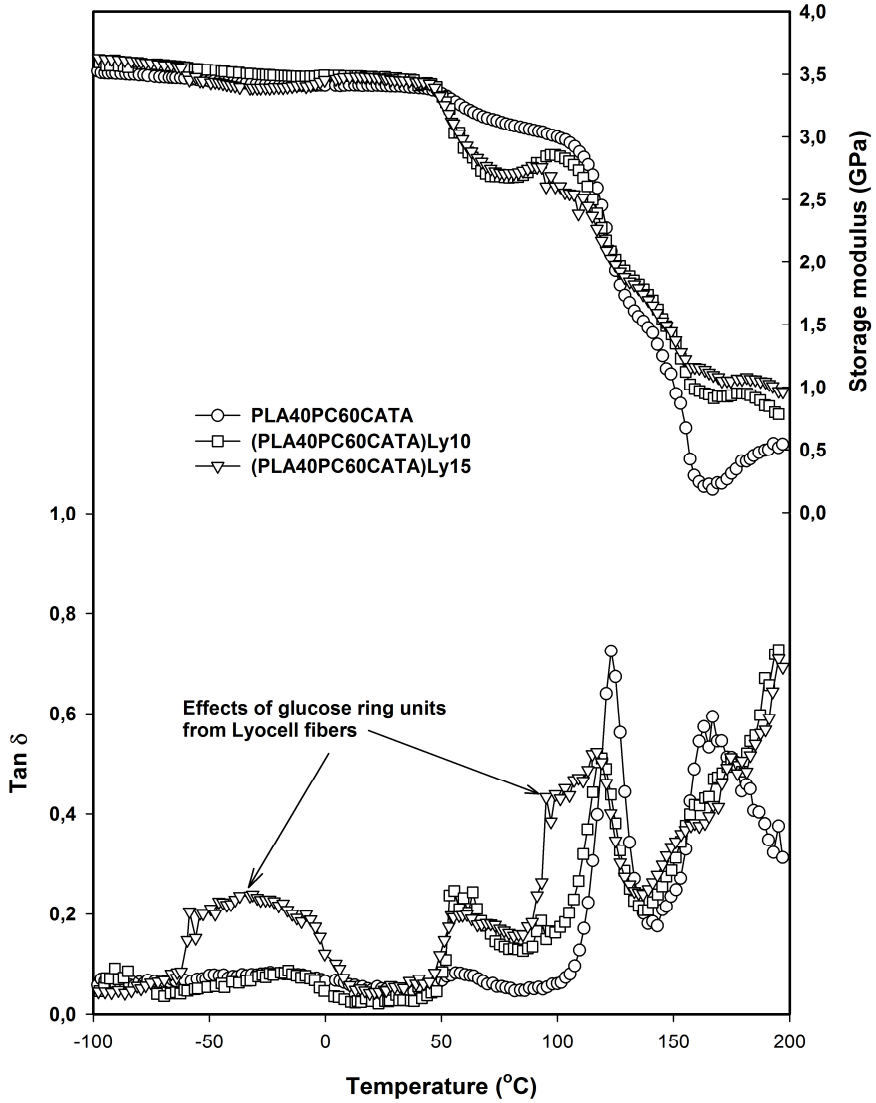

Figure 11. DMTA of the blends (PLA40/PC60/CATA)Ly with different content of fibers

Moreover, the storage modulus of PLA40PC60CATA does not show the re-crystalline of PLA because of the acting of a catalyst, which was explained in Chapter 3. Nevertheless, the addition of fibers changed the thermo properties of the materials. The composites obtained the re-crystallize processing by losing storage modulus after the T_g of PLA. This implies that the fibers have reaction between PLA and PC and affect the thermo behavior properties of the materials. This evidence confirmed the mechanism reaction hypothesis above.

4. Morphology

The fracture surfaces of (PLA40PC60)Ly15 are reported in Figures 12A and 12B. Almost all fibers pull out after cracking indicating that there are poor interactions between the fibers and polymer matrix. The high magnification of SEM images shows a notable gap between the fibers and matrix. In addition, the morphology of the polymer matrix performed clear phase separations as seen in Figure 12C. Due to the high surface tension of Polycarbonate, the domains of Polylactic acid do not have adhesion with the PC matrix. Similar to fibers, gaps were also obtained between the PLA domains and PC matrix. Although the aspect ratio of Lyocell fibers is higher than the critical aspect ratio and the stress can transfer from matrix to fibers, the mechanical properties of PLA40PC60Ly15 decreased and defected due to the heterogeneous structures of the materials and poor interaction between the components.

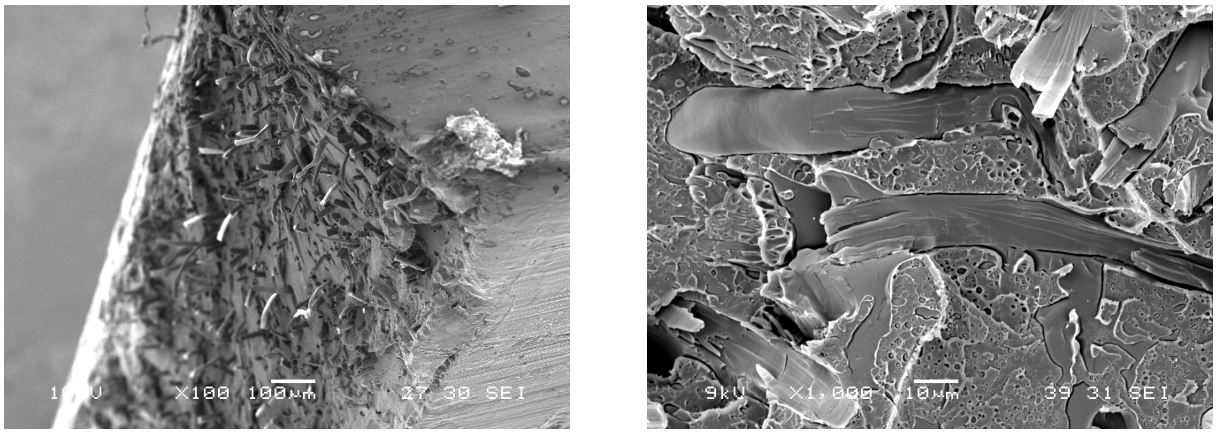

Figures 12 SEM of (PLA40/PC60)Ly15

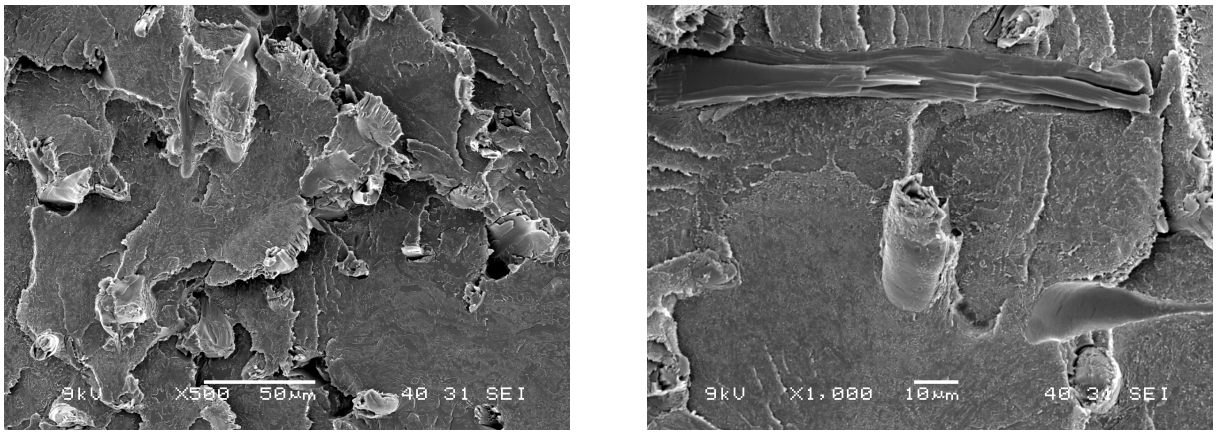

Figures 12 SEM of (PLA40/PC60/CATA)Ly15

To the contrary, the morphology of (PLA40PC60CATA)Ly15 shows perfect interaction between the fibers and matrix as shown in Figure 12D. It is evident that most of the fibers were stressed until broken down. Moreover, in Figure 12E, the morphology of the matrix seems co-continuous phases and perfect adhesion between PLA and PC or homogenous like copolymers instate of phase separations as PLA40PC60Ly15. This morphology confirmed that there are not only reactions between fibers and matrix, which are also confirmed by the FTIR and B factors, but also between the PLA and PC. The morphology of composites with the presence of a catalyst adequately authenticates our focus and explains why we used a catalyst as a factor to increase the mechanical and thermo resistance of composites.

V. CONCLUSIONS

The mechanical properties and thermo resistance as well as morphology of PLA40PC60 and Lyocell fibers are investigated carefully. Young's modulus of composites increases while the amount of cellulose fibers increases, but the material will not change the tensile strength significantly because of the poor interaction between the fibers and matrix as well as between the PLA and PC phases. The presence of Lyocell fibers not only decreases the elongation at break, but also facilitates the degradation process of the composites, which are shown in the tensile and TGA testing. Moreover, the fibers prevent the re-

crystalline process of PLA in the PLA40PC60 matrix due to losing the storage modulus of materials at low heat rates from the DMTA analysis.

However, catalysts can help overcome the negative properties of the PLA40PC60Ly15 composites. The mechanical properties of the materials at the same fiber content increase at the same fiber content as comparing to the composites without a catalyst. The new chemical links between fibers and matrix are obtained so that the thermo resistance and mechanical properties of the composites are enhanced. This was not only confirmed by the FTIR analysis, but also by the DMTA and SEM results. The homogenous phase or co-continuous phase between PLA and PC were performed, and the adhesion between the fibers and matrix was perfect, which fit well with the proposed mechanism reaction of blends. The exploitation actions of a catalyst in the formulation process of a copolymer to increase the interaction between fibers and a matrix can open the doors to new processing methods on production of green composites, bio-base or hybrid bio-degradable composites. This will counterbalance the negative properties of low mechanical properties and thermo resistance of biopolymers, potentially broadening its applications in electronics, car components, and in food packaging.

** This chapter was submitted Journal Composite Part A*

Acknowledgment

The authors gratefully acknowledge the financial support of the FORBIOPLAST (Forest Resource Sustainability through Bio-Based-Composite Development) project – Contract No. 212239-FP7-KBBE, funded by the European Commission under the 7th Framework Programme (FP7) (http://www.forbioplast.eu). Thanks to Dr Markus Gobl of Lenzing Aktiengesellschaft – Lenzing (Austria) for providing us the Tencel fibres. The authors wish also to acknowledge Ms Irene Anguillesi for performing DMTA and TGA tests.

VI. REFERENCES

1. Mohanty AK, Misra M, Hinrichsen G. Biofibres, biodegradable polymers and biocomposites: An overview. Macromolecular Materials and Engineering 2004;276:1–24.

2. Tsuji H, Fukui I. Enhanced thermal stability of poly (lactide)s in the melt by enantiomeric polymer blending. Polymer 2003;44:2891–2896.

3. Kido T, Yoshimura M, Yoka K. Japan published Patent Application 1995;109413.

4. Takehara A, Onoki T, Kageyama F. Japan, published Patent Application 2007;131795.

5.Ishihara J. Kuyama H, Ozeki E, Ishitoku T, Tanaka M, Sakamoto N. Crosslinked polycarbonate and polylactic acid composition containing the same. European Patent Application 1999;EP0896013.

6. RTP Co. Website Engineering Bioplastic Compounds. Available at: http://www.rtpcompany.com/info/flyers/bioplastic.pdf. Accessed on March 2013.

7. PolyOne Co. Website. reSoundTM Biopolymer Compounds (RS1200-0001 &RS1200-0002). Available at: http://www.polyone.com/en-us/products/engresincompund/pages/ reSound.aspx. Accessed on March 2013.

8. Suarez H, Barlow WJ, Paul DP. Mechanical properties of ABS/polycarbonate blends. Journal of Applied Polymer Science, 1984;29:3253–3259.

9. Warth H, Chen SC, Wang C, Wang Y, Li HC. Blend of aromatic polycarbonate and polylactic acid, the method for preparing the same and the use thereof. United State Patent 2012;US8242197B2.

10. Plackett D, Andersen TL, Pedersen WB, Nielsen L. Biodegradable composites based on L-polylactide and jute fibres. Composite Science Technology 2003;63:1287-1269.

11. Zini E, Baiardo M, Armelao L, Scandola M. Biodegradable polyesters reinforced with surface-modified vegetable fibers. Macromolecular Bioscience 2004;4:286-295.

12. Graupner N. Application of lignin as natural adhesion promoter in cotton fibre-reinforced poly(lactic acid) (PLA) composites. Journal of Material Science 2008;43:5222-5229

13. Graupner N, Herrmann A, Mussig. Natural and man-made cellulose fibre-reinforced poly (lactic acid)(PLA) composites: An overview about mechanical characteristics and application areas. Composite Part A 2009;40:810-821.

14. Bax B, Mussig J. Impact and tensile properties of PLA/Cordenka and PLA/flax composites. Composite Science and Technology 2008;68:1601-1607.

15. Bledzki AK, Jaszkiewicz A, Scherzer D. Mechanical properties of PLA composites with man-made cellulose and abaca fibres. Composite Part A 2009;40:404-412.

16. Teramoto N, Urata K, Ozawa K, Shibata M. Biodegradation of aliphatic polyester composites reinforced by abaca fiber. Polymer Degradable Stability 2004;86:401-409.

17. Garcia M, Garmendia I, Garcia J. Influence of natural fiber type in eco-composites. Journal of Applied Polymer Science 2008;107:2994-3004.

18. Threepopnatkul P, Kaerkitcha N, Athipongarporn N. Effect of surface treatment on performance of pieapple leaf fibers-polycarbonate composites. Composites Part B 2009;40:628-632.

19. Zini E, Baiardo M, Armelao L, Scandola M. Biodegradable polyesters reinforced with surface-modified vegetable fibers. Macromolecular Bioscience 2004;4:286-295.

20. Takatani M, Ikeda K, Sakamoto K, Okamoto T. Cellulose esters as compatibilizers in wood/poly (lactic acid) composite. Journal of Wood Science 2008;54:54-61.

21. Plackett D. Maleated Polylactide as an interfacial compatibilizer in biocomposites. Journal of Polymers and the Environment 2004;12:131-138.

22. Lee SH, Ohkita T. Mechanical and thermal flow properties of wood flour–biodegradable polymer composites. Journal of Applied Polymer Science 2003;90:1900-1905.

23. Petinakis E, Yu L, Edward G, Dean K, Liu HS, Andrew D. Effect of matrix–particle interfacial adhesion on the mechanical properties of Poly(lactic acid)/Wood-flour micro-composites. Journal of Polymers and the Environment 2009;17:83-94.

24. Finkenstadt VL, Liu LS, Willett JL. Evaluation of poly(lactic acid) and sugar beet pulp green composites. Journal of Polymer Environment 2007;15:1-6.

25. Islam MS, Pickering KL, Foreman NJ. Influence of accelerated ageing on the physico-mechanical properties of alkali-treated industrial hemp fibre reinforced poly(lactic acid) (PLA) composites. Polymer Degradation Stability 2010;95:59-65.

26. Shanks RA, Hodzic A, Ridderhof D. Composites of poly(lactic acid) with flax fibers modified by interstitial polymerization. Journal of Applied Polymer Science 2006;99:2305-2313.

27. Shibata M, Ozawa K, Teramoto N, Yosomiya R, Takeishi H. Biocomposites made from short abaca fiber and biodegradable polyesters. Macromolecular Materials and Engineering 2003;288:35-43.

28. Gregorova A, Hrabalova M, Wimmer R, Saake B, Altaner C . Poly(lactic acid) composites reinforced with fibers obtained from different tissue types of Picea Sitchensis. Journal Applied Polymer Science 2009;114:2616-2623.

29. Pilla S, Gong SQ, O'Neill E, Yang LQ, Rowell RM. Polylactide-recycled wood fiber composites. Journal of Applied Polymer Science 2009;111:37-47.

30. Li SH, Wang CP, Zhuang XW, Hu Y, Chu FX. Renewable resource-based composites of Acorn powder and Polylactide bio-plastic: Preparation and properties evaluation. Journal of Polymer Environment 2011;19:301–311.

31. Carrillo F, Martin G, Lopez-Mesas M, Colom X, Canavate J. High modulus regenerated cellulose fibers-reinforced cellulose acetate butyrate biocomposites. Journal of Computer Materials 2011;45:1733–1740.

32. Phuong TV, Lazzeri A. "Green" biocomposites based on cellulose diacetate and regenerated cellulose microfibers: Effect of plasticizer content on morphology and mechanical properties. Composites Part A 2012;43:2256–2268.

33. Cox HL. The Elasticity and Strength of Paper and Other Fibrous Materials. British Journal of Applied Physics 1952;3:72-79.

34. Nardone VC, Prewo KM. On the strength of discontinuous silicon carbide reinforced aluminum composites. Scripta Metallurgica et Materialia 1986;20:43-48.

35. Kim HG, Kwac LK. Evaluation of elastic modulus for unidirectionally aligned short fibers composites. Journal of Mechanical Science and Technology 2009;23:54-63.

36. Kim HG. A study on the prediction of elastic modulus in short fibers composites materials. Transactions of the Korean Society of Mechanical Engineers A 2005;29:318-324.

37. Kim HG. Effects of fibers aspect ratio evaluated by elastic analysis in discontinuous composites. Journal of Mechanical Science and Technology 2008;22:411-419.

38. Taya M, Arsenault RJ. A comparison between a shear lag type model and an Eshelby type model in predicting the mechanical properties of short fibers composites. Scripta Metallurgica et Materialia 1987;21:349-54.

39. Halpin JC, Kardos JL. The Halpin-Tsai equations: a review. Polymer Engineering and Science 1976;16:344-352.

40. Tandon GP, Weng GJ. The effect of aspect ratio of inclusions on the elastic properties of unidirectionally aligned composites. Polymer Composites 1984;5:327-333.

41. Eshelby, JD. The determination of the elastic field of an ellipsoidal inclusion, and related problems. Proceedings of the Royal Society of London 1957;A241:376-396.

42. Mori T, Tanaka K. Average stress in the matrix and average elastic energy of materials with misfitting inclusions. Acta Metallurgica 1973;21:571–574.

43. Pukánszky B. Influence of interface interaction on the ultimate tensile properties of polymer composites. Composites 1990;21:255–262.

44. Robinson IM, Robinson JM. The influence of fibre aspect ratio on the deformation of discontinuous fibre-reinforced composites, Journal of Material Science 1994;29:4663-4677.

45. López DE, Goodwin AG, , Bruce DA, Lotero E. Transesterification of triacetin with methanol on solid acid and base catalysts. Applied Catalysis A 2005;295:97–105.

46. Zięba A, Drelinkiewicz A, Chmielarz B, Matachowskia L, Stejskalc J. Transesterification of triacetin with methanol on various solid acid catalysts: A role of catalyst properties. Applied Catalysis A 2010;387:13-25.

47. Raman MA, Santic D, Spagnoli G, Romorino G, Penco M, Phuong TV, Lazzeri A. Biocomposites beased on Lignin and plasticized Poly(L-Lactic acid). Journal of Applied Polymer Science 2013;129: 202–214.

48. Szmel G, Klebert S, Sajo I, Pukanszky B. Thermal analysis of cellulose acetate modified with caprolactone. Journal of Thermal Analysis and Calorimetry 2008;91:715-722.

Chapter 5

Analysis on the influence of interface interactions on the mechanical properties of nanofiller and short fiber- reinforced polymer composites

I. INTRODUCTION

In recent years there has been a rapid growth in the development and application of nanofiller- and natural short fiber-reinforced thermoplastic polymer composites. In correspondence with this interest, increasing efforts have been devoted to better understand and measure the micro-mechanical parameters, which control the structure-property relationships in such composites. The properties of filled thermoplastic composites result from both nanoparticle/fiber and matrix properties and the ability to transfer stresses across the nanoparticle/fiber-matrix interface. Variables such as the volume fraction, aspect ratio, tensile strength, orientation of the nanoparticle or the short fiber as well as the interfacial strength are of primary importance to determine the mechanical properties of these composites. In particular, the ability to transfer stresses across the interface is often discussed in terms of 'adhesion' but is, in fact, related to a complex combination of factors such as surface energy of the reinforcing phase, adhesion strength of the interphase and the thickness of the coating layer. Therefore, it is not surprising if the nature of 'adhesion' is still a matter of debate in the literature and many techniques have been developed to measure it. For continuous fiber composites, 'adhesion' is generally related to the interfacial shear strength (τ or IFSS) or to the interlaminar shear strength (ILSS), which is somehow related to IFSS yet still a different parameter. Several experimental methods have been developed for their determination. These can be divided into two general categories: the single (direct testing) and the multiple fiber tests (indirect testing). The direct- or single fiber- testing methods aim at measuring the interfacial adhesion of

individual fibers in a matrix (microcomposites), while the indirect- multiple fiber- methods consider the collective behavior of fibers in a matrix (real composite) and estimate the interface strength via simplistic models. The experimental methods for single fibers are mainly the pull-out and the fragmentation tests and provide measures of IFSS [1,2]. In the case of multiple parallel fibers, the most important experimental techniques for the determination of ILSS are the Short Beam Interlaminar Shear and the Iosipescu Shear tests. There is no general consensus about which of these tests gives the most reliable measurements, but the situation is further complicated in the case of nanoparticle- or short fiber-reinforced thermoplastic composites since these techniques do not lend themselves to an easy extension for these types of composites.

Several methods have been recently developed for deriving values for τ (the IFSS) and η_o (a fiber orientation factor) from tensile stress-strain curve of the composite and the fiber length distribution based on modifications of the Kelly-Tyson equation [3,4]. Bader and Bowyer [5-7] presented a method for deriving values for τ and η_o from a simple combination of the tensile stress-strain curve and the composite fiber length distribution. Recently, Thomason improved this method and illustrated its application to injection molded glass-fiber-reinforced thermoplastic composites. Furthermore, he showed how the analysis could be extended to obtain the average fiber stress at composite failure, σ_{uf} [8].

Although developed originally for composites containing spherical particles, the semi-empirical equation proposed by Pukánszky [9] to describe the effects of filler volume fraction, φ_f, and interface interactions on yield stress and tensile strength of particulate-filled polymers has been recently successfully applied to anisotropic fillers such as layered silicate nanoparticles, multi-walled carbon nanotubes (MWCNTs), and wood fibers [10-12].

In Pukánszky's method and interaction parameter *B*, that considers the capacity of stress transfer between various components, can be easily calculated by knowing the yield stress of composites filled with different volume percentages of particle fillers.

Despite its simplicity and widespread use in characterize nanoparticle- and short fiber-reinforced composites, the adimensional Pukánszky *B*-factor is not related with physical-mechanical parameters such as the interfacial shear strength, τ, and other experimental variables like filler volume fraction, aspect ratio (a_r) and orientation factor.

In this paper we explore the relation between Pukánszky's interaction parameter *B* and these parameters, which are known to have a strong effect on the mechanical properties of composites. We present a modification of sPukánszky's approach by comparing it with the Kelly-Tyson equation to make a connection between the *B*-factor and the relevant physical-mechanical parameters. We apply this new approach to nanoparticle- and short fiber-reinforced thermoplastic composites. Values of τ and η_o obtained using this improved version of the original model are presented and discussed. We furthermore show how the analysis enables us to achieve values of the interfacial shear strength similar to those already published in the literature.

II. THEORETICAL ANALYSIS

The reinforcing effect of a filler or a fiber is expressed quantitatively by the following equation proposed by Pukánszky [9]:

1) $$\sigma_c = \sigma_m \frac{1-\varphi_f}{1+2.5\varphi_f} \exp\left(B\varphi_f\right)$$

In this equation, terms σ_c and σ_m are the yield stress of the composite and of the matrix, respectively, while the $(1-\varphi_f)/(1+2.5\varphi_f)$ term indicates the effective decrease of useful cross section due to filler introduction. The term $\exp(B\varphi_f)$ considers the filler-matrix interactions, by means of the interaction parameter *B* that considers the capacity of stress transfer between various components. For fillers, the interaction parameter depends on the thickness of the interphase, and the strength of the interaction is shown in the following equation:

2) $$B = \left(1 + A_f \rho_f l\right) ln \frac{\sigma_i}{\sigma_m}$$

where A_f, ρ_f, l, σ_i are the specific surface area and the density of the filler, the thickness of the interphase and the strength of interaction, respectively, that can be evaluated by knowing the yield stress of composites filled with different volume percentages of particle fillers [13]. Alternatively, the thickness of the interphase between particles and matrix can be evaluated by using the Shen–Li model which assumes the formation of a non-homogeneous interphases [14-15]. In this model, the mechanical properties of the medium at the microscopic scale do not change abruptly at the interface between the spherical particle and the polymeric matrix, but a transition region (or interphase) exists, in which the properties continuously relax until reaching those of the pure matrix at sufficiently long distances from the center of the filler particle.

We can write Eq. (1) in linear form:

3) $$\log(\sigma_{red}) = \log \frac{\sigma_c(1+2.5\varphi_f)}{\sigma_m(1-\varphi_f)} = B\varphi_f$$

and plotting the natural logarithm of reduced tensile strength, σ_{red}, against volume fraction (this graph will be called Pukánszky's plot in the following) should result in a linear correlation, the slope of which is proportional to the interaction parameter *B*.

According to the Kelly-Tyson model, the strength of the composite can instead be estimated by a simple modification of the mixture rule. Two cases must be identified, depending on whether the average length of the fibers, *L*, is lower or larger than the critical length, L_c, which is the minimum length necessary such that the stress is efficiently transferred from the matrix to the fibers, so that the center of the fiber reaches the ultimate (tensile) strength σ_f:

4) $$L_c = \frac{\sigma_f D}{2\tau} = \frac{\sigma_f L}{2\tau a_r}$$

where *D* is the diameter of the fibers.

For a composite containing more than a certain volume fraction, φ_{min}, the Kelly-Tyson model leads to the following equation ($\varphi > \varphi_{min}$):

5) $\sigma_c = \eta_o \sigma_f (1 - \frac{L_c}{2L})\varphi_f + \sigma'_m(1 - \varphi_f) = \eta_o \varphi_f \sigma_f (1 - \frac{\sigma_f}{4\tau a_r}) + \sigma'_m(1 - \varphi_f)$

where σ'_m represents the stress borne by the matrix when the strain of the composite is such that the fibers are strained to their ultimate tensile strain, ε_c.

Substituting σ_c from Eq. (5) into Eq. (3) we get

6) $$\log(\sigma_{red}) = \log \frac{\eta_o \varphi_f \sigma_f \left(1 - \frac{\sigma_f}{4\tau a_r}\right) + \sigma'_m(1 - \varphi_f)}{\sigma_m} + \log \frac{(1 + 2.5\varphi_f)}{(1 - \varphi_f)}$$

The second logarithmic term on the r.h.s. of Eq. (6) is approximately linear with φ_f in the range $0 \leq \varphi_f \leq 0.6$:

7) $$\log \frac{(1 + 2.5\varphi_f)}{(1 - \varphi_f)} \cong 3.04\varphi_f$$

The first logarithmic term on r.h.s. of Eq. (6) can be written as:

8) $$\log \frac{\eta_o \varphi_f \sigma_f \left(1 - \frac{\sigma_f}{4\tau a_r}\right) + \sigma'_m(1 - \varphi_f)}{\sigma_m} = \log \frac{\sigma'_m - \varphi_f \left[\sigma'_m - \eta_o \sigma_f \left(1 - \frac{\sigma_f}{4\tau a_r}\right)\right]}{\sigma_m} =$$

$$= \log \frac{\sigma'_m}{\sigma_m}\left[1 - \varphi_f \left[1 - \eta_o \frac{\sigma_f}{\sigma'_m}\left(1 - \frac{\sigma_f}{4\tau a_r}\right)\right]\right] = \log \frac{\sigma'_m}{\sigma_m} + \log \left[1 - \varphi_f \left[1 - \eta_o \frac{\sigma_f}{\sigma'_m}\left(1 - \frac{\sigma_f}{4\tau a_r}\right)\right]\right]$$

The latter equation, when $\varphi_f \to 0$, can be approximated into:

9) $$\log \frac{\sigma'_m}{\sigma_m} + \log \left[1 - \varphi_f \left[1 - \eta_o \frac{\sigma_f}{\sigma'_m}\left(1 - \frac{\sigma_f}{4\tau a_r}\right)\right]\right] \cong$$

$$\log \frac{\sigma'_m}{\sigma_m} - \varphi_f \left[1 - \eta_o \frac{\sigma_f}{\sigma'_m}\left(1 - \frac{\sigma_f}{4\tau a_r}\right)\right]$$

We can thus rewrite Eq. (6) in the following way:

10) $$\log(\sigma_{red}) = \log \frac{\sigma'_m}{\sigma_m} - \varphi_f \left[1 - \eta_o \frac{\sigma_f}{\sigma'_m}\left(1 - \frac{\sigma_f}{4\tau a_r}\right)\right] + 3.04\varphi_f$$

We observe that a Pukánszky's plot of Eq. (10) will give a straight line with slope

11) $$B = 3.04 - \left[1 - \eta_o \frac{\sigma_f}{\sigma'_m}\left(1 - \frac{\sigma_f}{4\tau a_r}\right)\right] \approx 2.04 + \eta_o \frac{\sigma_f}{\sigma'_m}\left(1 - \frac{\sigma_f}{4\tau a_r}\right)$$

and intercept $\log\frac{\sigma'_m}{\sigma_m}$ for $\varphi_f = 0$. When $\frac{\sigma'_m}{\sigma_m} \approx 1$ the straight line passes from the origin of the axis, as in the original Pukánszky's plot. Therefore Eq. (10) provides the theoretical basis for the extension of Pukánszky model for short fiber- and nanofiller-reinforced composites. In general, the plot of $\log(\sigma_{red})$ for short fiber- reinforced composites is not linear with φ_f but we can obtain *B* from the derivative of the $\log(\sigma_{red})$ vs. φ_f in the limit of $\varphi_f \to 0$.

From Eq. (11) we see that the interaction parameter *B* is dependent upon the tensile strengths of the matrix and of the fibers or fillers, the aspect ratio, the orientation factor and the interfacial shear strength. Eq. (11) enables us to calculate the maximum value for *B*, considering continuous aligned fibers:

12) $$B_{max} \approx 2.04 + \frac{\sigma_f}{\sigma'_m} \cong 2.04 + \frac{E_f \varepsilon_f}{E_m \varepsilon_f} = 2.04 + \frac{E_f}{E_m}$$

Eq. (11) also enables to estimate the IFSS from the value of *B*[1]:

13) $$\tau = \frac{\sigma_f}{4a_r\left[1-\frac{B-2.04}{\eta_o\frac{\sigma_f}{\sigma'_m}}\right]}$$

Eqs. (5), (10) and (11) are valid only when the fibers exceed a certain minimum volume fraction, φ_{min}, see Fig. 1, that can be estimated by considering that a composite will undergo immediate fracture if [16]:

14) $$\sigma_c \geq \sigma_m(1-\varphi_f) + \eta_o \sigma_f \frac{L_c}{2L}\varphi_f$$

where the last term takes into account the fact that fibers that have ends within $L_c/2$ of the cross-section at which the first fiber fails will not be broken. Now, substituting for σ_c from Eq. (5),

15) $$\eta_o \sigma_f (1-\frac{L_c}{2L})\varphi_f + \sigma'_m(1-\varphi_f) > \sigma_m(1-\varphi_f) + \eta_o \sigma_f \frac{L_c}{2L}\varphi_f$$

[1] In general, comparing Eq. (1) with Eq. (5) leads to the following expression:

$$\tau = \frac{\sigma_f}{4a_r\left\{1-\frac{\sigma_m(1-\varphi_f)}{\eta_o\varphi_f\sigma_f}\left[\frac{\exp(B\varphi_f)}{(1+2.5\varphi_f)}-\alpha\right]\right\}} \text{ for } L_f > L_c$$

where $\alpha = \frac{\sigma'_m}{\sigma_m}$.

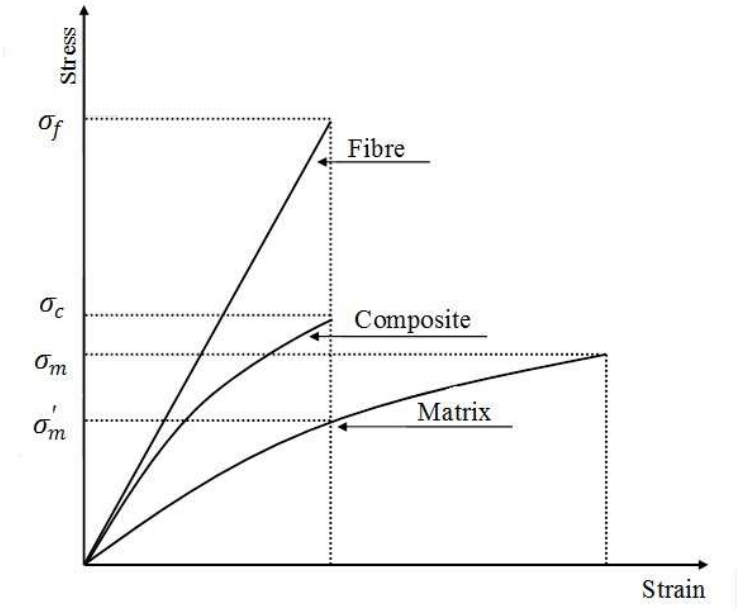

Figure 1a. Schematic representation of mechanical behavior for composites with $\varphi > \varphi_{min}$

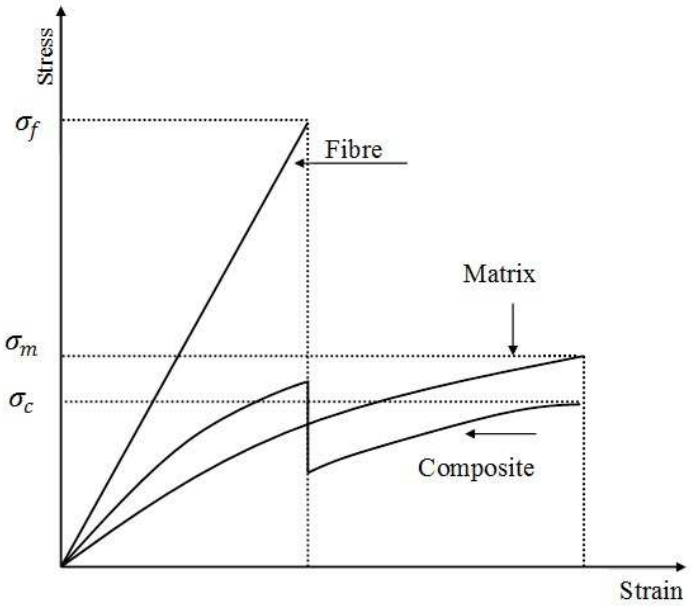

Figure 1a. Schematic representation of mechanical behavior for composites with $\varphi < \varphi_{min}$

we obtain φ_{min}, as follows:

(16) $$\varphi_{min} = \frac{\sigma_m - \sigma'_m}{\eta_o \sigma_f \left(1 - \frac{L_c}{L}\right) + \sigma_m - \sigma'_m} = \frac{\sigma_m - \sigma'_m}{\eta_o \sigma_f \left(1 - \frac{\sigma_f}{2\tau a_r}\right) + \sigma_m - \sigma'_m} \; (L > L_c)$$

At volume fractions less than φ_{min}, the strength of the composite is given by the equality in Eq. (14).

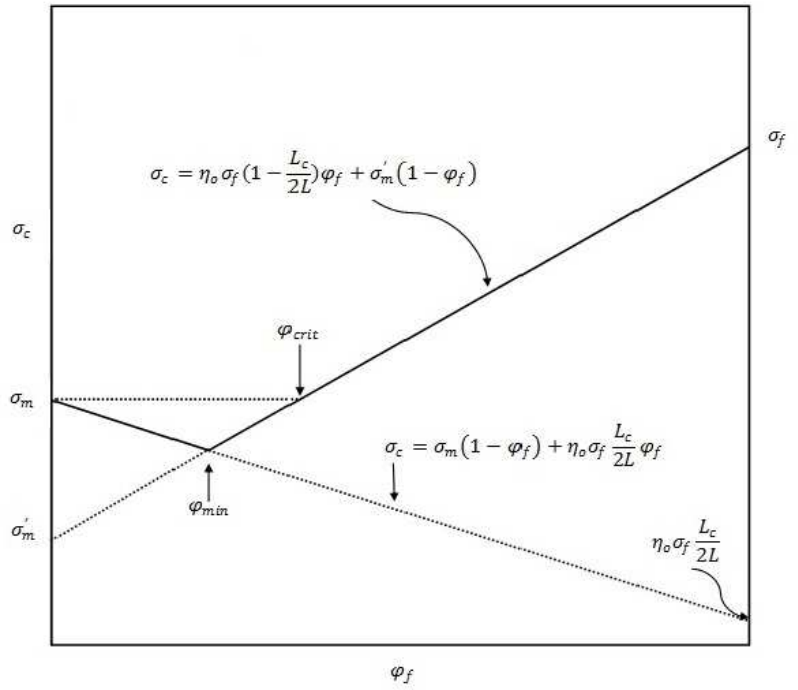

Figure 1c. theoretical variation of composite strength, σ_c, with volume fraction, φ_f, of nanofiller or short fiber reinforcement (c).

Therefore, the strength of the composite will be always greater the strength of the unreinforced matrix, when:

(17) $$\sigma_m(1 - \varphi_f) + \eta_o \sigma_f \frac{L_c}{2L}\varphi_f > \sigma_m$$

that is:

(18) $$\sigma_m < \eta_o \sigma_f \frac{L_c}{2L} = \frac{\sigma_f^2}{4\tau a_r}$$

If $\sigma_m > \eta_o \sigma_f \frac{L_c}{2L}$, this defines a critical volume fraction in the composite, φ_{crit}, necessary for composite strength to be greater than the strength of the unreinforced matrix, i.e. corresponding to the case $\sigma_c = \sigma_m$. The critical volume fraction is given by the following expression [16]:

19) $$\varphi_{crit} = \frac{\sigma_m - \sigma'_m}{\eta_o \sigma_f \left(1 - \frac{L_c}{2L}\right) - \sigma'_m} = \frac{\sigma_m - \sigma'_m}{\eta_o \sigma_f \left(1 - \frac{\sigma_f}{4\tau a_r}\right) - \sigma'_m}$$

Comparing Eqs. (16) and (19), we can see that $\varphi_{min} = \varphi_{crit}$ when $\sigma_m = \eta_o \sigma_f \frac{L_c}{2L} = \eta_o \frac{\sigma_f^2}{4\tau a_r}$

From Eq. (11) we can write:

20) $$\sigma'_m (B - 2.04) = \eta_o \sigma_f \left(1 - \frac{\sigma_f}{4\tau a_r}\right)$$

and substituting into Eq. (10):

21) $$\varphi_{crit} = \frac{\sigma_m - \sigma'_m}{\eta_o \sigma_f \left(1 - \frac{\sigma_f}{4\tau a_r}\right) - \sigma'_m} \cong \frac{\sigma_m - \sigma'_m}{\sigma'_m (B - 2.04) - \sigma'_m} = \frac{\frac{\sigma_m}{\sigma'_m} - 1}{B - 3.04}$$

The last equation sets a condition for the value of *B* above which the nanofillers or the fibers show a reinforcing action, B_{crit}:

22) $$B_{crit} \cong 3.04 + \frac{\frac{\sigma_m}{\sigma'_m} - 1}{\varphi_{crit}} \approx 3$$

Comparing Eq. (1) with Eq. (14), we can calculate the value of *B* corresponding to φ_{min}:

23) $$\sigma_m (1 - \varphi_{min}) + \eta_o \sigma_f \frac{L_c}{2L} \varphi_{min} = \sigma_m \frac{1 - \varphi_{min}}{1 + 2.5\varphi_{min}} \exp\left(B_{min} \varphi_{min}\right)$$

Solving for B_{min} we get:

24) $$B_{min} = \frac{1}{\varphi_{min}} \log\left\{\frac{1 + 2.5\varphi_{min}}{1 - \varphi_{min}} \left[(1 - \varphi_{min}) + \eta_o \frac{\sigma_f}{\sigma_m} \frac{L_c}{2L} \varphi_{min}\right]\right\}$$

Considering the approximation given by Eq. (7), we can write:

25) $$B_{min} \cong 3.04 + \frac{\log\left[(1 - \varphi_{min}) + \eta_o \frac{\sigma_f L_c}{\sigma_m 2L} \varphi_{min}\right]}{\varphi_{min}}$$

And with a suitable rearrangement:

26) $$B_{min} \cong 3.04 + \frac{\log\left[1+\varphi_{min}\left(\eta_o \frac{\sigma_f L_c}{\sigma_m 2L}-1\right)\right]}{\varphi_{min}}$$

For small values of φ_{min}, we can further approximate as follows:

27) $$B_{min} \approx 2.04 + \eta_o \frac{\sigma_f}{\sigma_m}\frac{L_c}{2L} = 2.04 + \eta_o \frac{\sigma_f^2}{4\tau\sigma_m a_r}$$

B_{min} is the minimum value of B for which it is possible to predict the tensile strength of the composite from the modified rule of mixtures and that enables to estimate τ from Eq. (13).

From Eq. (27) we see that the minimum interaction parameter B_{min} is dependent upon the tensile strengths of the matrix and of the fibers, the aspect ratio of the fibers, the orientation factor, and the interfacial shear strength.

Again, following Kelly and Davies [16], we now consider the case when $L = L_c$. From Eq. (16) where it is evident that $\varphi_{min} = 1$, thus the failure of the composite will occur by flow of the matrix.

However, from Eq. (18), it is evident that a strengthening effect will occur when:

28) $\sigma_m < \eta_o \frac{\sigma_f}{2}$ that is when $B_{min} \approx 2.04 + \eta_o \frac{\sigma_f}{2\sigma_m} > 3.04$

in this case, the strength of the composite will be given by

29) $$\sigma_c = \eta_o \frac{\sigma_f \varphi_f}{2} + \sigma_m\left(1-\varphi_f\right)$$

In an analogous way, we get:

30) $$B = \frac{\log\left\{\frac{1+2.5\varphi_f}{\sigma_m\left(1-\varphi_f\right)}\left[\eta_o \frac{\sigma_f \varphi_f}{2} + \sigma_m\left(1-\varphi_f\right)\right]\right\}}{\varphi_f}$$

For small values of φ_f we can approximate into:

31) $$B \cong 2.04 + \eta_o \frac{\sigma_f}{2\sigma_m} = B_{min}$$

Finally, for the case when $L < L_c$, it is apparent from Eq. (16) that φ_f is always $< \varphi_{min}$, so the failure of the composite occurs by plastic flow of the matrix. Thus the strength of the composite will be given by [16]:

32) $$\sigma_c = \frac{\eta_o \tau a_r \varphi_f}{2} + \sigma_m(1-\varphi_f)$$

Substituting σ_c from Eq. (1), we get

33) $$B = \frac{\log\left\{\frac{1+2.5\varphi_f}{\sigma_m(1-\varphi_f)}\left[\frac{\eta_o \tau a_r \varphi_f}{2}+\sigma_m(1-\varphi_f)\right]\right\}}{\varphi_f} \cong 2.04 + \frac{\eta_o \tau a_r}{2\sigma_m}$$

Solving this equation for the IFSS, we find:

34) $$\tau = \frac{2\sigma_m(B-2.04)}{\eta_o a_r}$$

Eq. 34 shows that the interfacial shear strength is directly proportional to *B*. It is important to note that for values of *B* smaller than 2.04, $\tau < 0$, which means that the fillers or the fibers do not show any reinforcing action on the matrix. Therefore, we can conclude that 2.04 is the lower limit for *B* for the application of Eqs. (13) and (34) in the estimation of the IFSS, τ.

III. DISCUSSION

Pukánszky's equation for tensile strength, originally developed for composites reinforced with quasi-spherical fillers [9], has been recently extended to nanofibers, carbon nanotubes and short natural fibers [10-12], although no theoretical justification for the use of such an equation for this type of composites has been provided so far in the literature. In this paper we propose a new interpretation of Pukánszky's model based on the classical Kelly–Tyson approach for short fiber composites [3, 16]. With this approach it was possible to find a correlation between Pukánszky's interaction factor *B* and the IFSS, τ. From Eq. (11) we can predict that *B* will increase with the tensile strengths of the fibers or fillers, their aspect ratio, orientation factor and the interfacial shear strength, and decrease upon increasing the stress reached by the matrix when the strain of the composite is such that the fibers are strained to their ultimate tensile strain, σ_m'.

In the present section we will show some examples of applications of this new approach with reference to some published data reported in the recent literature.

Bilotti *et al.* [10,17] showed the results of tensile tests carried out on sepiolite clay/polyamide 6 nanocomposites obtained by melt compounding and compared with similar nanocomposites prepared with two organically modified montmorillonite clays, identified by the geographic location from which they were mined, i.e., Yamagata, Japan (Kunipia-P hereafter MMT-JP) and Wyoming, USA (Cloisite hereafter MMT-USA) [18-19].

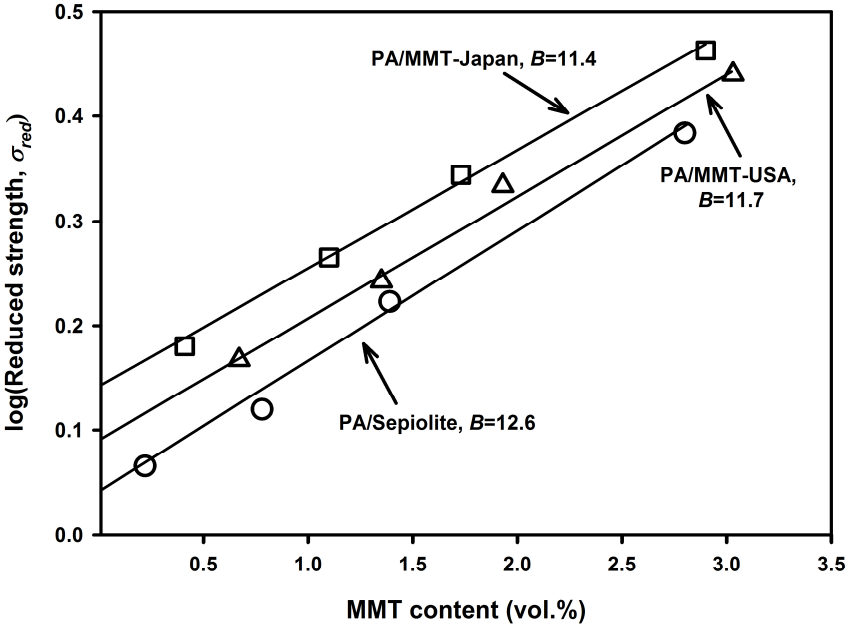

Figure 2. Pukánszky's plot of the data from Bilotti's data [25]

In Figure 2, we replotted Pukánszky's plot of the data from Bilotti, and we show the data regression lines, calculated without forcing them to pass through the origin of the Cartesian axis, for the three series of nanocomposites. In Tab. 1 we report the values of *B* and σ_m'obtained by the Pukánszky's model, as modified by Eq. (11). It can be observed that the *B* values are approximately constant for all types of nanocomposites. Also the values of σ_m' are similar but significantly larger than the tensile strength of the unmodified matrix, $\sigma_m = 69.7$ (MPa). This can be explained by considering that, in the case of nanocomposites, the immobilized layer of polymer chains that forms the interface will alter the

polymer – filler interaction at the molecular level, since the different structural organization of the matrix at the interface, with respect to the original matrix, hinders the polymer chain mobility [20].

Starting from these data we can estimate the IFSS of these composites. The aspect ratio reported in Tab. 2 has been calculated by Bilotti et al. [10,17] from experimental data of Young's modulus, using a_r as the fitting parameter of the Halpin-Tsai equations and considering an elastic modulus of all the nanoclays of 200 GPa [10, 21].

Material	σ'_m (MPa)	B	a_r	σ_f (MPa)	η_o	τ (MPa)	B_{max}
PA6/Sepiolite[a]	81.76	12.6	50	2500	0.6	29.5	32.6
PA6/MMT-USA[a]	76.38	11.7	36	2500	0.6	34.2	34.7
PA6/MMT-Japan[a]	80.13	11.4	45	2500	0.6	28.7	33.2
PP/MWCNT[b]	34.38	7.4	40	1720	0.6	13.1	52.1
PP/wood flour no MAPP[c]	17.04	3.8	12.6	300	0.6	7.2	19.6
PP/wood flour with MAPP[c]	17.04	5.8	12.6	300	0.6	9.2	19.6

Table 1. Values recalculated from original experimental data from [12,24] a); b) data from [25]; c) data from [11].

A difficulty arises in the estimation of σ_f, since no published data are available – to the authors' knowledge – on the tensile strength of individual nanoclay platelets. By considering that these nanoclays may possess the same tensile strength of industrially-produced alumina-silica fibers with similar Young's modulus (150-250 GPa), we assume a value of 2500 MPa in our calculations [22].

Bilotti reports a partial inplane orientation of sepiolite needle-like clays, thus we assume an orientation factor of 0.6 in our estimations. Tab. 1 reports the results of the calculation of IFSS for the three systems. Values of τ in the range 28-35 MPa are obtained from Eq. 13), with insignificant differences among the three types of nanoclays. Also the calculated value falls well in the expected range.

Figure 3 shows the dependence of *B* on the aspect ratio, a_r, calculated from Eq. 11) using the data in Tab. 1. As we can see, *B* monotonically rises until a plateau value of about 20.3 is obtained for PA6/Sepiolite. In the case $\eta_o = 1$, we obtain from Eq (12) B_{max} = 32.6 as reported in Tab. 1. For PA6/MMT-USA and PA6/MMT-Japan, the same calculations give 34.7 and 33.2.

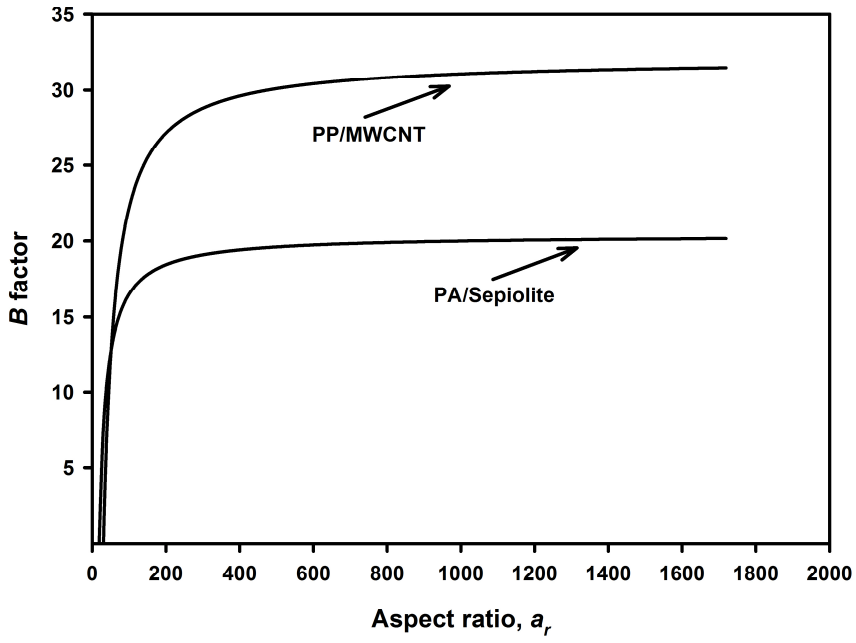

Figure 3. The dependence of *B* on the aspect ratio.

These figures compare well with the largest *B* values published according to Százdi *et al.* [23], which are below 25, although the same authors predict a value of about 200 for a completely exfoliated silicate on the basis of the linear dependence of *B* on the specific surface area.

The specific surface area of a nanoclay platelet can be related to its aspect ratio. By definition, the specific surface is given by:

35) $$A_S = \frac{A}{M} = \frac{A}{\rho V} = \frac{2\pi r^2}{\rho \pi r^2 h} = \frac{2}{\rho h}$$

For a platelet, the aspect ratio is defined as the ratio of mean diameter of a circle of the same area as the face of the plate to the mean thickness of the platelet, $a_r = d/h$, thus:

36) $$A_s = \frac{2}{\rho d} a_r$$

For a nanoclay, both ρ and d are constant for each specific type, while h can decrease with the degree of exfoliation. Thus, our model predicts that the relation between B and aspect ratio and specific surface area cannot be linear until complete exfoliation is attained. In fact, Eq. 12) related B_{max} with the ratio of the tensile strength of the nanofiller to the stress reached by the matrix when the composites fails. Before leaving Figure 3, where a constant τ is assumed, we also note that for values of a_r < 20, B is negative which means that the filler is actually detrimental for the tensile strength of the composites.

Polypropylene (PP) multi-walled carbon nanotube (MWNT) composites offer another interesting example of the model proposed in this paper. We consider the data published by Satapathy *et al.* [12, 24], which we replot in Figure 4. From the Pukánszky plot we obtain a value of B = 7.36 and $\sigma_m' = 34.38$ MPa. Extracting a value of IFSS from these data, using Eq. (13), requires knowledge of the tensile strength, aspect ratio and orientation factor of the MWCNTs. The MWNTs used by the group of Satapathy have been produced using chemical vapor deposition (CVD), and have a diameter in the range of 10 to 15 nm, lengths between 0.1 and 10 μm, giving an average aspect ratio of 40 [12, 24].

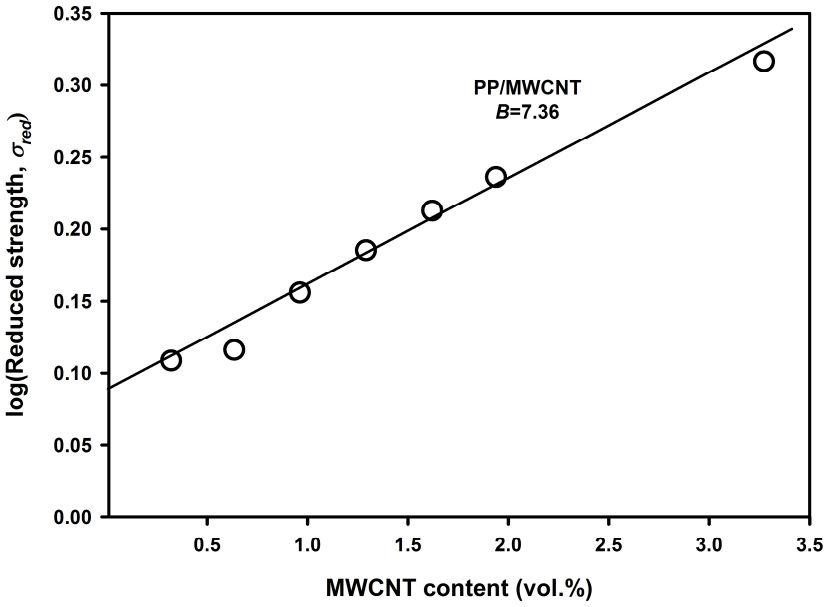

Figure 4. Pukánszky's plot from Satapathy's data [12,24]

By using the value of tensile strength, 1.72 GPa, measured by Pan *et al.* [25], on CVD-grown aligned MWCNTs we can estimate an IFSS of 13.1 MPa. Using these data in Figure 3 we observe that by increasing the aspect ratio an asymptotic value of B is reached at 31.5. For aligned MWCNT Eq. (12) provides an estimate of B_{max} = 52.1.

The data of Satapathy *et al.* [12, 24] are also replotted in the Pukánszky plot of Figure 5 together with the theoretical predictions of Eqs. (6) and (10). As it can be observed, the experimental data lie in the range where the curve obtained from the modified rule of mixture – Eq. (6) – can be approximated by Eq. (10). Significant deviations between the two curves only arise for volume fractions above 0.05.

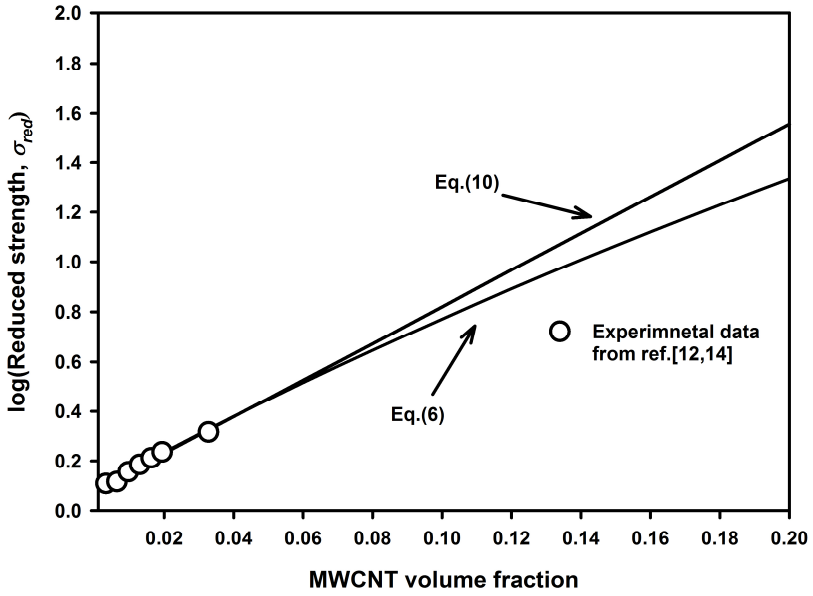

Figure 5. Comparison of the prediction of Eq.6 and Eq.10

with experimental data of Satapathy

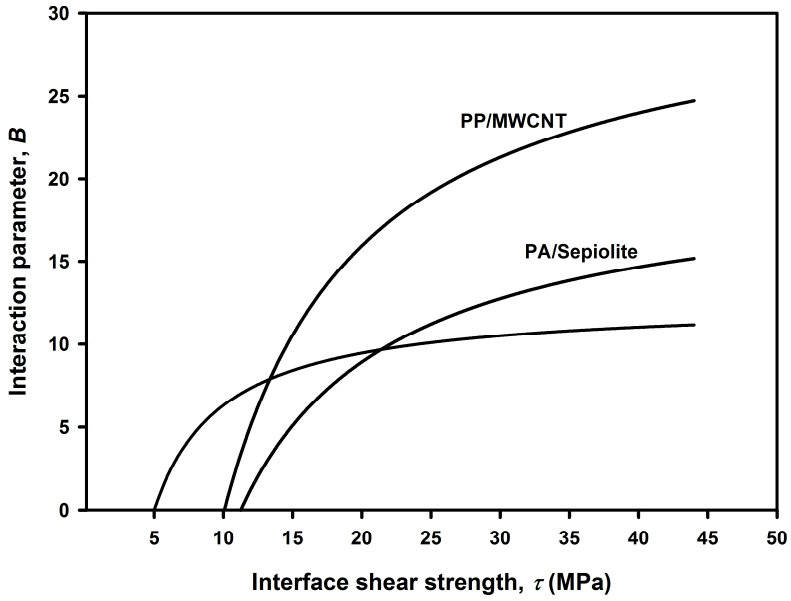

Figure 3. The dependence of *B* on the aspect ratio.

Finally, we examine some data published by the group of Prof. Pukánszky on PP/wood flour composites [11]. In this work, an ethylene-propylene random copolymer ethylene-propylene random copolymer (Tipplen R 359 from TVK Plc. - Tiszai Vegyi Kombinát - Hungary) has been mixed with lignocellulosic fibers (Arbocel FT 400 from Rettenmaier GmbH, Germany). To improve interfacial adhesion a maleic anhydride modified polypropylene PP (MAPP - Orevac CA 100 from Arkema Inc., Colombes Cedex, France) was used. The MAPP/wood ratio was chosen as 0.1.

Figure 7 shows the semi-log plot of reduced tensile strength as a function of the volume fraction for the two series of PP/wood flour composites: with and without modification with PP-*g*-MA. From the values of the interaction parameter obtained and reported in Tab. 1, we can calculate the IFSS. Again, we are faced with some assumptions since no information is provided in [11] to allow us to determine the orientation factor; moreover, we do not know the interface strength of the wood fibers.

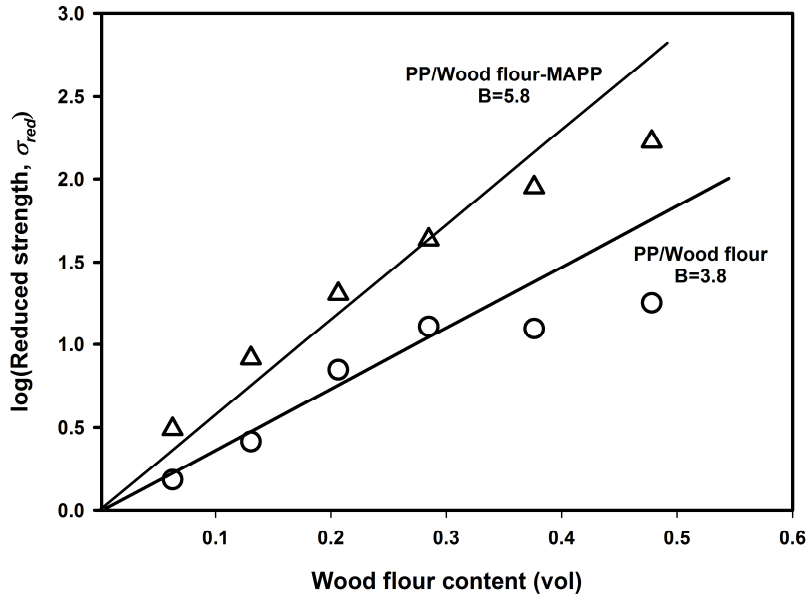

Figure 7. Pukánszky's plot of the data from Pukánszky [11]

Considering the literature on lignocellulosic fibers we find values between 130 and 600 MPa [26-30]. Assuming σ_f = 300 MPa and an orientation factor η_o = 0.6, the IFSS for the composites with PP/wood flour not treated with PP-*g*-MA is estimated to be 7.2 MPa. This is in agreement with the value of 7.9 MPa found by Rodriguez *et al.* [31] for corn stalk fiber reinforced PP. For PP/PP-*g*-MA/wood flour composites, the estimated interface shear strength rises to 9.2 MPa, with an increase of about 30%. This value of τ is substantially lower than that found from Rodriguez *et al.* [31] for composites containing 6% MAPP, corresponding to 15.5 MPa. This can be explained by the fact that the addition of PP-*g*-MA has brought the IFSS very close to its maximum predicted according to the von Mises criterion, $\tau = \sigma_m/\sqrt{3} =$ 9.8 MPa [32-33]. It has to be noted that all values of IFSS in Tab. 1 are below the respective values predicted by this condition.

IV. CONCLUSIONS

The Pukánszky model for the tensile strength, originally developed for filled composites, has been recently used with success for short fiber reinforced composites and various nanocomposites, although no theoretical justification has been provided so far for this new use. In this paper the Pukanszki equation has been analyzed in terms of the Kelly-Tyson model for the prediction of composite strength. In this way, it was possible to establish a direct link between Pukanszki's interaction parameter *B* and fundamental material parameters such as tensile strengths of the matrix and of the fibers, the aspect ratio of the fibers, the orientation factor and the interfacial shear strength IFSS. Also it was possible to determine the minimum value of *B* for which is possible to predict the tensile strength of the composite from the modified rule of mixtures, as well the maximum value that *B* can achieve in the case of continuous aligned fibers with the same type of matrix, fiber and interface shear strength. Moreover, a critical volume fraction, φ_{crit}, was defined corresponding to the minimum amount of filler content necessary for the

composite strength to be greater than the strength of the unreinforced matrix, i.e. corresponding to the case $\sigma_c = \sigma_m$. It was also shown that for this condition $B_{crit} \cong 3$.

From this analysis it was possible to express the interfacial shear strength in terms of *B* and other materials parameters, Eq. (13). From such an equation, it is possible to verify the monotonical relation between *B* and IFSS that has been suggested previously in the literature.

A few examples of calculations of the IFSS, τ, from Pukánszky's interaction factor *B* have been provided, using published literature values relating to nanocomposites with organically modified nanoclays and carbon nanotubes, as well as composites reinforced with short natural fibers. All results obtained fall within the value expected from similar literature values and below the maximum predicted according to the von Mises criterion, $\tau = \sigma_m/\sqrt{3}$.

The new equations presented in this paper provide a theoretical basis for the use of the Pukánszky's model in the case of nanocomposites and discontinuous fiber composites. Compared to the traditional Kelly-Tyson approach, the interaction factor B enables to give a rapid estimate of the interface shear strength even when fundamental material constants such as fiber tensile strength, aspect ratio and orientation factor as well as the stress in the matrix when the composites breaks, cannot be simply evaluated. This new approach can therefore be appreciated in research and development of new composites in industrial environments.

**This chapter was submitted Composite Science and Technology Journal*

Acknowledgment

The authors gratefully acknowledge the financial support of the FORBIOPLAST (Forest Resource Sustainability through Bio-Based-Composite Development) project – Contract No. 212239-FP7-KBBE, funded by the European Commission under the 7th Framework Programme (FP7) (http://www.forbioplast.eu).

V. REFERENCES

1. Hull D, Clyne TW. An introduction to composite materials, 2nd ed. Cambridge University Press, Cambridge 1996.
2. Matthews FL, Rawlings RD. Composite materials: Engineering and science. CRC Press, Boca Raton 1999.
3. Kelly A, Tyson WR, Tensile properties of fibre-reinforced metals: Copper/tungsten and copper/molybdenum. Journal of the Mechanics and Physics of Solids 1965;13:329-350.
4. Piggott MR. Short fibre polymer composites: A fracture-based theory of fibre reinforcement. Journal of Composite Materials1994;28:588-606.
5. Fu SY, Lauke B. Effects of fibre length and fibre orientation distributions on the tensile strength of short-fibre-reinforced polymers. Composites Science and Technology 1996;56:1179-1190.
6. Bowyer WH, Bader MG. On the reinforcement of thermoplastics by perfectly aligned discontinuous fibres. Journal of Material Science 1972;7:1315-1321.
7. Bader MG, Bowyer WH. An improved method of production for high strength fibre-reinforced thermoplastics. Composites 1973;4:150-156.
8. Thomason JL, Interfacial strength in thermoplastic composites - at last an industry friendly measurement method?. Composites Part A 2002;33:1283-1288.
9. Pukánszky B. Influence of interface interaction on the ultimate tensile properties of polymer composites. Composites 1990; 21: 255–62.
10. Bilotti E, Zhang R, Deng H, Quero F, Fischer HR, Peijsa T. Sepiolite needle-like clay for PA6 nanocomposites: An alternative to layered silicates. Composites Science and Technology 2009;69:2587–2595.

11. Renner K, Kenyó C, Móczó J, Pukànszky B. Micromechanical deformation processes in PP/wood composites: Particle characteristics, adhesion, mechanisms. Composites Part A 2010;41:1653-1661.
12. Satapathy BK, Ganß M, Pötscke P, Weidisch R. Stress transfer and fracture mechanisms in carbon nanotube-reinforced polymer nanocomposites. Cap 7 in: Vikas Mittal V (ed). Optimization of Polymer Nanocomposite Properties. Wiley-VCH Verlag. Weinheim 2010.
13. Voros G, Fekete E, Pukànszky B. An interphase with changing properties and the mechanism of deformation in particulate-filled polymers. The Journal of Adhesion 1997;64:229-250.
14. Shen L, Li J. Effective elastic moduli of composites reinforced by particle or fiber with an inhomogeneous interphase. International Journal of Solids and Structures 2003;40:1393–1409.
15. Cioni B, Lazzeri A. The role of interfacial interactions in the toughening of precipitated Calcium Carbonate–Polypropylene nanocomposites. Composite Interfaces 2012;17:533–549.
16. Kelly A, Davies GJ. The principles of the fibre reinforcement of metals. International Materials Reviews 1965;10:1-77.
17. Bilotti E. Polymer/Sepiolite clay nanocomposites, PhD Thesis, University of London, 2009.
18. Fornes TD, Yoon PJ, Keskkula H, Paul DR. Nylon 6 nanocomposites: the effect of matrix molecular weight. Polymer 2001;42:9929-9940.
19. Fornes TD, Hunter DL, Paul DR. Effect of sodium montmorillonite source on nylon 6/clay nanocomposites. Polymer 2004;45:2321-2331.
20. Pitsa D, Danikas MG. Interfaces features in polymer nanocomposites: A review of proposed models. Nano 2011;6:497-508.
21. Chen B, Evans JRG. Elastic moduli of clay platelets. Scripta Materialia 2006;54:1581–1585.
22. Bunsell AR, Berger MH. Ceramic fibres, Chap 7 in High-performance fibres, Ed. Hearle JWS, CRC Press, Boca Raton FL 2000.

23. Százdi L, Pozsgay A, Pukánszky B. Factors and processes influencing the reinforcing effect of layered silicates in polymer nanocomposites. European Polymer Journal 2007;43:345-359.
24. Ganß M, Satapathy BK, Thunga M, Weidisch R, Pötschke P, Jehnichen D. Structural interpretations of deformation and fracture behavior of polypropylene/multi-walled carbon nanotube composites. Acta Materialia 2008;56:2247–2261.
25. Pan ZW, Xie SS, Lu L, Chang BH, Sun LF, Zhou WY, Wang G, Zhang DL. Tensile tests of ropes of very long aligned multiwall carbon nanotubes. Applied Physics Letters 1999;74:3152–3154.
26. Méndez JA, Vilaseca F, Pèlach MA, López JP, Barberà L, Turon X, Gironès J, Mutjé P. Evaluation of the reinforcing effect of ground wood pulp in the preparation of polypropylene-based composites coupled with maleic anhydride grafted polypropylene. Journal of Applied Polymer Science 2007;105:3588–3596.
27. El Mansouri NE, Espinach FX, Julian F, Verdaguer N, Torres L, Llop MF, Mutje P. Research on the Suitability of organosolv semi-chemical triticale fibers as reinforcement for recycled HDPE composites. Bioresources 2012;7:5032-5047.
28. Vilaseca F, Valadez-Gonzalez A, Herrera-Franco PJ, Pèlach MÀ, López JP, Mutjé P. Biocomposites from abaca strands and polypropylene. Part I: Evaluation of the tensile properties. Bioresource Technology 2010;101:387-395.
29. Vallejosa ME, Espinach FX, Julián F, Torrese Ll, Vilaseca F, Mutjé P. Micromechanics of hemp strands in polypropylene composites. Composites Science and Technology 2012;72:1209–1213.
30. Venkateshwaran N, ElayaPerumal A. Modeling and evaluation of tensile properties of randomly oriented Banana/Epoxy composite. Journal of Reinforced Plastics and Composites 2011;30:1957-1967.

31. Rodriguez M, Rodriguez A, Bayer RJ, Vilaseca F, Girones J, Mutje P. Determination of corn stalk fibers' strength through modeling of the mechanical properties of its composites. Bioresources 2010;5:2535-2546.
32. Di Landro L, Di Benedetto AT, Groeger J. The effect of fiber-matrix stress transfer on the strength of fiber-reinforced composite materials. Polymer Composite 1988;9:209-222.
33. Pegoretti A, Della Volpe C, Detassis M, Migliaresi C. Thermomechanical behaviour of interfacial region in carbon fibre/epoxy composites. Composites Part A 1996;27A:1067–1074.

Chapter 6: General Conclusions

In the research focus of this dissertation, the mechanical properties, thermal stability and morphology of biocomposites based on cellulose diacetate (CDA), plasticized with a combination of reactive and non-reactive plasticizers and reinforced with fibers from natural resources, were investigated and results were reported in Chapter Two. Values of tensile strength and Young's modulus decreased with the increasing of plasticizer content. A good compromise between processing and mechanical properties for the composites with Lyocell cellulose fibers was obtained for the systems where CDA is plasticized with 20 wt% Triacetin (TA). The presence of GPE not only improved processability but also increased values of elongation at break in the materials produced. The glass transition temperature T_g decreased due to the effect of the primary plasticizer, as investigated by DMTA testing. SEM micrographs evidenced that, in samples with 20 wt% TA, the fibers were stressed until break with just a small amount being pulled-out. The adhesion of the polymeric matrix with the fibers improved by the addition of GPE, possibly because of the formation of strong chemical bonds with the polymer matrix through the epoxy groups of GPE. Therefore, this coupling agent can be applied to the blends, in which the polymer matrix has OH or NH groups, to increase the interaction between the fiber and matrix.

Moreover, the mechanical properties of the cellulose diacetate composite with different natural fillers were determined as a reference. Considering both processing conditions, the economic aspects and availability of raw materials on the market, biocomposites based on plasticized CDA reinforced with regenerated cellulose (Lyocell) microfibers could become an interesting option for the production of "green" biocomposites.

However, cellulose diacetate presents a disadvantage in processing by extrusion. It seems difficult to improve the elongation at break of cellulose diacetate through plasticizers and processing by extrusion. The author tried to increase the content of the plasticizer GPE and TA but the elongation at break, tensile and modulus decreased due to a decrease in the interaction between polymer chains of the materials. Moreover, it was attempted to blend plasticized cellulose diacetate with different biopolymers and toughness agents to enhance the toughness of materials. However, the cellulose diacetate has very high surface tension and was immiscible with the components in blends. In addition, the TA and polymer matrix have physical interactions as shown by the analysis of TGA. It will be possible that the plasticized polymers and composite cannot maintain the mechanical properties for long time in outdoor conditions. This point can limit the application of materials.

To develop biocomposites with good mechanical properties and able to maintain them for long periods of time that are inexpensive and that have high thermo resistance for different applications, it is necessary to develop a matrix with those properties first. For these reasons, blends of polylactic acid and polycarbonate with and without a catalyst were investigated carefully in Chapter Three. The effect of a catalyst and temperature on the mechanical properties of blends showed that the materials can obtain high miscibility processing at 230°C. Additionally, the blends with multi-catalysts in DMTA analysis presented a new peak on tan delta, which is between the relaxation temperature of PLA and PC, as evidence of the formation of a copolymer. Moreover, the data of TGA shows an increased thermal resistance in blends containing a catalyst. It also indicates that the new copolymer is formulated on that processing condition.

The mechanical properties of blends with varying amounts of polylactic acid demonstrated that Young's modulus of blends improve as the PLA amount is increased. The blends obtained the maximum elongation at break as the phases of blends were inverted. More specifically, they fit well with some

current models of mechanical properties. As the catalyst was added, Young's modulus of materials was enhanced thanks to the increasing interface of polymers by the formulation of new copolymers.

DSC and DMTA confirmed that as the content of PC increased, the crystallinity of materials was reduced. More specifically, the formula PLA40PC60 –CATALYST showed that the materials would not lose storage modulus after the temperature at T_g of PLA, namely no crystalline processing in that zone. Due to the catalyst, the links between PLA and PC were increased. Consequently, the PLA lessened the mobility and the crystalline process could not be obtained. These advantageous properties broadened the application possibility of materials as compared to current polymers based on PLA. In addition, the SEM and TEM confirmed once again the effect of a catalyst on the morphology of blends. By reducing the surface tension of PC and the new copolymer, the interactions between domain and matrix improved, and the size of the domains increased. The biodegradation tests demonstrated that the materials combined with a catalyst slightly decreased the percent of degradation after 70 days, but the speed of degradation was higher than with physical blends.

In Chapter Three, a new "hybrid" biopolymer was formulated by blending PLA and PC. Although the polycarbonates are not biodegradable, they are recyclable and thus are still friendly to the environment. To decrease the environmental impact of materials and to pursue the main focus of development of biocomposites, PLA/PC copolymer blends with Tencel fiber are reported in chapter four. The mechanical properties and thermo resistance as well as morphology of PLA40PC60 and Lyocell fibers are investigated carefully. Young's modulus of composites increases while the amount of cellulose fibers increases, but the material will not change the tensile strength significantly because of the poor interaction between the fibers and matrix as well as between the PLA and PC phases. The presence of Lyocell fibers not only decreases the elongation at break, but also facilitates the degradation process of the composites, which are shown in the tensile and TGA testing. Moreover, the fibers prevent the re-

crystalline process of PLA in the PLA40PC60 matrix due to losing the storage modulus of materials at low heat rates from the DMTA analysis.

However, catalysts can help overcome the negative properties of the PLA40PC60Ly15 composites. The mechanical properties of the materials at the same fiber content increase as compared to the composites without a catalyst. The new chemical links between fibers and matrix are obtained so that the thermo resistance and mechanical properties of the composites are enhanced. This was not only confirmed by the FTIR analysis, but also by the DMTA and SEM results. The homogenous phase or co-continuous phase between PLA and PC were achieved, and the adhesion between the fibers and matrix was perfect, which fit well with the proposed mechanism reaction of blends. The exploitation actions of a catalyst in the formulation process of a copolymer to increase the interaction between fibers and a matrix can open the doors to new processing methods on production of green composites, bio-based or hybrid bio-degradable composites. This will counterbalance the negative properties of low mechanical properties and thermo resistance of biopolymers, potentially broadening its applications in electronics, car components, and in food packaging.

In the development the new types of biocomposites with increased interaction between the fiber and matrix by practical experiment, we found that the theory in determining the interface shear strength (IFSS) of short fiber and fillers is still open, and this effect is not considered by the theory, although this is an important parameter on the mechanical properties of composites. For that reason, we developed a new method for predicting IFSS by an expression of Pukánszky's model and of the Kelly-Tyson Davies model, which is the focus of Chapter Five.

In this chapter, it was possible to establish a direct link between Pukanszky's interaction parameter B and fundamental parameters of the material such as tensile strengths of the matrix and of the fibers, the aspect ratio of the fibers, the orientation factor and the interfacial shear strength IFSS. It was also possible to determine the minimum value of *B* for which it is possible to predict the tensile strength of the

composite from the modified rule of mixtures, as well the maximum value that B can achieve in the case of continuous aligned fibers with the same type of matrix, fiber, and interface shear strength. From this analysis it was possible to express the interfacial shear strength in terms of B and other material parameters. It is possible to verify the monotonical relation between B and IFSS that has been suggested previously in the literature. A few examples of calculations of the IFSS, τ, from Pukánszky's interaction factor B have been provided, using published literature values relating to nanocomposites with organically modified nanoclays and carbon nanotubes, as well as composites reinforced with short natural fibers. This method will be used to determine TFSS from our experimental data in the previous chapter, which will confirm the effect of the coupling agent on the interface shear strength of composite. In the future, this new method will be used to compare with Thomason, Fu-Lauke or the current model in calculatin the IFSS fiber composite.

The research focus of this dissertation was achieved. New types of biocomposites based on renewable resources and recycled polymers were developed that have high mechanical properties, thermo resistances, that are biodegradable and recyclable. They will express the applications of biopolymers and biocomposites in different life applications such as food trays, electric components, cell phone covers, car components, and helmets. In particular, new methods for increasing the interaction between fibers in different polymeric matrices were obtained. They can be applied for different biopolymers and biofibers present in the market to improve the mechanical properties and fracture toughness of biocomposite materials. Moreover, the new model for estimating the interface shear strength of fibers/fillers are useful for predicting the mechanical properties of biocomposites not only in research, but also in production. The prediction of the IFSS of nanofillers in the matrix can be applied, something that was never estimated before in the theory.

More specifically, materials were also developed on an industrial scale for the production of "green composites" with a pilot scale extrusion machine. The products of this thesis not only apply to Italian plastic companies but also to European projects:

- FP7 – KBBE project FORBIOPLAST (Forest Resource Sustainability through Bio-Based Composite Development). 2010-2012.

- FP7-KBBE project DIBBIOPACK. (Development of injection and blow extrusion molded biodegradable and multifunctional packages by nanotechnologies: improvement of structural and barrier properties, smart features, and sustainability). 2012-2013

- FP7-KBBE project BIOBOARD (Bio-Board for a sustainable protein-based paper coating system) 2012- 2013.

- FP7-KBBE project OliPHA (Functional sustainable packaging)

- Thermozeta Company - Milano – Italy, producer of coffee caps.

- Fiat Company - Torino- Italy - producer of car components

- Acetati Spa – Verbania - Italy - producer of helmet, sport components, etc.

- Mircotech - Venizia - Italy - producer of mixing pellets and fillers for plastic components

- Euromaster - Prato - Italy - producer of mixing pellets for plastic components

SCIENTIFIC PRODUCTIONS

A. PATENTS:

1. International Application Patent PTC – WO2012/025907A1 - “COPOLYMER BASED ON POLYESTER AND AROMATIC POLYCARBONATE”, published on 1st – March, 2012. Andrea lazzeri, Vu Thanh Phuong, Patrizia Cinelli.

2. Italian Application Patent “COPOLIMERI A BASE DI POLIESTERI E PLASTIFICANTI REATTIVI PER LA PRODUZIONE DI FILM DA IMBALLAGGIO TRASPARENTI E BIODEGRADABILI” . Andrea Lazzeri, Vu Thanh Phuong, Patrizia Cinelli – Applied.

B. PUBLISHED INTERNATIONAL PAPERS:

1. Composite Part A: ““Green” Biocomposites Based on Cellulose Diacetate and Regenerated Cellulose Microfibers: Effect of Plasticizer Content on Morphology and Mechanical Properties” .Thanh vu Phuong, Andrea Lazzeri –Volume 43, Issue 12, December 2012, Pages 2256–2268.

2. Journal Applied of Polymer Science:“Biocomposites Based on Lignin and Plasticized Poly (L-lactic Acid)”. Md. Arifur Rahman, Diego De Santis, Gloria Spagnoli, Giorgio Ramorino, Maurizio Penco, Thanh Vu Phuong , Andrea Lazzeri. – Published online, DOI: 10.1002/app.38705.

C. PUBLISHED INTERNATIONAL CONFERENCE PAPERS

1. Thanh vu Phuong, Andrea Lazzeri. “Green” Biocomposites Based on Cellulose Diacetate and Regenerated Cellulose Microfibers: Effect of Plasticizer Content on Morphology and Mechanical Properties”. ECCM 15th – Venice – Italia.

2. Thanh Vu Phuong, Patrizia Cinelli, Andrea Lazzeri“Green” Biocomposites Based on Cellulose Diacetate and Regenerated Cellulose Microfibers: Effect of Plasticizer Content on Morphology and Mechanical Properties” BiPoco 2012 in Siofok – Hungary

3. Thanh Vu Phuong, Patrizia Cinelli, MarizioPenco, Andrea Lazzeri “ Copolymer based on polyester and aromatic polycarbonate" BiPoco 2012 in Siofok – Hungary.

4. Thanh Vu Phuong,Andrea Lazzeri“Green” Biocomposites Based on Cellulose Diacetate and Regenerated Cellulose Microfibers: Effect of Plasticizer Content on Morphology and Mechanical Properties”. 2st Workshop on Green Chemistry and Nanotechnologies in Polymer Chemistry, Riga, Latvia 5-6 of May 2011.

5 .Thanh vu Phuong, Andrea Lazzeri“Green” Biocomposites Based on Cellulose Diacetate and Regenerated Cellulose Microfibers: Effect of Plasticizer Content on Morphology and Mechanical Properties” 32nd International SAMPE EUROPE Conference / JEC 2011 – PARIS – from 25-29/3/2011.

6. “Pubblicazionesu USB, Crete 2012 3rd International Conference on industrial and hazardous waste management” - Workshop “Diffusion of waste-related cleaner technologies: how R&D contributes to sustainable solutions”, 12-14 Settember 2012, Creta, Grecia, “Bio-composites based on forest derived materials and biodegradable polymers” A. Lazzeri, P. Cinelli, T. V. Phuong, I. Anguillesi; pp7

C. ATTENDING INTERNATIONAL PROJECTS:

1. FP7 – KBBE projectFORBIOPLAST (Forest Resource Sustainability through Bio-Based Composite Development). 2010-2012.

2. FP7-KBBE project DIBBIOPACK.(Development of injection and blow extrusion molded biodegradable and multifunctional packages by nanotechnologies: improvement of structural and barrier properties, smart features, and sustainability)2012-2013

3. FP7-KBBE project BIOBOARD (Bio-Board for a sustainable protein-based paper coating system) 2012- 2013.

4. FP7 – KBBE project EVOLUTION(The Electric Vehicle revOLUTION enabled by advanced materials highly hybridized into lightweight components for easy integration and dismantling providing a reduced life cycle cost logic). 2012-2013.

D. COOPERATION WITH COMPANIES:

1. Thermozeta Company - Milano – Italy, producer of coffee caps.

2. Fiat Company - Torino- Italy - producer of car components

3. Acetati Spa – Verbania - Italy - producer of helmet, sport components, ect.

4. Mircotech - Venizia - Italy - producer of mixing pellets and fillers for plastic components

5. Euromaster - Prato - Italy - producer of mixing pellets for plastic components.

Acknowledgement

This study has benefited greatly from the help of many individuals and institutions.

First and foremost, I am indebted to my supervisor, Professor Andrea Lazzeri who has built my knowledge and capacity through his guidance. "No teachers, no winners" is a saying that Vietnamese students learn by heart. This dissertation would not have been possible without the constant support of my supervisor. His valuable instructions in research methodology led me to attain essential academic growth and behavioral science. Beyond scientific understandings, he provided me with comprehension in terms of social experiences, culture and history. Specially, his dedication and perspectives on education would be a good sample for my career in the future.

I consider it an honor to work with all my colleagues in Multifunctional, Bio-Ecocompatible Materials Laboratory. Special thanks to Ms. Irene Anguillesi who taught me laboratorial skills and instruments. I am fortunate to have Dr. Patrzia Cinelli, Dott. Letizia Bacheci, Dr. Xuetao Shi, Dr. Fabia Galatini who gave inspiring discussion and shared interest in the research. Also, I would like to extend my thanks to Ms Laura Maley for tirelessly reviewing and correcting my research dissertation and English writing. With their assistance, I have greatly widened my intellectual horizons.

My sincere thanks go to Microtech and Comac Companies for supporting me in putting my researches into practical manufacture.

For financial support during my PhD program, I would like to appreciate the support I had been receiving from FP7-KBBE projects - Forbioplast (Forest resource sustainability through bio-based composite development) and OliPHA (Functional sustainable packaging). Also, I wish to express my appreciation to University of Pisa and Department of Civil Engineering and Industry which have provided with excellent research facilities to complete the study.

Most important, I owe a lifelong debt of love and gratitude to my parents for their continuous encouragement and support during the challenging time in Italy. My thanks are due to my wife for shouldering all the laborious work at home and taking care of our little son when I am away doing research.

Last but not least, I convey my sincere thanks to all my professors, staff, colleagues and friends, whose names I am unable to mention, but who nevertheless were extremely helpful in many ways.